COMPUTER SIMULATION OF A GROWTH FACTOR SIGNAL TRANSDUCTION PATHWAY

FRANCES A. BRIGHTMAN

A thesis submitted in partial fulfilment of the

requirements of Oxford Brookes University

for the degree of Doctor of Philosophy

January 2001

ABSTRACT

Although growth factor signalling has been a focus of intensive study, there are still a number of unresolved issues in this field that traditional experimental approaches have been unable to address; of particular interest are the mechanisms underlying signalling specificity. Numerous descriptive models have been proposed, although these remain largely untested, and minimal quantitative analysis has been undertaken. Where mathematical modelling has been applied, the intention has often been to examine the potential properties that biological signalling systems might exhibit, rather than to explain observed phenomena. The objective of this work was to investigate growth factor signal transduction mechanisms through the application of computer modelling techniques, and thereby obtain a novel, dynamic perspective on cell signalling processes.

A kinetic model of EGF-induced Ras/MAPK cascade activation has been developed, and implemented as a computer simulation; the model is consistent with experimental data for the PC12 cell type. During the development process, a number of qualitative models of EGF signalling were evaluated. The completed simulation provides support for the putative mechanism of EGF-stimulated Ras activation, but suggests that the mechanistic details of EGF receptor tyrosine kinase activation have little functional significance at a systemic level. However, the compartmentalization of signalling intermediates was implicated as an important regulatory feature, whilst negative feedback regulation of the pathway was shown to be a critical process in terminating signalling to the MAPK cascade. A subsequent sensitivity analysis of the simulated EGF signalling pathway reinforced these findings, and highlighted a possible regulatory role for the relative expression levels of signalling intermediates; the extent and duration of Ras/MAPK cascade activation were found to be dependent upon the effective concentration of several components of the pathway. Furthermore, feedback down-regulation was shown to confer a high degree of integral stability on the Ras/MAPK cascade, so that activation of the terminal kinase, ERK, was largely insensitive to variations in signal intensity above the level at which the feedback mechanism operates. Hence, although the MAPK cascade was demonstrated to exhibit an ultrasensitive response to EGF, the potential for the cascade to operate as a 'metabolic switch' is likely to be suppressed when embedded within a negative feedback loop. It seems more probable that inherent ultrasensitivity in the MAPK cascade plays a role in filtering out background noise, or amplifying the rate of ERK activation. Consolidating much of the preceding work, a novel hypothesis was proposed to account for the specificity of EGF and NGF signalling in PC12 cells: the contrasting patterns of Ras/MAPK cascade activation observed in response to these stimuli are most likely to be engendered by differential feedback regulation of the cascade.

Whilst the model compares favourably with similar, published models of growth factor signalling, it provides a more detailed and accurate representation, and a valuable *in silico* experimental system. The merit of a modelling approach for studying signal transduction is clearly demonstrated, but the potential for future expansion of the model is also recognised, enabling further investigation of the factors that define specific responses to growth factor signals.

ACKNOWLEDGEMENTS

Firstly, I would like to express my sincere gratitude to Prof. David Fell, not only for his invaluable guidance, assistance and encouragement throughout my time as a Ph.D. student, but also for inspiring my interest in theoretical biochemistry, and providing me with the opportunity to pursue that interest. My thanks also go to Dr. Simon Thomas, partly as a mentor, for being willing to share his knowledge and expertise with me on a day-to-day basis, but also as a friend, for his unlimited confidence in my abilities. I am also indebted to Drs. Alan Betteridge and Mark Poolman, for their unfailing willingness to help, and for providing valuable suggestions and advice on many occasions.

I wish to thank Lisa Cornwell, Kaye Bellman, Richard and Donna Goode, and Dennis Wiggins, for their friendship and support over the course of my academic career. Without these people, I would not have had the chance to fulfil this ambition. For also inspiring me to realise my aspirations, I would like to acknowledge Gary Ward, Pamela Biss and Maria Kutar.

Finally, I cannot thank Richard Harrison enough for taking a genuine interest in this work, and having a desire to help wherever possible. For his enduring patience, support and encouragement, I am immensely grateful.

CONTENTS

ABBREVIATIONS

ADP:	Adenosine diphosphate
AP2:	Adaptor protein 2
ATP:	Adenosine triphosphate
CPP:	Coated pit protein
CRD:	(Raf) Cysteine-rich domain
EGF:	Epidermal growth factor
EGFR:	EGF receptor
ERK:	Extracellular signal-regulated kinase
ERK1:	ERK isozyme 1
ERK2:	ERK isozyme 2
ERKP:	Phosphorylated ERK
ERKPP:	Phosphorylated ERKP
FGF:	Fibroblast growth factor
FRS2:	Fibroblast growth factor receptor substrate 2
GAP:	Ras GTPase activating protein
GDP:	Guanosine diphosphate
GEF:	Guanine-nucleotide exchange factor
Grb2:	Growth factor receptor binding protein 2
GTP:	Guanosine triphosphate
Hsp90:	90 kDa heat-shock protein
IGF-I:	Insulin-like growth factor-I
IGF-IR:	Insulin-like growth factor-I receptor
KSR:	Kinase suppressor of Ras
MAPK:	Mitogen-activated protein kinase
MEK:	MAPK or ERK kinase
MEK1:	MEK isozyme 1
MEK2:	MEK isozyme 2
MEKP:	Phosphorylated MEK
MEKPP:	Phosphorylated MEKP
MKP:	MAPK phosphatase
MP1:	MEK partner 1
NGF:	Nerve growth factor
PH:	Pleckstrin homology
PI-3K:	Phosphatidylinositol 3-kinase
PKA:	Protein kinase A
PKC:	Protein kinase C
$cPLA_2$:	Cytosolic phospholipase A_2
PLCγ:	Phospholipase Cγ
PP2A:	Protein phosphatase 2A
PTPase:	Protein tyrosine phosphatase
Ras-GDP:	GDP-bound Ras
Ras-GTP:	GTP-bound Ras
RBD:	(Raf) Ras-binding domain
Rsk:	Ribosomal S6 kinase
RTK:	Receptor tyrosine kinase
SH2:	Src homology 2
SH3:	Src homology 3

Shc:	Src homology and collagen domain protein
ShcP:	Phosphorylated Shc
SNT:	*suc*1-associated neurotrophic factor target
SOS:	Son of sevenless homologue protein
TrkA:	High affinity NGF tyrosine kinase receptor
VHR:	*vaccinia* H1-related phosphatase

CHAPTER 1

BACKGROUND TO THE THESIS

1.1 INTRODUCTION

This initial chapter serves to outline the motivation for the work documented in the thesis, by providing an overview of current issues in the field of growth factor signal transduction, and an introduction to the application of theoretical modelling techniques in the study of biochemical systems. A more comprehensive review of the contextual literature follows in subsequent chapters.

1.2 GROWTH FACTOR SIGNAL TRANSDUCTION

1.2.1 SIGNAL TRANSDUCTION AND SIGNALLING SPECIFICITY

Many of the individual cells of multicellular organisms communicate with each other indirectly through soluble signalling molecules, as a means of co-ordinating and regulating systemic behaviour. Extracellular signalling molecules bind to and activate receptors expressed by their target cells, to initiate a cascade of molecular events within the cell. The signal is thereby relayed from the cell surface to the cytosolic or nuclear targets responsible for generating the cellular response, through the process of signal transduction (171).

Cell specialization enables different cell types to respond differentially to the same chemical signal, according to their particular complement of receptor proteins and intracellular mediators. Conversely, different signalling molecules may interact with the same cell type, but evoke contrasting responses through the activation of distinct receptors and transduction cascades (296). These features of cell signalling enable the behaviour of the target cell to be regulated in a highly specific manner, often in accordance with the selective activation of a particular signalling pathway (303). However, this rather simplistic scheme is complicated by a high degree of interaction, or 'cross-talk', between parallel intracellular pathways, many of which eventually converge upon common components of the cell signalling network; for example, the

mitogen-activated protein kinase (MAPK) cascade (74, 233). Hence, there is an apparent paradox: extracellular signalling molecules bind with a high degree of selectivity to cell surface receptors, but although a reduction in specificity is subsequently introduced by the initiation of generic intracellular events, a highly specific cellular response is still achieved (74, 151). This phenomenon is particularly exemplified by growth factor signalling.

1.2.2 GROWTH FACTOR SIGNALLING PATHWAYS

Growth factors are a family of polypeptide signalling molecules that play a central role in regulating the proliferation, survival and differentiation of the majority of eukaryotic cell types (298, 300). A number of growth factors mediate their cellular actions by interacting with a group of cell surface receptors that have intrinsic protein tyrosine kinase activity, termed receptor tyrosine kinases (RTKs) (300, 376). These receptors comprise an extracellular ligand-binding domain, a single transmembrane region and a cytosolic protein tyrosine kinase domain (300, 376). The binding of a growth factor to the ligand-binding domain activates the cytosolic kinase domain, thereby inducing tyrosine phosphorylation of both the receptor (autophosphorylation) and intracellular effectors[1] (300). These events constitute the first steps in a signal transduction cascade that ultimately results in the activation of target proteins involved in cell cycle control and the regulation of cell growth. The signal is propagated by a network of cytosolic protein kinases, the vast majority of which are serine/threonine kinases, and other intracellular mediators; transmission of the signal is largely through rapid, reversible changes in the phosphorylation state of cellular proteins, which influence direct interactions between signalling intermediates and enzymatic activity (171).

Whilst it seems a reasonable assumption that different growth factor RTKs might activate distinct intracellular transduction cascades, and that proliferation and differentiation are associated with specific pathways, this is not generally the case. There is considerable overlap in the identity of the signal transducing molecules utilized by different RTKs to transmit the signal from the cell surface to diverse cellular targets, and no effectors have yet been discovered that are uniquely associated with a given receptor or a particular cellular response. In some instances, the nature of the response

[1] In this context, the term 'effector' refers to an element of a signal transduction cascade that mediates the effect(s) of an upstream component of the cascade.

induced by a certain RTK appears to be dependent on the cellular context; for example, activation of the fibroblast growth factor (FGF) receptor induces proliferation in fibroblasts, but differentiation of PC12 cells (217). This is not however, a definitive answer, and cannot explain why different RTKs may activate apparently identical signalling pathways, yet generate opposing responses in the same cell type; for example, the receptors for mitogens and differentiation factors in PC12 cells (53, 217).

A plausible hypothesis is that such phenomena arise through the translation of quantitative, rather than qualitative, differences in the signal into a distinct biological response. For example, it has been argued that variations in the frequency, amplitude or duration of particular signalling events (74, 217, 303), relative expression levels of signal transducing molecules in different cell types (11, 302), or differential affinities of RTKs for alternative ligands (75) or signalling effectors (265, 296, 302), may determine the cell fate.

1.2.3 CURRENT PERSPECTIVES IN CELL SIGNALLING

The biochemical mechanisms underlying growth factor signal transduction and signalling specificity have long been a focus of attention. Many of the individual components of cellular signal transduction networks have been identified and characterized in isolation, yet how they function as an integrated system within the cell is still poorly understood. Numerous mechanistic models of growth factor signalling have been proposed, largely on the basis of qualitative experimental evidence, but a lack of quantitative data means that these models may well place too much emphasis on irrelevant or inconsistent observations, or be founded upon false assumptions. Hence, much of the currently accepted understanding of how cellular signalling systems operate may be invalid. In order to clarify this issue, an explicit investigation of the functional and regulatory properties of signal transduction networks is essential. Evidently, it would be preferable to study these properties within the cellular environment, but unfortunately, the direct analysis of biochemical systems is still hindered by numerous technical constraints. Theoretical modelling techniques can however, represent a feasible alternative to more established practical methodologies, as they provide a means of investigating the properties of biochemical systems in a simulated 'physiological' situation (144).

1.3 THEORETICAL ANALYSIS OF BIOCHEMICAL SYSTEMS

1.3.1 MODELLING BIOCHEMICAL SYSTEMS

A model can be defined as a simplification, or abstraction, of a real system (141). Biochemical models usually take the form of a mathematical description of the structural and dynamic properties of the system, formulated as a set of first-order ordinary differential equations that describe the net rate of change of the system variables. These equations are generally derived from mathematical expressions that define the kinetic behaviour of the component reactions of the system (for example, from enzyme rate laws or ligand-binding equilibria), and their solution provides a means of characterizing the behaviour of the system. The variables to be modelled are usually levels of biochemical intermediates and flux through a particular pathway or cellular sub-system (kinetic and thermodynamic constants, enzyme concentrations, or the concentrations of external effectors are regarded as model parameters), and there are two general approaches: calculation of the steady state flux and metabolite concentrations, or time course simulation, where system behaviour is followed as a function of time from a specified starting point.

There are also two extremes in model complexity. Biochemical systems typically constitute an extensive network of reactions, with many interdependent variables. An idealized 'skeleton' model provides a greatly simplified representation of such a system, comprising only the fundamental dynamic features (141). A high degree of abstraction can be achieved by significantly reducing the number of variables and parameters, amalgamating sequences of reactions into single processes, and (under certain circumstances) using linear approximations to rate laws. This allows the model to be expressed in terms of a system of linear differential equations, for which it is possible to determine an analytical solution. Despite the mathematical tractability of this approach, it has a serious disadvantage; the resulting model may lack sufficient realism to permit any meaningful analysis of the system behaviour, and would be incapable of representing phenomena that emerge through system non-linearity, such as the existence of multiple steady states. At the other extreme are 'synthetic' models (108), in which a large quantity of empirical data is consolidated to provide a highly detailed representation of the system. Models of this type allow simulated experiments to be conducted, although a possible drawback is that the model can be almost as complex as the actual system, and hence equally difficult to study (141). Furthermore, this inherent

complexity can only be represented satisfactorily by a system of non-linear differential equations, which cannot be solved analytically. Computer modelling techniques enable the numerical solution of these equations, either by numerical integration or direct solution, and hence provide a valuable computational tool for investigating the behaviour of biochemical systems; purpose-written computer software for modelling biochemical systems is widely available, for example 'SCAMP' (295), 'Gepasi' (226, 227), and 'MIST' (91). Most models are a compromise between these extremes and the degree of mathematical abstraction employed is largely determined by the intended function of the model, that is, whether the purpose is to qualitatively describe the behaviour of the system being modelled, or accurately predict that behaviour in quantitative terms. As a broad generalization, the simplest model that is consistent with the real system is used (141).

A model of a biological system may be viewed as a hypothesis that aims to explain the behaviour of the system (141). This hypothesis can be tested by comparing the functional attributes of the model with experimental observations. Although close agreement with quantitative data is a more rigorous test of the validity of a model, the capacity to represent fundamental qualitative characteristics of the real system may be sufficient to substantiate the model under certain circumstances; for example, if it is possible to reproduce system behaviour that can only arise under a restricted set of conditions, such as sustained oscillations or hysteresis. Similarly, compatibility with time course data, rather than steady state data, is a more stringent criterion for model verification (141). There may in fact be several hypotheses that can be considered, by changing the mathematical structure of the model and varying the model parameters. In order to find the best fit between the model and a set of experimental data, a variety of model optimization methods may be employed; these invoke an algorithm that iteratively assesses the quality of the fit and adjusts the model parameters accordingly, until an optimal fit is obtained (108, 109). A model may be eliminated if it can be shown to be incompatible with the data, although it is not possible to conclusively prove that any particular model is the definitive representation of a system (141). Alternatively, as a model often forms a composite representation of experimental data derived from different sources, inconsistencies in this data may be revealed through modelling the system. If the behaviour of a model can be demonstrated to be compatible with experimental observations, the essential dynamic features of the system are likely to have been correctly assumed, although the model parameters will

not necessarily reflect actual physiological values (141). The validated model can, nonetheless, be viewed as a tool for investigating the properties of the system.

1.3.2 QUANTITATIVE ANALYSIS OF METABOLIC CONTROL AND REGULATION

Any study of the regulatory properties of a biochemical system generally involves identifying the components of the system that have the greatest influence on flux and metabolite concentrations, the means by which external signals interact with these components, and the overall response of the system to such signals (141). It is becoming more widely acknowledged that this type of study is best approached from a quantitative perspective. One such technique that is routinely employed in a number of disciplines, in various forms, is sensitivity analysis. This method is used to quantify the degree of control that individual factors exert on the behaviour of the system as a whole.

Metabolic control analysis is a form of sensitivity analysis that is specifically applicable to biochemical systems; it is the most widely accepted and implemented quantitative approach to the study of metabolic control, and has both theoretical and experimental applications (101). The theory was originally proposed independently by Kacser and Burns (167) and Heinrich and Rapoport (142), but since these approaches are essentially equivalent in their mathematical formulation, a common terminology was subsequently established (35). The underlying premise is that the control of the behaviour of a metabolic system is not localized within one element of the system, but distributed throughout the system components. Hence, contrary to the prevalent view that a single 'rate-limiting' step is responsible for the overall rate of flow through a metabolic pathway, flux is considered to be a property of the entire system (167). Individual metabolite concentrations and overall flux are treated as variables of the system, which are established by the dynamic interaction of the various system parameters (167). The relative contribution of each parameter in determining a particular variable, within the context of the intact system, can be represented mathematically in the form of a control coefficient (169). A comprehensive account of the theory and applications of metabolic control analysis has been provided by Fell and colleagues (100, 168).

Theoretical modelling provides a convenient basis for subjecting a biochemical system to quantitative sensitivity analysis, which can be carried out simply by altering any system parameter or variable and determining the response of the system (141, 144). Similar regulatory studies can also be carried out on an experimental basis, but manipulation of the structure, or parameters, of a real biological system is possible only to limited extent (141). Moreover, the isolation procedure typically disrupts the structural organization or normal cellular functioning, and such studies are normally carried out under optimal rather then physiological conditions. Theoretical analysis, particularly when approached from a computer modelling perspective, is generally more practicable and far more rapid than carrying out a comparative experimental study (108, 109). Due to their intrinsic complexity, biochemical systems frequently demonstrate properties that are not necessarily intuitive, and computer simulation can facilitate a greater understanding of their behaviour than might be gained through more conventional approaches (108).

1.4 Aims of the Thesis

The overall purpose of the work documented in this thesis was to apply the techniques of computer simulation and quantitative sensitivity analysis to a study of the dynamic behaviour and regulatory properties of signal transduction pathways in general. This broad objective was broken down into three project goals.

- To construct a computer simulation of a generic signal transduction pathway.
- To utilize this simulation in an investigation of the general functional and regulatory properties of a typical transduction network, and more specifically, to study the dependence of signalling specificity on the kinetic properties of signalling events within the simulated pathway.
- To complement this study of a kinetic model with a quantitative sensitivity analysis of the pathway, such as metabolic control analysis, to assess the control features of the system in more general terms.

These goals evolved during the lifetime of the project, and hence the actual aims of the thesis diverge somewhat from those proposed initially.

- To introduce a detailed computer simulation of a representative growth factor signal transduction pathway, the behaviour of which is consistent with experimental observation, in conjunction with a discussion of a number of issues arising during the development of the model.

- To present a sensitivity analysis of the simulated pathway, conducted with the intention of assessing the robustness of the model and exploring possible functional and regulatory features of the real system.

- To compare the dynamic and regulatory features of the simulated pathway with those of published quantitative models of modular components of cellular signalling networks, and consider whether these models provide an appropriate representation of the system *in vivo*.

- To report and discuss the findings of a quantitative analysis of growth factor signalling specificity carried out using the completed model, accompanied by a discussion of the significance of these findings.

- To submit a number of general conclusions regarding the application of a computer modelling approach to studying mechanisms of cellular signal transduction, supported by the work undertaken.

1.5 OVERVIEW OF THE THESIS

1.5.1 CHAPTER 2: THE EPIDERMAL GROWTH FACTOR SIGNAL TRANSDUCTION PATHWAY

This chapter provides the basis for the subsequent derivation of a computer model of growth factor signalling, and constitutes a critical review of the considerable body of pertinent literature that has accumulated over many years intensive study of the epidermal growth factor (EGF) signal transduction system.

1.5.2 CHAPTER 3: DEVELOPMENT OF A COMPUTER SIMULATION OF EGF SIGNAL TRANSDUCTION

The majority of the work underlying the thesis is documented in this chapter, starting with the specification of a computer simulation of the EGF signal transduction pathway, which is followed by an account of the development and refinement of the

model. A modular approach was adopted for this process; the pathway was sub-divided conceptually into three 'modules', corresponding to three sub-cellular compartments within which specified groups of events were considered to take place: the cell surface (extracellular face of the plasma membrane), a compartment immediately adjacent to the inner face of the plasma membrane, and the cytosol. Each module was bounded by events for which published experimental data are readily available. These individual modules were ultimately combined to form the complete model. The methodology employed at each stage of the development process is described, including the evaluation of a number of mechanistic models of EGF signalling proposed in the literature, and validation of the model through comparison of the simulated behaviour with experimental data. This provides a narrative account of model development, and reflects the recursive nature of this process.

1.5.3 CHAPTER 4: SENSITIVITY ANALYSIS OF THE EGF SIGNALLING PATHWAY

The robustness of the behaviour of the simulated pathway is explored in this chapter, which begins by describing a methodology for analysing the sensitivity of the model to variations in simulation parameters. The results of this analysis are presented and discussed, with reference to the possible significance of the findings within a physiological setting.

1.5.4 CHAPTER 5: MATHEMATICAL MODELLING APPLIED TO SIGNAL TRANSDUCTION: A CRITICAL REVIEW

This chapter places the work covered in the thesis into context, and documents a comparison of the simulated EGF signal transduction pathway with similar models of growth factor signalling. A survey of the theoretical study of signal transduction is provided, with particular emphasis being placed upon a number of recently published quantitative studies that demonstrate the inherent properties of a central component of cell signalling networks, the MAPK cascade. The likely operation of the MAPK cascade within the cellular environment is considered by comparing the range of potential behaviours predicted for the isolated cascade, with the simulated operation of the cascade within the more realistic context of an intact signalling pathway. Finally, the structural and dynamic features of the simulation are also compared with those demonstrated by similar kinetic models of growth factor signalling systems.

1.5.5 CHAPTER 6: QUANTITATIVE ANALYSIS OF EGF AND NGF SIGNALLING SPECIFICITY IN PC12 CELLS

Mitogens, such as EGF, and differentiation factors, such as nerve growth factor (NGF), induce opposing responses in the PC12 cell line, despite activating the same signalling pathway. The background to this well-documented, but as yet unexplained phenomenon is provided in this chapter. A methodology for investigating the basis of specificity in growth factor signalling is then described, and the results of this analysis are presented and discussed. The chapter concludes with the proposal of a novel hypothesis, suggested by the findings, that explains the phenomenon.

1.5.6 CHAPTER 7: GENERAL CONCLUSIONS

A general summary of the conclusions that can be drawn from the preceding chapters is given, with the intention of assessing the applicability of computer modelling techniques to the study of cellular signalling networks, and highlighting the capacity of this approach to provide significant insights into the behaviour of these systems. The chapter is completed by a discussion of the potential for further enhancements to the work detailed in the thesis.

CHAPTER 2

THE EPIDERMAL GROWTH FACTOR SIGNAL TRANSDUCTION PATHWAY

2.1 INTRODUCTION

The intention at the outset of the project was to construct a detailed model of a signal transduction pathway, to serve as an experimental system for examining the properties of cell signalling. A comprehensive survey of the relevant literature indicated that probably the best characterized cellular signalling pathway is that of the growth factor, EGF. This system was therefore selected as a suitable candidate to form the basis of the model.

This initial chapter constitutes a review of the accumulated body of knowledge concerning EGF signal transduction. Since several authors have suggested that the specificity of the cellular response to growth factors may arise from quantitative differences in signalling events occurring at the level of the receptor (217, 296, 340), particular emphasis is placed upon ligand-induced RTK activation and internalization. The mechanisms underlying these processes are not clearly defined, and this account reflects an attempt to extract a cohesive model of EGF-induced activation of the EGF receptor (EGFR), from the seemingly contradictory published material.

2.2 EPIDERMAL GROWTH FACTOR

EGF is a polypeptide hormone that stimulates the proliferation and differentiation of numerous cell types, although principally epithelial cells, and exerts its effects through interaction with a specific plasma membrane receptor (EGFR) that has intrinsic protein tyrosine kinase activity (reviewed in refs. 43, 44, 158). The structure and configuration of the receptor has been deduced from its cDNA sequence; the mature EGFR is a 170-kDa glycoprotein, consisting of an extracellular ligand-binding domain, a single transmembrane region, and an intracellular protein tyrosine kinase domain (341). The binding of EGF to its receptor stimulates a series of both rapid and delayed responses:

autophosphorylation of receptor tyrosine residues, tyrosine phosphorylation of exogenous substrates, hydrolysis of phosphatidyl inositol and elevation of intracellular Ca^{2+} levels (43, 44, 158). In addition, EGF-EGFR complexes rapidly cluster within cell surface clathrin-coated pits, and are subsequently internalized and degraded, although there is some evidence for a degree of receptor recycling to the cell surface (43). The physiological events following ligand binding are dependent upon activation of the receptor tyrosine kinase (60, 115, 148); hence, this appears to be an essential step in the signal transduction cascade.

2.3 ACTIVATION OF THE EGF RECEPTOR

2.3.1 DIMERIZATION AND ACTIVATION

Since the ligand-binding and catalytic domains of receptor tyrosine kinases are separated by the plasma membrane, across which ligand-induced activation of the receptor must be transmitted, Ullrich, Schlessinger and Yarden (300, 342, 376) suggest that they can be viewed as membrane-associated allosteric enzymes. However, the transmembrane signal transduction mechanism remains unresolved. Two types of model have been proposed for activation of the EGFR, both of which are apparently supported by experimental evidence. The first is an intramolecular model, which states that the external binding of EGF induces a conformational change in the receptor that is transmitted through the transmembrane domain to activate the cytosolic tyrosine kinase domain (114, 186, 323). The alternative, more generally accepted model is an intermolecular mechanism, termed the allosteric oligomerization model, in which receptor activation is governed by dimerization (298, 374, 375). According to this scheme, inactive monomeric EGF receptors are in equilibrium with activated dimeric EGF receptors. It is assumed that the binding affinity of the dimers toward EGF is higher than that of the monomers, and hence the preferential binding of EGF to receptor dimers shifts the equilibrium to favour the active dimeric state (299, 300). EGF thereby stabilizes and enhances the formation of receptor dimers (384).

Homologous, ligand-induced receptor dimerization is common to all growth factor receptors with tyrosine kinase activity (302), many of which have also been shown to form heterodimers with closely related members of the same RTK family (355). EGF-induced dimerization of the EGFR has been detected in detergent-solubilized

preparations (22, 374), in isolated plasma membranes (65, 115, 248), and in intact cells (65, 314), and has been shown to be an inherent property of the extracellular ligand-binding domain of the receptor (159, 197). The binding of EGF to the EGFR induces a conformational change in this domain (127), which has been suggested to stimulate receptor-receptor association (197). Dimerization brings the cytoplasmic domains of the two receptors into close proximity, thus promoting and stabilizing interactions between adjacent domains; this is claimed to facilitate intermolecular receptor autophosphorylation and activation (300, 342). Both reversible (374, 375) and irreversible (39) mechanisms of ligand-induced EGFR dimerization have been proposed however, the precise molecular details are still not entirely understood, and whether this constitutes the actual mechanism of receptor activation remains unclear.

Experimental evidence has been presented that dimerization parallels receptor activation (39), precedes autophosphorylation (308), and increases the affinity of the EGFR for EGF (22, 106, 319, 374, 375, 384), supporting the conclusion that the dimeric form of the receptor represents an active high-affinity state, whilst the monomeric receptor is presumed to constitute an inactive low-affinity state. This model is consistent with the apparent precedence of high-affinity receptors in mediating EGF signal transduction (13, 78, 375), but conflicts with reports that aggregation is not an absolute requirement for receptor activation (47, 186, 248) or stimulation of the early cellular responses to EGF (45). The assumption that ligand-induced dimerization is a prerequisite for transduction of the signal across the plasma membrane may therefore be questionable. In addition, apparent high-affinity receptors can be activated by EGF (78); hence, even if dimerization increases ligand-binding affinity, it may not necessarily determine receptor activation. This might imply that activation is an intramolecular event, although deletions or substitutions in the transmembrane region of the receptor, which should be critical for intramolecular signal transduction, do not affect the ability of EGF to activate the EGFR kinase (42).

In order to explain these seemingly contradictory observations, an alternative, non-allosteric activation model has more recently been proposed (106), in which high-affinity receptors correspond to dimeric complexes in an intermediary inactive state, that can be fully activated only upon EGF binding (320). According to this model, the association of EGF with pre-existing receptor dimers induces a reorientation of the constituent monomers, brought about by stereochemical interaction of the bound EGF

molecules (106). This motion is presumed to be transmitted by corresponding rotation of the transmembrane and cytoplasmic domains, enabling the tyrosine kinase domains to achieve a relative configuration that facilitates mutual activation.

Although this seems a plausible hypothesis, in that it incorporates aspects of both intramolecular and intermolecular models of EGFR activation, a serious criticism of the accepted justifications for both types of model has been raised by Gates and King (111). They allege that the evidence supporting an intramolecular model is based primarily upon the absence of receptor aggregation coincident with autophosphorylation, and is therefore indirect. However, evidence that receptor dimerization induces EGFR activation is founded on using agents other than EGF to cross-link the receptor, such as lectins or antibodies. Whilst these agents can stimulate aggregation and autophosphorylation of the solubilized receptor (320, 374), they do not increase tyrosine kinase activity in intact cells or membranes (78, 111, 320). Hence, the apparent activation of the EGFR brought about by cross-linking agents in detergent solution is likely to be artefactual, as this merely constitutes the prevention of a decrease in tyrosine kinase activity caused by solubilization (111). These studies cannot therefore be used to support either an intermolecular or an intramolecular mechanism, as they are unlikely to be relevant to ligand-induced EGFR activation in intact cells (45). Indeed, it may be that the mechanism by which EGF activates the EGFR within the plasma membrane is not the same as that in solution (45, 46).

In conclusion, a confounding array of evidence has accumulated concerning EGFR activation, and there is little consensus on the mechanism by which this is brought about. Ligand binding is the predominant regulator of EGFR activity, and is required to induce a fully active receptor conformation (353). Kinetic analysis demonstrates that EGF activation of the EGFR leads to an increase in apparent and absolute affinity for ATP and other substrates, and increases the apparent, but not absolute V_{max} of the tyrosine kinase (270). Furthermore, EGF-induced activation seems to stabilize the ternary complex, and thereby promotes the formation of the phosphorylated product; EGF thus appears to induce conformational changes that increase the affinity of the receptor for its substrates, allowing them to be more readily phosphorylated (270). Both dimeric and monomeric EGFR are enzymatically active, although the dimer has a higher affinity for exogenous substrates than the monomer (36). Hence, EGFR dimers would seem to represent the active form of the receptor, and receptor activation may

indeed be facilitated by EGF-induced dimerization. These conclusions do not however, take into consideration the effect of EGF-induced EGFR autophosphorylation on tyrosine kinase activity; whilst self-phosphorylation is not an absolute prerequisite for catalytic activity (206, 307, 347), accumulating evidence suggests that autophosphorylation may play a role in promoting maximal activation of the enzyme (15, 16, 347).

2.3.2 THE ROLE OF RECEPTOR AUTOPHOSPHORYLATION IN EGFR ACTIVATION

Numerous studies indicate that the C-terminal region of the EGFR is an important regulatory domain (24, 52, 59, 176, 259, 347, 354). EGF stimulation has been shown to promote rapid self-phosphorylation of the EGFR on a number of tyrosine residues located in the extreme C-terminus (88), via an intramolecular reaction (18, 352). Intermolecular autophosphorylation of these residues has also been demonstrated, both for the solubilized receptor (149, 308) and in intact cells (150). This does not exclude an intramolecular autophosphorylation mechanism *in vivo* (149, 150), yet EGF-induced receptor activation displays apparent second-order kinetics, implying that intermolecular phosphorylation within the EGFR dimer may be the activating step (150). In order to determine the role of autophosphorylation in EGFR activation, it is therefore important to establish whether this process directly affects tyrosine kinase activity. Some experimental data seems to indicate that EGFR autophosphorylation increases EGFR kinase activity towards exogenous substrates (16, 208, 316, 347), particularly for peptides closely resembling physiological targets, such as phospholipase Cγ (PLCγ) (152), whereas others have found that autophosphorylation has little (147) or no (89, 130) effect on catalytic activity. There is however some agreement that autophosphorylation may alter substrate specificity (24, 89) or affinity (16, 147).

Kinetic analysis has indicated that the autophosphorylation sites act as alternate substrates or competitive inhibitors of exogenous substrates (16), which conversely inhibit self-phosphorylation (49, 93), by competing for the active site (16, 271). Self-phosphorylation therefore removes this inhibitory constraint (16, 147, 316), effectively increasing the affinity of the enzyme for the substrate and promoting substrate phosphorylation (15, 24, 208). Bertics and colleagues (15, 16) have therefore postulated that self-phosphorylation may have a role in modulating EGFR activity; the autophosphorylation sites have an intrinsic negative regulatory role and self-

phosphorylation may thus serve as a mechanism for the suppression of basal kinase activity in the non-activated state, but also a means of achieving maximal activity secondary to ligand-induced activation. A slightly different view is that autophosphorylation serves to generate a stimulation threshold, which must be exceeded to induce a normal mitogenic response (147). Alternatively, as phosphorylated tyrosine residues form binding sites for Src homology 2 (SH2) domain-containing proteins associated with signal transduction (reviewed in refs. 66, 266), autophosphorylation is mandatory for interaction of the EGFR with signalling effectors containing SH2 domains (271), and may increase the affinity for these molecules by generating SH2 binding sites. This is in fact supported by studies showing that autophosphorylation of the EGFR induces a significant conformational change in the catalytic domain of receptor (36, 152), which may expose sites for SH2 interactions (36).

A coherent view of EGFR activation is therefore that ligand binding activates the receptor by inducing a conformational change in the extracellular domain of the receptor, which facilitates dimerization. This process transduces the signal across the plasma membrane, by promoting and stabilizing a configuration that favours autophosphorylation of the protomeric intracellular C-terminal domains (156). Autophosphorylation promotes further conformational changes in the catalytic domain, which remove an inhibitory constraint, allowing exogenous substrates to gain access to the active site and effectively increasing the affinity of the EGFR for its target molecules (342); this step is likely to correspond to the exposure of SH2 binding sites. Activation would therefore appear to be an intermolecular process, since it would be dependent upon dimerization, although the autophosphorylation mechanism could still be either intramolecular or intermolecular. Despite invoking a fundamentally intermolecular mechanism for EGFR activation, this is not necessarily an allosteric model, as it is not implicit that the dimeric receptor has a higher affinity for EGF than receptor monomers. The final step required to complete the picture of EGFR activation is therefore to establish whether the generation of apparent high affinity binding sites is associated with receptor dimerization.

2.3.3 AFFINITY HETEROGENEITY IN EGF-EGFR INTERACTION

Since the validity of an allosteric activation model depends upon equating high-affinity receptors with the dimeric EGFR, considerable effort has focused on characterizing these receptors. Although studies investigating the kinetics of EGF-EGFR interaction have implied the presence of at least two affinity classes of EGF receptors (13, 14, 282), there is no direct biochemical evidence for two stable populations of EGFR with different affinities for EGF (13, 352). Furthermore, evidence has been presented that the emergence of high-affinity binding sites is independent of the oligomeric state of the receptor (249, 346), and may be determined by factors such as the phosphorylation status of the receptor (363), association of the receptor with the cytoskeleton (344, 358), or interaction with other proteins that modulate binding affinity (346). The probable basis of apparent affinity heterogeneity has in fact been elucidated through studies investigating the mechanism of EGF-EGFR complex internalization. Several mathematical models describing the dynamics of EGF-EGFR binding and internalization have been proposed, which can generally be classified as either two-state or three-state ('ternary-complex') models.

2.3.3.1 Two-state internalization models

In most cell types ligand-induced receptor internalization can be regarded as a first-order process (348, 359, 360), implying that although more than one process may be involved, there is only a single 'rate-limiting' step, corresponding to receptor occupancy (361). Receptor-ligand binding and internalization can therefore be described using a two-state model, in which the only events modelled explicitly are ligand binding and subsequent receptor-ligand complex internalization, with no intermediate steps being considered. This is illustrated in Figure 2.1 below.

A model of this type has been developed by Waters and colleagues (348) to describe EGF-EGFR internalization in foetal rat lung cells. The endocytic step was assumed to be a simple first-order process; replacing the first-order endocytic term for internalization with a second-order term, in order to represent receptor dimerization, resulted in a poorer fit to experimental data. Thus, it was concluded that although dimerization may occur, it is not 'rate-limiting' for endocytosis. However, the fit of the model to the data was relatively poor at high free ligand concentrations; the measured

rise in receptor-ligand complexes at high EGF concentrations was steeper than that predicted by the model. This was interpreted as indicating the presence of two classes of receptors, with differing affinity for the ligand, although no change in affinity at high EGF concentrations was directly observed.

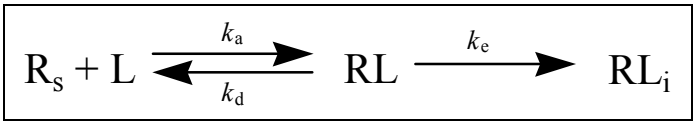

Figure 2.1 A two-state model describing receptor-ligand binding and internalization
R_s, free surface receptor; L, free ligand; RL, surface receptor-ligand complex; RL_i, internalized receptor-ligand complex; k_a, receptor-ligand association rate constant; k_d, receptor-ligand dissociation rate constant; k_e, endocytic rate constant.

A similar model, including terms for recycling of receptor-ligand complexes and a time delay for ligand degradation, was employed to investigate EGFR internalization in NIH-3T3 cells (349). The model was however, found to be unable to account for some feature of EGF binding in this cell type, as the dissociation rate constant for the receptor-ligand complex (k_d) was found to increase with occupancy, whereas the endocytic rate constant (k_e) decreased. This was again attributed to the existence of two affinity classes.

Ligand binding parameters are generally derived from equilibrium binding data expressed in the form of a Scatchard plot; this allows the apparent affinity constants and average number of receptors per cell to be estimated (43). In almost all cell lines investigated, Scatchard analysis of EGF equilibrium binding data generates a non-linear plot (14), whereas two-state binding and internalization models predict a linear Scatchard plot (219). Evidently, a simple two-state scheme for ligand binding and internalization is therefore not entirely consistent with experimental observations. Under conditions where internalization is arrested (for example, at low temperature), a non-linear Scatchard plot indicates occupancy-dependent affinity (112). Equilibrium binding data for EGF and the EGFR usually generate plots that exhibit negative curvature (366), with decreased effective affinity at high receptor occupancy (219). As such non-linearity can arise if there is actual heterogeneity in the binding affinities of

the receptors (366), this curvature can be interpreted as indicating the presence of two different populations or affinity classes of receptors, a major class of low-affinity receptors and a minor class of high-affinity receptors (43).

On the basis of Scatchard analysis of EGF equilibrium binding data, a model of EGF-EGFR internalization has been proposed that assumes two receptor populations, which differ in their affinity for the ligand (97). The high-affinity state is suggested to arise from a conformation that is stabilized by receptor aggregation within cell surface coated pits, and as this state is also assumed to exhibit enhanced affinity for the 'endocytic apparatus', it is internalized at a higher rate than the low-affinity state. This interpretation may however, be flawed; data derived from equilibrium binding studies are often compromised, as these studies are usually conducted with intact cells at temperatures at which post-binding events, such as internalization and ligand degradation, are not precluded (43). Consequently, this data may not necessarily indicate the existence of multiple receptor affinity classes, and an alternative explanation may be more likely.

2.3.3.2 Three-state models

In addition to affinity heterogeneity, a non-linear Scatchard plot can indicate cooperative, two-step or multivalent binding (112). The dissociation of EGF from human fibroblasts at 4 ºC has been shown to be a biphasic process; in conjunction with the typical negative curvature of the EGF equilibrium binding plot, this could indicate two sequential binding events (219). Thus, a number of three-state or 'ternary complex' models have been proposed (112, 219, 359), in which the receptor-ligand complex further associates with a cell surface interaction molecule prior to internalization, as illustrated below in Figure 2.2. The interaction molecule has been equated with a specific 'internalization component' in coated pits, which mediates rapid, ligand-induced internalization of occupied receptors (359). Thus, ligand binding may result in a structural alteration in receptors, facilitating interaction with coated pit components, and consequent clustering in coated pits (112).

This elementary two-step binding and internalization model has since been developed to accommodate a number of further experimental observations. It has been noted that occupied receptors are cleared from the cell surface more rapidly than unoccupied

receptors (360). In addition, mutant receptors lacking protein tyrosine kinase activity exhibit decreased ligand-induced internalization, that is a low k_e, which does not vary with occupancy (59, 115). These observations have led to the proposal that there may be two endocytic pathways in operation, corresponding to a ligand-independent and a ligand-induced mechanism. Unoccupied and tyrosine kinase inactive receptors are internalized via a low-affinity/high-capacity constitutive pathway, which displays first-order kinetics and is likely to correspond to background turnover (59, 115, 356). Occupied receptors are however, endocytosed through a high-affinity/low-capacity mechanism, characterized kinetically as a second-order process (59, 210).

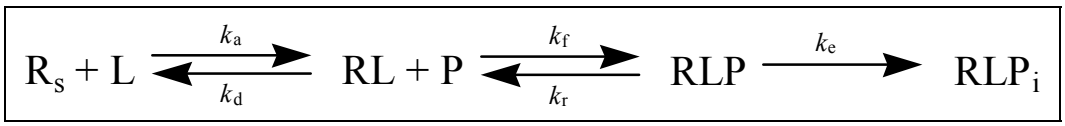

Figure 2.2 A three-state model describing receptor-ligand binding and internalization
R_s, free surface receptor; L, free ligand; RL, surface receptor-ligand complex; P, free surface interaction molecule; RLP, surface ligand-receptor-interaction molecule complex; RLP_i, internalized receptor-ligand-interaction molecule complex; k_a, receptor-ligand association rate constant; k_d, receptor-ligand dissociation rate constant; k_f, receptor-ligand-interaction molecule association rate constant; k_r, receptor-ligand-interaction molecule dissociation rate constant; k_e, endocytic rate constant.

A comprehensive model of EGF-EGFR internalization, which takes these observations into account, has been proposed by Wiley and others (210, 322, 362). In the absence of tyrosine kinase activity, EGF receptors are internalized through the default constitutive (210, 362), or 'smooth-pit' pathway (322). Ligand binding induces a conformational change in the receptor that results in kinase activation, and enables interaction of the occupied receptor with specific binding sites in clathrin-coated pits (322, 362). These sites are presumed to be adaptor proteins that, in association with clathrin, form an integral part of the coat (267). As kinase activity is necessary for the association of occupied EGFR with coated pits (210), and hence ligand-induced internalization (59, 115), tyrosine phosphorylation of the internalization component may be required in order to stabilize the interaction between EGFR and the coated pit, and thereby generate the apparent increase in the affinity of the receptor for the

endocytic apparatus (210, 362). All cell surface receptor-ligand complexes are assumed to be functionally active (322), except for those bound to the internalization component; as the association between the EGFR and the coated pit is presumed to be stabilized by phosphorylation of the coated pit protein, it is considered unlikely that an exogenous substrate could gain access to the catalytic domain of the EGFR within the cell surface ternary complex (322). Internalized receptor-ligand complexes, free receptors and ligand are localized within endosomal structures, wherein they are sorted to recycling or degradation processes (322).

A number of lines of investigation have subsequently confirmed many aspects of this model, and highlighted the role of receptor autophosphorylation in ligand-induced internalization. Ligand- and temperature-dependent binding of EGFR to coated pit adaptors has been observed *in vivo* (315), and requires the regulatory C-terminus of the receptor molecule, shown to be necessary for ligand-dependent endocytosis (241). It has also been established that association of the EGFR with adaptor protein (AP) 2, a major component of cell surface coated pits, requires tyrosine kinase activity (241). Receptor autophosphorylation appears to be necessary for internalization of the EGF-EGFR complex (316), but phosphorylated tyrosine residues of the receptor do not directly participate in adaptor protein binding; indeed, these proteins lack the requisite SH2 domains for binding to phosphotyrosine residues (241). Contrary to an inherent assumption in the model of EGFR internalization described above, it therefore seems unlikely that ternary complex formation blocks the access of exogenous substrates to the active site, as the mechanism for binding of the EGF-EGFR complex to adaptor proteins is likely to be different to that for association of the activated receptor kinase with effector molecules. The process of ligand-induced internalization requires endocytic codes, which correspond to sequences of 4-6 amino acids containing obligatory tyrosine or phenylalanine residues (52). Activation of the EGFR has therefore been proposed to cause an autophosphorylation-dependent conformational change that exposes concealed endocytic codes in the C-terminus (36), effectively releasing an inhibitory constraint (59, 316), and enabling specific interaction of the receptor-ligand complex with AP2 (241). Autophosphorylation has subsequently been demonstrated to significantly enhance adaptor protein binding, by increasing the affinity of the receptor for these proteins (241).

The multivalent binding of receptors to ligand and coated pit adaptor proteins can give rise to the typical Scatchard plot curvature exhibited by EGF-EGFR binding data, and hence apparent affinity heterogeneity (112). In cells that typically exhibit high surface receptor densities (A431, NIH-3T3), k_e decreases with receptor occupancy, eventually reaching a stable minimum (59, 349, 359). This is consistent with saturation of the endocytic mechanism (59, 359). Thus, high levels of occupied receptors may overload the component necessary for endocytosis (359). Under conditions where internalization is not impeded and the coated pit adaptor is not saturated, linear Scatchard plots are obtained. However, if saturation occurs as the ligand concentration increases, the Scatchard plot becomes non-linear (112). Two-step binding models can mimic either positive or negative cooperativity, depending upon the kinetic parameters (112): if the endocytic rate is much less than the rate of receptor-ligand dissociation ($k_e << k_d$), then saturation of the endocytic system occurs and apparent negative cooperativity is observed; however, if the rate of receptor-ligand dissociation is far slower than the endocytic rate ($k_d << k_e$), then apparent positive cooperativity is obtained. A qualitative change in the Scatchard plot can thus arise, without cooperativity of receptor binding and with no change in affinity for the ligand (112). Hence, saturation of the component that mediates ligand-induced internalization via the coated pit pathway, the adaptor proteins, may be responsible for the apparent emergence of multiple affinity classes of receptor (359).

Despite the majority of evidence favouring a multivalent two-step binding model for EGF-EGFR binding and internalization, Felder and colleagues (97) have raised a number of objections to such models, primarily citing reports that kinase activity is not necessary for ligand-induced internalization, but rather for normal intracellular trafficking (98, 148). However, these studies were carried out at high levels of receptor occupancy, which preclude discrimination between induced and constitutive internalization, as the latter can attain a significant net rate of endocytosis when the receptor number and ligand concentration are high (210). They have also argued that the endocytic apparatus is unlikely to be limiting, as the capacity for fibroblasts to internalize the transferrin receptor through coated pits is considerable, even when the receptor is overexpressed, although the saturable component may be specific for the occupancy-induced internalization of EGFR (359).

The most plausible alternative to a three-state model in which occupied receptors associate with coated pit adaptors, is a variant of this particular model in which the cell surface interaction molecule corresponds to a second receptor molecule (219). Hence, in accordance with an allosteric model of EGFR activation, ligand-induced dimerization of EGF receptors may account for the emergence of multiple affinity classes of receptors at high receptor occupancy (375). Equilibrium models for EGF-induced EGFR dimerization have been developed, in which the dimer is formed by two monomeric EGF-EGFR complexes and has a higher affinity for EGF than the monomer (199, 252, 309). However, these models predict that a Scatchard plot of equilibrium binding data will exhibit curvature characteristic of positive cooperativity (199, 219, 309), which is inconsistent with the majority of experimental observations (366). Thus, in order to account for the more typical negative curvature of the Scatchard plot, a model based upon negative cooperativity within the receptor dimer has been proposed, although this explanation was also found not to be entirely satisfactory (366). Hence, the current evidence appears to favour the association of receptor-ligand complexes with a coated pit interaction molecule as the basis for apparent negative cooperativity (219).

2.3.4 SUMMARY

A complete description of the first steps in the EGF signal transduction pathway is likely to include ligand-induced EGFR dimerization, which may facilitate tyrosine kinase activation and autophosphorylation as described in the preceding sections, but can be eliminated as the source of the affinity heterogeneity suggested by Scatchard analysis of EGF-EGFR equilibrium binding data. This conclusion would seem to argue against the allosteric model of EGFR activation, particularly as this model relies upon the emergence of high-affinity EGF binding sites at high receptor occupancy, which contradicts the majority of experimental data for intact cells. It is also interesting to note that direct measurement of the 'on' (k_f) and 'off' (k_r) rate constants for receptor-ligand binding have revealed that the increased affinity of solubilized EGFR dimers for EGF largely arises through a decrease in k_r (384), whereas high-affinity EGFR-EGF binding at the cell surface is characterized by an increase in k_f (13). Whilst it is still possible therefore that there is an intrinsic difference in EGF binding affinity between monomeric and dimeric EGFR, this is unlikely to constitute a source of affinity heterogeneity in intact cells, and is probably obscured within this environment by an

apparent reduction in receptor affinity at high receptor occupancy, resulting from the association of the activated EGFR with coated pit adaptor proteins. Ligand-induced autophosphorylation effects this interaction by revealing binding sites for the adaptor proteins on the EGFR C-terminus, in addition to enabling the association of the receptor with SH2 domain-containing effectors. Autophosphorylation therefore has an important dual function in mediating the cellular responses to EGF, and is effectively synonymous with EGFR tyrosine kinase activation. As discussed in the following section, this is the key event in the transduction of the extracellular signal, represented by EGF, to the cellular targets responsible for generating the mitogenic response (342).

2.4 MITOGENIC SIGNALLING THROUGH THE EGF RECEPTOR

2.4.1 RAS: A 'MOLECULAR SWITCH' IN GROWTH FACTOR SIGNAL TRANSDUCTION

The signal initiated at the plasma membrane by the activated EGFR is transmitted to the cytosolic MAPK cascade via the guanine-nucleotide binding protein, Ras (301). There are three, closely related, 21-kDa mammalian Ras proteins, denoted H-, K- and N-Ras. The activation state of these molecules is regulated by the bound GDP/GTP ratio; GTP-bound Ras is generally considered the form that is functionally active in signal transduction (85). Ras proteins undergo conformational changes in response to the successive binding of GDP and GTP. In the active GTP-bound conformation, Ras has the capacity to interact with effector molecules, and thereby transmit the signal downstream, whereas the inactive GDP-bound conformation specifically interacts with upstream regulators (294). Ras can hence be viewed as a molecular switch, which alternates between active and inactive states, in the control of proliferation and differentiation (294).

This cycling of Ras between active and inactive forms is not spontaneous, but is regulated within the cell by two classes of proteins, GTPase activating proteins (GAPs) and guanine-nucleotide exchange factors (GEFs). GAPs enhance the low intrinsic catalytic activity of Ras, and thereby act as negative regulators of Ras activation, whereas GEFs accelerate the inherently low rate of GDP-GTP substitution, and hence activate Ras (reviewed in ref. 85). The net cellular level of Ras activation is therefore determined by the relative activity of these factors. In the quiescent state, the majority of cellular Ras is present in the GDP-bound form (85), but this is rapidly converted to

the active form in response to RTK stimulation (294). An increase in the level of activated Ras could theoretically be brought about by a reduction in the activity of GAPs or an increase in GEF activity. Nevertheless, growth factor-induced activation of Ras is generally mediated by acceleration of GDP-GTP exchange, and therefore through the elevation of Ras GEF activity (31, 107, 202, 203, 225).

2.4.2 EGF-INDUCED RAS ACTIVATION

The signal transducing mechanism that links RTK and Ras GEF activation has been delineated in some detail, and is mediated by interactions between the activated receptor and a group of non-catalytic cytosolic proteins that contain SH2/Src homology 3 (SH3) domains. SH2 domains are modular components that bind specifically to phosphotyrosine residues, the specificity of the interaction being determined by the short linear sequences of residues adjoining the phosphotyrosine (66, 266); hence, the association of the RTK with SH2 domain-containing proteins is facilitated by receptor autophosphorylation. The role of SH3 domains in signal transduction is less well defined, although they are also involved in co-ordinating protein-protein interactions (reviewed in refs. 66, 266).

The principal component in the sequence of events leading to growth factor-induced Ras activation is the 'adaptor' protein, Grb2 (84). This molecule is the mammalian homologue of the nematode *Caenorhabditis elegans* Sem-5 and *Drosophila* Drk proteins; it is a short polypeptide with no intrinsic catalytic activity, consisting of a central SH2 domain flanked by two SH3 domains. The predominant function of Grb2 appears to be coupling other signalling molecules, in particular, activated RTKs with the Ras activator, SOS. Mammalian SOS proteins are homologous to *Drosophila* Son of sevenless, and function as GEFs for Ras (30, 54, 90). The N- and C-terminal SH3 domains of Grb2 bind cooperatively to proline-rich sequences in the C-terminus of SOS, and in the majority of cell-types, Grb2 and SOS form a constitutive complex (54, 204, 284), although this association has also been found to be inducible by EGF in Rat1 fibroblasts (30). The Grb2-SOS complex is found in the cytosol in quiescent cells, but is recruited to the plasma membrane upon EGF stimulation where it forms a stable complex with the activated EGFR (30), through binding of the Grb2 SH2 domain to the phosphotyrosine residues of the autophosphorylated receptor (209). The

association of SOS with membrane phosphoinositides, through an N-terminal pleckstrin homology (PH) domain, may also be involved in mediating the anchoring of SOS to the plasma membrane (21, 57, 85). These events are apparently responsible for activating SOS, and thereby for promoting nucleotide exchange on Ras, resulting in Ras activation (30, 54, 57, 107).

There are three possible mechanisms whereby the catalytic activity of SOS might be stimulated by complex formation (107, 204, 284). It is conceivable that the binding of Grb2-SOS to the EGFR might constitute a means for allosteric regulation of SOS activity, but association of the Grb2 SH2 domain with phosphotyrosine does not appear to induce a conformational change that could be transmitted to SOS (70). Another plausible mechanism is through the tyrosine phosphorylation of SOS by the activated EGFR, but although SOS possesses a number of consensus phosphorylation sites, there is little detectable phosphotyrosine (62). The possibility that appears to be the most consistent with the available data is that EGF-dependent translocation of cytosolic SOS to the plasma membrane, where Ras is localized, is sufficient to elevate GDP-GTP exchange activity, purely by bringing SOS into the vicinity of its substrate (30). No change in the intrinsic guanine-nucleotide exchange activity of SOS has been detected after EGF stimulation (30, 107), implying that GDP-GTP exchange on Ras is enhanced indirectly, by an increase in the local concentration of SOS, rather than by direct potentiation of SOS activity. Furthermore, theoretical analysis has substantiated claims that an increase in the effective concentration of SOS at the plasma membrane, through membrane localization, could be sufficient to increase the extent of the interaction between SOS and Ras, and thereby engender Ras activation (179). Support for this hypothesis is also provided by studies indicating that the artificial localization of SOS to the plasma membrane, through the insertion of direct membrane targeting sequences, is sufficient to stimulate Ras activation (9, 276). It should however, be noted that an enhancement of GEF activity in cell extracts following RTK activation has also been reported (202, 203).

This particular model for EGF-induced Ras activation is generally accepted, but Downward (85) has pointed out that it is largely based on analogy with the *Drosophila Sevenless* system, and that in other systems, the SOS pathway may not be the predominant means of activating Ras, or there may be alternative combinations of adaptors and exchange factors; for example, in a number of cell types, the adaptor

protein Shc has also been implicated in mitogenic signalling. This protein contains one SH2 domain, but no SH3 domains. Shc has been shown to be recruited to the plasma membrane and tyrosine phosphorylated in response to EGF, and to associate with the autophosphorylated EGFR via its SH2 domains (133, 268, 287). Furthermore, growth factor stimulation has been demonstrated to induce the association of Grb2-SOS with tyrosine phosphorylated Shc, via the SH2 domain of Grb2 (90, 285). Thus, the association of Grb2-SOS with the activated EGFR, via Shc, may constitute an alternative mechanism for activating Ras (273).

Although it seems that activated Ras may be involved in regulating several signal transduction cascades in mammalian cells (173), the critical mitogenic effector of Ras is the serine/threonine protein kinase, Raf (10).

2.4.3 THE ACTIVATION OF RAF

There are three mammalian Raf isoforms, with apparently non-redundant functions: A- and B-Raf, and (c-)Raf-1 (187). Raf-1 has a generalized role in cell growth and development, and as such, has been the most intensively studied isoform, whereas A- and B-Raf are involved predominantly in neurological development and have attracted far less attention.

Raf-1 contains two distinct N-terminal domains that mediate the GTP-dependent binding of Ras: the aptly termed Ras-binding domain (RBD) and a cysteine-rich domain (CRD) (29, 153). Direct physical association with Ras instigates Raf activation, through the recruitment of cytosolic Raf to the plasma membrane, where some additional factor stimulates Raf kinase activity (198, 328). Whereas the RBD is sufficient for the redistribution of cytosolic Raf to the plasma membrane, the CRD is also required for efficient Raf kinase activation (187). The nature of this secondary activation process is uncertain, but Ras evidently plays a direct role in Raf activation further to membrane recruitment (205, 230, 283, 333), as well as facilitating additional activation events.

One such event is likely to correspond to the phosphorylation of membrane-localized Raf, mediated by members of the Src family of tyrosine kinases, or protein kinase C (PKC) (201, 234). Both tyrosine (215) and serine (140) phosphorylated Raf-1 has been

detected in mammalian cells. Tyrosine phosphorylation has been shown to enhance Raf-1 kinase activity (94, 215), and may be essential for activation (80, 166), but since Src and activated Ras have synergistic roles in Raf-1 activation (215, 329), an additional Ras-mediated event is required for maximal activation. The role of serine phosphorylation is more ambiguous and whereas PKCα has been reported to phosphorylate and activate Raf-1 (188), serine phosphorylation by protein kinase A (PKA) is associated with the suppression of Raf-1 kinase activity (131). Recent reports have somewhat clarified the issue, by revealing that the phosphorylation of both Ser-338/339 and Tyr-340/341 contributes to maximal Raf-1 activation (81, 218), although phosphorylation at further, unidentified sites may also be involved (187). Conversely, the dephosphorylation of Ser-259, catalysed by protein phosphatase 2A (PP2A), is also required for Raf-1 activation (1), whilst PKA-mediated phosphorylation of Ser-43 reduces the affinity of Raf-1 for Ras-GTP and hence down-regulates Raf activity (367).

Although Raf phosphorylation is clearly an important regulatory feature, whether this process is directly responsible for Raf activation at the plasma membrane has yet to be resolved, and there is evidence for the involvement of additional activators, such as membrane phospholipids and lipid metabolites (37). An alternative proposal is that Raf dimerization may provide a means of activation (96, 211). The N-terminus of Raf-1 exerts an inhibitory influence on kinase activity (71), possibly by impeding the access of substrates to the catalytic C-terminus. By altering the conformation of Raf, dimerization could either release this inhibitory constraint, or promote autophosphorylation, and thereby enhance kinase activity. Furthermore, as Ras can spontaneously dimerize within an environment analogous to the plasma membrane (160), Raf dimerization, and thereby activation, could be induced by association with dimeric Ras (187). Dimerization has however, been found to be a relatively weak activator of Raf-1, and hence the physiological relevance of this process is unclear (234), although the binding of Ras to the CRD has been shown to alleviate Raf-1 autoinhibition (71).

The enigma of Raf kinase activation has been further complicated by the discovery that Raf-1 associates, within a multimeric complex, with a number of putative regulatory proteins (201, 234); for example, the phosphoserine binding protein family, 14-3-3, kinase suppressor of Ras (KSR), the 90 kDa heat-shock protein (Hsp90) and the adaptor protein, Cdc37. KSR and 14-3-3 may form a scaffolding complex that couples

Raf-1 to upstream activating kinases, such as PKC and Src, and to MEK, the downstream effector of Raf, whereas Hsp90 and Cdc37 act as chaperones that stabilize the tertiary structure of Raf, but may also link Raf-1 with upstream tyrosine kinases and with MEK (187).

It is therefore difficult to form an intelligible picture of the various contributing events, but a model of Raf-1 activation has recently been proposed that attempts to integrate the plethora of regulatory mechanisms that have been reported (187). In this model, dimeric 14-3-3 binds to phosphoserine-259/261 of Raf-1, stabilizing the inactive form of the kinase. Binding to Ras-GTP localizes Raf-1 to the plasma membrane, where Raf associates with PP2A, and destabilizes the interaction between 14-3-3 and phosphoserine-259; this facilitates the dephosphorylation of phosphoserine-259 and thereby releases 14-3-3 to recruit upstream activators, such as PKC and Src (187). Although attractive in its relative simplicity, this is unlikely to constitute a definitive model of Raf activation that is universally applicable, particularly given the observed differences in the response of the different Raf isozymes to growth factor stimulation; for example, whereas B-Raf is serine/threonine phosphorylated, it is not as extensively tyrosine phosphorylated as Raf-1 (166, 261, 326), since it lacks comparable regulatory tyrosine phosphorylation sites (166), and may be activated solely through interaction with Ras-GTP (187). The finer details of the actual physiological mechanism(s) in operation therefore remain obscure, but the activation of Raf is evidently initiated by Ras-dependent plasma membrane translocation, and constitutes the final link in a pathway that transmits the signal initiated at the cell surface by the activated EGFR, to the cytosolic MAPK cascade (10).

2.4.4 THE MAPK CASCADE

Raf is the first of a cascade of three cytosolic protein kinases that together represent a key functional unit in signal transduction. The only apparent function of Raf is to activate the 'dual-specificity' (threonine/tyrosine) kinase, MAPK/ERK kinase (MEK), which in turn seems to be the sole activator of the serine/threonine kinase, MAPK or extracellular signal-regulated kinase (ERK) (10, 38, 72, 233). In combination, Raf, MEK and ERK comprise just one example of a cytosolic MAPK module; there are at least three such cascades in mammalian systems (201), which are differentially activated in

response to growth factors, hormones, cytokines and other stimuli (110). This specificity is at least partly achieved through the co-ordination of kinase interactions by scaffolding or anchoring proteins. A candidate scaffold protein for the Raf/MEK/ERK cascade is KSR, which may increase the efficiency of signalling through the cascade by coupling MEK to upstream activators and downstream effectors, or possibly modulates the kinetics of cascade activation (187).

There are two isoforms of both MEK and ERK expressed in all mammalian cell types, the functional roles of which may be partially redundant (187); MEK1 and MEK2 are both 44-kDa enzymes, whereas ERK1 and ERK2 are 44- and 42-kDa isozymes (201). MEK family kinases are activated through phosphorylation at two regulatory serine residues within the sequence Ser-Met-Ala-Asn-Ser (123, 280, 383), catalysed by activated Raf (6). Although both isoforms of MEK are targets for B-Raf and Raf-1 *in vitro*, with Raf-1 catalysing the phosphorylation of both serine residues with equal efficiency, A-Raf does not activate MEK2 and stimulates a relatively weak activation of MEK *in vivo* (6, 123, 272, 369, 371). Phosphorylation of either serine residue is sufficient to at least partially activate MEK kinases (6, 123, 280). Activated MEK catalyses the phosphorylation of ERK at regulatory threonine and tyrosine residues within a conserved Thr-Glu-Tyr sequence; both isozymes of MEK display similar affinity for ERK1 and ERK2 (79), although MEK1 has a lower specific activity (382). However, the specialized adaptor protein, MEK partner 1 (MP1), links MEK1 specifically with ERK1 (187), and may thereby increase the efficiency of ERK1 activation by MEK1. Both MEK isoforms may also have greater specificity for tyrosine residues, as ERK threonine phosphorylation is preceded by tyrosine phosphorylation (137). Unlike MEK, the phosphorylation of both regulatory residues (tyrosine and threonine) is required for the activation of ERK (8).

Among the diverse substrates of ERK are nuclear transcription factors, such as c-Myc and c-Jun (38, 73, 201, 233). Clearly, in order to interact with these proteins, the migration of ERK into the nucleus is necessary, and has in fact been observed following growth factor stimulation (58, 339). The onset of this process is rapid, typically within 5-30 minutes of stimulation (depending on the cell type), and persists for several hours. The mechanism by which this translocation is achieved has yet to be conclusively determined, but could be facilitated by dimerization of phosphorylated ERK (64), and the kinetic characteristics of the process are consistent with active

uptake into the nucleus (201). In contrast, MEK apparently remains within the cytosol following growth factor stimulation, although there is evidence for a nuclear MEK export mechanism, implying that there is some movement of MEK into the nucleus (201).

Through the phosphorylation and activation of transcription factors, ERK may influence the expression of particular genes associated with cell growth and differentiation. In addition, ERK has the potential to regulate a number of other aspects of the mitogenic response, such as cytoskeletal reorganization, metabolic changes and the release of second messengers, through the phosphorylation of other cellular substrates, including the microtubule-associated protein, tau, ribosomal S6 kinases (Rsk) and cytosolic phospholipase A_2 ($cPLA_2$) (38, 73, 233). Rather than representing the culmination of the signal initiated at the cell surface by EGF, the activation of ERK therefore constitutes a branch-point at which this signal is deflected along a number of divergent pathways. The means by which the signal is transduced beyond ERK are however, not yet entirely understood, and although many putative substrates for ERK have been identified, whether these actually represent physiological targets remains to be established. It is clear however, that ERK occupies a central position in the regulation of a number of cellular processes.

2.4.5 SUMMARY

Activation of the EGFR-TK initiates the transfer of a mitogenic signal, from the plasma membrane to diverse cellular targets, via the small guanine-nucleotide binding protein, Ras, and a MAPK cascade formed by Raf, MEK and ERK protein kinases. The signal itself consists of a sequence of phosphorylation and protein-protein binding events, many of which facilitate the regulatory translocation of signalling intermediates. Thus, EGF apparently activates membrane-anchored Ras by inducing recruitment of the guanine-nucleotide exchange factor, SOS, to the plasma membrane, mediated by the association of SOS with the adaptors Grb2 and Shc, and the activated EGFR. Localization of SOS to the plasma membrane enhances GEF activity, and thereby accelerates GDP/GTP exchange on Ras, probably by increasing the local concentration of SOS and hence, the effective affinity of the Ras-GDP/SOS interaction.

The mechanism by which Raf is activated is less well defined, but also depends upon the translocation of Raf to the plasma membrane, induced by activated Ras, in addition to one or more phosphorylation steps. Finally, Raf is responsible for activating MEK, and thereby ERK, which represents a critical branch-point in the cascade; the efficiency of signalling through the MAPK cascade is possibly modulated by co-localization of the components through association with scaffolding proteins. Equally important, in regulating signal transmission, are the processes that terminate signalling along this pathway. Although less attention has paid to this aspect, the mechanisms involved in down-regulating EGF signal transduction through Ras, Raf, and ERK have begun to emerge.

2.5 DOWN-REGULATION OF EGF SIGNALLING

In the normal functioning of the cell, the signal instigated by EGF is generally transient; prolonged activation of many components of the EGF signal transduction pathway is frequently associated with a transformed phenotype. Down-regulation of EGF signalling occurs at multiple levels of the cascade and is achieved by a number of means, including both termination of the signal initiated by the EGFR, and inactivation of the individual components of the pathway (38).

2.5.1 THE FUNCTIONAL ROLE OF EGF-EGFR INTERNALIZATION

Until recently, the role of EGFR internalization in mitogenic signalling was inconclusive. Receptor down-regulation, or the loss of receptors from the cell surface through endocytosis and degradation, ensures that active complexes are removed and made unavailable for subsequent ligand binding. This process is generally considered to function as a physiological mechanism for modulating mitogenic signalling, and preventing unregulated cell proliferation (59, 356). The majority of the available experimental data are however, contradictory.

Several studies have indicated that receptor-mediated endocytosis does indeed attenuate EGFR signalling. Internalization, via the coated pit pathway, of an EGFR mutant truncated at residue 973 is significantly reduced (59, 356), presumably as this mutation prevents the receptor-ligand complexes from associating significantly with coated pit adaptor proteins (322). However, the truncated receptor retains a functional

tyrosine kinase domain, and cells transfected with the receptor respond mitogenically to EGF, implying that cell surface EGFR complexes are responsible for mitogenic signalling (59, 356). Nevertheless, conflicting evidence suggests that internalized receptor complexes are responsible for generation of the mitogenic signal (195, 238), and the majority of receptor-ligand complexes are, in fact, located intracellularly. Several studies have demonstrated that the internalized EGFR retains its association with EGF (193, 243, 318), ability to dimerize (314) and autophosphorylation status (243). The activation state of the internalized receptor in intact cells is however more controversial; whereas some evidence implies that the EGFR tyrosine kinase may be functionally inactive once internalized (98, 222), others have concluded that EGFR may still be active at the prelysosomal stage of cellular processing (105, 242, 243).

The role of internalization is therefore likely to be more complex than simple down-regulation of the mitogenic signal (242); for example, as the inhibition of endocytosis greatly increases the transforming potential of EGFR (356), internalization may provide feedback signals, allowing normal mitogenesis without cell transformation. A recent study has in fact clarified the possible functional significance of ligand-induced internalization, and demonstrates that whilst the internalized EGFR is capable of mitogenic signalling via activation of the small guanine-nucleotide binding protein, Ras, signalling through a divergent pathway, involving the activation of PLCγ, is attenuated by receptor internalization (134, 136). Hence, the purpose of ligand-induced EGFR internalization may be to selectively down-regulate particular signalling pathways activated by the occupied receptor, without affecting others.

Whilst it is evident that EGFR signalling is also modulated by other means, for example, through a negative feedback mechanism involving PLCγ-PKC (56), these aspects are beyond the scope of the project and will not be discussed further here. The reader is however, referred to reviews concerning the regulation of EGF signalling, through transmodulation by heterologous signalling pathways and heterodimerization, for further information (161, 231, 342).

2.5.2 ATTENUATION OF RAS SIGNALLING

EGF stimulation typically induces a rapid, but transient activation of Ras in many cell types. A number of possible mechanisms for the attenuation of signalling through Ras have been identified, perhaps reflecting the critical role of Ras in transmitting the signal to the MAPK cascade.

Upstream of Ras, the signal initiated by the EGFR is presumably down-regulated by dephosphorylation of phosphorylated RTK substrates, including Shc and the EGFR itself (183), catalysed by unspecified protein tyrosine phosphatases (PTPases). Candidate PTPases involved in this process include the SH2 domain-containing SHP-2, and a number of trans-membrane PTPases (38). The time course of EGFR substrate dephosphorylation has however, been shown not to correlate with that of Ras inactivation; EGF-induced tyrosine phosphorylation of the EGFR and Shc was found to persist after activated Ras had reverted to the inactive basal state (350). Hence, the specific termination of Ras signalling is probably attributable to some other mechanism.

The activity of cellular GAPs is likely to be involved in maintaining Ras in an inactive state in unstimulated cells, and also in restoring this state following growth factor stimulation (85). The prototypic GAP is a 120-kDa cytosolic protein containing a number of N-terminal SH2 and SH3 domains (220, 364). The SH2 domains mediate the association of GAP with activated RTKs (7, 172, 174), localizing the molecule to the plasma membrane, and *in vivo* tyrosine phosphorylation of GAP has been demonstrated in response to growth factor stimulation (92, 172). Since the affinity of GAP for Ras-GTP is comparatively low, and as both are expressed at low levels, it is reasonable to speculate that GAP might only act upon Ras when localized to the membrane (297). Furthermore, it seems that the SH2 domain-mediated interaction of GAP and the activated RTK may modulate the interaction of GAP with Ras (113), although tyrosine phosphorylation of GAP does not affect the catalytic activity (85). Moreover, only a fraction of cellular GAP has been shown to migrate to the plasma membrane in response to growth factor stimulation (85), and it seems unlikely that this is solely responsible for the rapid attenuation of Ras signalling, particularly as the association of GAP with the EGFR has been reported to only marginally suppress GAP activity (305).

In fact, growth factor-induced Ras activation appears to be down-regulated, and desensitized, primarily through the negative feedback phosphorylation of SOS. The activation of the MAPK cascade, by a number of growth factors, has been shown to result in feedback serine/threonine phosphorylation of SOS, causing dissociation of the Shc-Grb2-SOS complex (55, 61, 76, 194, 269, 286, 351). Although one study reported EGF-induced dissociation of Grb2 and SOS (194), others have not observed any change in the status of the Grb2-SOS complex (146, 183, 269, 286), rather, inactivation of Ras following EGF stimulation has been suggested to result from dissociation of the Grb2-SOS complex from Shc, or the EGFR (146, 183, 269, 286). This is consistent with an observed decrease in the affinity of Grb2-SOS for tyrosine phosphorylated EGFR and Shc, following SOS phosphorylation (32, 286). The feedback phosphorylation of SOS has been demonstrated to correlate with the rapid deactivation of Ras (194), and is generally attributed to ERK (34, 62), although downstream targets of ERK, such as p90 Rsk-2, have also been implicated (83, 145). Other evidence suggests that the kinase responsible for feedback SOS phosphorylation varies with the identity of the cell surface receptor, and that the fate of the Grb2-SOS complex depends upon the site of phosphorylation, which may explain the observation that activation of the Raf/MEK/ERK cascade is not always required or sufficient to induce SOS phosphorylation (184, 381).

2.5.3 REGULATION OF THE RAF/MEK/ERK CASCADE

The overall activity of the Raf/MEK/ERK cascade is a function of the relative activities of upstream activators of these kinases and the protein phosphatases that dephosphorylate, and hence deactivate them. Since ERK must be phosphorylated on both a regulatory threonine and a tyrosine residue in order to be catalytically active (8), dephosphorylation of either residue is sufficient to deactivate the enzyme, whereas dephosphorylation of both regulatory serine residues is required for the inactivation of MEK (6, 123). As the activation status of Raf may also be regulated by phosphorylation, it is likely that the inactivation of Raf is also mediated by dephosphorylation (80). Up to three classes of phosphatase are possibly involved in regulating the activity of MEK, ERK, and Raf: serine/threonine specific and 'dual-specificity' (threonine/tyrosine) phosphatases (DSPs), and PTPases (201). Although the identity of the enzymes that are physiologically relevant has yet to be confirmed, there are a number of likely candidates.

Several of these are structurally related members of the DSP family, specifically termed MAPK phosphatases (MKPs), which can be further sub-divided according to their sub-cellular location: those that are localized within the nucleus, such as MKP-1 and -2, and cytosolic MKPs, for example MKP-3 and -4 (175, 201). Although these enzymes have been shown to inactivate ERK both *in vitro* and *in vivo* (201), implying that they are involved in the down-regulation of growth-factor stimulated ERK activation, their role in mammalian systems is unclear, but may vary with the particular cell type (175, 228). Cytosolic MKPs are expressed in a limited number of cell types, are not inducible by mitogens (128, 235, 236), and may regulate the activity of ERK within the cytosol. In contrast, nuclear MKPs are immediate early gene products, induced by stress and growth factors, and not expressed in quiescent cells. Although nuclear MKP expression generally correlates with ERK inactivation, in many cells the latter occurs within 15-20 minutes, and is not blocked by protein synthesis inhibitors (5, 50, 368). Mitogen-induced MKPs are therefore unlikely to play a major role in the rapid deactivation of ERK, but since they are induced by ERK activation, and not normally evident until 30-60 minutes after growth factor stimulation, may be involved in the negative feedback regulation of ERK following translocation to the nucleus (175, 201, 337).

Serine/threonine specific phosphatases, in particular cytosolic PP2A, have long been implicated in the regulation of MAPK cascades, and may have multiple targets within the cascade; PP2A has been reported to form a stable complex with, and to dephosphorylate, Raf-1 (228), and to dephosphorylate and inactivate MEK and ERK *in vitro* (8, 119). Furthermore, PP2A-specific inhibitors have been shown to activate ERK *in vivo* (124, 138). In fact, convincing evidence has been presented that PP2A is the key phosphatase responsible for the rapid inactivation of both MEK and ERK following growth factor stimulation in a number of mammalian cell types (5, 50). PP2A is proposed to act in conjunction with an unspecified PTPase that dephosphorylates the regulatory tyrosine residue of ERK, with PP2A-catalysed threonine dephosphorylation reputedly being the 'rate-limiting' step for ERK inactivation (5). The role of the PTPase has been suggested to be played by *vaccinia* H1-related phosphatase (VHR) (337). This enzyme is constitutively expressed and confined to the nucleus, and hence not likely to be immediately involved in the rapid deactivation of ERK, but may participate in maintaining ERK in an inactive state in quiescent cells.

2.5.4 SUMMARY

A number of mechanisms operate concurrently to attenuate the signal initiated by EGF and transmitted via the EGFR and Ras to the Raf/MEK/ERK cascade. The signal is terminated by feedback phosphorylation of SOS, catalysed by ERK or some other MEK-dependent kinase, which results in the dissociation of EGFR-Shc-Grb2-SOS signalling complexes and diminishes SOS GEF activity towards Ras. The basal activation state of Ras is recovered through the activity of GAPs, whilst the other components of the pathway are down-regulated by dephosphorylation. Cytosolic PP2A appears to be the predominant phosphatase involved in the rapid deactivation of Raf, MEK and ERK, although specific MKPs may also be involved in the long-term suppression of ERK activity. In addition, recent evidence suggests that Raf-1 is the target of feedback inhibition, although the nature of this regulatory mechanism is not known (187). Finally, neither EGFR internalization, nor dephosphorylation of the EGFR substrates, seem to play a part in the rapid dissolution of the signal, although they are likely to be important for longer-term desensitization of the system.

CHAPTER 3

DEVELOPMENT OF A COMPUTER SIMULATION OF THE EGF SIGNAL TRANSDUCTION PATHWAY

3.1 INTRODUCTION

A detailed kinetic model of the EGF signal transduction pathway has been developed, describing the sequence of events that links ligand-induced activation of the EGF receptor at the cell surface with activation of the cytosolic Raf/MEK/ERK phosphorylation cascade, and incorporating much of the data discussed in the previous chapter. A specification of the completed model, and the means by which this has been implemented as a computer simulation, are presented in the initial section of this chapter, whilst the subsequent sections provide a discursive account of the model development process.

3.2 SPECIFICATION OF A COMPUTER SIMULATION OF EGF SIGNAL TRANSDUCTION

3.2.1 MODEL DESCRIPTION

A schematic representation of the model is provided in Figure 3.1 below; this specifically depicts the signalling cascade initiated by the treatment of PC12 cells with EGF. The first step is the binding of EGF (L in the reaction scheme) to the monomeric cell surface EGFR (R_s), to form a receptor-ligand complex (RL) (199). After ligand binding, RL complexes associate to yield the $R2L2_s$ dimer (199, 309). Activation of the intrinsic protein tyrosine kinase occurs simultaneously with dimerization (39).

Only the active $R2L2_s$ species is internalized via a ligand-induced pathway (210), through binding to cell surface coated pit adaptor proteins (CPP). Internalization of $R2L2_s$ yields an intracellular dimeric species ($R2L2_i$), which rapidly dissociates to form the monomeric species (R_i).

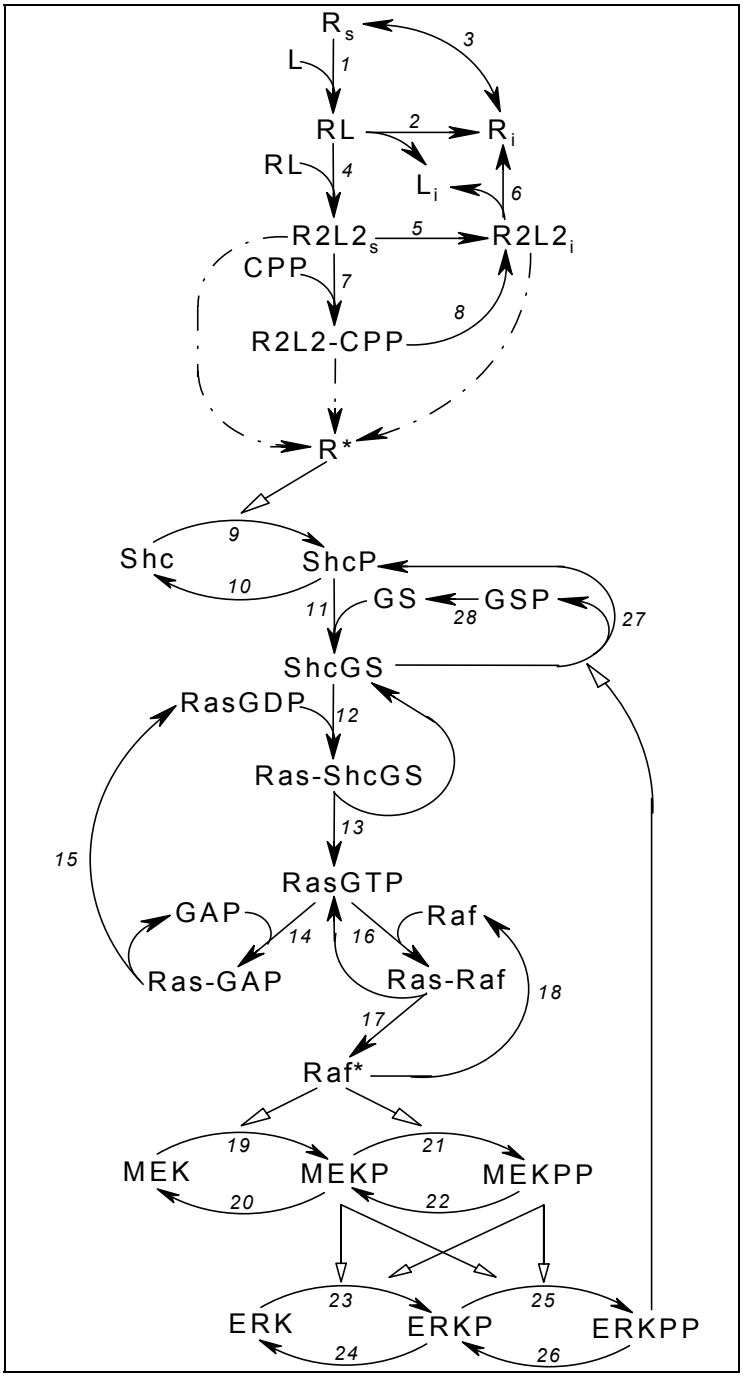

Figure 3.1 Reaction scheme for the kinetic model of the EGF signal transduction pathway

R_s, free cell surface receptor; L, ligand; RL, cell surface receptor-ligand complex; $R2L2_s$, cell surface dimeric receptor-ligand complex; CPP, coated pit protein; R2L2-CPP, receptor-ligand-coated pit protein complex; $R2L2_i$, internal dimeric receptor-ligand complex; R_i, internal receptor; L_i, internal ligand; R*, generic term denoting all active species of receptor (R2L2, R2L2-CPP and $R2L2_i$), introduced for ease of illustration, although all active species are modelled as separate entities; Shc, Src homology and collagen domain protein; GS, complex formed by Grb2, growth factor receptor binding protein 2 and SOS, Son of sevenless homologue protein; ShcGS, complex formed by Shc and GS; Ras-GDP, inactive, GDP-bound Ras; Ras-ShcGS, complex formed by Ras-GDP and ShcGS; Ras-GTP, active, GTP-bound Ras; GAP, Ras GTPase activating protein; MEKP and MEKPP phosphorylated MEK species; ERKP and ERKPP phosphorylated ERK species; GSP, phosphorylated GS. Filled arrowheads denote protein-protein binding, or the conversion of a signalling intermediate from one form to another, whereas unfilled arrowheads indicate catalytic interactions. The numbering of the reactions is arbitrary.

Inactive R_s and RL complexes are internalized through a constitutive mechanism (210), as are $R2L2_s$ complexes not associated with coated pits. Once internalized, the ligand dissociates from the receptor (L_i) and is subsequently degraded. Internalized R_i is then recycled to the cell surface.

Activated receptors ($R2L2_s$, $R2L2_i$ and R2L2-CPP) catalyse the tyrosine phosphorylation of the adaptor protein, Shc (268), yielding ShcP, which then associates with a constitutive complex (GS), formed by the adaptor protein, Grb2, and the guanine-nucleotide exchange factor, SOS (54, 204, 284) to form the ternary complex, ShcGS (90, 285). It is assumed that only uncomplexed ShcP may be dephosphorylated by cellular PTPases (291). Formation of ShcGS recruits SOS to the plasma membrane where Ras is localized (90). Interaction of Ras-GDP with ShcGS forms a Ras-ShcGS complex, and enables SOS to stimulate the conversion of inactive Ras-GDP to active Ras-GTP (90).

Ras-GTP may bind to GAP, yielding a Ras-GAP complex and stimulating the intrinsic GTPase activity of Ras, so that Ras-GTP is converted to Ras-GDP (220). Alternatively, Ras-GTP may bind to Raf to generate the Ras-Raf complex. This recruits Raf to the plasma membrane and facilitates Raf kinase activation (216); the latter is associated with growth factor-induced serine/threonine phosphorylation of Raf (261, 326).

Activated Raf* catalyses the phosphorylation of two MEK serine residues; both MEKP and MEKPP are catalytically active (6). MEKP and MEKPP activate ERK by catalysing the phosphorylation of a tyrosine and a threonine residue, but only ERKPP is active (8). Dephosphorylation of Raf*, MEKP, MEKPP and ERKPP is catalysed by the same serine/threonine phosphatase, PP2A, however, ERKP/ERKPP is also dephosphorylated by a currently unidentified PTPase (228). Feedback regulation of the pathway is mediated by the inhibitory serine/threonine phosphorylation of SOS, catalysed by ERKPP, resulting in dissociation of the Shc-GS complex to yield ShcP and GSP (85). GS is regenerated by dephosphorylation.

For ease of reference, a copy of Figure 3.1, which can be folded out to accompany the text in later sections of the thesis, is supplied in Appendix I.

3.2.2 IMPLEMENTATION OF THE MODEL AS A COMPUTER SIMULATION

3.2.2.1 Derivation of kinetic equations

The model described above has been implemented using the public domain biochemical kinetics simulation software packages, Gepasi 3.2 (226, 227) and SCAMP (295). The user defines the simulation in terms of the signalling components and interactions shown in the reaction scheme (Figure 3.1), and specifies the appropriate rate equations and kinetic constants for these events. From this data, the software derives a system of differential equations, termed kinetic or balance equations, which describe the change in the concentrations of the signalling intermediates over time. For any given component of the system, the rate of change of the concentration is given by the total rate of production (that is, the sum of the net rates of the reactions that generate the component), minus the total rate of consumption. A summary of the set of kinetic equations describing the dynamics of the model is provided in Table 3.1.

3.2.2.2 Moiety conservation equations

Since the simulation is intended to represent the operation of the EGF signalling system over a relatively short time scale (of the order of tens of minutes, rather than hours), cellular processes that influence the absolute concentrations of signalling molecules over a longer time scale, such as protein synthesis, are beyond the scope of the model. The total concentrations of a number of protein moieties are therefore considered to be at an effective steady state, and hence assumed to remain constant throughout the simulated time period (141). The appropriate moiety conservation equations are given in Table 3.2.

3.2.2.3 Rate equations

The majority of the enzyme-catalysed reactions represented in the model follow Michaelis-Menten kinetics, with the rate of the reaction given by an equation of the form: V_{max} [S]/(K_m + [S]), where V_{max} = maximal enzyme rate, K_m = Michaelis constant and [S] = concentration of substrate.

Table 3.1 Kinetic equations comprising the mathematical model of the EGF signal transduction pathway, illustrated in Figure 3.1

v_n corresponds to the net rate of reaction number, n, of the reaction scheme given in Figure 3.1.

$d[L]/dt = -v_1$
$d[R_s]/dt = v_3 - v_1$
$d[RL]/dt = v_1 - v_2 - v_4$
$d[R_i]/dt = v_2 + v_6 - v_3$
$d[L_i]/dt = v_2 + v_6$
$d[R2L2_s]/dt = v_4 - v_5 - v_7$
$d[R2L2_i]/dt = v_5 + v_8 - v_6$
$d[R2L2\text{-}CPP] = v_7 - v_8$
$d[Shc]/dt = v_{10} - v_9$
$d[ShcP]dt = v_9 - v_{10}$
$d[GS]/dt = v_{28} - v_{11}$
$d[GSP]/dt = v_{27} - v_{28}$
$d[ShcGS]/dt = v_{11} + v_{13} - v_{12} - v_{27}$
$d[Ras\text{-}GDP]/dt = v_{15} - v_{12}$
$d[Ras\text{-}ShcGS]/dt = v_{12} - v_{13}$
$d[Ras\text{-}GTP]/dt = v_{13} + v_{17} - v_{14} - v_{16}$
$d[GAP]/dt = v_{15} - v_{14}$
$d[Raf]/dt = v_{18} - v_{16} - v_{17}$
$d[Ras\text{-}GAP]/dt = v_{14} - v_{15}$
$d[Ras\text{-}Raf]/dt = v_{16} - v_{17}$
$d[Raf^*]/dt = v_{17} - v_{18}$
$d[MEK]/dt = v_{20} - v_{19}$
$d[MEKP]/dt = v_{19} + v_{22} - v_{20} - v_{21}$
$d[MEKPP]/dt = v_{21} - v_{22}$
$d[ERK]/dt = v_{24} - v_{23}$
$d[ERKP]/dt = v_{23} + v_{26} - v_{24} - v_{25}$
$d[ERKPP]/dt = v_{25} - v_{26}$

Table 3.2 Moiety conservation equations for the model of EGF signal transduction

$[R]_{Total} = [R_s] + [RL] + 2[R2L2_s] + 2[R2L2\text{-}CPP] + 2[R2L2_i] + R_i$
$[Shc]_{Total} = [Shc] + [ShcP] + [ShcGS] + [Ras\text{-}ShcGS]$
$[GS]_{Total} = [GS] + [GSP] + [ShcGS] + [Ras\text{-}ShcGS]$
$[Ras]_{Total} = [Ras\text{-}GDP] + [Ras\text{-}ShcGS] + [Ras\text{-}GTP] + [Ras\text{-}GAP] + [Ras\text{-}Raf]$
$[GAP]_{Total} = [GAP] + [Ras\text{-}GAP]$
$[Raf]_{Total} = [Raf] + [Ras\text{-}Raf] + [Raf^*]$
$[MEK]_{Total} = [MEK] + [MEKP] + [MEKPP]$
$[ERK]_{Total} = [ERK] + [ERKP] + [ERKPP]$

V_{max} is used when the enzyme concentration is fixed, i.e. where the enzyme is not an integral part of the system (such as PP2A or PTPase), but when the enzyme is also a model variable (for example, ERK), V_{max} is given by $[E]_t \times k_{cat}$, where $[E]_t$ = enzyme concentration at time, t, and k_{cat} = specific activity. Although it is important to consider the reversibility of enzyme-catalysed reactions and product inhibition in the construction of a metabolic model, this is not crucial for this particular model of signal transfer, where each enzymatic process is directly linked to an opposing reaction.

The Michaelis-Menten equation is not used to represent the activation of guanine-nucleotide exchange on Ras, catalysed by SOS (Figure 3.1, reactions 12 and 13), or Ras GTP hydrolysis, catalysed by GAP (Figure 3.1, reactions 14 and 15). Rather, these processes are modelled explicitly as two successive reactions, an initial enzyme-substrate binding equilibrium, where $K_m \approx$ equilibrium dissociation constant, K_d, and subsequent irreversible enzyme-product dissociation, equivalent to the catalytic step, where k = enzyme specific activity, k_{cat}.

The rates of production and consumption of ATP are assumed to be balanced, and hence the cellular ATP:ADP ratio is regarded as constant (144); furthermore, the reported K_m values of the protein kinases for ATP are much lower than [ATP] (104, 214, 270, 274, 281, 290). The rate equations for these reactions therefore simplify to a single-substrate formulation. Similarly, the cellular GTP:GDP ratio is considered constant, and [GTP] is much greater than the K_m value of SOS for GTP (132). Hence, [GTP] is not limiting for the guanine-nucleotide exchange reaction, which is therefore modelled as a first-order process.

All other reactions are represented by mass-action kinetics, with the rate of the reaction given by an expression of the form k_f [A][B] - k_r [C][D], where k_f = forward rate constant, k_r = reverse rate constant, [A] and [B] are the reactant concentrations, [C] and [D] are the product concentrations, and K_d is given by k_r/k_f.

In order to account for steps corresponding to the intracellular processing of internalized receptor-ligand complexes, which are not explicitly included in the model, the rate of receptor internalization (Figure 3.1, steps 2, 5 and 8), as well as the subsequent ligand dissociation (Figure 3.1, step 6) and receptor recycling steps (Figure 3.1, step 3), are modified by a time delay factor of the form:

$$d(t) = \varepsilon + (1 - \varepsilon)\,[1 - e^{-(t/\Delta T)^3}].$$

The internalization rate constant therefore becomes a function of time of the type $k(t) = kd(t)$, where εk = rate constant before addition of ligand, k = steady state rate constant after the addition of ligand, and ΔT = time delay (112). Where the process involves cell surface receptor species (Figure 3.1, steps 2, 3, 5 and 8), the rate of the reaction is further modified by a factor, f, representing the fraction of receptors located within cell surface endocytic structures (112). The number of coated pit adaptor proteins is assumed to remain effectively constant over the simulated time period, and is thus accounted for in the rate constant governing the association of activated receptors with coated pit proteins (Figure 3.1, step 7; ref. 112).

3.2.2.4 Units and values of simulation parameters

The initial concentrations of signalling molecules, and the values assigned to the appropriate rate constants, are given in Table 3.3. Signalling intermediates not listed in the table are assumed to have an initial concentration of zero.

Inspection of the kinetic equations listed in Table 3.1 indicates that EGF (L) is consumed by the system, whereas internalized ligand (L_i) is produced. In order to represent a thermodynamically open system and, at least in principle, enable the attainment of a steady state, the concentrations of these molecules are regarded as system parameters, and are therefore fixed at a constant value throughout the simulation (144). All other concentrations are regarded as variables of the system that evolve over the simulated time period, in accordance with the kinetic equations shown above in Table 3.1.

The rates of the individual reactions and maximal enzyme rates (V_{max}) are expressed in units of molecule cell^{-1} minute^{-1}. Concentrations of signalling intermediates and Michaelis constants (K_m) are given in molecule cell^{-1}. First- and second-order rate constants are expressed in units of minute^{-1} and molecule^{-1} minute^{-1} respectively, except the forward rate constant for ligand binding, which is expressed in M^{-1} minute^{-1}; as this reaction occurs at the cell surface, [EGF] is given in nM.

Table 3.3 Parameter values for the EGF signal transduction model

k_n corresponds to the first- or second-order rate constant, for reaction number, n, of the reaction scheme given in Figure 3.1; V_n is the maximal enzyme rate and K_{mn} the corresponding Michaelis constant. Where possible, the values listed are specific for PC12 cells.

Reaction	Parameter values	Reference
1	$[L] = 1.0 \times 10^2$; $[R]_{Total} = 1.5 \times 10^4$; $[R_s] = 1.11 \times 10^4$; $[R_i] = 3.9 \times 10^3$; $k_1 = 3.8 \times 10^8$; $k_{-1} = 0.73$	(112, 157, 185, 239, 245, 340, 348, 360)[a]
2	$k_2 = 0.70$; f = 0.20; $\varepsilon = 0.12$; $\Delta T = 6.5$	(112)
3	$k_3 = 4.84 \times 10^{-2}$; $k_{-3} = 0.70$; f = 0.20; $\varepsilon = 0.12$; $\Delta T = 6.5$	(112)
4	$k_4 = 1.383 \times 10^{-3}$	(39, 143, 199)[b]
5	$k_5 = 0.35$; f = 0.20; $\varepsilon = 0.12$; $\Delta T = 6.5$	(112)[c]
6	$k_6 = 0.35$; $\varepsilon = 0.12$; $\Delta T = 6.5$	(112)
7	$k_7 = 1.0$; $k_{-7} = 3.47 \times 10^{-4}$; f = 0.20	(112)
8	$k_8 = 0.35$; $\varepsilon = 0.12$; $\Delta T = 6.5$	(112)
9	$[Shc] = 3.0 \times 10^4$ [d]; $k_9 = 12$; $K_{m9} = 6.0 \times 10^3$	(135, 257)
10	$V_{10} = 3.0 \times 10^5$; $K_{m10} = 6.0 \times 10^3$	(17, 27, 177)[c]
11	$[GS] = 2.0 \times 10^4$ [a]; $k_{11} = 2.0 \times 10^{-3}$; $k_{-11} = 3.8$	(63, 135)
12	$[Ras\text{-}GDP]_0 = 1.98 \times 10^4$; $[Ras\text{-}GTP]_0 = 2.0 \times 10^2$; $k_{12} = 1.63 \times 10^{-2}$; $k_{-12} = 10$	(102, 163, 200, 237, 260, 275)[d]
13	$k_{13} = 15$	(163, 200, 260)[d]
14	$[GAP] = 1.5 \times 10^4$ [a]; $k_{14} = 5.0 \times 10^{-3}$; $k_{-14} = 60$	(28, 135)[c]
15	$k_{15} = 7.2 \times 10^2$	(2, 113, 247)[c]
16	$[Raf] = 1.0 \times 10^4$; $k_{16} = 1.2 \times 10^{-3}$; $k_{-16} = 3.0$	(19, 102, 331)[c]
17	$k_{17} = 27$	(17, 177)[c]
18	$V_{18} = 9.7 \times 10^4$; $K_{m18} = 6.0 \times 10^3$	(17, 27, 155, 177)[c]
19	$[MEK] = 3.6 \times 10^5$; $k_{19} = 50$; $K_{m19} = 9 \times 10^3$	(17, 102, 104, 155, 177, 214, 216, 264)[c]
20	$V_{20} = 9.2 \times 10^5$; $K_{m20} = 6.0 \times 10^5$	(17, 27, 155, 177)[c]
21	$k_{21} = 50$; $K_{m21} = 9.0 \times 10^3$	(17, 104, 155, 177, 214, 216, 264)[c]
22	$V_{22} = 9.2 \times 10^5$; $K_{m22} = 6.0 \times 10^5$	(17, 27, 155, 177)[c]
23	$[ERK] = 7.5 \times 10^5$; $k_{23} = 8.3$; $K_{m23} = 9.0 \times 10^4$	(17, 102, 137, 155, 177)[c]
24	$V_{24} = 2.0 \times 10^5$; $K_{m24} = 6.0 \times 10^5$	(17, 27, 155, 177)[c]
25	$k_{25} = 8.3$; $K_{m25} = 9.0 \times 10^4$	(17, 137, 155, 177)[c]
26	$V_{26} = 4.0 \times 10^5$; $K_{m26} = 6.0 \times 10^5$	(17, 27, 155, 177)[c]
27	$k_{27} = 1.6$; $K_{m27} = 6.0 \times 10^5$	(177, 274, 281)[c]
28	$V_{28} = 75$; $K_{m28} = 2.0 \times 10^4$	(17, 27, 155, 177)[c]

[a] The value specified for k_1 was determined from the reported K_d (157) and assumed k_{-1} (see section 3.3.1.5), and is consistent with the range of typical values reported for this parameter (185, 239, 348, 360).

[b] Dimerization is assumed to be effectively irreversible (39); k_4 was derived from the estimated association constant, K_a, for dimerization (199), with an upper limit being determined by the number of receptor-receptor collisions sec^{-1} (143).

[c] The values assigned to the parameters are consistent with a range of measured or estimated values given in the literature.

[d] No estimates specific for SOS are available, but the values assigned to the parameters are consistent with those reported for the mammalian homologue of the yeast CDC25 protein, Ras-GRF.

3.3 METHODOLOGY AND EVALUATION

For the purposes of model development, the EGF signal transduction pathway depicted in Figure 3.1 was divided into three conceptual sub-systems, or 'modules'. These components correspond to sub-cellular locations within which defined groups of signalling events are presumed to take place. Hence, the 'top-level' module constitutes a self-contained model of EGF-induced EGFR activation at the cell surface, whilst the 'bottom-level' component represents the activation of the cytosolic MAPK cascade formed by Raf, MEK and ERK protein kinases, mediated by activated Ras. These two sections are linked by an 'intermediate' module comprising a sequence of signalling events occurring at the plasma membrane, beginning with phosphorylation of the adaptor protein, Shc, by the activated EGFR, and formation of a complex between phosphorylated Shc, Grb2 and SOS, and terminating with activation of the guanine-nucleotide binding protein, Ras. The individual components were developed successively, and coupled in turn to the preceding module(s), to ultimately form the complete simulation. In addition, a negative feedback interaction between the MAPK cascade and the intermediate, Ras activation module was incorporated. Figure 3.2 provides an illustration of the modular nature of the simulation.

Each module is bounded by signalling events for which experimental data are readily available, enabling validation of the model at three landmark stages of development. The methodology employed in composing each module, as well as the steps taken to assess the validity of the simulation at each stage of its evolution, are discussed in detail in the following sections. Where appropriate, an account of the use of the simulation as a tool for evaluating various models of EGF signal transduction is also given.

3.3.1 THE 'TOP-LEVEL' MODULE: EGFR ACTIVATION AND INTERNALIZATION

Although experimental evidence clearly demonstrates a link between EGFR dimerization, activation and high-affinity ligand binding, this remains somewhat controversial, as made apparent in the preceding chapter. However, the account also reflected an attempt to reconcile the many, apparently conflicting models describing EGF-EGFR interaction at the cell surface, and to thereby derive a coherent model of this key signalling event, as illustrated by Figure 3.3 below. This 'integrated' model specifically describes the binding of EGF to the EGFR, EGF-EGFR aggregation,

RTK activation, autophosphorylation and subsequent internalization through the coated pit pathway, and has been realized as the top-level component of the simulation. A mathematical model describing the EGF-EGFR endocytic pathway in Balb/c 3T3 cells, developed by Gex-Fabry and DeLisi (112), was selected to form the structural basis of the top-level module, since it embodies several fundamental features of the integrated model: receptor-ligand binding and internalization, through both the constitutive and ligand-induced (coated pit) pathways, as shown in Figure 3.4 below.

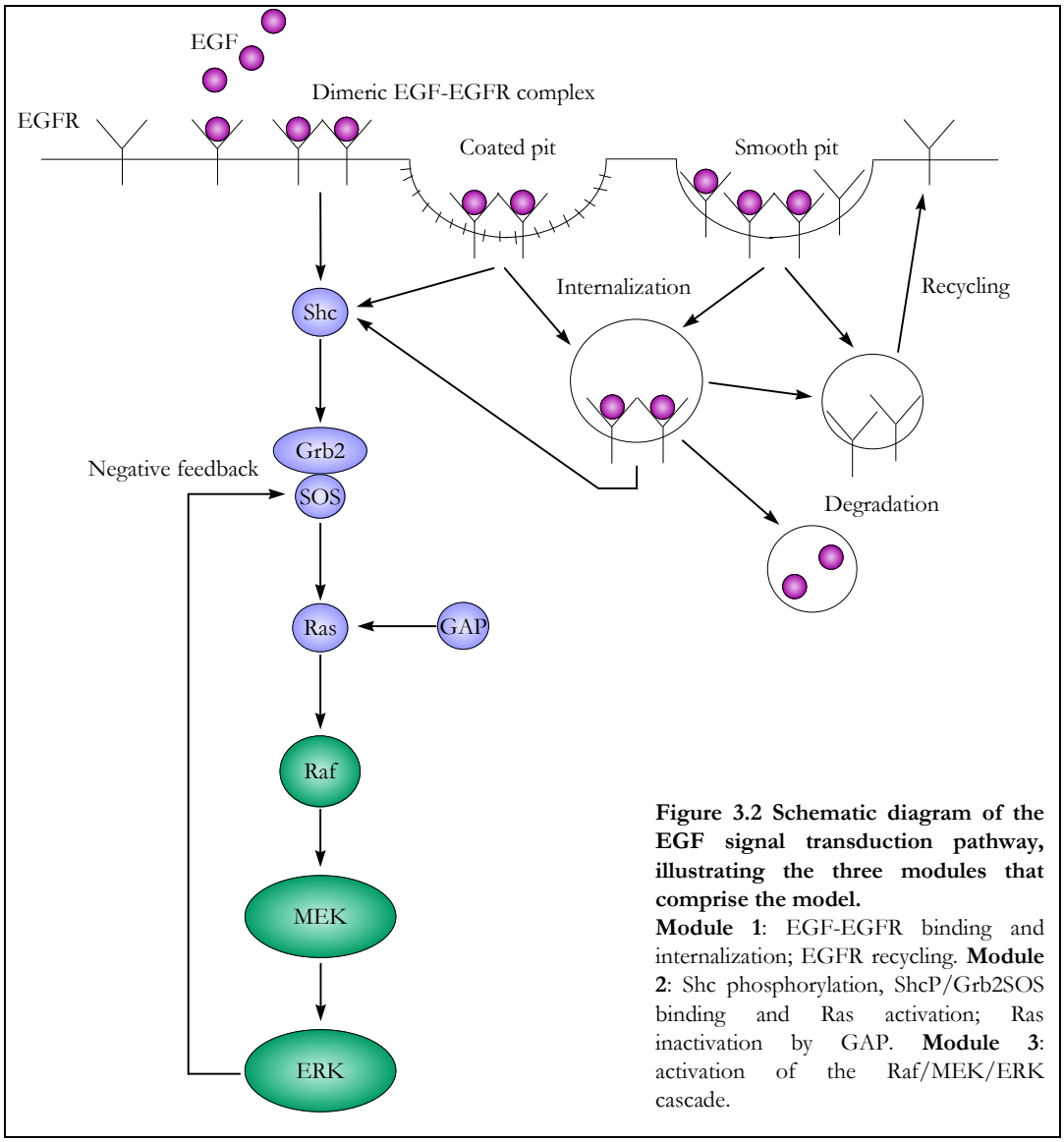

Figure 3.2 Schematic diagram of the EGF signal transduction pathway, illustrating the three modules that comprise the model.
Module 1: EGF-EGFR binding and internalization; EGFR recycling. **Module 2**: Shc phosphorylation, ShcP/Grb2SOS binding and Ras activation; Ras inactivation by GAP. **Module 3**: activation of the Raf/MEK/ERK cascade.

Figure 3.3 Contrasting conceptual models of EGF-induced EGFR activation and internalization

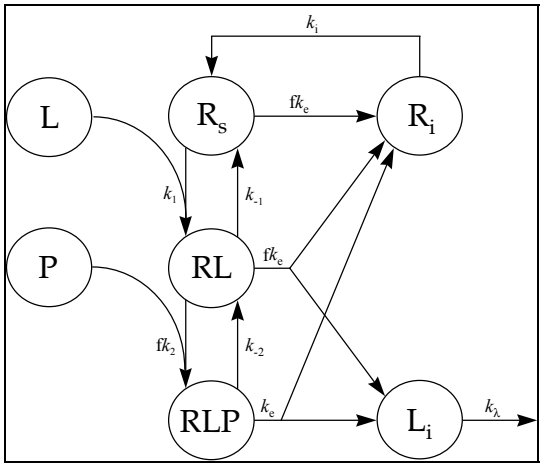

Figure 3.4 Gex-Fabry and DeLisi's (112) model of the EGFR endocytic pathway
L, free ligand; R_s, free surface receptor; RL, surface receptor-ligand complex; P, free coated pit protein; RLP, receptor-ligand-coated pit protein complex; R_i, internal receptor; L_i, internalized ligand; f, fraction of receptors in coated pits; k_e, endocytic rate constant; k_i, internalization constant; k_λ, rate constant for ligand degradation.

Events that are not taken into account in this scheme include receptor aggregation, autophosphorylation and activation; neither is their impact on the internalization process considered. This outline model was therefore modified to include both ligand-induced receptor dimerization and activation; the resulting simulation was subsequently employed in evaluating the principal models for these processes, in order to determine which is the most consistent with published experimental observations.

3.3.1.1 EGF-induced EGFR dimerization

The reactions shown in Figure 3.5 below depict the ligand binding and receptor aggregation equilibria that are possible when oligomerization is confined to the formation of receptor dimers (199, 366).

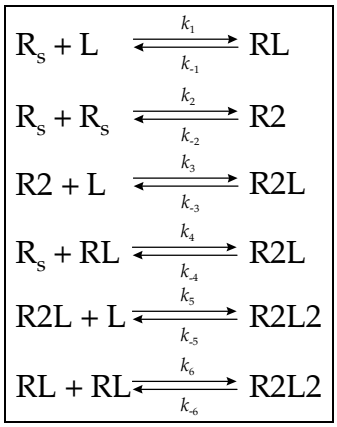

Figure 3.5 Possible binding and aggregation reactions in a receptor dimerization scheme (199, 366)
R2, receptor dimer; R2L, R2L2, ligand-dimer complexes.

A number of lines of experimental evidence suggest that in order to adequately model EGFR dimerization and consequent RTK activation, it is only necessary to introduce a step representing dimer formation into the model, and that the remaining reactions shown in Figure 3.5 (reactions 2 to 5) can reasonably be omitted.

- In the absence of ligand there is little (199, 366), or no EGFR dimerization (309); Canals (39) reported a small fraction of EGFR in the dimeric form in the absence of

EGF, but this was not considered to be functionally active and was regarded as an artefact of the experimental methodology.

- EGF induces aggregation (366).

- EGF is monomeric in solution, and the stoichiometry of EGF to EGFR in the occupied dimeric receptor is 1:1, with no evidence for a 1:2 EGF-EGFR complex being found (199).

- In addition, only dimeric forms of the EGFR that are equimolar in stoichiometry with EGF are catalytically active (309).

Hence, only the binding of ligand to the monomeric receptor and the formation of dimeric receptor-ligand complexes apparently occur to a significant extent (199, 366).

In adapting the model of the EGFR endocytic pathway, it was assumed that in the absence of EGF, the EGFR is diffusely distributed on the cell surface (317), and there is no receptor dimerization (309). EGF binds only to monomeric EGFR to form a receptor-ligand complex (199). Subsequent to ligand binding, the occupied receptors redistribute to clathrin-coated pits (317), where they aggregate to yield the R2L2 dimer (97, 199). A step representing ligand-induced dimerization was therefore interposed between the ligand binding and coated pit binding steps depicted in Figure 3.4; internalization of receptor dimers through the constitutive pathway was also included. In order to maintain a thermodynamically open system, additional steps were inserted representing the dissociation of bound ligand from internalized dimeric receptors, and trafficking of the resultant ligand and receptor molecules to intracellular pools, for degradation or recycling, respectively. Although the original model of Gex-Fabry and DeLisi (112) considers ligand degradation, this process was omitted from the adapted model and L_i was treated as a system parameter of fixed value.

3.3.1.2 EGF-induced autophosphorylation and activation of the EGFR

Receptor dimerization is required for, and occurs simultaneously with RTK activation (39), in a reaction that displays second-order kinetics with respect to the concentration of EGFR. Activation is therefore likely to proceed via an intermolecular mechanism (375). Dimerization also enhances autophosphorylation (22, 308), which has been

shown to result in increased RTK activity (16, 152, 208, 347). EGFR dimerization may therefore promote a conformational change in the protomers that facilitates self-phosphorylation of the cytoplasmic domains (22, 149), and thereby activate the RTK. Thus, regardless of the autophosphorylation mechanism, which has been reported to be both intramolecular (18, 352) and intermolecular (149, 150, 308), receptor activation is apparently a bimolecular process (150). This is the mechanism assumed in the model, and consequently the R2L2 dimer is the only species that is catalytically active (309). Both cell surface (356) and internalized (134, 242) occupied dimers are considered to be functionally active, including those associated with coated pit adaptor proteins. A separate autophosphorylation/activation step, following dimerization, was initially added to the reaction scheme, although this was later found to be an unnecessary addition (see section 3.3.1.8). Hence, in the final version of the module, dimerization is assumed to be synonymous with RTK activation.

Although monomeric EGFR does display some RTK activity, this is low compared to that associated with the dimeric form, and presumably represents basal autophosphorylation of the non-activated monomers (39). This is unlikely to contribute significantly to mitogenic signalling, since the dephosphorylated form of the non-activated receptor is liable to be rapidly regenerated by cellular phosphatases, thus preventing the monomer from achieving full activity (16). Hence, it was not considered necessary to specifically include the basal level of monomeric RTK activity in the model.

3.3.1.3 EGF-EGFR internalization and apparent EGFR affinity heterogeneity

Following dimerization, the EGFR dimer is able to form heterocomplexes with other cellular proteins (309). RTK activity is necessary for binding of the receptor-ligand complex to the coated pit component (210, 241). Hence, only the R2L2 species is able to associate with coated pit adaptor proteins, and thereby be internalized via the induced pathway (59, 115).

A functional RTK domain is also required for the emergence of apparent high-affinity binding sites (97), which has been presumed to correspond to dimer formation (319). However, models based on this assumption predict that ligand binding will display apparent positive cooperativity (199, 309), which is inconsistent with the majority of

experimental data (366). Furthermore, there is no direct evidence for two stable populations of EGFR with differing affinities for EGF, although the emergence of apparent affinity subclasses can arise from the multivalent binding of receptors to both ligand and coated pit protein (112). The association of the activated R2L2 dimer with coated pit adaptor proteins is therefore assumed to generate apparent affinity heterogeneity, although this phenomenon is not explicitly represented in the model.

As the monomeric receptor and receptor-ligand complexes are considered to be inactive, these are internalized via the constitutive pathway (210), as are activated R2L2 dimers not associated with the cell surface coated pit.

3.3.1.4 Rate equations

All reactions were assumed to conform to mass-action kinetics, including the EGFR dimerization and autophosphorylation/activation step (Figure 3.1, step 4). The reaction kinetics for the EGFR tyrosine kinase (EGFR-TK) are consistent with a sequential Bi-Bi rapid equilibrium catalytic mechanism (270). However, as the cellular concentration of ATP is far in excess of the reported K_m value for this substrate (352), the enzyme is saturated with respect to ATP and hence the rate equation for the reaction simplifies to a single substrate Michaelis-Menten function. Furthermore, since the autophosphorylation reaction occurs within the receptor dimer, the enzyme concentration increases in parallel with that of the substrate and saturation of the enzyme with respect to the substrate is not possible. Hence, typical Michaelis-Menten kinetics do not apply and the autophosphorylation reaction, corresponding to receptor activation, can be modelled as a first-order process that follows mass-action kinetics.

Occupied monomers undergo a single internalization/ligand-dissociation step (Figure 3.1, step 2), whereas in the case of occupied dimers, these events are represented by two sequential steps; thus, the internalization of dimeric receptors is not coincident with ligand dissociation (Figure 3.1, steps 5 and 8, and reaction 6). This measure was taken to allow for a pool of internalized, ligand-bound dimers that remain catalytically active prior to lysosomal degradation (134, 243), or in the case of this particular model, recycling. Both steps were still assumed to be subject to the same time delay function and governed by the same rate constant (see section 3.2.2.3). It is recognized that this provides a highly simplified representation of real events, but the assumed mechanistic

details, and indeed the values for the parameters governing these steps, were found to have little impact on the time courses of Shc phosphorylation or Ras/MAPK cascade activation (sections 4.3.2.1. and 6.4). However, these factors were relevant to the pattern of receptor down-regulation (section 4.3.1).

3.3.1.5 Derivation of quantitative data

At this early stage of development, the simulation was not intended to specifically reflect the PC12 cell system, but rather, in order to enable a direct comparison with the original model of Gex-Fabry and DeLisi (112), the isolated top-level module was designed to represent the processes of EGF-induced EGFR activation and internalization in fibroblasts. Hence, estimates of kinetic parameters were derived from a number of appropriate sources and subsequently refined, by employing parameter fitting methods, to improve the fit with the original model of EGFR endocytosis.

The rate constant for dissociation of the receptor-ligand complex (Figure 3.1, step 1; Figure 3.4, k_{-1}) was retained from the original model (112), as this was found to be a typical of the values reported in the literature for the fibroblast system (185, 210, 219, 322, 348, 356, 359, 360, 362). Parameters for receptor distribution ($[R_s]_0$, $[R_i]_0$ and f), coated pit protein binding (Figure 3.1, step 7; Figure 3.4, k_2), internalization (Figure 3.1, steps 2, 3, 5, 6 and 8; Figure 3.4, k_e) and receptor recycling (Figure 3.1, step 3; Figure 3.4, k_i) were also retained (112), although rate constants for processes involving dimeric species were modified by a factor of two.

Initial estimates of kinetic data for receptor dimerization (Figure 3.1, step 4) were derived from equilibrium constants for EGFR association on membrane vesicles, determined by Wofsy and colleagues (366), or for dimerization of the EGFR extracellular domain, reported by Lemmon and co-workers (199). These sources specify equilibrium binding constants either in units of μg protein receptor^{-1} (i.e. μg protein molecule^{-1}) (366) or M^{-1} (199), whereas values in units of (molecule/cell)$^{-1}$ are required in order to maintain dimensional consistency within the simulation. In order to convert these data into equilibrium constants appropriate for dimerization at the cell surface, estimates of total cell volume and total plasma membrane protein per cell were used as conversion factors. Estimates of the latter were derived from a number of sources and found to range between 0.6 and 13.5 pg, for a variety of cell types (3, 324,

372). Values within this range were used to calculate the appropriate equilibrium constants for receptor dimerization at the cell surface, as shown in Box 3.0 below.

Box 3.0 Conversion of K_a from units of μg protein receptor^{-1} (μg protein molecule^{-1}) to (molecule/cell)$^{-1}$

Assuming 6 pg plasma membrane protein cell^{-1}:

$K_{a4} = 2.1 \times 10^{-6}$ μg protein molecule^{-1} (ref. 366)

$= 2.1 \times 10^{-6}$ μg protein molecule^{-1} / 6.0×10^{-6} μg protein cell^{-1}

$= 0.35$ (molecule/cell)$^{-1}$

$K_{d4} = 1 / 0.35$ molecule cell^{-1}

$= 2.85$ molecule cell^{-1}

The actual value used for total plasma membrane protein content was found however, not to significantly influence the behaviour of the model. In order to calculate kinetic parameters from the equilibrium constants, it was necessary to assume that dimerization at the cell surface is diffusion-limited. This is reasonable, given the rapid onset of autophosphorylation in response to growth factor stimulation (178). The rate of association of the two receptor monomers was therefore assumed to be no greater than the rate of receptor-receptor encounters (0.03 s^{-1}) (143), and the appropriate dissociation rate constants were derived from this value and the calculated equilibrium constants for dimerization. The quantitative data used in the original model, in addition to the parameters for ligand binding and dimerization derived from the literature, are presented below in Table 3.4.

3.3.1.6 Validation of the simulation and parameter fitting

The original model of Gex-Fabry and DeLisi (112), depicted in Figure 3.4, has been shown previously to be consistent with experimental observations in terms of reproducing the time course of EGFR down-regulation in Balb/c 3T3 cells; the model correctly predicts that after 30 minutes continuous exposure to a fixed concentration of

EGF, 25% of the receptors remain unoccupied at the cell surface, 74% are located intracellularly and around 1% are bound to coated pit protein at the cell surface, as illustrated by Figure 3.6 below.

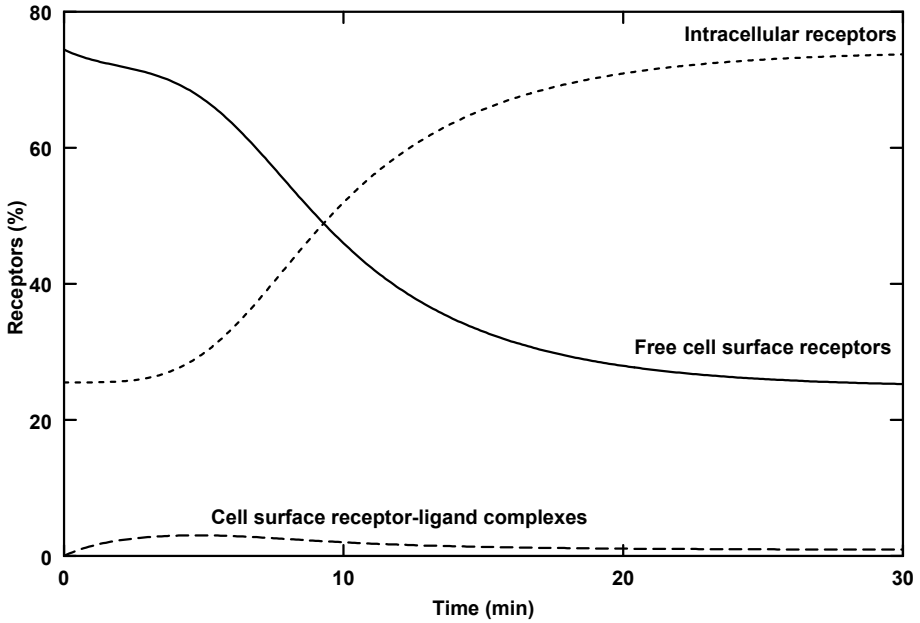

Figure 3.6 Time course of EGFR down-regulation
The number of free receptors on the cell surface (R_s), number of receptor-ligand complexes on the surface (RL) and number of intracellular receptors (R_i) are plotted as a percentage of the total number of receptors per cell. The data were obtained from a reconstruction of Gex-Fabry and DeLisi's model of the EGFR endocytic pathway (Figure 3.4 and ref. 112), implemented in Gepasi 3.2. The simulation parameters are given in Table 3.4.

In order to validate the modifications to the original model, and the estimated dimerization parameters, the patterns of receptor down-regulation predicted by the original model and the top-level simulation module were compared. Using the estimated parameters, the temporal and quantitative behaviour of the simulation was found to deviate significantly from that of the original model. Hence, kinetic parameters for ligand binding, coated pit protein binding, receptor dimerization and recycling were adjusted using the fitting capability of Gepasi 3.2 (226, 227). A number of fitting algorithms were examined, but due to inherent differences between these methods in terms of the type of problem for which they are best suited, only two were found to be appropriate in this instance: the Hooke and Jeeves, and L-BFGS-B methods.

The compatibility of the simulation with the original model was initially found to depend predominantly upon the rate constant for receptor-ligand association (k_1). Consequently, this parameter was set at the value specified for the original model (112), whereas the rate constant for dissociation of the receptor-ligand complex (k_{-1}) was allowed to vary between limits determined by values specified in the literature (185, 210, 219, 322, 348, 356, 359, 360, 362). The other parameters to be fitted were also allowed to vary between feasible limiting values. By employing this strategy, a number of acceptable parameter sets were obtained; substituting any of these sets of values into the simulation resulted in time-dependent behaviour that was compatible with that of the original model, with no discernible difference in the quantitative distribution of receptor species after 30 minutes. A summary of the fitted parameters sets is given below in Table 3.4.

3.3.1.7 Comparison of calculated and fitted parameter values

A number of observations can be made concerning the data shown in Table 3.4 below. The equilibrium constants reported for receptor-ligand binding on plasma membrane vesicles (366) or in solution (199), and the association rate constants derived from these (K_{d1}; k_1), differ by at least one order of magnitude from that assumed by the original model. As the behaviour of the simulation is highly dependent upon the value of the equilibrium constant for ligand binding, this may be the predominant reason why the simulations based upon this data were inconsistent with the original model. In contrast, the fitted parameter sets yield equilibrium constants for ligand binding that are similar to the value in the original model, presumably as the fitted values for dissociation of the receptor-ligand complex are relatively consistent.

Fitted values of the association rate constant for dimerization (k_4) were significantly lower than the original estimate, which was based upon the rate of receptor-receptor encounters at the cell surface (143). As this value does not discriminate between receptor-ligand complexes and free cell surface receptors, it was viewed as a maximum. It is therefore not surprising that the fitted value is somewhat lower, particularly as it is conceivable that not every receptor-receptor interaction facilitates dimerization.

Table 3.4 Estimated and fitted parameters for the 'top-level' module

K_{dn} corresponds to the equilibrium dissociation constant for reaction number, n, of the reaction scheme given in Figure 3.1; k_n is the corresponding first- or second-order rate constant for the reaction.

	Estimated Values			Fitted Values		
Parameter	Original model (ref. 112)	Membrane vesicles (ref. 366)[a]	Solubilized EGFR (ref. 199)	L-BFGS-B (a)[b]	L-BFGS-B (b)[b]	Hooke and Jeeves
Receptor distribution						
$[R_s]_0$, molecule cell^{-1}	7.3×10^4	-	-	-	-	-
$[R_i]_0$, molecule cell^{-1}	2.5×10^4	-	-	-	-	-
f	0.20	-	-	-	-	-
Ligand binding						
[L], nM	0.33	0.33	0.33	-	-	-
K_{d1}, M	7.1×10^{-9}	1.0×10^{-7}	4.0×10^{-7}	1.7×10^{-8}	1.1×10^{-8}	8.8×10^{-9}
k_1, M^{-1} min^{-1}	8.15×10^7	5.8×10^6	1.45×10^6	-	-	-
k_{-1}, min^{-1}	0.58	0.58	0.58	1.35	0.88	0.72
Dimerization						
K_{d4}, molecule cell^{-1}	-	2.85	2.0×10^6	2.3×10^5	7.8×10^5	1.4×10^6
k_4, molecule^{-1} min^{-1}	-	1.8	1.8	4.3×10^{-3}	6.9×10^{-4}	2.1×10^{-3}
k_{-4}, min^{-1}	-	5.13	3.6×10^6	9.9×10^2	5.4×10^2	3.0×10^3
CPP binding						
k_7, min^{-1}	0.24	-	-	0.29	0.56	1.0
k_{-7}, min^{-1}	0.0	-	-	5.0×10^{-5}	0.35	4.7×10^{-4}
Internalization						
k_2; k_{-3}; $2k_5$; $2k_6$; $2k_8$, min^{-1}	0.70	-	-	-	-	-
ΔT, min	6.5	-	-	-	-	-
ε	0.12	-	-	-	-	-
Recycling of receptors						
k_3, min^{-1}	4.9×10^{-2}	-	-	4.8×10^{-2}	4.8×10^{-2}	4.8×10^{-2}

[a] Assuming 6 pg plasma membrane protein cell^{-1}

[b] Denotes fitting of the parameters over different ranges of values

The equilibrium constants for receptor dimerization (K_{d4}), specified for EGFR on membrane vesicles (366) or in solution (199), and the dissociation rate constants derived from these (k_{-4}), also differ considerably from each other. The fitted kinetic parameters for receptor dimerization are quite variable, however, the forward and reverse rate constants were found to vary consistently within approximately the same ratio, to yield equilibrium constants that were comparable to that specified for dimerization of the solubilized extracellular domain of the EGFR (199). This is somewhat surprising, as the fitted data describe the dynamic behaviour of the EGF-EGFR endocytic pathway in intact cells, and hence might have been predicted to be more consistent with the equilibrium constant specified for dimerization of the EGFR on membrane vesicles (366).

The values of the equilibrium constants reported in these published studies reflect constraints placed upon these parameters, in order for them to be consistent with a particular model of dimerization. Lemmon and co-workers (199) discovered that the solubilized EGFR displayed apparent positive cooperativity with respect to ligand binding, and have attributed this to the existence of two different affinity classes of receptor, corresponding to monomers and dimers. In contrast, Wofsy and colleagues (366) have developed a model of negative cooperativity within the receptor dimer, to account for the observation that EGF binding to EGFR on intact cells typically displays this type of behaviour. In the current study, computer simulation of EGF-EGFR interaction at the cell surface, and parameter fitting for this environment, have indicated that the equilibrium constants specified by this group are not consistent with experimental observations. This could possibly be viewed as evidence that the model favoured by Wofsy and co-workers (366) is actually invalid, and it seems more likely that the binding of EGFR to plasma membrane proteins is responsible for apparent negative cooperativity in the association of EGF with dimeric EGFR (219). Furthermore, the results of the current study appear to support the model of Lemmon and colleagues (199), although it must be noted that this model is not necessarily applicable to the holo-receptor under physiological conditions, and it may be coincidental that the fitted value for the dimerization equilibrium constant is comparable to that specified by this group. Nonetheless, it is plausible that although there is positive cooperativity in the binding of EGF to dimeric EGFR in isolation (199, 309), this process may typically exhibit negative cooperativity at the cell surface, due to association of the receptor-ligand complex with coated pit adaptor proteins (112, 219).

Although there is some variation within the fitted values for coated pit protein binding (k_{-7}), and between these values and the data in the original model, the latter are not definitive, as they constitute estimated values (112). Therefore, any of the fitted values may also be considered acceptable. Furthermore, in the original model, receptor internalization is not regarded as a saturable equilibrium process, since $k_{-7} = 0$ (112), but a better fit was obtained by assuming $k_{-7} > 0$. This results in a very low value for K_{d7}, in comparison with the total number of receptors, consistent with the proposed high-affinity, but low-capacity ligand-induced internalization mechanism (59, 210).

The rate constant for receptor recycling (k_3) is apparently invariant, and is perhaps a critical value in determining the behaviour of the simulation. This is a reasonable proposal, as the 'recycling' step constitutes a simplification of the scheme to accommodate intracellular processing events that have not been modelled explicitly; in reality, the majority of the internalized receptors are degraded, and replaced by *de novo* synthesis of further receptor molecules, with only a small proportion being recycled to the cell surface (43).

3.3.1.8 Analysis of the simulated time courses of EGFR dimerization and activation

The compatibility of the simulation with the time course of EGFR down-regulation in intact cells suggests that the assumptions made in attempting to reconcile the differences between proposed models of EGF-EGFR activation and internalization, and in adapting the original model to incorporate receptor dimerization, may adequately represent the sequence and mechanism of events that occur in the physiological situation. Nonetheless, in order to enable a more complete assessment of the behaviour of the simulation, the predicted time courses of ligand-induced receptor dimerization and activation were also investigated.

Since much of the published experimental work regarding these properties of the EGFR has been carried out using the detergent-solubilized receptor, the simulation was simplified to represent this experimental system, in order to allow a direct comparison with experimental data. This necessitated a number of modifications.

- All reactions except ligand binding (Figure 3.1, step 1), receptor dimerization and autophosphorylation/activation (Figure 3.1, step 4) were eliminated.
- Receptors were quantified in units of molar concentration, rather than number per cell.
- The equilibrium constant and kinetic constants for ligand binding retained the same dimensions, however, it was necessary to amend those for dimerization in order to reflect the dynamics of receptor-receptor interaction in solution, rather than at the cell surface.

An initial estimate of the ligand binding equilibrium constant for the solubilized receptor was obtained (375), from which the association rate constant was derived. In order to calculate this parameter, it was necessary to assume that solubilization of the receptor affects only the rate of association of ligand and receptor, and hence that the dissociation rate constant in solution is the same as at the cell surface. An initial estimate of the equilibrium constant for dimerization of the solubilized extracellular domain of the EGFR was also obtained (199), however, this is likely to be too low to allow significant dimerization to take place at EGFR concentrations that are typical in solubilized receptor studies (39, 309), and possibly inappropriate for the holo-receptor. Consequently, an arbitrary estimate of this value was made and used to calculate the association rate constant for this process, assuming that the dissociation rate constant of the solubilized dimer is the same as at the cell surface.

The simplified model was assessed on its capacity to reproduce the EGF stimulus-response curve for dimerization of the detergent-solubilized receptor, and time course of receptor dimerization at 1 μM EGF (39). Whilst the model was apparently compatible with the EGF stimulus-response data, it did not adequately predict the dimerization time course at either of two EGFR concentrations. In order to improve the fit to the experimental data, parameter fitting for the ligand binding and dimerization reactions was attempted, although it became evident that it was not possible to resolve a distinct set of parameters that enabled the model to adequately simulate all aspects of the behaviour of the solubilized receptor system; a satisfactory fit to the stimulus-response data was obtained at the expense of the fit to the time course data, and vice versa. This implied that, contrary to the conclusions drawn above regarding the more comprehensive model of EGF-EGFR interaction at the cell surface, the fundamental mathematical structure of the model was somehow incorrect.

Based on experimental observations, Canals (39) has proposed that dimerization is an irreversible step, and therefore, with sufficient time, proceeds to completion at high EGF concentrations. However, an inherent assumption in the simulation is that receptor dimerization is an equilibrium process; i.e. dimeric receptor-ligand complexes may dissociate into the monomeric species. Furthermore, the experimental data indicate that there is a fraction of the dimeric form present before the introduction of EGF to the system, although this was likely to be an artefact of the methodology used (39), and incorporating this pre-existing dimer into the simulation did not alter the fit to

either set of data. Yet, by modifying the simulation to reflect an irreversible dimerization mechanism, i.e. by eliminating the dissociation rate constant for the dimeric receptor, it was possible to determine a set of parameters that enabled a satisfactory fit to the time course data at both EGFR concentrations. These values were subsequently refined to also allow an adequate fit to the stimulus-response data. The fitted parameters, in addition to the initial estimates and the values reported by Canals (39), are presented in Table 3.5, whilst the fit of the simulation to both the stimulus-response and time course data is illustrated below in Figures 3.7 and 3.8.

From Table 3.5 it is apparent that the fitted parameters differ somewhat from the initial estimates, which might be expected, as the latter are based upon a simplifying assumption and hence represent largely arbitrary values. The fitted value for the ligand-binding equilibrium constant (K_{d1}) differs by approximately one order of magnitude from the reported value for the solubilized receptor (375), and is comparable to the fitted values for interaction of EGF-EGFR at the cell surface (Table 3.4). Similar discrepancies are however, evident for reported estimates of this parameter at the cell surface; hence, this is not likely to represent a significant error. The fitted value for the dimerization rate constant (k_4) differs almost by a factor of three from that determined by Canals (39) on the basis of the same set of experimental data, however, substituting this higher value into the simulation resulted in a poorer fit to the data. This discrepancy was investigated and found to be due to another fundamental difference between the computer simulation and the model of EGFR dimerization proposed by Canals (39).

Table 3.5 Parameter values for ligand binding and dimerization in the detergent-solubilized EGFR system

Parameter	Estimated Values	Reported in ref. 39	Fitted Values
Ligand binding			
K_{d1}, M	1.0×10^{-7}	1.0×10^{-7}	6.7×10^{-9}
k_1, M^{-1} min^{-1}	8.8×10^{6} [a]	-	1.5×10^{7}
k_{-1}, min^{-1}	0.88 [b]	-	0.10
Dimerization			
K_{d4}, M	2.0×10^{-8}	-	-
k_4, M^{-1} min^{-1}	2.7×10^{10} [a]	6.0×10^{7}	2.25×10^{7}
k_{-4}, min^{-1}	5.4×10^{2} [b]	-	-

[a] Calculated

[b] Estimated from the fitted value for the dissociation rate constant at the cell surface, given in Table 3.4.

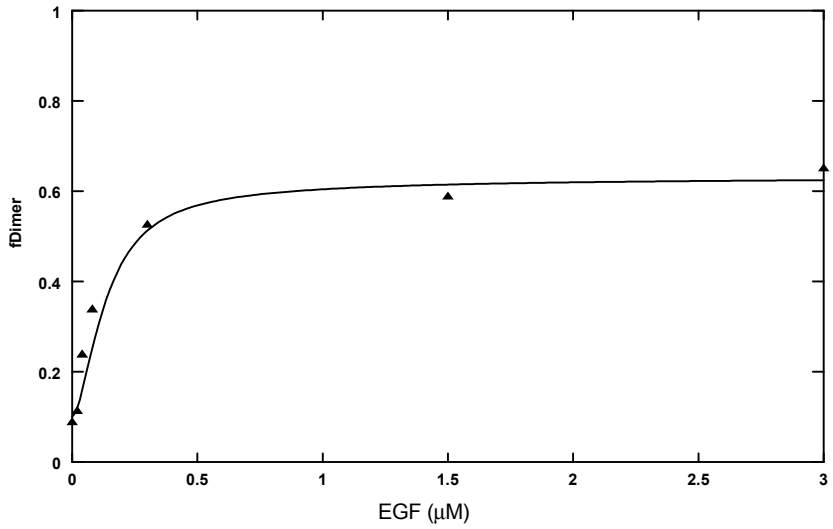

Figure 3.7 EGF stimulus-response curve for solubilized EGFR dimerization
Experimental data (discrete symbols) have been replotted from Canals (39); 30 nM EGFR was incubated for 1 minute with the indicated concentrations of EGF. The fitted curve (solid line) shows the stimulus-response profile predicted by the model of solubilized EGFR dimerization; the simulation parameters are listed in Table 3.5. Dimeric receptors are plotted as a fraction (fDimer) of total receptors in the system.

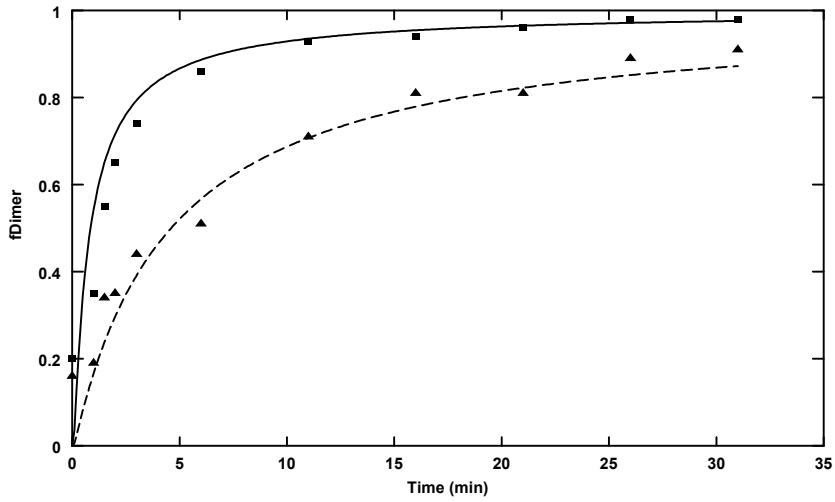

Figure 3.8 Time course of solubilized EGFR dimerization
Experimental data have been replotted from Canals (39); 30 nM (■) or 5 nM (●) EGFR was incubated for the indicated times with 1 μM EGF. The fitted curves show the time course predicted by the model of solubilized EGFR dimerization, at 30 nM (solid line) and 5 nM (dashed line) EGFR, and 1 μM EGF. Other simulation parameters are listed in Table 3.5. Dimeric receptors are plotted as a fraction (fDimer) of total receptors in the system.

The stimulus-response curve (Figure 3.7) indicates that increasing the concentration of EGF above 1 μM does not promote an increase in EGFR dimerization during a 1 minute incubation period, and the time course data at 1 μM EGF (Figure 3.8) suggests that only minimal dimerization takes place during this period. The model of Canals (39) is therefore based on the assumption that ligand binding is complete before significant

dimerization occurs, i.e. within 1 minute, so that the ligand binding process can be effectively eliminated from the model, with the equilibrium concentration of occupied monomer in solution prior to the onset of dimerization being represented as an external parameter of the system. Altering the solubilized receptor simulation to reflect this hypothesis resulted in a good fit to the experimental data with the parameters specified by Canals (39). An implied assumption in this model however, is that the position of the ligand binding equilibrium, and the rate at which this is attained, are governed solely by the equilibrium constant for the process. This assumption is valid, if receptor-ligand binding is considered in isolation. However, where ligand binding forms part of a system that allows subsequent receptor-ligand complex dimerization, this assumption is incorrect; the ligand binding equilibrium will then also be influenced by the dimerization process, so that the kinetic properties of both events will determine the equilibrium concentration of the receptor-ligand complex, which cannot therefore be treated as an external parameter of the system.

The influence of receptor-ligand complex dimerization on the equilibrium properties of ligand binding can be illustrated by comparing the time course for receptor-ligand binding in isolation, with that of the solubilized receptor simulation, which considers ligand binding as an integral part of the system. The position of the ligand binding equilibrium is in fact determined by the relative values of the equilibrium constant for ligand binding and the dimerization rate constant. If the ligand binding equilibrium constant is assumed to be that reported in the literature (375), and the dimerization rate constant is relatively high, such as that calculated by Canals (39), the position of the ligand binding equilibrium, i.e. the equilibrium concentration of the receptor-ligand complex, is affected quite considerably, as shown in Figure 3.9A below. In contrast, the time course of receptor-ligand binding at the fitted values of the kinetic parameters, exhibits a somewhat different pattern of behaviour, as shown in Figure 3.9B below. The fitted ligand binding equilibrium constant is approximately one order of magnitude greater than that reported in the literature (375), so that although the fitted dimerization rate constant is still high, the position of the ligand binding equilibrium now approaches that in the isolated situation. The speed at which this equilibrium is attained is also more rapid, although this is largely a function of the relative values of the EGF-EGFR association and dissociation rate constants.

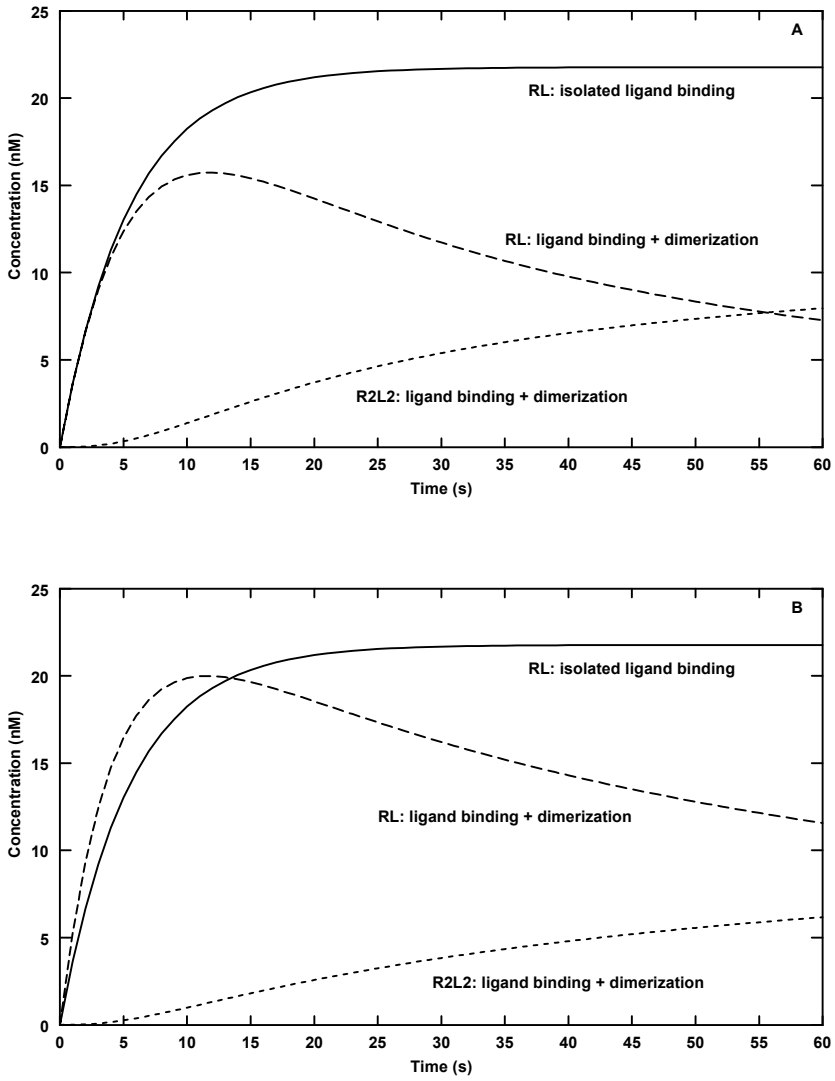

Figure 3.9 Simulated time courses of EGF-EGFR binding and dimerization

The time course of receptor-ligand binding was computed over 1 minute, in isolation and with subsequent receptor dimerization, at 30 nM EGFR and 1 μM EGF. (**A**) Ligand binding, $K_{d1} = 1.0 \times 10^{-7}$ M ($k_1 = 1.0 \times 10^7$ M^{-1} min^{-1}, $k_{-1} = 1.0$ min^{-1}); dimerization, $k_4 = 6.0 \times 10^7$ M^{-1} min^{-1}. (**B**) Ligand binding, $K_{d1} = 6.7 \times 10^{-9}$ M ($k_1 = 1.5 \times 10^7$ M^{-1} min^{-1}, $k_{-1} = 0.1$ min^{-1}); dimerization, $k_4 = 2.25 \times 10^7$ M^{-1} min^{-1}. The results are expressed as the concentrations of monomeric receptor-ligand complexes (RL) and occupied dimers (R2L2).

If the fitted parameters are indeed appropriate for the experimental system, this suggests that the position of the ligand binding equilibrium is not significantly affected by dimerization, and it is apparent from Figure 3.9B that ligand binding does reach an equilibrium before appreciable dimerization occurs. However, there is no justification for assuming this equilibrium is completely independent of subsequent dimerization, or that the equilibrium concentration of the receptor-ligand complex can be treated as an external factor. Hence, based on this incorrect supposition, and through assuming the reported ligand binding equilibrium constant is accurate, Canals (39) has apparently

overestimated the dimerization rate constant. Yet, unless it is assumed that dimerization is effectively irreversible, the simulation is inconsistent with the dimerization time course and stimulus-response data, which may possibly be considered as validation of this particular hypothesis.

Assuming irreversible dimerization, the activation time course of the solubilized receptor system was also investigated. In order to model the catalytic activity of the EGFR tyrosine kinase (EGFR-TK), values for the kinetic properties of the EGFR-TK were required. As discussed above, the autophosphorylation/activation step was initially modelled as a distinct process, subsequent to dimerization, governed by a first-order rate constant representing the fraction of dimeric receptors autophosphorylated/activated per unit time; this was initially assigned an arbitrary value of 1.0 min^{-1}. However, in agreement with the observation that dimerization parallels activation (39), the fit to EGFR-TK activation data was unaffected by omitting the separate activation step, and assuming that all occupied receptors become catalytically active upon dimerization. Occupied dimeric species were therefore presumed to have a catalytic potential corresponding to the specific activity of the EGFR-TK. A number of estimates for this constant were obtained, as shown below in Table 3.6.

The median of these values was used as an initial estimate of the specific activity; this was subsequently found to be too high and an optimal value of 3.2 mol min^{-1} mol^{-1} enzyme protein was established through parameter fitting. The solubilized receptor simulation demonstrates a good fit to the experimental data, as shown in Figure 3.10 below, which suggests that this represents an acceptable model of ligand-induced EGFR activation.

Table 3.6 Estimates of EGFR-TK specific activity

Substrate	Specific activity (mol min^{-1} mol^{-1} enzyme protein)	Reference
Tyr-771 of PLCγ	0.75	(152)
Synthetic peptide ($L_{11}G_1$)	1.75	(352)
Synthetic peptide ($L_{12}G_1$)	2.10	(93)
Shc	4.70	(257)
Angiotensin II	10.5	(16)
"	11.0	(352)
Src homology peptide	13.2	(16)
"	16.4	(352)

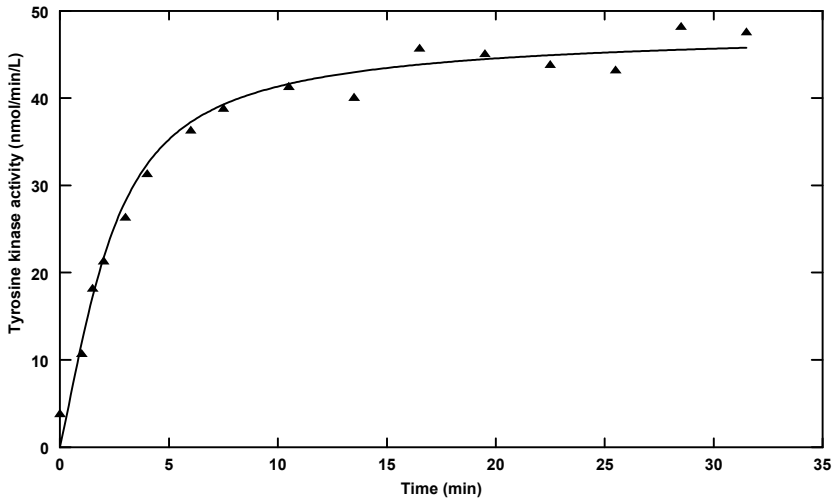

Figure 3.10 Time course of solubilized EGFR activation
Experimental data (discrete symbols) have been replotted from Canals (39); 15 nM EGFR was incubated for the indicated times with 1 μM EGF. The fitted curve (solid line) shows the corresponding time course predicted by the model of solubilized EGFR dimerization. Receptor tyrosine kinase activity is expressed in terms of the total catalytic capacity of the activated receptor dimers (nmol phosphate incorporated into an exogenous substrate min^{-1} l^{-1} enzyme). The specific activity of EGFR-TK was taken to be 3.2 mol min^{-1} mol^{-1} enzyme protein; other simulation parameters are given in Table 3.5.

3.3.1.9 Revision of the cell surface simulation

The simplified model of dimerization and activation of the solubilized EGFR diverges from the earlier simulation of EGF-EGFR interaction at the cell surface, by assuming that EGFR dimerization is an irreversible process. The cell surface model was therefore altered to accommodate this mechanism of EGFR dimerization, and the impact on the time-dependent behaviour of the model was assessed. Further parameter fitting was required to fully optimize the values of the kinetic constants for dimerization and coated pit protein binding, and several sets of parameters were obtained that enabled the model to adequately fit the pattern of receptor down-regulation predicted by the original model. A summary of the revised values of these parameters is presented below in Table 3.7.

The majority of these values differ very little from those fitted by assuming that EGFR dimerization at the cell surface is an equilibrium process (shown previously in Table 3.4), with the only significant variation being in the dimerization rate constant (k_4). The value of this parameter is slightly closer to the upper limit set by the estimated rate of receptor-receptor encounters at the cell surface, consistent with the assumption that dimerization is diffusion-limited rather than reaction-limited. The impact of altering the mechanism of EGFR dimerization appears to be minimal; the mechanism that is

assumed may be relatively unimportant in the cell surface model, as once formed, activated dimers are subject to rapid internalization, and under these circumstances the reaction cannot proceed to completion, even if effectively irreversible.

Table 3.7 Revised parameter values for the 'top-level' module

Parameter	Previous range (from Table 3.4)	Revised value
Ligand binding		
K_{d1}, M	1.1×10^{-9} - 8.8×10^{-9}	8.9×10^{-9}
k_1, M^{-1} min^{-1}	-	8.15×10^{7}
k_{-1}, min^{-1}	0.72 - 1.35	0.73
Dimerization		
k_4, $molecule^{-1}$ min^{-1}	6.9×10^{-4} - 2.1×10^{-3}	1.383×10^{-3}
k_{-4}, min^{-1}	5.4×10^{2} - 3.0×10^{3}	-
CPP binding		
k_7, min^{-1}	0.29 - 1.0	1.0
k_{-7}, min-1	5.0×10^{-5} - 0.35	3.47×10^{-4}

3.3.1.10 Summary

The preceding sections have described the development of the top-level module of a computer simulation of EGF signal transduction, through the adaptation of a mathematical model of the EGF-EGFR endocytic pathway in Balb/c 3T3 cells to incorporate terms for ligand-induced EGFR dimerization and activation. The simulation embodies an attempt to reconcile a number of apparently conflicting models of the mechanisms of ligand-induced EGFR activation and internalization, and thereby to form a cohesive representation of these events. The behaviour of the simulation has been shown to be consistent with experimental observations from intact cells. This should not be viewed as conclusive proof that the assumptions made in reconciling these models, and in adapting the original model to include receptor dimerization, correspond to the physiological sequence and mechanism of events, nor that the fitted parameters reflect the true kinetics of the system. Rather, these simplifying assumptions constitute a possible model of EGF-EGFR interaction that is compatible with the actual mechanism in operation at the cell surface.

Detailed simulation of this first step in the EGF signal transduction pathway has enabled some of the proposed models of EGFR dimerization to be evaluated, based on their compatibility with experimental observations. A model assuming negative cooperativity within the receptor dimer at the cell surface was found not to be

compatible with experimental data from this environment. Hence, it was concluded that apparent negative cooperativity in EGF-EGFR binding *in vivo* is more likely to be the result of receptor-ligand complex association with coated pit adaptor proteins. The majority of EGFR dimerization models assume that dimer formation is an equilibrium process, yet an irreversible mechanism of dimerization was found to be equally consistent with the data, although the rate constant reported in the literature for this process was shown to have been overestimated on the basis of a mistaken assumption regarding the dynamic properties of the system. Thus, it seems that the physiological mechanism of dimerization may not be relevant to a consideration of the functional properties of EGF signal transduction.

3.3.2. THE 'INTERMEDIATE' MODULE: RAS ACTIVATION

Since the revised top-level module was found to adequately reflect ligand-induced activation of the EGFR *in vivo*, it was used as the basis for extending the simulation of EGF signal transduction to include activation of the GTP-binding protein, Ras. Before development of this second module could proceed however, it was necessary to decide upon a strategy for dealing with processes involving signalling intermediates contained within separate cellular compartments; for example, the signalling events linking two conjoining modules, such as the phosphorylation of Shc by EGFR-TK, and the activation of the MAPK cascade, mediated by Ras.

3.3.2.1 Sub-cellular compartmentalization

A 'multi-compartment' simulation was initially considered as a solution to the problem, with the cell surface forming one compartment and the intracellular space immediately adjacent to the plasma membrane representing another, the intention being that the cytosol would ultimately comprise a third compartment in the later stages of development. This approach appeared to offer the advantage of allowing many of the kinetic parameters used in the model to be expressed in terms of molar concentration, in which experimentally derived data are generally reported, rather than in units of amount. However, in order to formulate a multi-compartment model, the simulation software required the rates of any 'user-defined' reactions (i.e. those that must be specified by the user, since they are not included in the reaction database supplied with

the software), and associated second-order rate constants, to be expressed in amount per unit time, thus obviating the purpose of such a model in this instance.

Nonetheless, it was considered necessary to account for the compartmentalization of signalling intermediates, particularly since the recruitment of effectors such as SOS and Raf to the plasma membrane plays such a vital role in signal transmission (187). Indeed, theoretical and experimental studies, conducted by Kholodenko (179), Haugh (134, 135) and colleagues, have clearly demonstrated the importance of sub-cellular localization in regulating signal transduction processes. The approach adopted in extending the simulation was therefore to continue with the implementation of a single compartment model, by converting all relevant data (for example, concentrations of signalling intermediates, second-order rate constants and Michaelis constants) to units of amount rather than concentration. As these units are independent of volume, they are suitable for specifying interactions between signalling molecules within different cellular compartments, of differing volumes. The conversion of data between units of moles l^{-1} and molecule $cell^{-1}$ was carried out using estimated volumes of the appropriate sub-cellular compartments as conversion factors, thereby accounting for the compartmentalization of signalling intermediates, without the need for explicitly modelling separate compartments. This is described in more detail in section 3.3.2.5. In order to implement this model however, it was necessary to assume that the interactions between the intermediates are not diffusion-limited.

No data conversion was required for the completed top-level module, EGFR activation at the cell surface, since the data specified for this module were already expressed in units of amount. Although the signalling events comprising the intermediate module are presumed to occur exclusively within the compartment adjacent to the membrane, only GDP/GTP exchange on Ras, catalysed by SOS, involves participating molecules that are co-localized to this site. The remaining interactions at this level are between molecules, such as Ras, that are restricted to this compartment and others that are assumed to be homogeneously distributed throughout the cell, for example, Raf. This particular interaction links Ras with the remainder of the final, MAPK cascade module, which is located cytosolically.

3.3.2.2 EGFR-TK phosphorylation of Shc, and the formation of a Shc-Grb2-SOS complex

As discussed in the previous chapter, there are two possible routes through which the activated EGFR mediates the activation of Ras: either by the direct association of the adaptor protein Grb2 with the autophosphorylated receptor, or through the phosphorylation of the adaptor Shc by EGFR-TK, with the consequent formation of a complex between phosphorylated Shc and Grb2. Either route instigates the recruitment of the guanine-nucleotide exchange factor, SOS, to the plasma membrane, where it encounters its target molecule, Ras (85). The critical route for Ras activation induced by EGF seems however, to be mediated by Shc, whilst the formation of EGFR-Grb2-SOS complexes apparently plays a minor role (12, 291, 292); immunoprecipitation of Shc from membrane fractions of EGF-stimulated Rat1 cells removes around 93% of the total Ras GEF activity (291), whilst the micro-injection of an anti-Shc antibody into intact Rat1 cells inhibits mitogenic signalling by 81% (292). Moreover, the affinity of Grb2-SOS for tyrosine phosphorylated Shc is ten-fold greater than for the phosphotyrosine EGFR (63), so that a far greater proportion of Grb2 associates with Shc than directly with the activated EGFR (291). Hence, the sub-set of all possible signalling complexes that could be represented in the model was restricted to those including Shc. The consequences of this simplification to the reaction scheme are reviewed in section 5.3.1.3.

Contrary to a widely accepted premise, that the formation of a stable complex between Shc and the activated EGFR is essential for signal transduction, there is convincing evidence that this is not required for EGF-induced tyrosine phosphorylation of Shc and activation of Ras. Although the time course of Ras activation is consistent with the kinetics of Shc tyrosine phosphorylation (133, 291), no correlation between EGFR-Shc complex formation and the activation of Ras is evident (12, 291). Furthermore, EGFR deletion mutants lacking the major autophosphorylation and SH2 domain-binding sites are still capable of inducing the tyrosine phosphorylation of Shc and the formation of Shc-Grb2-SOS ternary complexes, as well as Ras and MAPK activation (121, 313). Hence, the mechanism assumed in the model was that transient association of Shc with the activated EGFR is sufficient for catalysing the tyrosine phosphorylation of Shc, and consequently for mitogenic signalling, through the formation of a trimeric Shc-Grb2-SOS complex that is independent of the receptor (12, 121).

The majority of tyrosine phosphorylated Shc remains localized to the plasma membrane following EGF stimulation (287). The mechanism through which this might

be achieved in the absence of stable association with the activated EGFR is not clear, but non-receptor tyrosine kinases, such as members of the Src family, also induce Shc phosphorylation and complex formation at the plasma membrane without forming a stable complex with Shc; it therefore seems reasonable that the same, unknown, mechanism might be involved in both instances (313). The eventual recycling of Shc to the cytosol parallels tyrosine dephosphorylation (287). The cellular phosphatases for which phosphorylated Shc is a target have not been identified, but for the purposes of model development, phosphorylated Shc was considered to be subject to generalized protein tyrosine phosphatase activity; given that the phosphorylation status of the ShcP-Grb2-SOS complex is relatively prolonged (291), the phosphotyrosine of complexed Shc was presumed to be protected from this activity.

Since Grb2 and SOS are found in a constitutive complex in the majority of mammalian cell types (54, 204, 284, 291), the Grb2-SOS binding equilibrium was excluded from the model. Inclusion of this process, modelled using experimentally derived quantitative data, was found to have no effect on the simulated behaviour of the system.

These assumptions enabled considerable simplification of the model. Many of the theoretically possible combinations of the signalling proteins Shc, Grb2 and SOS, as well as multiple species of activated EGFR, could be omitted without any loss of functionality, resulting in a 'streamlined' model that could be more readily implemented and analysed.

3.3.2.3 The regulation of Ras activation by SOS and GAP

The ratio of GTP/GDP bound forms of Ras, and hence the Ras activation state, is determined by the relative activities of the regulatory proteins, SOS and GAP. Whereas SOS catalyses the release of bound GDP, and its replacement by cytosolic GTP, GAP simulates the intrinsic GTPase activity of Ras (85). Hence, Ras can be viewed as a molecular switch in mitogenic signalling that cycles between two interconvertible forms (294), with SOS and GAP playing the roles of the enzymes that catalyse these conversions (85). The catalytic mechanisms of SOS and GAP, and the rate equations employed in modelling their role in the system, are discussed further in the following section.

Given that the relevance of the association of GAP with the activated EGFR is unclear, but that this interaction does not appear to significantly affect the catalytic activity of GAP, it was not included in the model. Furthermore, since the rate of guanine-nucleotide exchange on Ras and Ras GTPase activity are extremely low in the absence of SOS and GAP respectively, it was also not considered necessary to reflect these intrinsic properties within the model.

3.3.2.4 Rate equations

As discussed above, the EGFR-TK has been shown to demonstrate reaction kinetics that are consistent with a sequential Bi-Bi rapid equilibrium catalytic mechanism (270), but since the cellular ATP concentration is far greater than the reported K_m value of the enzyme for ATP (270, 352), the rate equation for phosphorylation of Shc by the EGFR-TK (Figure 3.1, step 9) therefore simplifies to a single-substrate Michaelis-Menten function. The dephosphorylation of Shc (Figure 3.1, step 10) was also assumed to follow Michaelis-Menten kinetics (77, 380), whereas the ShcP/Grb2-SOS binding step (Figure 3.1, step 11) was modelled using mass-action kinetics.

There were two possible approaches for representing the Ras activation-inactivation cycle in the model, suggested by the catalytic mechanisms of GAP and Ras GEFs, such as SOS. Formation of a complex between Ras-GDP and a GEF significantly decreases the affinity of Ras for the nucleotide, and thus promotes the dissociation of bound GDP. The resulting binary Ras-GEF complex binds cytosolic GTP, with the subsequent release of the GEF (200). Ras GEFs therefore have a dual function: they destabilize the interaction between Ras and GDP (200), and stabilize a nucleotide-free intermediate (132, 192), but do not expressly favour the formation of the active Ras-GTP complex. Rather, the role of the GEF appears to be to catalyse the attainment of an equilibrium between active and inactive states, the position of which is determined by the ratio of cellular GDP/GTP concentrations and respective nucleotide affinities (200). Whilst Ras does have a slightly higher affinity for GTP than GDP (192, 200, 279), the cellular concentration of GTP is around 20-fold greater than that of GDP, so that dissociated GDP is primarily replaced with GTP (132).

GAP directly associates with Ras-GTP, and has been proposed to function by either inducing the conversion of Ras from a catalytically inefficient configuration to a

GTPase competent conformation, or to play a more active role by supplying residues required for enhanced GTP hydrolysis (364). Biochemical and structural evidence indicates that GAP both stabilizes a GTPase competent configuration and provides a critical arginine residue that directly participates in the GTPase reaction (364). Following the rapid conversion of Ras-GTP to Ras-GDP, GAP dissociates from Ras (220).

The options available were therefore either to directly implement a complete binding equilibrium scheme for GDP/GTP exchange on Ras, stimulated by SOS (200), or to treat this as single step that conforms to the Michaelis-Menten model for an enzyme-catalysed process (132, 163). Similarly, the interaction between Ras and GAP might be represented directly (28), or GAP-enhanced GTP hydrolysis could be modelled as an enzyme-catalysed reaction that follows Michaelis-Menten kinetics, even though the active site is located within Ras (2, 113, 247).

An appraisal of these possible approaches was conducted by formulating two independent kinetic models of SOS-dependent Ras activation, and implementing these as Gepasi 3.2 simulations for comparison with experimental data. A model representing a comprehensive Ras-GEF-guanine-nucleotide binding scheme, based upon the work of Lenzen and colleagues (200), was found to predict an incorrect pattern of Ras activation: the stability of the Ras-GDP-SOS complex was found to be too great, resulting in an unsatisfactorily low rate of Ras-GTP generation. In contrast, a simulation representing SOS-dependent guanine-nucleotide exchange on Ras as an enzyme-substrate reaction was found to predict an adequate degree of Ras-GTP accumulation. Superficially, it would appear that the latter might be a better strategy for modelling this, and also the GAP-catalysed reaction steps.

However, taking this approach might place a significant restriction upon later model development: it would preclude the direct representation of competition between GAP, and the Ras effector, Raf, for binding to Ras-GTP (331). This competition may have some physiological relevance, since the binding of Ras-GTP to either protein would clearly affect the availability of Ras to participate in an alternative interaction, by removing a proportion of activated Ras from the cellular pool. Furthermore, within the cellular environment, it is unlikely that the concentrations of Ras-GDP or Ras-GTP would be sufficiently in excess of SOS and GAP to be saturating. Under these

circumstances, the Michaelis-Menten equation is not strictly applicable, and the overall rate of the reaction becomes dependent upon the rate at which the enzyme and substrate interact to form a complex.

Thus a compromise was determined, where the interconversions of active and inactive forms of Ras, catalysed by GAP and SOS, were represented as two-step processes with an initial enzyme-substrate binding equilibrium, where $K_m \approx K_d$, and a subsequent irreversible enzyme-product release step, equivalent to the catalytic step, where k = enzyme specific activity, k_{cat}. These explicit representations of the Michaelis-Menten model account for steps 12 to 15 of the reaction scheme shown in Figure 3.1. As cellular [GTP] is assumed to be constant, and is far greater than reported K_m values of Ras GEFs for GTP (132), this substrate is not limiting for the guanine-nucleotide exchange reaction, which can therefore be modelled as a first-order process.

This approach avoids the unnecessary complication of modelling an entire binding scheme for all possible permutations of Ras, guanine-nucleotide, SOS and GAP, but incorporates the important aspects of this scheme, by accounting for the removal of enzyme and substrate from the cellular pools. Implementation of this model in isolation was found to produce a similar level of Ras activation to that predicted by model in which the corresponding reactions were represented by true Michaelis-Menten kinetics, but also adequately reflected the dynamics of the binding equilibria.

3.3.2.5 Parameter values

In order to facilitate a comparison of the time-dependent behaviour of the simulation with experimental data describing the time course of EGF-induced Shc phosphorylation and Ras activation in Rat1 fibroblasts (291), quantitative data appropriate for this cell type were used in implementing the model described above.

Where applicable, the parameter values for the top-level module were adjusted to reflect the Rat1 system, rather than Balb/c 3T3 fibroblasts. Rat1 cells express approximately the same number of EGFR per cell (194), but the relative distribution of these receptors between the cell surface and intracellular compartments was assumed to be the same as in Balb/c 3T3 cells, as were the EGFR ligand binding characteristics

(112). The parameter values for EGFR dimerization, internalization and recycling determined for the top-level module were also unchanged.

No estimates of the total number of Shc or Grb2-SOS expressed per cell were available, although it is reasonable to suppose that the expression levels of these proteins are within the same range as that of the EGFR (between 1×10^4 and 1×10^5 molecules cell^{-1}) (135). The total number of Ras molecules per cell has been estimated at 2×10^4 in NIH 3T3 fibroblasts (102), and in PC12 cells, around 1% of the cellular complement of Ras is GTP-bound in the basal state (237, 275); it seems likely that the expression level of GAP would be of the same order.

Kinetic parameters for the tyrosine phosphorylation of Shc by the activated EGFR-TK (Figure 3.1, step 9) were assigned values determined *in vitro* (257). Estimates of cellular concentrations and kinetic parameters for protein phosphatases vary widely, with K_m values in the range 10-15000 nM, k_{cat} values varying between 0.1 and 50 s^{-1} and concentrations ranging between 0.1 and 1000 nM (17, 27, 155, 177). Values reflecting this range were therefore used to represent cellular protein phosphatase activity, and more specifically, the dephosphorylation of phosphorylated Shc (Figure 3.1, step 10); V_{max} was taken as $[E]_{Total} \times k_{cat}$.

The association rate constant for the formation of a complex between phosphotyrosine Shc and Grb2-SOS (k_{11}) was calculated from the reported equilibrium dissociation constant for this process *in vitro* (63), assuming a dissociation rate constant of 6 min^{-1} (0.1 s^{-1}); this value is typical of those reported for interactions between SH2 domain-containing proteins and high affinity phosphopeptides (99, 263).

Michaelis constants reported for mammalian SOS homologues range from 0.7 to 400 μM (163, 200, 260) whilst that for p120GAP is estimated to be in the range 5-60 μM (2, 113, 247). Since this parameter is approximately equivalent to the equilibrium dissociation constant for enzyme-substrate binding, rate constants for the association of Ras-GDP/SOS (k_{12}) and Ras-GTP/GAP (k_{14}) were calculated from these estimates, assuming arbitrary values for the dissociation rate constant of 6 min^{-1} and 600 min^{-1} respectively; the latter is comparable to the reported rate of Ras-GTP dissociation from Raf (331). The reported specific activities of mammalian Ras GEFs vary between 0.02 and 4 s^{-1} (163, 200, 260), and that for p120GAP ranges from 5 to 20 s^{-1} (2, 113, 247).

Values representative of these estimates were used as the rate constants governing the irreversible enzyme-product release, or catalytic steps (k_{13} and k_{15}).

The majority of signalling events comprising the intermediate module can be viewed as an interaction between one molecule that is able to freely diffuse through the cytosol, and another that is restricted in its three-dimensional movement, through localization to the plasma membrane; for example, the dephosphorylation of Shc by unspecified cellular PTPases. These events were therefore considered to be spatially confined to a compartment immediately adjacent to the plasma membrane, representing only a fraction of the total cytosolic volume.

In such cases, any second-order rate constants (containing a concentration term) were converted from units of moles l^{-1} to molecule $cell^{-1}$ using a conversion factor equivalent to the volume of this compartment. Given that the width of the compartment corresponds to molecular dimensions (between 1 and 10 nm) (223), and assuming a cell radius of 5 μm (4) and a total cytosolic volume of 1×10^{-12} l (102), the volume was estimated to be 1.7×10^{-15} l $cell^{-1}$ (for a compartment of width 5 nm). Assuming homogeneous distribution of the freely diffusing molecule throughout the cytosol, this approach accounts for the proportion located at any one time within the sub-cellular compartment adjacent to the plasma membrane, and thereby reflects a reduction in the effective rate of the reaction arising through partial segregation of the participating molecules.

SOS-catalysed guanine-nucleotide exchange on Ras is an exception to this generalization, as both proteins are localized to the plasma membrane. This increases the local concentration and apparent affinity of the interacting proteins, and thereby the extent of the reaction, by up to three orders of magnitude (179). Hence, the K_d for Shc-Grb2-SOS/Ras-GDP binding was converted to units of molecule $cell^{-1}$ using the estimated volume of the juxtamembrane compartment as a conversion factor, reflecting the increased effective affinity of SOS for Ras within this environment. However, where only one of the interacting proteins is localized to the plasma membrane, the extent to which this interacts with a cytosolic protein is not enhanced (179), and the effective affinity constant (K_d or K_m) is the same as if the two proteins were both located cytosolically. The cytosolic volume was therefore used as a factor for converting the affinity constants for all other signalling events represented at the

intermediate level into the appropriate units. The converted values of the estimated simulation parameters are shown below in Table 3.8.

Table 3.8 Estimated parameter values for the combined top-level and intermediate, Ras activation, modules

k_n corresponds to the first- or second-order rate constant, for reaction number, n, of the reaction scheme given in Figure 3.1; V_n is the maximal enzyme rate and K_{mn} the corresponding Michaelis constant. All other parameter values as shown in Tables 3.4. and 3.7.

Parameter	Estimated Values	Reference
Receptor distribution		
$[R_s]_0$, molecule cell^{-1}	7.6×10^4	(112, 194)
$[R_i]_0$, molecule cell^{-1}	2.4×10^4	(112, 194)
Ligand binding		
$[L]_0$, nM	1.3×10^2	(291)
Shc phosphorylation		
[Shc], molecule cell^{-1}	5.0×10^4	(135)
k_9, min^{-1}	4.7	(257)
K_{m9}, molecule cell^{-1}	4.65×10^5	(257)
ShcP dephosphorylation		
V_{10}, molecule cell^{-1} min^{-1}	1.0×10^5	(17, 27, 177)
K_{m10}, molecule cell^{-1}	1.0×10^5	(17, 27, 155, 177)
ShcP/Grb2-SOS binding		
[Grb2-SOS], molecule cell^{-1}	5.0×10^4	(135)
k_{11}, molecule^{-1} minute^{-1}	3.23×10^{-4}	(63, 99, 263)
k_{-11}, min^{-1}	6.0	(99, 263)
Ras-GDP/ShcP-Grb2-SOS binding		
$[\text{Ras-GDP}]_0$, molecule cell^{-1}	1.98×10^4	(102, 237, 275)
$[\text{Ras-GTP}]_0$, molecule cell^{-1}	2.0×10^2	(102, 237, 275)
k_{12}, molecule^{-1} minute^{-1}	3.68×10^{-2}	(132, 163, 200)
k_{-12}, min^{-1}	6.0	-
Ras GDP/GTP exchange		
k_{13}, min^{-1}	25	(132, 163, 200)
Ras-GTP/GAP binding		
[GAP]	1.5×10^4	(135)
k_{14}, molecule^{-1} minute^{-1}	5.0×10^{-4}	(2, 113, 247)
k_{-14}, min^{-1}	6.0×10^2	-
GTP hydrolysis		
k_{15}, min^{-1}	1.0×10^3	(2, 113, 247)

3.3.2.6 Validation of the model

Within minutes of EGF stimulation *in vivo*, 50-80% of total cellular Shc translocates to the plasma membrane and is tyrosine phosphorylated (287). Figure 3.11 illustrates that in Rat1 cells, EGF-induced tyrosine phosphorylation of Shc reaches a maximum within 1 minute of EGF stimulation, but begins to decline after 2.5 minutes and approaches the basal level by 20 minutes (291), despite continuous exposure to EGF. A similarly rapid response is observed in hepatocytes (178).

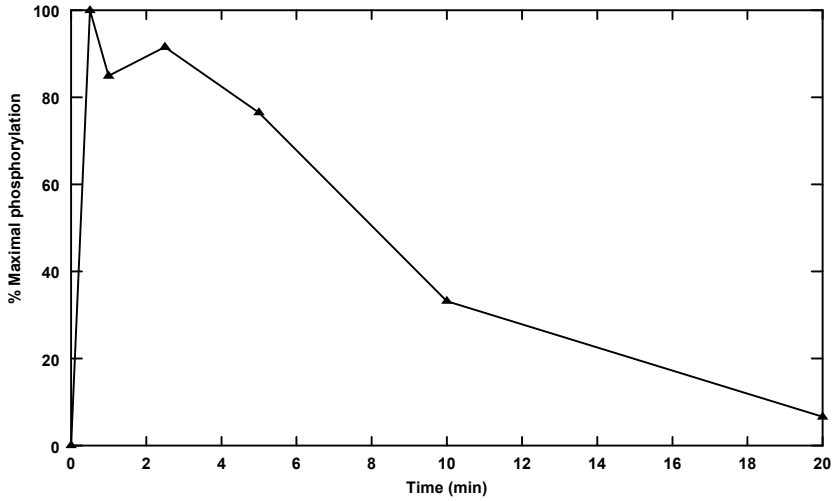

Figure 3.11 Time course of EGF-induced tyrosine phosphorylation of Shc in Rat1 cells

The data have been replotted from Sasaoka *et al.* (291); Rat1 fibroblasts were treated with 130 nM EGF for the indicated times. The results are expressed as the percentage of maximal tyrosine phosphorylation, and reflect the phosphorylation status of both free and complexed Shc.

A simulation consisting of the combined top-level and intermediate modules, implemented using the estimated values of parameters for Shc phosphorylation and Ras activation given in Table 3.8, was found to predict a time-dependent pattern of EGF-induced tyrosine phosphorylation of Shc which diverged from that observed experimentally: the initial response was delayed, with peak phosphorylation being achieved after around 5 minutes of EGF stimulation, and there was inadequate down-regulation of the response, as Figure 3.12 demonstrates. These data reflect the tyrosine phosphorylation status of both free and complexed forms of Shc, and the inconsistencies between the simulated and experimental time courses can partly be explained by considering the fate of the individual forms of phosphorylated Shc separately.

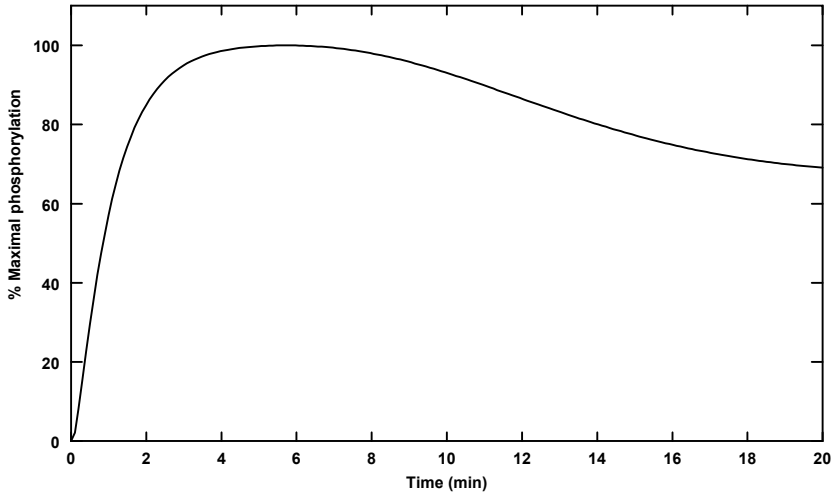

Figure 3.12 Simulated time course of EGF-induced Shc tyrosine phosphorylation in Rat1 cells
The simulation are parameters given in Table 3.8. The data are expressed as the percentage of maximal tyrosine phosphorylation, and reflect the phosphorylation status of both free and complexed Shc.

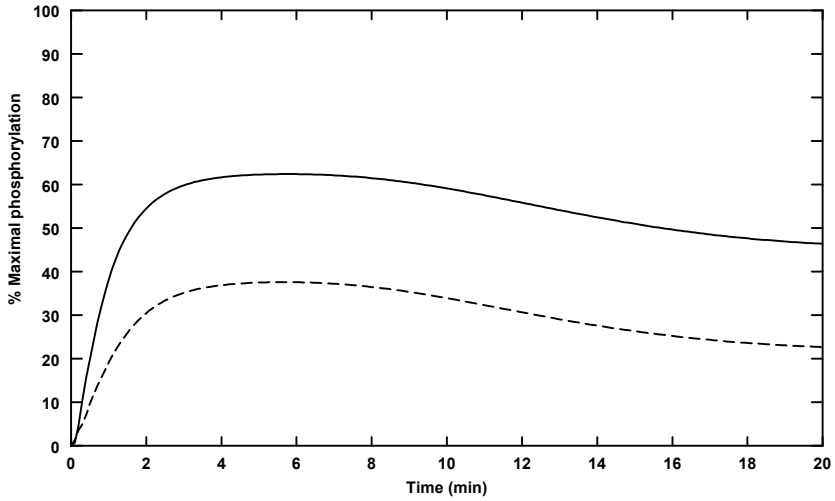

Figure 3.13 Simulated time courses of free Shc and Shc-Grb2-SOS complex tyrosine phosphorylation in Rat1 cells
The curves indicate the time courses of EGF-induced Shc-Grb2-SOS complex (solid line) and free Shc (dashed line) tyrosine phosphorylation. The simulation parameters are given in Table 3.8. The data are expressed as the percentage of maximal tyrosine phosphorylation.

The simulation predicts that the majority of tyrosine phosphorylated Shc forms a stable complex with Grb2-SOS, in agreement with experimental observations (178, 291). Since the phosphotyrosine of complexed Shc is assumed to be inaccessible to phosphatase activity, the majority of Shc therefore remains tyrosine phosphorylated throughout the simulated time period, as shown in Figure 3.13. Hence, the simulated pattern of sustained Shc phosphorylation predominantly reflects the high stability of

the Shc-Grb2-SOS complex, suggesting that in order for the phosphorylation state of Shc to return to the basal level, this stability must be reduced.

As discussed in the previous chapter, such a reduction in stability is brought about within the cell by feedback serine/threonine phosphorylation of SOS (32, 286), catalysed by ERK or a kinase downstream of the MAPK cascade (34, 62, 83, 145), which results in dissociation of the Shc-Grb2-SOS complex (55, 61, 76, 269, 286, 351); this presumably enables cellular phosphatases to gain access to Shc phosphotyrosine, which would otherwise be sequestered from phosphatase activity through Shc complex formation. Inhibitory feedback phosphorylation of SOS was not included in the model at this stage of development, and it is therefore not entirely surprising that the simulated behaviour of the system did not adequately reflect the down-regulation of EGF-induced Shc tyrosine phosphorylation typically observed in intact cells. However, other errors in the predicted Shc phosphorylation response, such as the rate at which peak phosphorylation is attained, are also the likely to reflect inaccuracies in the estimated values of the simulation parameters governing Shc tyrosine phosphorylation by the EGFR-TK, and ShcP/Grb2-SOS association.

The time course of EGF-induced Ras activation generated by the simulation was also found to differ considerably from reported for Rat1 cells; in this cell type, the proportion of Ras in the active GTP-bound state reaches a peak of around 20% within 5 minutes of EGF stimulation, but begins to decline after this time point (291). In contrast, the simulation predicts that more than 80% of total Ras is activated within only 1 minute, and that this level of activation is sustained for the remainder of the simulated time period (data not shown). This discrepancy in the down-regulation of Ras activation is again likely to be due to the absence of the feedback phosphorylation of SOS in the model, since this constitutes the primary mechanism for the specific attenuation of Ras signalling (351); dissociation of the Shc-Grb2-SOS complex at the plasma membrane, induced by SOS phosphorylation, releases Grb2-SOS to the cytosol and thereby isolates membrane-localized Ras from GEF activity. In addition, the predicted extent of maximal Ras activation, and the elevated rate at which this is achieved, may arise through errors in the estimated values of the simulation parameters.

In order to rationalize the predominant source of the error in the model, an attempt was made to determine a set of parameter values that might enable the simulation to

reproduce the patterns of Shc tyrosine phosphorylation and Ras activation typical of Rat1 cells, using the parameter fitting capability of Gepasi 3.2. However, no such set of values could be resolved, indicating that the model was likely to be structurally incorrect, rather than simply formulated using inaccurate estimates of parameter values. This was not unexpected, since at this stage of development the simulation was clearly deficient in terms of both a mechanism that regulates the status of the key Shc-Grb2-SOS signalling complex, as highlighted above, and also interactions between Ras and its target effector, Raf. The inadequacy of the model in reflecting the kinetics of EGF-induced Shc tyrosine phosphorylation and Ras activation in the absence of these interactions suggests that they play a fundamental role in determining the dynamic properties of the system, although it was also possible that there may have been other unforeseen omissions from the model. It was therefore decided to proceed with the planned development of the simulation, building upon the combined top-level and intermediate modules, and to review the compatibility of the model with experimental data upon the completion and integration of the final, MAPK module.

3.3.2.7 Summary

The preceding sections have described the formulation of the intermediate module of a computer simulation of the EGF signal transduction pathway. This component was intended to represent Ras activation, through tyrosine phosphorylation of the adaptor, Shc, by the activated EGFR-TK, and the formation of a ternary complex comprising phosphorylated Shc, the Grb2 adaptor protein and the Ras GEF, SOS, at the plasma membrane. Mechanisms for down-regulating the signal, through Shc dephosphorylation and GAP-stimulated Ras-GTP hydrolysis, were also included at this stage of model development. Combined with the completed top-level module, representing EGF-induced EGFR activation, this was expected to provide a dynamic simulation of EGF-stimulated Ras activation in Rat1 fibroblasts.

The time-dependent behaviour of the simulation was however, found to be incompatible with experimental data describing the EGF-induced tyrosine phosphorylation of Shc and activation of Ras *in vivo*. This discrepancy was ascribed primarily to the absence of a critical regulatory interaction from the model: the inhibitory feedback phosphorylation of SOS, catalysed by ERK, or a downstream target of this kinase, that causes disassembly of the Shc-Grb2-SOS complex. The

fundamental importance of this mechanism in terminating Ras signalling is emphasised by the inability of the incomplete simulation to reflect the behaviour of the actual system. Furthermore, this appears to confirm that Shc dephosphorylation and the antagonism of Ras activation by GAP play a secondary role, by dispersing any residual signal and inactivating individual components of the pathway, thereby enabling the system to revert to the basal activation state (see section 2.5.3).

Given that the simulation in its current form was clearly deficient as a model of Ras activation, it was decided to proceed with development of the final, MAPK cascade module, and to subsequently link this with the top-level and intermediate components through both Ras-mediated Raf activation, and feedback SOS phosphorylation. By taking this approach, it was envisaged that all the key elements of the system influencing the dynamics of Shc phosphorylation and Ras activation would be accounted for, resulting in a more appropriate model of both these intervening events, and the pathway as a whole.

3.3.3 THE FINAL MODULE: THE MAPK CASCADE

In the final stage of model development, a component representing the cytosolic Raf/MEK/ERK cascade was combined with the existing top-level and intermediate modules, to provide a complete simulation of EGF-induced ERK activation. To enable a comparison with available experimental data, the existing modules were previously intended to represent EGF signal transduction in fibroblasts. However, the simulation was tailored at this final stage to reflect the PC12 cell system, for the purpose of conducting a subsequent analysis of the properties of the system that determine the contrasting patterns of EGF and NGF-induced activation of the pathway in this particular cell type.

3.3.3.1 Ras-mediated Raf activation

All three mammalian Raf isoforms contribute to MAPK cascade activation in the PC12 cell line, but Raf-1 is activated transiently by both EGF and NGF, whilst A-Raf and B-Raf are responsible for sustained MEK and ERK activation in response to NGF (365). As discussed in the previous chapter, the precise details of the physiological mechanism of Raf activation remain elusive. A-Raf and Raf-1 are apparently activated in a similar

manner, through binding to Ras-GTP and phosphorylation at regulatory tyrosine and serine residues, but B-Raf activation is somewhat different (216, 218). Like Raf-1, B-Raf is localized to the cytosol in quiescent cells (326), but directly associates with Ras-GTP (164, 232) and is thereby translocated to the plasma membrane (216). A fundamental difference in the processes underlying Raf-1 and B-Raf activation results from the substitution of the B-Raf residues homologous to Tyr-340/341 of Raf-1 with aspartate residues (Asp-447/448) (166). B-Raf is therefore not tyrosine phosphorylated in response to growth factor stimulation (166, 261). Furthermore, the regulatory serine residue corresponding to Ser-338 of Raf-1 (Ser-445) is constitutively phosphorylated in B-Raf (218). These isoform-specific differences confer elevated basal kinase activity on B-Raf in comparison with Raf-1 (216), and suggest that B-Raf may be activated simply through binding to Ras-GTP (187).

Hence, Ras-GTP would be expected to be sufficient to activate isolated B-Raf, and this conclusion is apparently supported by some studies, in which the activity of partially purified B-Raf was assayed in a 'cell-free' system (254, 258). Another study however, demonstrates that purified phosphorylated B-Raf is not activated in the presence of Ras-GTP (338), implying that an additional activation factor is required. This is most likely to correspond to some mechanism in operation at the plasma membrane, since Ras-mediated membrane recruitment appears to be an essential element in B-Raf activation *in vivo* (216). *In vitro*, B-Raf activation mediated by Ras-GTP can be further enhanced by phospholipid cofactors (191), possibly reflecting a physiological activation mechanism. Alternatively, as growth factor stimulation has been shown to enhance B-Raf serine/threonine phosphorylation *in vivo* (326, 338), in a manner that correlates with kinase activation (165, 261), phosphorylation at unidentified regulatory sites cannot be excluded as an activating process.

For the purposes of model development, B-Raf was therefore considered to be activated both by binding to Ras-GTP, and through some additional mechanism, facilitated by Ras-mediated localization to the plasma membrane. The nature of this additional activating process is uncertain, but was presumed to correspond to serine/threonine phosphorylation at unspecified sites. As the mechanism of B-Raf activation assumed in the model is essentially the same as that putatively assigned to both A-Raf and Raf-1, these isoforms were not represented separately, but treated as a single cellular pool. Additional factors implicated in Raf activation, such as

dephosphorylation of a constitutive phosphoserine residue catalysed by PP2A (1), or modulation of catalytic activity by membrane phospholipids (37), although not directly implied, are not necessarily excluded.

Although it is not known whether other Raf isoforms must stay bound to Ras-GTP in order to remain catalytically active, Raf-1 is only transiently associated with Ras-GTP (328), and continued interaction with Ras is not required to sustain Raf-1 activation (198). Rather, Raf-1 is anchored to the plasma membrane independently of Ras, subsequent to membrane recruitment (328). The same was therefore assumed for A- and B-Raf.

Scaffolding proteins such as 14-3-3, Hsp90 and Cdc37 may have an important role in enhancing the specificity and efficiency of signal transduction, by coupling Raf to upstream activators and the downstream effector, MEK (187). However, in the absence of any relevant data, it was considered preferable to disregard these interactions rather than incorporate them into the model, which would necessitate making numerous, possibly invalid, simplifying assumptions.

Scant attention has been paid to the mechanism of Raf deactivation, but Raf-1 dephosphorylation is associated with inactivation of the enzyme (80), and presumably, since A-Raf is activated by the same means, this isoform may also be inactivated in the same way. Similarly, phosphatase treatment of activated B-Raf substantially reduces the *in vitro* kinase activity (326). Hence, deactivation of Raf in the model was considered to correspond to dephosphorylation, catalysed by the dual-specificity serine/threonine phosphatase, PP2A (228).

3.3.3.2 MEK and ERK activation

Both MEK isoforms (MEK1/2) are phosphorylated and activated by Raf, and both are capable of phosphorylating and activating either ERK 1 or ERK2 (187). MEK1 and MEK2 are also similar in terms of their mode of activation, as are both ERK isoforms, and hence these kinases were represented in the model as single cellular pools of MEK and ERK, respectively.

MEK kinases are activated through two separate phosphorylation events, at the sequence Ser-Met-Ala-Asn-Ser (123, 280, 383), catalysed by activated Raf (6);

phosphorylation of either residue was regarded as sufficient to activate MEK (6, 123, 280). Although there are minor differences in the specificity of the various isoforms of Raf for MEK1 and MEK2 (272, 369), these were not taken into account in the model, since the Raf isoforms were not considered separately. Activated MEK catalyses the phosphorylation of ERK at a conserved Thr-Glu-Tyr sequence (137); the lower specific activity of MEK1 (382) was not directly accounted for, given the representation of MEK1 and MEK2 as a single functional unit in the model. The phosphorylation of both regulatory residues was considered to be required for the activation of ERK (8).

MEK and ERK are co-localized within the cell through association with scaffolding proteins (110), such as KSR and MP1 (187), but as the necessary data are not available, no direct attempt was made to account for the effects of this phenomenon.

Both MEK and ERK are inactivated through phosphoserine and phosphothreonine dephosphorylation, catalysed by PP2A, whilst ERK is also phosphotyrosine dephosphorylated by an unspecified PTPase (5). Since the simulation was intended to represent activation of the MAPK cascade over a period of only 60 minutes continuous growth factor stimulation, translocation of ERK to the nucleus and dephosphorylation by nuclear MKPs were not considered.

3.3.3.3 Feedback SOS phosphorylation

As discussed above, EGF-induced Ras activation appears to be down-regulated primarily through the feedback phosphorylation of SOS, which results in dissociation of the Shc-Grb2-SOS complex (55, 61, 76, 269, 286, 351) and inactivation of guanine-nucleotide exchange on Ras (194). Feedback SOS phosphorylation is generally attributed to ERK (34, 62), and the majority of studies have noted only dissociation of the Grb2-SOS complex from Shc, or from the EGFR, with the association status of the Grb2-SOS complex remaining unaffected (146, 183, 269, 286). This particular scheme of events was therefore directly represented in the model. ShcP-Grb2-SOS complexes associated with Ras-GDP were presumed not to represent a target for ERK. In addition, functional Grb2-SOS is assumed to be reconstituted by dephosphorylation, although the specific phosphatase(s) involved in this process are not known.

3.3.3.4 Rate equations

Given that the K_m values for ATP reported for the kinases of the MAPK cascade are lower than cellular [ATP] (104, 214, 274, 281, 290), and assuming that the phosphatases involved also conform to the Michaelis-Menten model, the majority of the reactions comprising this final component of the simulation were represented by single-substrate Michaelis-Menten kinetics.

The exception to this generalization is Ras-mediated Raf activation, which was modelled in a manner analogous to that used to implement the reactions catalysed by SOS and GAP. This event is represented by an initial rapid Ras-GTP/inactive Raf binding equilibrium (Figure 3.1, step 16) (120, 331), followed by an irreversible step in which activated Raf is released from Ras (Figure 3.1, step 17). Although an inherent assumption is that this activation step corresponds to the phosphorylation of Raf at the plasma membrane, one or more additional events may actually be involved in this process, and this particular representation of Raf activation does not exclude alternative or additional activating steps. Furthermore, this scheme enables competition between Raf and GAP for binding to activated Ras to be considered.

3.3.3.5 Parameter values

Where appropriate, quantitative data specific for PC12 cells were employed in the model. The total number of EGFR expressed per cell, as well as the equilibrium dissociation constant and association rate constant for receptor-ligand binding were altered to reflect the PC12 system; the latter was derived by assuming the same k_r as in fibroblasts (k_{-1}), and calculating k_f (k_1) from the reported K_d (K_{d1}) for PC12 cells (157). All other parameters in the top-level module were retained. Similarly, in the absence of any more appropriate estimates, the values of the intermediate module parameters were also left unchanged at this stage.

The association and dissociation rate constants for the Ras-GTP/Raf binding equilibrium (k_{16} and k_{-16}) were initially assigned values reported for the interaction of the Raf-1 RBD with a Ras-GTP analogue complex (331). Specific values of these parameters for A- and B-Raf have not been reported. Although the Raf activation step was not modelled explicitly as a phosphorylation event, the rate constant for the release

of activated Raf from Ras-GTP (k_{17}) was initially considered to be equivalent to that estimated for the phosphorylation and activation of Raf (17, 177).

Specific estimates of the number of Raf, MEK and ERK molecules per cell were used (102), but initial values of the kinetic parameters for the activated forms of these kinases (Figure 3.1, steps 19 to 27, odd numbers) were derived from a variety of sources (17, 27, 155, 177); these are detailed in Table 3.9. Parameter values appropriate for Raf-1 were used to represent all the Raf isoforms, although B-Raf has been noted to have a greater affinity for MEK, and elevated kinase activity, in comparison with Raf-1 (216, 264, 272), whereas A-Raf has somewhat lower catalytic activity (216).

Kinetic parameters associated with dephosphorylation of the components of the cascade, and of phosphorylated SOS (Figure 3.1, steps 18 to 28, even numbers), were assigned values consistent with a range of estimates given in section 3.3.2.5 for cellular phosphatases (17, 27, 155, 177).

The recruitment of cytosolic Raf by membrane-associated Ras can be classified as an interaction between a membrane-localized protein, Ras, and one that is diffusely distributed throughout the cytosol, Raf. However, Raf activation and presumably inactivation occur at the plasma membrane, and these processes were therefore assumed to be confined within a compartment of defined volume, adjacent to the plasma membrane. The remainder of the MAPK cascade was considered to be homogeneously distributed within the cytosol. SOS phosphorylation was also presumed to take place at the plasma membrane, but this results in the release of Grb2-SOS from the complex formed with phosphorylated Shc, and the recycling of Grb2-SOS to the cytosol; SOS dephosphorylation was therefore assumed to be a cytosolic process.

Using the same rationale described previously (section 3.3.2.5), the relevant quantitative data were modified by a factor representing either the volume of the juxtamembrane compartment or the cytosolic volume, as appropriate, in order to convert from molar units to amount per cell. The converted values of all the estimated parameters are given below in table 3.9.

Table 3.9 Estimated parameter values for the combined top-level, intermediate and MAPK modules

k_n is the first- or second-order rate constant, for reaction number, n, of the reaction scheme given in Figure 3.1; K_{dn} is the corresponding equilibrium dissociation constant. V_n is the maximal enzyme rate and K_{mn} the corresponding Michaelis constant. All other parameter values are as shown in Tables 3.4, 3.7 and 3.8.

Parameter	Estimated Values	Reference
Receptor distribution		
$[R_s]_0$, molecule cell^{-1}	1.11×10^4	(112, 340)
$[R_i]_0$, molecule cell^{-1}	3.9×10^3	(112, 340)
Ligand binding		
$[L]_0$, nM	1.0×10^2	(245)
K_{d1}, M	1.9×10^{-9}	(157)
k_1, M^{-1} min^{-1}	3.8×10^8	-
k_{-1}, min^{-1}	0.73	-
Ras-GTP/Raf binding		
k_{16}, molecule^{-1} minute^{-1}	4.6×10^{-3}	(331)
k_{-16}, min^{-1}	4.0×10^2	(331)
Raf activation		
k_{17}, min^{-1}	26	(17, 177)
Raf inactivation		
V_{18}, molecule cell^{-1} min^{-1}	6.12×10^3	(17, 27, 177)
K_{m18}, molecule cell^{-1}	6.0×10^5	(17, 27, 155, 177)
MEK phosphorylation		
[MEK], molecule cell^{-1}	3.6×10^5	(102)
k_{19}; k_{21}, min^{-1}	6.0	(17, 177)
K_{m19}; K_{m21}, molecule cell^{-1}	4.8×10^5	(104)[a]
MEK dephosphorylation		
V_{20}; V_{22}, molecule cell^{-1} min^{-1}	3.6×10^6	(17, 27, 177)
K_{m20}; K_{m22}, molecule cell^{-1}	6.0×10^5	(17, 27, 155, 177)
ERK phosphorylation		
[ERK], molecule cell^{-1}	7.5×10^5	(102)
k_{23}; k_{25}, min^{-1}	1.45	(214)[b]
K_{m23}; K_{m25}, molecule cell^{-1}	2.04×10^5	(214)[b]
ERK dephosphorylation		
V_{24}; V_{26}, molecule cell^{-1} min^{-1}	3.6×10^6	(17, 27, 177)
K_{m24}; K_{m26}, molecule cell^{-1}	6.0×10^5	(17, 27, 155, 177)
SOS phosphorylation		
k_{27}, min^{-1}	1.4	(281)[c]
K_{m27}, molecule cell^{-1}	2.4×10^7	(281)[c]
SOS dephosphorylation		
V_{28}, molecule cell^{-1} min^{-1}	3.6×10^6	(17, 27, 177)
K_{m28}, molecule cell^{-1}	6.0×10^5	(17, 27, 155, 177)

[a] Value specified for phosphorylation of MEK by Raf-1

[b] Reported for phosphorylation of ERK2 by v-mos activated MEK1

[c] Value given for phosphorylation of the oncoprotein, TAL2, by ERK2

3.3.3.6 Validation of the completed simulation

At this stage of development, the simulation was structurally complete, and validation of the dynamic properties of the model was carried out by assessing the predicted time courses of Ras, MEK and ERK activation in comparison with those typically observed in PC12 cells. Numerous reports have demonstrated that the continuous stimulation of PC12 cells with EGF concentrations that generate a maximal response (157), results in a rapid, transient activation of Ras, MEK and ERK. The level of Ras-GTP rapidly reaches a maximum of up to 20% of total Ras within 2 minutes exposure to EGF, but declines to between 5 and 10% within 10 minutes and gradually returns to the basal level within 60 minutes (12, 237, 275). Similarly, MEK and ERK activation are maximal within 2-5 minutes, but MEK activation rapidly declines to less than 15% of the peak value within 30 minutes (339, 340), whilst ERK activation declines to between 7 and 40% of the maximum level by 30 minutes, and to between 9 and 23% within 60 minutes (5, 245, 335, 339, 340). Examples of typical experimental time courses of EGF-induced Ras, MEK and ERK activation in PC12 cells are given in Figure 3.14 below.

In order to compare the time-dependent behaviour of the computer simulation of EGF signal transduction with these experimental observations, the time courses of Ras, MEK and ERK activation were computed over 60 minutes continuous exposure to 100 nM EGF, at which a maximal cellular response is achieved (157). The simulated time courses of EGF-induced Ras, MEK and ERK activation were considerably different to those obtained experimentally, both in terms of the extent of activation of these components of the cascade, and once again, in the absence of any significant down-regulation of the response (data not shown). Since the major structural features of the pathway were believed to have been adequately represented at this stage, parameter fitting using Gepasi 3.2 was attempted, but with little success. This however, was attributed to a possible limitation of the fitting algorithms in solving a problem of the complexity associated with the model; the existence of a negative feedback interaction within the pathway considerably increases system complexity, by introducing interdependencies between several variables. Thus, an alternative approach was taken, whereby the parameters were fitted manually.

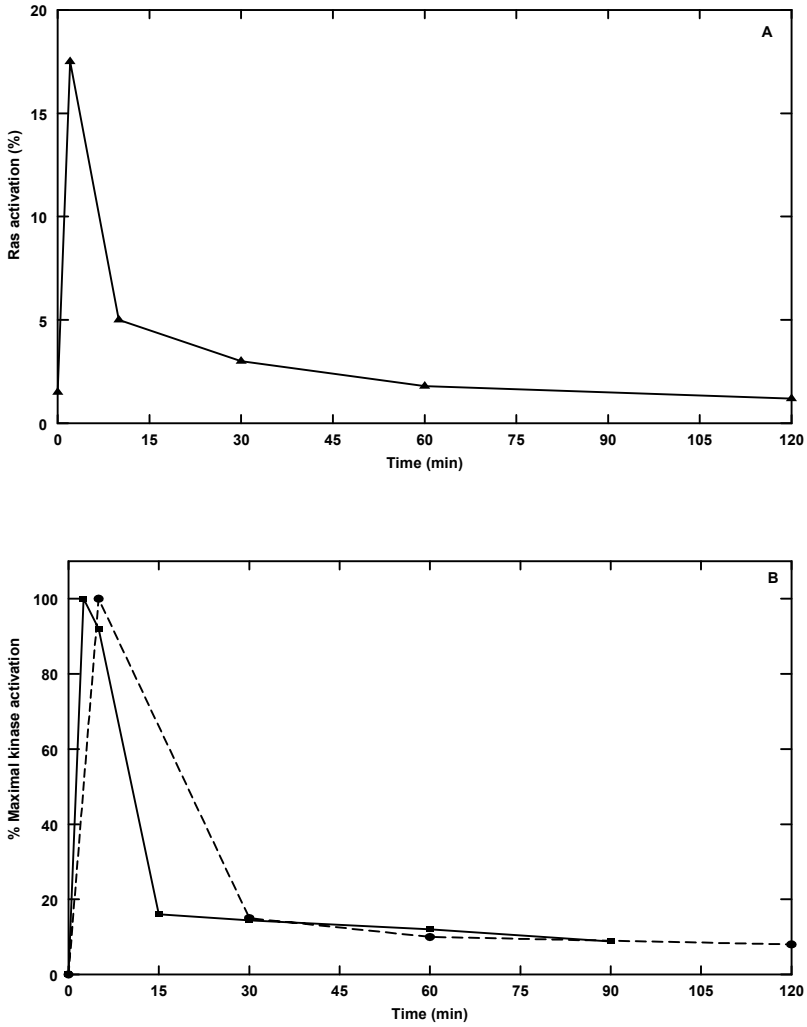

Figure 3.14 Experimental time courses of EGF-induced Ras, MEK and ERK activation in PC12 cells

PC12 cells were incubated for the indicated times with a saturating concentration of EGF. The data have been replotted from: (**A**) Muroya *et al.* (340), expressed as the percentage of total Ras in the GTP-bound form; (**B**) Traverse *et al.* (340) and Teng *et al.* (335), expressed as the percentage of maximal MEK (solid line, ■) or ERK (dashed line, ●) activation, respectively.

By employing a form of sensitivity analysis, the influence of the various parameters on the dynamic properties of the system was examined, and used as a rational basis for resolving a set of appropriate parameter values. Three aspects of system behaviour, or variables, were considered: the time to peak activation of Ras, MEK and ERK, the extent of maximal activation of these components of the cascade, and the level of activation remaining after 60 minutes EGF stimulation. To assess the sensitivity of these features of the system to variations in parameter values, the value of a selected parameter was changed from its original value (whilst maintaining all other parameters at their original values) and the effect on the simulated behaviour was observed. The majority of simulation parameters for the intermediate and MAPK cascade modules

were initially examined, except for the number of Ras, Raf, MEK and ERK molecules per cell, since variations in these values are essentially equivalent to variations in the kinetic parameters of the MAPK cascade. Those from the top-level module were also excluded, as the behaviour of this module had already been shown to be consistent with that *in vivo* (section 3.3.1.6). Parameter values were varied over appropriate ranges, consistent with either measured or estimated values specified in the literature (see sections 3.3.2.5 and 3.3.3.5), using the parameter scanning facility of Gepasi 3.2. For each parameter value, the corresponding values of the selected variables were recorded, thereby allowing the change in these variables over a spectrum of parameter values to be examined from a quantitative perspective.

The data generated by this analysis were represented graphically as a plot of log variable against log parameter value, an example of which is shown in Figure 3.15.

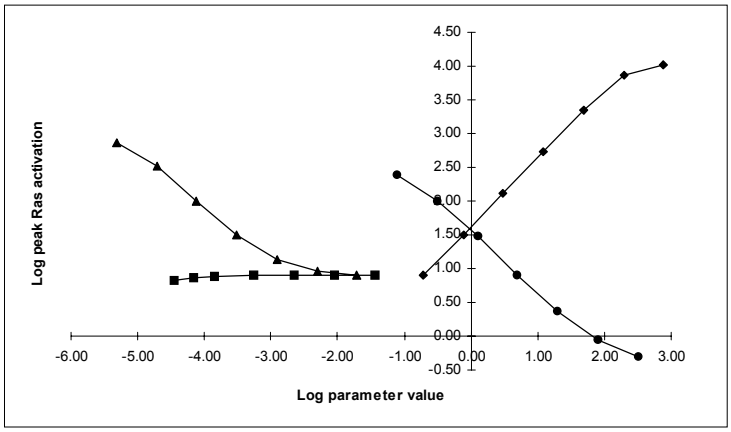

Figure 3.15 Sensitivity of peak EGF-induced Ras activation to variations in selected simulation parameters

Sensitivity of the selected variable to the rate of: Ras-GDP/ShcP-Grb2-SOS binding, k_{12} (■); Ras GDP/GTP exchange, k_{13} (◆); Ras-GTP/GAP binding, k_{14} (▲); and Ras-GTP hydrolysis, k_{15} (●). [EGF] = 100 nM; other simulation parameters are listed in Tables 3.3 and 3.9.

A separate plot was produced for each variable, illustrating the relative sensitivity of a particular variable to variations in several parameters. The parameter that has the greatest influence on the selected variable corresponds to the plot with the steepest gradient; in the example shown in Figure 3.15, the rate constant for the guanine-nucleotide exchange reaction (k_{13}) appears to have the greatest effect on the extent of Ras activation over the range of values examined, whilst the rate of Ras-GDP/Shc-Grb2-SOS binding (k_{12}) has little discernible influence on this variable. An appropriate

value for the selected parameter (i.e. one that generates simulated behaviour that is compatible with the experimental data) can be estimated from this plot, allowing the value assigned to the parameter to be adjusted accordingly. This methodology was repeated, with the newly fitted parameter eliminated from the analysis at each iteration, until an optimal fit to the data for all three aspects of system behaviour was established. By following this approach, a set of parameters (given in Table 3.10) was obtained that enabled the simulation to accurately reproduce the experimentally determined time courses of EGF-induced Ras, MEK and ERK activation in PC12 cells, as shown in Figure 3.16 below (cf. Figure 3.14), implying that the model is an adequate representation of these events within the cell.

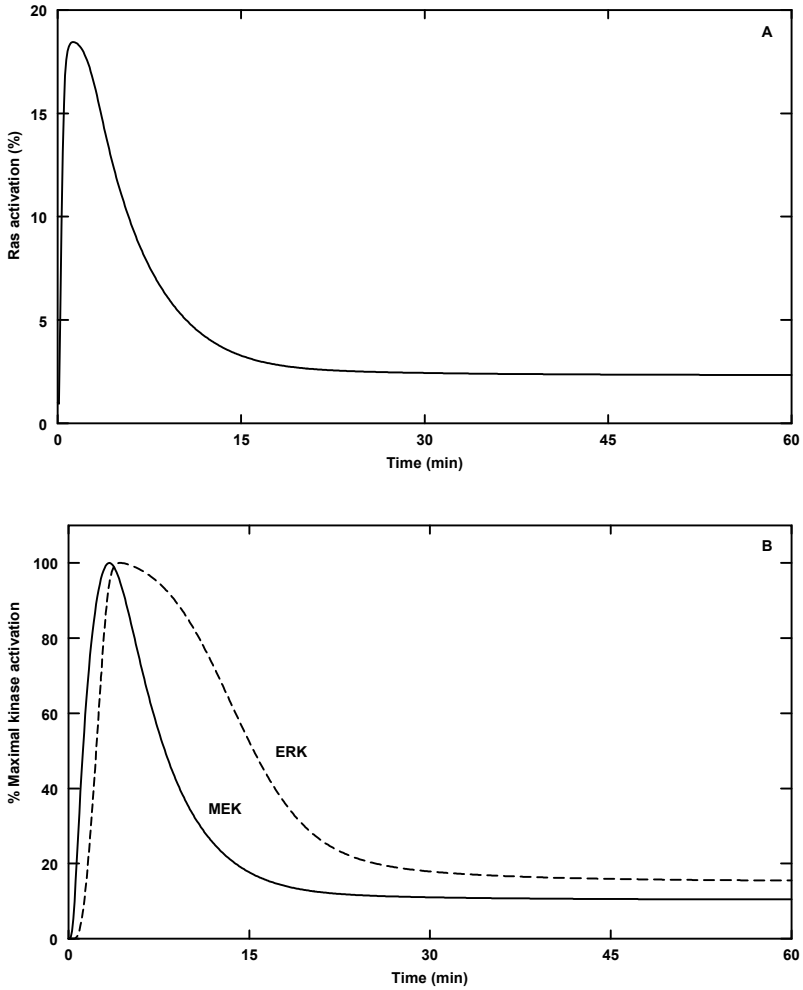

Figure 3.16 Simulated time courses of EGF-induced Ras, MEK and ERK activation in PC12 cells

The data are expressed as (**A**) the percentage of total Ras in the GTP-bound form and (**B**) the percentage of maximal MEK (solid line) and ERK (dashed line) activation. The time courses were computed over 60 minutes continuous exposure to 100 nM EGF; other simulation parameters are given in Table 3.10.

Thus, Ras activation reaches a peak of around 19% within 2 minutes of EGF stimulation, whilst MEK and ERK activation are maximal within 5 minutes. Despite continuous exposure to EGF, the activation level of Ras declines to 5% by 10 minutes, and approaches the basal level (approximately 2%) within 60 minutes. Similarly, MEK and ERK activation levels diminish to 11% and 15% of the maximal response, respectively, within 30 minutes. These simulated responses are typical of those observed in PC12 cells stimulated with a saturating concentration of EGF, as described above. Furthermore, the simulation correctly predicts that around 20% activation of Ras is sufficient to induce almost 100% ERK activation (102) (data not shown).

As discussed in the previous section, an incomplete simulation, consisting of only the top-level and intermediate modules, was unable to correctly reproduce the time course of EGF-induced Shc phosphorylation typically observed in fibroblasts. This failing was attributed primarily to a structural deficiency in the model, rather than any significant error in the estimated values of the simulation parameters. Thus, in order to establish whether the completed simulation was indeed an acceptable model of signal transduction from the activated EGFR to the MAPK cascade, this aspect of the simulated behaviour was reviewed.

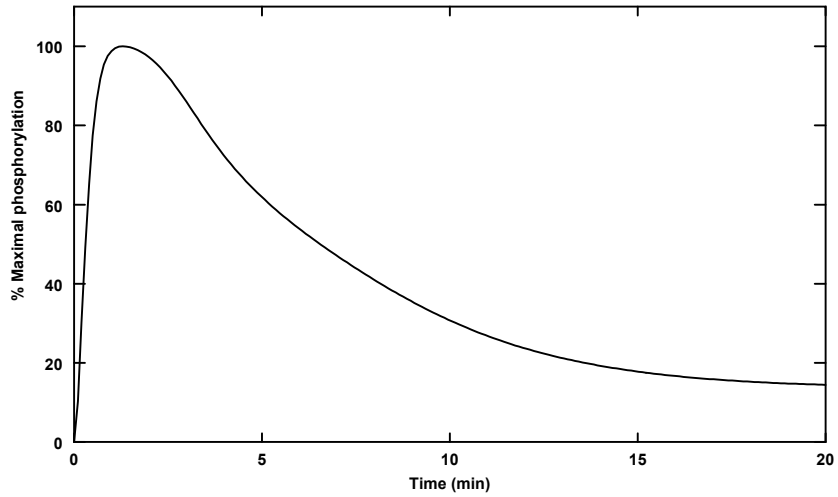

Figure 3.17 Simulated time course of EGF-induced Shc tyrosine phosphorylation in PC12 cells

The data are expressed as the percentage of maximal tyrosine phosphorylation, and reflect the phosphorylation status of both free and complexed Shc. The time course of phosphorylation was computed over 20 minutes continuous exposure to 100 nM EGF; other simulation parameters are given in Table 3.10.

No experimental data describing the pattern of EGF-induced Shc phosphorylation in PC12 cells were available. However, the activation of Ras and the MAPK cascade induced by EGF in this cell type is similarly transient in fibroblasts, and it seems plausible that the respective time courses of Shc phosphorylation might also be comparable. As Figure 3.17 illustrates, the completed simulation predicts a time-dependent pattern of EGF-induced Shc phosphorylation that is indeed compatible with that observed in fibroblasts (cf. Figure 3.11 above), suggesting that this may also be applicable in the PC12 cell type; maximal tyrosine phosphorylation is observed within 1 minute of EGF stimulation, but declines after 2.5 minutes, reaching a level that is less than 15% of the peak value by 20 minutes.

The only major change made to the intermediate module during completion of the simulation was structural, i.e. the incorporation of the feedback phosphorylation of SOS, and the parameter values for this component were not altered greatly during the model fitting process described above (see Table 3.10 below). This apparently confirms that the main source of error in the incomplete simulation was indeed the omission of this key regulatory mechanism, and supports the earlier proposal that this mechanism is of primary importance in down-regulating EGF signalling within the cell, in terms of both Ras activation and Shc phosphorylation (section 3.3.2.6).

3.3.3.7 Comparison of estimated and fitted parameter values

Table 3.10 provides a summary of the estimated and fitted parameter values for the intermediate and MAPK cascade simulation modules; initial estimates that were found to be appropriate are not recorded in the table. The majority of the fitted values do not vary greatly from the estimated values, although there are a few anomalies.

The most notable discrepancies are shown by the estimated and fitted values for the parameters defining the kinetics of Raf or GAP association with Ras-GTP. In order to generate a simulated rate and extent of MEK and ERK cascade activation compatible with that observed experimentally, the fitted dissociation rate constant for the binding of Ras-GTP to Raf (k_{-16}) was necessarily two orders of magnitude lower than the estimated value for this process. However, the latter was determined through an *in vitro* assay of the interaction between a Ras-GTP analogue complex and the RBD fragment of Raf-1 (331).

Table 3.10 Estimated and fitted parameter values for the completed simulation

k_n or V_n corresponds to the first- or second-order rate constant for reaction number, n, of the reaction scheme given in Figure 3.1; K_{mn} corresponds to the appropriate Michaelis constant. All other parameter values are as shown in Table 3.3. Where possible, the values listed are specific for PC12 cells.

Parameter	Estimated Values	Fitted values
Shc phosphorylation		
[Shc], molecule cell^{-1}	5.0×10^4	3.0×10^4
k_9, min^{-1}	4.7	12
K_{m9}, molecule cell^{-1}	4.65×10^5	6.0×10^3
ShcP dephosphorylation		
V_{10}, molecule cell^{-1} min^{-1}	1.0×10^5	3.0×10^5
K_{m10}, molecule cell^{-1}	1.0×10^5	6.0×10^3
ShcP/Grb2-SOS binding		
[Grb2-SOS], molecule cell^{-1}	5.0×10^4	2.0×10^4
k_{11}, molecule^{-1} minute^{-1}	3.23×10^{-4}	2.0×10^{-3}
k_{-11}, min^{-1}	6.0	3.8
Ras-GDP/ShcP-Grb2-SOS binding		
k_{12}, molecule^{-1} minute^{-1}	3.68×10^{-2}	1.63×10^{-2}
k_{-12}, min^{-1}	6.0	10
Ras GDP/GTP exchange		
k_{13}, min^{-1}	25	15
Ras-GTP/GAP binding		
K_{d14}, molecule cell^{-1} (calculated)	1.2×10^6	1.2×10^4
k_{14}, molecule^{-1} minute^{-1}	5.0×10^{-4}	5.0×10^{-3}
k_{-14}, min^{-1}	6×10^2	60
GTP hydrolysis		
k_{15}, min^{-1}	1.0×10^3	7.2×10^2
Ras-GTP/Raf binding		
K_{d16}, molecule cell^{-1} (calculated)	8.7×10^4	2.5×10^3
k_{16}, molecule^{-1} minute^{-1}	4.6×10^{-3}	1.2×10^{-3}
k_{-16}, min^{-1}	4.0×10^2	3.0
Raf activation		
k_{17}, min^{-1}	25	27
Raf inactivation		
V_{18}, molecule cell^{-1} min^{-1}	6.12×10^3	9.7×10^4
K_{m18}, molecule cell^{-1}	6.0×10^5	6.0×10^3
MEK phosphorylation		
k_{19}; k_{21}, min^{-1}	6.0	50
K_{m19}; K_{m21}, molecule cell^{-1}	4.8×10^5	9.0×10^3
MEK dephosphorylation		
V_{20}; V_{22}, molecule cell^{-1} min^{-1}	3.6×10^6	9.2×10^5
K_{m20}; K_{m22}, molecule cell^{-1}	6.0×10^5	6.0×10^5

Table 3.10 Continued

Parameter	Estimated Values	Fitted values
ERK phosphorylation		
k_{23}; k_{25}, min^{-1}	1.45	8.3
K_{m23}; K_{m25}, molecule cell^{-1}	2.04×10^5	9.0×10^4
ERK dephosphorylation		
V_{24}, molecule cell^{-1} min^{-1}	3.6×10^6	2.0×10^5
V_{26}, molecule cell^{-1} min^{-1}	3.6×10^6	4.0×10^5
K_{m24}; K_{m26}, molecule cell^{-1}	6.0×10^5	6.0×10^5
SOS phosphorylation		
k_{27}, min^{-1}	1.4	1.6
K_{m27}, molecule cell^{-1}	2.4×10^7	6.0×10^5
SOS dephosphorylation		
V_{28}, molecule cell^{-1} min^{-1}	3.6×10^6	75
K_{m28}, molecule cell^{-1}	6.0×10^5	2.0×10^4

This experimental system does not therefore, consider the binding of Ras to the Raf CRD, which is also likely to contribute to the overall affinity with which Raf binds Ras, and to the dynamics of the process. Thus, although the rate of dissociation of Ras from the isolated Raf RBD may indeed be high (120, 331), the overall rate of Ras-Raf dissociation could actually be somewhat lower, as this is also dependent on the Ras-binding characteristics of the CRD. This might perhaps explain why the fitted K_d for the Ras-Raf binding process (K_{d16}) is two orders of magnitude lower than that calculated from the estimated rate constants, but is actually more consistent with the value reported for Raf-1 in its entirety (229). Alternatively, the disparity between the estimated and fitted parameter values for Ras-Raf binding might reflect the difference between the *in vitro* and cellular environments. Membrane localization of signalling intermediates, such as Ras and Raf, can produce an increase in effective affinity, caused by a decrease in the dissociation rate constant resulting from 'macromolecular crowding' (179). Thus, it is plausible that the fitted parameter values may actually represent the *in vivo* system more faithfully than the original estimates. Although not immediately apparent, since the estimated and fitted values are consistent, the rate of Ras-GTP/Raf association (k_{16}) was also constrained within a narrow range, in order to generate the correct rate of MEK and ERK activation.

Similarly, the parameter fitting process suggests that the affinity of GAP for Ras-GTP is higher within the cell than measured *in vitro*, resulting from both a higher initial binding rate, and a lower dissociation rate than initially estimated. A rate of Ras-

GTP/GAP association (k_{14}) comparable to the rate of Ras-GDP/ShcP-Grb2-SOS binding (k_{12}) was found to be imperative in preventing the proportion of activated Ras exceeding experimentally determined levels, particularly in terms of the peak level of activation; down-regulation of the initial response was far less dependent upon these parameters. Even a reduced rate of Ras GDP/GTP exchange (k_{13}), or an increased rate of feedback SOS phosphorylation (k_{27}), was insufficient to counteract excessive peak Ras activation arising from a low rate of Ras-GTP/GAP binding. Although GAP is a cytosolic protein, the fitted K_d (K_{d14}) is actually more consistent with co-localization of GAP and Ras to the plasma membrane. Contrary to the assumptions made in developing the model (section 3.3.2.3), this implies that the anchoring of GAP to the plasma membrane within the vicinity of Ras, possibly through association with the activated RTK, is an important regulatory process (297). This would increase the effective affinity of the interaction between Ras and GAP (179), and thereby promote more efficient GTP hydrolysis than if GAP remained distributed throughout the cytosol, thus limiting the maximum level of Ras activation. Directly modelling the interaction between Ras-GTP and GAP has therefore revealed more detailed information about the functional properties of the system than might have been gained by representing this event as an enzyme-catalysed process, with the characteristics of enzyme-substrate binding governed by a single K_m.

The fitted parameter values for MEK and ERK phosphorylation (Figure 3.1, steps 19, 21, 23 and 35) also differ from those estimated, and suggest that MEK activation by Raf, and ERK activation by MEK, occur at a greater rate and with higher affinity within the cellular environment than indicated by *in vitro* measurements (104, 214). Although co-localization of Raf, MEK and ERK, through association with scaffolding proteins (110), was not directly considered in the model, this quantitative discrepancy may reflect an increase in the specificity and efficiency of MAPK cascade activation conferred by spatial organization of the cascade components (187); such an arrangement eliminates the limitations imposed by diffusion through the cytosol and thereby modulates the kinetics of cascade activation (27).

Nonetheless, a further consequence is that ERK is not only contained within a separate cellular compartment to its target, SOS, but also that both are restricted in their three-dimensional movement, through anchoring to the plasma membrane in the case of SOS, or through association within a cytosolic multi-protein complex in the case of

ERK. This may explain the low rate of SOS phosphorylation catalysed by ERK, and the relatively low affinity of this interaction (Figure 3.1, step 27). Although the fitted value for the rate of SOS phosphorylation is comparable to the estimated value, this is at the lowest extreme of a range of values determined *in vitro* for the specific activity of ERK, which varies between 1.4 and 120 min^{-1} (281). Similarly, the fitted K_m value is lower than expected, implying a higher affinity than that measured for the interaction between ERK and a number of *in vitro* substrates (281), but this is low in comparison with the values fitted for Raf and MEK. These fitted values could reflect the considerable limitations imposed upon the efficiency of SOS phosphorylation at the plasma membrane by the necessary diffusion of cytosolic ERK to this location.

Consistent with the hypothesis that scaffolding may serve to regulate interactions between proteins, both positively and negatively (110), this restriction, and the consequential low effective rate of SOS phosphorylation, may have some functional significance; these features of the cascade establish a delay in the negative feedback loop, which could give rise to a wave of activation (i.e. phosphorylation) that travels through the cell, possibly encoding a temporal signal (27, 177). Assuming a typical cell radius of between 5 and 50 μm, for a eukaryotic cell (4), and a diffusion coefficient for the movement of a soluble protein through the cytosol of 5×10^{-8} cm^2 s^{-1} (reported to be between 1×10^{-7} and 1×10^{-8} cm^2 s^{-1}) (27), the time taken for a cytosolic protein to travel from the cytosol to the plasma membrane can be estimated to be between approximately 5 and 500 seconds (0.083 and 8.33 minutes). Given that the reversible association of ERK with structural components of the cell, i.e. MAPK cascade scaffolding proteins, could substantially reduce the actual rate of diffusion (27), this range may even be rather conservative. Nonetheless, these estimates do illustrate how sequestration and localization of ERK within the cytosol could readily give rise to a substantial delay in the feedback circuit.

A conspicuous disagreement is found between the estimated and fitted values for the maximal rate of SOS dephosphorylation (V_{28}), the latter being several orders of magnitude lower than originally estimated. In fact, the fitted value is outside the range of values deemed appropriate for dephosphorylation within the cytosolic compartment, but is acceptable if SOS dephosphorylation occurs at the plasma membrane (see sections 3.3.2.5 and 3.3.3.5). In constructing the model, this process was assumed to take place within the cytosol, following the release of phosphorylated Grb2-SOS from

a complex formed at the plasma membrane with phosphorylated Shc. The fitted value for the rate of SOS dephosphorylation is therefore incompatible with this initial assumption, and furthermore, implies that this event actually occurs at the plasma membrane. A plausible explanation for this inconsistency may be that the diffusion of phosphorylated Grb2-SOS back into the cytosol, where it is dephosphorylated, is relatively slow, allowing a spatial gradient of the phosphorylated form (high close to the plasma membrane and low within the cytosol) to develop (27). The estimated time-scale for the diffusion of a soluble protein across the radius of the cell, given above, confirms that this is a possibility.

Thus, SOS dephosphorylation would be expected to occur largely in proximity to, although not directly at, the plasma membrane, since this is where the bulk of the phosphorylated form would be located. However, the rate of this process would be comparatively low, since the phosphatase involved would presumably be homogeneously distributed throughout the cytosol, and not located solely within the vicinity of its target, phosphorylated SOS. The rate of SOS dephosphorylation may therefore be limited both by diffusion of the substrate, and partial segregation from the phosphatase responsible for catalysing the reaction. Hence, the fitted parameter values for SOS dephosphorylation could reflect this limitation, which in fact may be essential for SOS phosphorylation to function as a regulatory mechanism; a high rate of SOS dephosphorylation, consistent with homogenous distribution throughout the cytosol of both phosphorylated SOS and the phosphatase involved, was found to result in persistent Ras and MAPK cascade activation, through rapid reconstitution of a functional Shc-Grb2-SOS complex. This observation was explored further during subsequent phases of the project (see Chapters 4, 5 and 6).

In reality, the cellular distribution of phosphorylated SOS is likely to be more complex than a simple gradient between the plasma membrane and the cytosol; activated ERK probably also phosphorylates free cytosolic Grb2-SOS, although this permutation is not accounted for in the simulation, whilst the delay in the feedback loop further contributes to the complexity of the system. Although contrary to those initially estimated, the fitted parameter values may therefore enable the simulation to approximate a highly complex temporal and spatial pattern of SOS and MAPK cascade phosphorylation, which cannot be directly represented due to the necessary simplifications made in constructing the model.

As previously suggested (3.3.2.6), the estimated rate of ShcP-Grb2/SOS association (k_{11}), calculated from the reported K_d for the *in vitro* binding of Grb2-mSOS1 and a Shc-derived phosphopeptide (63), was found to be inappropriate. Indeed, the fitted values for k_{11} and k_{-11} imply that the affinity of Grb2-SOS for ShcP is at least 10-fold greater *in vivo* than indicated by the initial estimates for these parameters. Finally, it can be noted that although the two steps involved in ERK dephosphorylation were initially assigned the same parameter values, a better fit to the data was obtained by discriminating quantitatively between these steps (Figure 3.1, steps 24 and 26). Thus, threonine dephosphorylation was assumed to precede tyrosine dephosphorylation (5), with a higher maximal rate, but similar affinity. An improved fit was also obtained by assuming a lower K_m for Shc phosphorylation catalysed by the EGFR-TK (K_{m9}); given that the initial estimate reflects a value determined through an *in vitro* assay (257), which is unlikely to be directly applicable within the cell, this is not remarkable. Other minor discrepancies in estimated and fitted parameter values for Shc, Raf, MEK and ERK dephosphorylation (Figure 3.1, steps 10, 18 to 26, even numbers) and Ras-GTP/ShcP-Grb2-SOS binding (Figure 3.1, step 12) are also not significant, since the initial values were arbitrary estimates and would therefore be expected to have some degree of inaccuracy. The fitted values of these parameters are all consistent with the appropriate estimated ranges.

3.3.3.8 Summary

This final section of the chapter has documented the completion of a computer simulation of EGF signal transduction, composed from three interconnected modules representing the activation of the EGFR at the cell surface, Ras activation at the plasma membrane and activation of the cytosolic MAPK cascade, respectively. The time-dependent behaviour of the simulation was shown to be compatible with the pattern of Ras, MEK and ERK activation typically observed in PC12 cells stimulated with EGF, indicating that the completed model is an adequate representation of EGF-induced MAPK cascade activation in this cell type. Furthermore, the time course of Shc phosphorylation predicted by the completed simulation was also found to be consistent with that observed *in vivo*, confirming that the earlier inability of an incomplete simulation to reflect this aspect of EGF signal transduction was correctly ascribed to the absence of a key regulatory mechanism from the model (section 3.3.2.6). This

mechanism, the feedback phosphorylation of SOS, was thereby identified as probably being of fundamental importance in the down-regulation of EGF signalling within the cellular environment, in terms of both Ras activation and Shc phosphorylation. The parameter fitting process also confirmed that the interaction of Ras-GTP with GAP is likely to be far less significant in down-regulating the initial peak in EGF-induced Ras activation (see section 3.3.2.7), but may have an important role in limiting the extent of this response.

Other, possibly significant observations include a greater predicted affinity of Ras-GTP for both GAP and Raf within the cell than suggested by *in vitro* estimates and similarly, a greater affinity of Raf for MEK, and MEK for ERK. Both findings imply that the sub-cellular localization of signalling intermediates may be an important regulatory feature, as previously speculated (section 3.3.2.1). Thus, the anchoring of Raf and GAP to the plasma membrane, in the vicinity of Ras-GTP, may increase the effective affinity of Ras-GTP binding, whilst the co-localization of MAPK components, through association with scaffolding proteins, may enhance the specificity and efficiency of signalling through cascade. The segregation of SOS from both ERK and cellular phosphatases could also have some relevance to the functional role of SOS phosphorylation as a feedback down-regulation mechanism; thus, separation from ERK establishes a time delay in the feedback circuit, whilst a low effective rate of SOS dephosphorylation is critical in maintaining desensitization of the system.

CHAPTER 4

SENSITIVITY ANALYSIS OF THE EGF SIGNALLING PATHWAY

4.1 INTRODUCTION

A common theme throughout the remainder of the thesis is an exploration of the properties demonstrated by the computer simulation of EGF signal transduction introduced in the previous chapter, and the feasibility of extrapolating these to growth factor signalling in general. These issues are directly addressed in the current chapter, with the presentation of the results of a sensitivity analysis of the model; this provides both a means of appraising the robustness of the simulated behaviour, and a quantitative basis for discussing the dynamic features of the system.

4.2 METHODOLOGY

The sensitivity of the simulated behaviour of the EGF signal transduction pathway to variations in system parameters was analysed using the same methodology described in section 3.3.3.6. Four aspects of system behaviour were considered in the analysis. Firstly, the distribution of receptor species after 60 minutes continuous exposure to EGF. For the purposes of this analysis, no distinction was made between monomeric and dimeric receptor species. The variables of interest were therefore defined as: free cell surface receptors, R_{Free} (directly equivalent to the species R_s, shown in the reaction scheme of Figure 3.1); cell surface receptor-ligand complexes, R_{Bound} (the sum of RL and R2L2); receptors associated with coated pit adaptor protein at the cell surface, R_{CPP} (corresponding to R2L2-CPP); and internalized receptor, R_{Int} (equivalent to R_i + $R2L2_i$), all expressed as a percentage of the total receptors in the system.

Also monitored were: the maximum extent of Shc phosphorylation, in addition to Ras and ERK activation (p_{Max}, expressed as a percentage of total cellular content); the time at which peak phosphorylation/activation is achieved (t_{Max}, expressed in minutes); and

the level of phosphorylation/activation remaining after 60 minutes EGF stimulation (p_{60}, expressed as a percentage of the total cellular content).

The values of several of the top-level module parameters were taken as invariant, as these define the dynamic properties of events that are not explicitly included in the model (i.e. those associated with the time delay function; see section 3.2.2.3 and ref. 112), and were therefore omitted from the analysis. The majority of the remaining parameters were however, varied over ranges consistent with previously estimated or experimentally determined values. In addition, the response to EGF was further investigated, by varying the simulated concentration over a range that elicits the full scope of cellular responses *in vivo* (157).

Where no definitive limiting values were available, for example for the endocytic rate constant, k_e, which features in a number of steps (reactions 2, 3, 5, 6 and 8 of the reactions scheme shown in Figure 3.1), the initial value was varied over two orders of magnitude. In the case of binding events for which several differing estimates of K_d are available, for example for Ras-GDP and SOS binding (132, 163, 200), the forward rate constant for the reaction was varied progressively, with the reverse rate constant remaining unchanged, to observe the effect of variations in K_d over the possible range evident from the literature[2]. The limits between which the influence of each parameter was investigated are given below in Table 4.1.

As described previously, a plot of log variable against log parameter was generated (section 3.3.3.6), and a dimensionless 'sensitivity coefficient', S_p^{v}, was defined as the slope of this plot (averaged over the whole range of values), or the ratio of the change in log variable to the change in log parameter; a value of zero denotes no discernible effect, a positive value indicates that the variable increases with the parameter, whilst a negative value indicates that an increase in the parameter results in a decrease in the variable over the range of values investigated. Comparison of these coefficients therefore allows a quantitative assessment of the relative influence of the simulation parameters on individual aspects of system behaviour.

[2] Variations of k_r over the same range, with k_f unchanged, would result in the same modulation of K_d, and hence this was not separately investigated.

Table 4.1 Ranges of values over which the specified simulation parameters were varied in the sensitivity analysis of the EGF signal transduction pathway

k_n or V_n corresponds to the first- or second-order rate constant for reaction number, n, of the reaction scheme given in Figure 3.1; K_n or K_{mn} corresponds to the appropriate equilibrium or Michaelis constant. Concentrations and affinity constants are expressed in molecule cell^{-1}; first-order and second-order rate constants are given in minute^{-1} and molecule^{-1} minute^{-1} respectively, unless otherwise specified. All values are appropriate for the sub-cellular compartment in which the reaction is assumed to take place, unless explicitly stated.

Parameter	Range of Values	Reference
Receptor-ligand binding		
[EGF], M	2.0×10^{-13} - 1.0×10^{-9}	(157, 245)
$[EGFR]_{Total}$	1.0×10^{4} - 1.0×10^{6}	(43)
k_1 (K_{d1}), M^{-1} min^{-1} (M)	7.3×10^{7} (1.0×10^{-8}) - 7.3×10^{9} (1.0×10^{-10})	(112, 185, 239, 348, 360)
Dimerization		
k_4	1.8×10^{-4} - 1.8×10^{-2}	(143)
CPP binding		
k_7, (K_{d7})	0.1 (3.47×10^{-3}) - 10 (3.47×10^{-5})	(112)
Internalization		
k_2; k_{-3}; k_5; k_6; k_8, min^{-1}	0.10 - 1.0	(112)
Shc phosphorylation		
[Shc]	1.0×10^{4} - 2.0×10^{5}	(135)
k_9	6.0 - 60	(135)
K_{m9}	6.0×10^{3} - 9.0×10^{6}	(17, 27, 155, 177)
ShcP dephosphorylation		
V_{10}, molecule cell^{-1} min^{-1}	0.6 - 3.0×10^{6}	(17, 27, 177)
K_{m10}, molecule cell^{-1}	6.0×10^{3} - 9.0×10^{6}	(17, 27, 155, 177)
ShcP/Grb2-SOS binding		
[Grb2-SOS]	1.0×10^{4} - 2.0×10^{5}	(135)
k_{11} (K_{d11})	2.0×10^{-3} (1.5×10^{3}) - 2.0×10^{-1} (15)	(63)
SOS/Ras-GDP binding		
$[Ras]_{Total}$	1.0×10^{4} - 2.0×10^{5}	(102)
k_{12} (K_{d12})	2.5×10^{-5} (4.1×10^{5}) - 6.0×10^{-2} (1.6×10^{2})	(163, 200, 260)
Ras GDP/GTP exchange		
k_{13}	1.2 - 2.4×10^{2}	(163, 200, 260)
Ras-GTP/GAP binding		
[GAP]	1.0×10^{4} - 2.0×10^{5}	(135)
k_{14} (K_{d14})	5.0×10^{-4} (1.2×10^{5}) - 5.0×10^{-2} (1.2×10^{3})	(113)
GTP hydrolysis		
k_{15}	3.0×10^{2} - 1.2×10^{3}	(2, 113, 247)
Ras-GTP/Raf binding		
[Raf]	1.0×10^{4} - 1.0×10^{6}	(102)
k_{16}(K_{d16})	1.2×10^{-4} (2.5×10^{4}) - 1.0×10^{-2} (2.5×10^{2})	(229)
Raf activation		
k_{17}	0.15 - 2.4×10^{2}	(17, 177)
Raf inactivation		
V_{18}	0.6 - 3.0×10^{6}	(17, 27, 177)
K_{m18}	6.0×10^{3} - 9.0×10^{6}	(17, 27, 155, 177)
MEK phosphorylation		
[MEK]	1.0×10^{4} - 1.0×10^{6}	(102)
k_{19}; k_{21}	1.5 - 2.4×10^{2}	(17, 27, 177)
K_{m19}; K_{m21}	6.0×10^{3} - 9.0×10^{6}	(17, 27, 104, 155, 177)

Table 4.1 Continued.

Parameter	Range of Values	Reference
MEK dephosphorylation		
V_{20}; V_{22}	3.6×10^2 - 1.8×10^9	(17, 27, 177)
K_{m20}; K_{m22}	6.0×10^3 - 9.0×10^6	(17, 27, 155, 177)
ERK phosphorylation		
[ERK]	1.0×10^4 - 1.0×10^6	(102)
k_{23}; k_{25}	1.45 - 2.4×10^2	(17, 27, 177, 214)
K_{m23}; K_{m25}	6.0×10^3 - 9.0×10^6	(17, 27, 155, 177, 214)
ERK dephosphorylation		
V_{24}; V_{26}	3.6×10^2 - 1.8×10^9	(17, 27, 177)
K_{m24}; K_{m26}	6.0×10^3 - 9.0×10^6	(17, 27, 155, 177)
SOS phosphorylation		
k_{27}	1.4 - 1.2×10^2	(281)
K_{m27}	6.0×10^3 - 9.0×10^6	- [a]
SOS dephosphorylation		
V_{28}	0.6 - 3.0×10^6	(17, 27, 177) [b]
K_{m28}	6.0×10^3 - 9.0×10^6	(17, 27, 155, 177) [b]

[a] The range of values reported for *in vitro* substrates (281) were found to be too high, and that used is consistent with the premise that the affinity of an interaction between a membrane-anchored and a cytosolic protein is the same as if the two partners were both located cytosolically (179).
[b] The fitted values for these parameters were found to be more consistent with an assumption that this event occurs at the plasma membrane (section 3.3.3.7); hence, a range of values appropriate for this environment was considered.

4.3 RESULTS AND DISCUSSION

The data resulting from the analysis described above are summarized in Tables 4.2 to 4.6 below, and discussed in the following sections.

4.3.1. RECEPTOR DISTRIBUTION

Only the top-level module parameters were found to exert an influence on the distribution of receptor species after continued exposure to EGF, and hence these results are tabulated separately in Table 4.2. The observation that variations in the intermediate and MAPK cascade module parameters have no effect on this aspect of simulation behaviour is not surprising, given the structure of the model, in which there is only a unidirectional link between the top-level and subsequent modules, through the phosphorylation of Shc by the activated EGFR-TK. In reality, components downstream of the EGFR in the signalling cascade are likely to modulate RTK activity through a variety of feedback mechanisms (161, 231, 342), and may thereby affect the distribution of active receptors between sub-cellular compartments.

Much of the data in Table 4.2 are not unexpected; for example, by promoting the redistribution of cell surface receptor species to the intracellular compartment (R_{Int}), an increase in the rate of internalization (k_2, k_{-3}, k_5 and k_8) dramatically decreases the amount of receptor associated with coated pit adaptor proteins (R_{CPP}), in addition to reducing the number of receptor-ligand complexes (R_{Bound}) and unoccupied receptors (R_{Free}). Although an enhanced rate (k_7) and affinity (K_{d7}) for the interaction of activated receptors with coated pit proteins produces a similar decrease in R_{Bound}, and a concomitant increase in R_{CPP}, this does not greatly affect R_{Free} or R_{Int}, suggesting that the low endocytic rate is a limiting factor for internalization through this route. Furthermore, consistent with a high affinity, but low capacity ligand-induced internalization mechanism (210, 359), K_d for the dissociation of active receptor dimers from coated pit proteins (K_{d7}) is extremely low in comparison with the total number of receptors: 3.47×10^{-4} molecule cell^{-1} compared to 1.5×10^{4} molecule cell^{-1}.

Table 4.2 Summary of the quantitative sensitivity analysis of the EGF signalling pathway: top-level module parameters

The results are expressed in the form of sensitivity coefficients, S_p^r, which quantify the influence that a particular parameter exerts on a specified variable.

Parameter	R_{Int}	R_{Free}	R_{CPP}	R_{Bound}
Internalization; k_2; k_{-3}; k_5; k_8	0.28	-0.18	-1.53	-0.39
CPP binding, k_7 (K_{d7})	0.06	0.05	0.36	-0.46
[EGF]	0.01	-0.36	1.11	0.72
Receptor-ligand binding, k_1 (K_{d1})	0.00	-1.00	0.01	0.00
Dimerization, k_4	0.00	-0.11	0.03	-0.03
$[EGFR]_{Total}$	0.00	-0.10	0.03	-0.02

Thus, given both the relatively low rate of endocytosis through both constitutive and coated pit pathways, and the saturability of the ligand-induced internalization mechanism, it is reasonable to surmise that these factors may limit the potential of other parameters to directly modify the distribution of receptors between the cell surface R_{Free}, R_{Bound} and R_{CPP} species, and the intracellular R_{Int} form. Indeed, the inability of the remaining parameters to substantially affect R_{Int}, R_{Bound} or R_{CPP} further supports this conclusion.

Conversely, the number of free cell surface receptors (R_{Free}) is moderately sensitive to changes in many of the parameters. Of these, EGF concentration has the greatest overall impact on the distribution of R_{Free}, in addition to R_{CPP} and R_{Bound}, as might be

expected; the value of this parameter directly establishes the extent of receptor-ligand binding (R_{Bound}), and consequently the amount of free cell surface receptor remaining (R_{Free}), as well as indirectly determining the extent of dimerization and association of activated receptor with coated pit protein (R_{CPP}). The range over which [EGF] was varied induces a full spectrum of responses, from virtually undetectable to almost maximal receptor occupancy, which is reflected in the magnitude of the calculated coefficients.

Since [EGF] has such a dramatic effect on receptor distribution, by directly influencing the maximal extent of receptor-ligand binding, the contrasting response of the system to the equilibrium and rate constants for this process (K_{d1} and k_1) is somewhat surprising. Contrary to an earlier unquantified observation, noted during the parameter fitting process (see section 3.3.1.6), the values assumed for these parameters appear to be of little importance to the overall steady state distribution of receptor species; the extent of their influence is restricted to R_{Free}, but is of less significance than immediately apparent, and merely constitutes a reduction in R_{Free} from a maximum of less than 1%, to a minimum of less than 0.01%.

This inconsistency can be accounted for by considering the concentration of EGF at which the sensitivity coefficients given in Table 4.2 were calculated: 100 nM, in comparison with a variable K_d for receptor-ligand binding (K_{d1}) of between 0.1 nM and 10 nM. This is also considerably greater than the EGF concentration of 0.33 nM at which the parameter fitting process was carried out. Hence, 100 nM EGF represents a saturating ligand concentration, at which a maximal response is achieved, and there is limited potential for an increase in the affinity (over the comparatively narrow range investigated) or the rate of receptor-ligand binding to augment the magnitude of response (although the time-scale may be affected). However, at the sub-saturating concentration of 0.33 nM, there is a greater margin for modulation of the response. That a saturating concentration of EGF imposes such a restriction on the sensitivity of the system to a corresponding increase in the rate (k_1) and affinity (K_{d1}) of receptor-ligand binding, is evidenced by reassessment of the sensitivity coefficients for these parameters at a sub-saturating EGF concentration of 0.1 nM[3], as shown in Table 4.3.

[3] Sensitivity coefficients for selected parameters were recalculated at a lower concentration of EGF in order to illustrate a particular point of discussion. A comprehensive sensitivity analysis of the model under these conditions

The significance of this increased sensitivity at low [EGF], in terms of the time course of receptor distribution, is illustrated by Figure 4.1 below; a 100-fold increase in k_1 (and hence also K_{d1}) at 0.1 nM EGF clearly shifts the time-frame of receptor-ligand binding, and substantially reduces the amount of free cell surface receptor, thereby increasing the proportion of the ligand-bound and coated pit-associated forms.

Table 4.3 Summary of the quantitative sensitivity analysis of the EGF signalling pathway at 0.1 nM EGF: top-level module parameters
The results are expressed in the form of sensitivity coefficients, S_p^r.

Parameter	R_{Int}	R_{Free}	R_{CPP}	R_{Bound}
Receptor-ligand binding, k_1 (K_{d1})	0.03	-0.28	1.11	0.64
Dimerization, k_4	0.00	-0.03	0.49	0.15
$[EGFR]_{Total}$	0.00	-0.03	0.26	0.12

Thus, repeating the sensitivity analysis at a sub-saturating EGF concentration confirms that the dynamic behaviour of the top-level module is strongly dependent on the kinetic constants for receptor-ligand binding under these conditions, as previously observed at 0.33 nM EGF. However, it should also be noted that a qualitatively similar pattern is observed over the simulated time-period, in terms of a transient peak in R_{Free}, R_{Bound} and R_{CPP} and a progressive increase in R_{Int}, culminating in the attainment of a steady state.

The minimal impact of variations in the rate of receptor-receptor association (k_4) at 100 nM (Table 4.2) provides a further example of the limiting effect of saturating EGF on the sensitivity of the system to changes in parameter values. An increase in the rate of dimerization increases the proportion of dimeric receptors accounted for in the variable R_{Bound}, marginally reducing R_{Free}, but the distribution of occupied receptors between the cell surface and intracellular compartments is unchanged. Recalculation of the coefficients at 0.1 nM (Table 4.3) demonstrates that the rate of dimerization does however, assume greater importance at a sub-saturating EGF concentration; the pattern observed under these conditions indicates a rise in both R_{CPP} and R_{Bound}, both of which are stimulated by enhanced dimer formation, as this increases the availability of activated receptors for binding to the coated pit proteins and modulates the position of the ligand binding equilibrium (demonstrated in section 3.3.1.8). Yet, even at the

was not carried out, although it is recognized that it may have been instructive to conduct such a parallel investigation.

lower EGF concentration, this factor is still less significant than the parameter values for receptor-ligand binding, supporting a previous conclusion that the dynamics of receptor dimerization are relatively unimportant in defining the time course of events at the cell surface (section 3.3.1.9). This is further exemplified by the high variability in the fitted values determined for this parameter (Table 3.4).

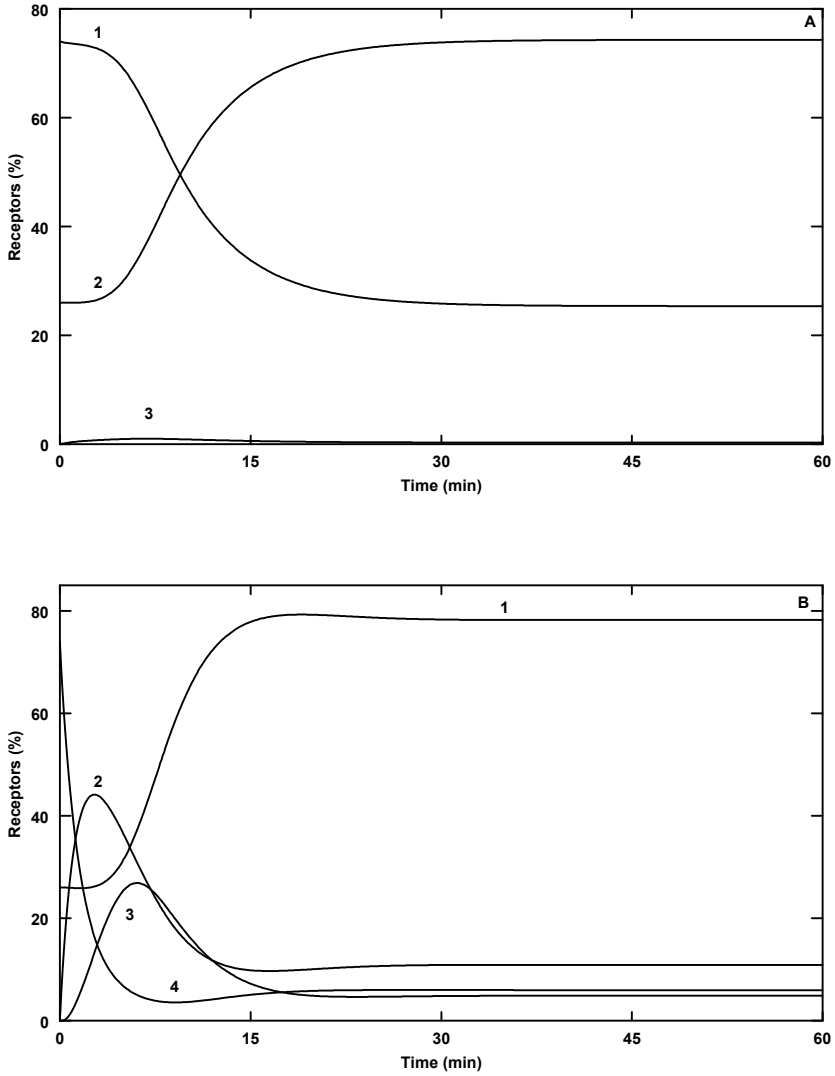

Figure 4.1 The influence of receptor-ligand binding parameters on the time-course of EGFR down-regulation

(**A**) The percentage of the total number of receptors per cell represented by R_{Int} (line 1), R_{Free} (line 2) and R_{Bound} + R_{CPP} (line 3; these cell surface, ligand-bound species were plotted together, since jointly they comprised < 1% of the total receptors); $k_1 = 7.3 \times 10^7$ molecule cell^{-1} min^{-1}. (**B**) R_{Int}, (line 1), R_{Bound} (line 2), R_{CPP} (line 3) and R_{Free} (line 4); $k_1 = 7.3 \times 10^9$ molecule cell^{-1} min^{-1}. The time courses were computed over 60 minutes continuous exposure to 0.1 nM EGF; other simulation parameters are listed in Table 3.3.

A striking similarity between the coefficients for $[EGFR]_{Total}$ and the rate constant for receptor dimerization at 100 nM EGF (Table 4.2), suggests that the marginal effect of

an increase in EGFR expression at this ligand concentration is probably associated with enhanced receptor dimerization. In common with a direct increase in the rate of receptor-receptor association, this is relatively ineffectual in altering the distribution of active receptor dimers between cell surface and intracellular compartments. Recalculation of the sensitivity coefficients for $[EGFR]_{Total}$ at 0.1 nM EGF (Table 4.3) confirms that this factor is more significant at low [EGF]. Furthermore, these values are again comparable to those determined for the rate of dimerization at the same ligand concentration, reinforcing the conclusion that an increased EGFR expression level mediates enhanced R_{CPP} and R_{Bound} by promoting dimerization.

In summary, few of the parameters of the top-level module are seemingly important in determining the extent of redistribution of receptors between the cell surface and intracellular compartments. This is largely due to the saturating concentration of EGF at which the sensitivity coefficients were determined, but also reflects the limited capacity of the combined constitutive and the ligand-induced internalization mechanisms. Thus, an increase in the number of receptors, or the dimerization rate, has little impact on the net rate of their association with coated pit proteins or internalization, but merely results in a greater proportion of the cell surface R_{Bound} form constituting receptor dimers. Other than [EGF] therefore, only variations in the endocytic rate constant, or in the parameters for receptor-ligand binding at low [EGF], are able to significantly alter the quantitative properties of the model, although the behaviour is qualitatively stable over the ranges of parameter values explored.

4.3.2 THE TIME COURSES OF SHC PHOSPHORYLATION, AND RAS AND ERK ACTIVATION

4.3.2.1 Top-level module parameters

Table 4.4 summarizes data describing the sensitivity of the time courses of Shc phosphorylation, in addition to Ras and ERK activation, to variations in parameter values for the top-level module. An initial observation is that although the pattern of Shc phosphorylation is modulated by variations in many of the parameters, few of these have any influence on Ras activation, and only [EGF] substantially affects the activation of ERK. Those that do influence the Ras/MAPK cascade, largely affect the timing of cascade activation, rather than the magnitude. It is particularly interesting to note that prolonged Shc phosphorylation (indicated by a positive sensitivity coefficient

for p_{60}), is not necessarily linked with sustained Ras and ERK activation, even though this constitutes an increase in the activating signal.

Table 4.4 Summary of the quantitative sensitivity analysis of the EGF signalling pathway: top-level module parameters

The results are expressed in the form of sensitivity coefficients, $S_p^{p'}$. All values were calculated at 100 nM EGF, unless otherwise stated.

	Shc			Ras			ERK		
Parameter	p_{Max}	t_{Max}	p_{60}	p_{Max}	t_{Max}	p_{60}	p_{Max}	t_{Max}	p_{60}
[EGF]	0.75	-0.23	0.69	0.30	-0.24	0.64	1.08	-0.18	1.26
$[EGFR]_{Total}$ (100 nM EGF)	0.12	-0.06	0.71	0.02	-0.25	0.00	0.00	-0.02	0.00
$[EGFR]_{Total}$ (0.1 nM EGF)	0.37	0.05	0.69	0.17	-0.40	0.01	0.02	-0.25	0.01
Receptor-ligand binding, k_1 (K_{d1})	0.00	0.00	0.00	0.00	0.00	0.00	0.00	0.00	0.00
Dimerization, k_4	0.00	-0.24	0.01	0.00	-0.15	0.00	0.00	-0.07	0.00
CPP binding, k_7 (K_{d7})	0.00	0.00	-0.07	0.00	0.00	0.00	0.00	0.00	0.00
Internalization, k_2; k_{-3}; k_5; k_8	-0.01	0.00	-0.06	0.00	0.00	0.00	0.00	0.00	-0.01
[Shc]	-0.76	0.00	-0.93	0.10	-0.20	0.00	0.01	-0.12	-0.01
Shc phosphorylation, k_9	0.29	-0.29	0.71	0.07	-0.58	0.00	0.00	-0.08	-0.01
Shc phosphorylation, K_{m9}	-0.43	0.30	-0.20	-0.36	0.30	-0.13	-0.38	0.19	-0.25
ShcP dephosphorylation, V_{10}	-0.05	0.05	-0.19	-0.02	0.00	0.00	0.00	0.02	0.01
ShcP dephosphorylation, K_{m10}	0.05	-0.03	0.37	0.01	-0.01	0.00	0.00	-0.01	0.00

These findings seemingly contradict the premise that a cascade arrangement of protein kinases, such as the Raf/MEK/ERK cascade, provides enhanced sensitivity to fluctuations in an upstream signal (155); in this case, in the kinetics of EGFR-TK activation or Shc phosphorylation. Any apparent conflict between the observed and proposed sensitivity of the Ras/MAPK cascade can be rationalized by a closer examination of the response of the system to EGF. As might be expected, the variation of EGF across a wide range of concentrations has the greatest impact on all the recorded variables, by affecting the rate and extent of receptor-ligand binding (discussed in the previous section), and thereby the critical event for initiation of the intracellular signalling cascade, EGFR-TK activation. By effectively increasing the amount of enzyme available to catalyse the phosphorylation of Shc, this enhances the rate (decreased t_{Max}) and extent (increased p_{Max} and p_{60}) of the reaction, which stimulates the activation of the Ras/MAPK cascade (t_{Max}, p_{Max} and p_{60} for Ras and ERK).

Of greater interest, although not directly apparent from the data given in Table 4.3, is that the MAPK cascade was found to demonstrate a 'switch-like' response, in terms of

the peak activation level (p_{Max}), to the primary stimulus, EGF, as shown in Figure 4.2; the MAPK cascade is either 'off', i.e. virtually no activation (<10%) of ERK, at a stimulus of less than 0.02 nM EGF, or 'on', i.e. almost maximal activation (>90%) above 0.1 nM EGF, with an intermediate peak activation level only being apparent across a narrow range of EGF concentrations. This type of behaviour, characterized by a large increase in the output of the cascade, i.e. the activation state of bottom-level kinase, in response to a small increase in the input, and an abrupt transition between inactive and active forms of the kinase, has been termed 'ultrasensitive' (116).

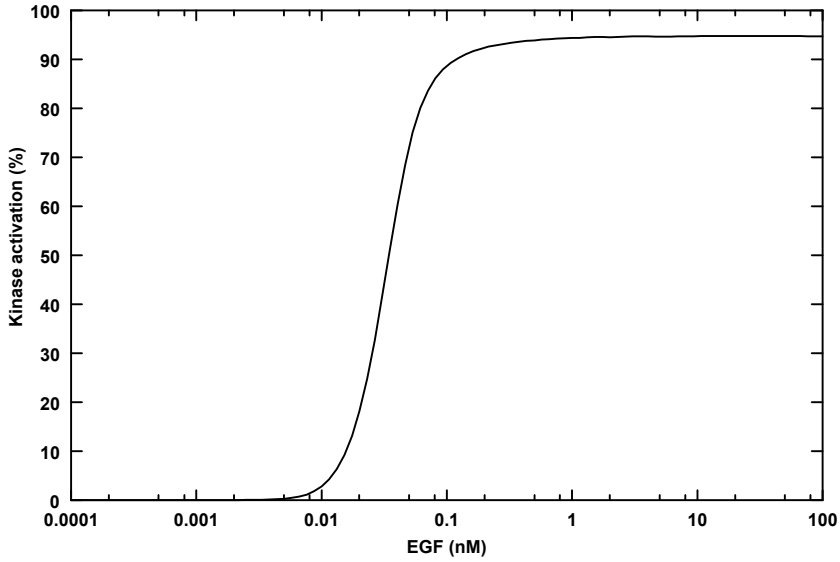

Figure 4.2 Predicted EGF stimulus-response curve for peak ERK activation (p_{max})
ERK activation is plotted as the percentage of total ERK in the catalytically active form. All other simulation parameters are listed in Table 3.3.

Contrary to the initial assessment, the MAPK cascade represented in the PC12 simulation apparently does have the capacity to respond with a high degree of sensitivity to an upstream signal. The degree of sensitivity amplification achieved between the cell surface and the MAPK cascade can be appreciated if an EGF concentration that induces almost maximal ERK activation, 0.1 nM, is compared with the concentration at which ligand binding is saturated, around 50 to 100 nM (see section 4.3.1). Moreover, this seems to provide a mechanism for rapidly and comprehensively converting inactive ERK to the catalytically active form in response to an external stimulus, consistent with the central role of this enzyme in many cellular processes (38).

Once maximally activated however, the Ras/MAPK cascade appears to relax to a self-determined steady state level of activation, regardless of the continuing external stimulus provided by EGF. Figure 4.3 indicates that, in common with peak ERK activation, the steady state level of ERK activation (corresponding to p_{60}) demonstrates a highly sensitive response to an EGF stimulus of between approximately 0.02 and 0.1 nM. At higher EGF concentrations, ERK is consistently switched 'on' (p_{Max} > 90%), as noted above (Figure 4.2). Similarly, steady state ERK activation becomes largely independent of this factor at a concentration in excess of 0.1 nM, but reaches a maximum that is significantly lower than the peak level ($p_{60} \cong 14\%$; Figure 4.3), in accordance with transient activation of the Ras/MAPK cascade.

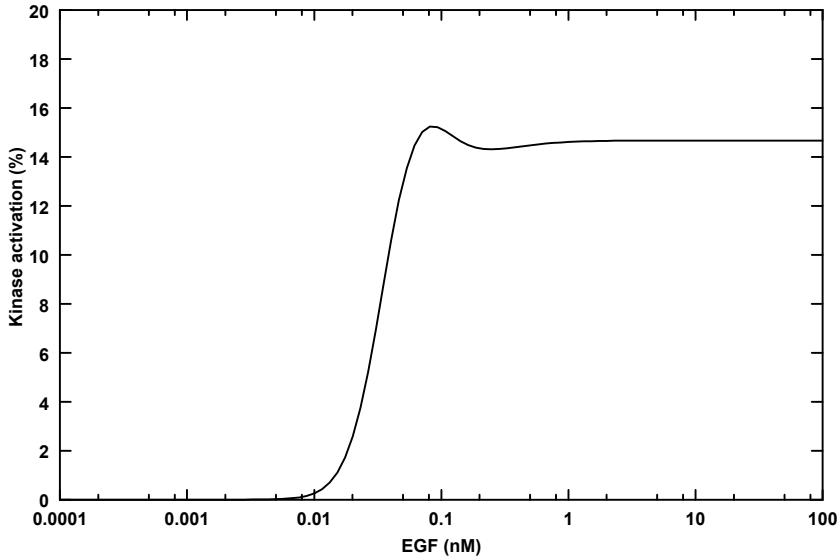

Figure 4.3 Predicted EGF stimulus-response curve for steady state ERK activation (p_{60})
ERK activation is plotted as the percentage of total ERK in the catalytically active form. All other simulation parameters are listed in Table 3.3.

Thus, although the capacity of the MAPK cascade to respond in a highly sensitive manner to a stimulus may initially result in the rapid activation of almost the entire cellular complement of ERK, it does not necessarily imply that this state is maintained. The obvious explanation is that ERK activation is accompanied by a proportional increase in the feedback phosphorylation of SOS, which rapidly down-regulates the Ras/MAPK cascade and desensitizes the pathway to further imminent activation, despite the continued presence of EGF. An increase in [EGF] above a threshold of around 0.02 nM does however, consistently reduce the time taken to attain peak ERK

activation (t_{Max}) until a minimum is reached at around 75 nM, as illustrated by Figure 4.4.

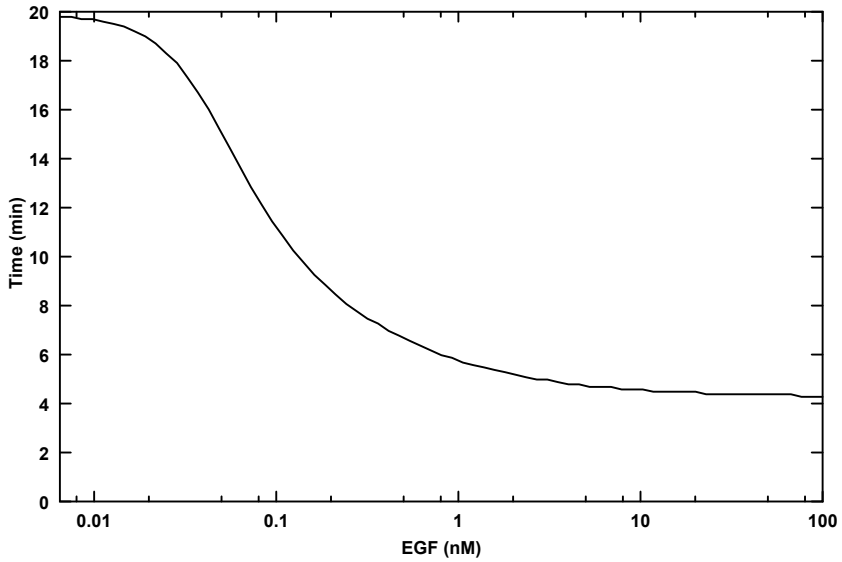

Figure 4.4 Predicted EGF stimulus-response curve for the time taken to attain peak ERK activation (t_{Max})
All other simulation parameters are listed in Table 3.3.

The general lack of sensitivity of the Ras/MAPK cascade to many factors operating at this level in the pathway, in terms of the peak activation achieved (p_{Max}), can therefore be defined as an artefact of the EGF concentration at which the sensitivity coefficients were calculated (> 0.1 nM); this level of stimulus induces the maximum possible response (Figure 4.2), which cannot be further amplified, but can be diminished (for example, in response to an increase in K_{m9} for Shc phosphorylation). The apparent stability of the steady state level of cascade activation is however, more significant. In principle, there appears to be scope for enhancement of the response seen at 0.1 nM EGF and above, as this constitutes a very low level of activation, perhaps by intensifying the signal transmitted through Shc. Yet, this limit is not exceeded, but is rigidly enforced through the negative feedback regulation of SOS (although p_{60} may not correspond temporally with the attainment of a steady state). The further implications of these observations are discussed later in this section, and in Chapter 5.

As noted above, [EGF] also has a significant influence on the kinetics of Shc phosphorylation. Other factors that have a generalized effect on this variable are the specific activity of the EGFR-TK (k_9), the expression level of the EGFR and the

availability of Shc; the sensitivity coefficients calculated for [Shc] are however, rather misleading. Increasing this parameter clearly reduces t_{Max}, but also falsely appears to diminish the extent of peak and steady state Shc phosphorylation; the actual amount of phosphorylated Shc that accumulates is virtually unchanged by an increase in [Shc], but the relative amount is consequently reduced, when expressed as a percentage of total Shc. The reason for this is clear when the K_m value of the EGFR-TK for Shc (K_{m9}), 6.0×10^3 molecule cell^{-1}, is compared with the range of [Shc] investigated, from 1×10^4 to 2×10^5 molecule cell^{-1}. Thus, the enzyme is operating under saturating conditions, and any increase in [Shc] has a marginal effect, as observed. The more marked sensitivity of the system as a whole to modulation of K_{m9} for Shc phosphorylation, over the range 6×10^3 to 9×10^6 molecule cell^{-1}, can conversely be explained by a corresponding shift from the zero-order to first-order domain, but also by a sharp decline in enzyme affinity.

Although the sensitivity of steady state receptor distribution to $[EGFR]_{Total}$ is reduced at a saturating concentration of EGF (100 nM EGF; see section 4.3.1), Table 4.3 indicates that $[EGFR]_{Total}$ still has an important role in determining the extent of Shc phosphorylation (p_{Max} and p_{60}) under the same conditions. Comparison with the corresponding sensitivity coefficients calculated at 0.1 nM EGF does however, confirm that this factor is more significant at low EGF concentrations. Although it is intuitive that an increase in $[EGFR]_{Total}$, or in the k_{cat} for the EGFR-TK (k_9), would enhance the amount of phosphorylated Shc, at very high values of these parameters the behaviour of the system as a whole was also found to diverge qualitatively from that typically observed.

In order to demonstrate this effect, activation of the pathway has been simulated at a low (sub-saturating) concentration of EGF, at which an almost maximal response is still achieved but the peak response is delayed, allowing better resolution of the response pattern at early time-points. At 0.1 nM EGF, an increase in the EGFR expression level within the typical physiological range of 1×10^4 to 2×10^5 molecule cell^{-1} (43) was found to progressively increase the peak phosphorylation level of Shc (p_{Max}), as expected, although the response remained transient. However, further increments in this parameter up to a maximum of 1×10^6 molecule cell^{-1}, approaching the EGFR expression level of several epithelial carcinoma cell lines (43), resulted in almost maximal Shc phosphorylation levels being maintained for the duration of the

simulated time-period (p_{60}). This effect was also observed in response to increasing k_{cat} for the EGFR-TK (k_9), and although less pronounced at 100 nM EGF, was still generally apparent for both parameters, as indicated by the sensitivity coefficients reported in Table 4.3.

A probable explanation is that the rate of the rise in phosphorylated Shc is in fact a function of the rates of both phosphorylation by the EGFR-TK, and dephosphorylation. In turn, the effective rate of the latter process is partly determined by the rate of feedback SOS phosphorylation, which primarily functions to down-regulate GEF activity, but also releases complexed phosphorylated Shc to become a target for phosphatase activity (see sections 3.3.2.6 and 3.3.3.6). At low $[EGFR]_{Total}$, the maximal rate of Shc phosphorylation is less than that of the dephosphorylation reaction. Activation of the feedback down-regulation loop therefore gives rise to a transient peak in phosphorylated Shc, but a moderate increase in k_9 or EGFR expression is able to enhance the rate at which this peak is achieved, and the extent of phosphorylation. However, as k_9 or $[EGFR]_{Total}$ increase above a level at which the maximal rate of phosphorylation is greater than that of dephosphorylation, this aspect of the feedback mechanism is effectively overwhelmed. This results in prolonged Shc phosphorylation, which reaches a more delayed peak as the reaction nears completion. This effect is illustrated in Figure 4.5 below.

This analysis implies that elevated EGFR expression would be associated with sustained Shc phosphorylation *in vivo*. Although data describing the time-dependent pattern of Shc phosphorylation in cells overexpressing the EGFR are not available, constitutive Shc phosphorylation has been observed in cell lines that overexpress ErbB2, a member of the same family of RTKs as the EGFR (327). Furthermore, it is clear that the expression level of EGFR assumed in the model is constrained within typical physiological limits, in order for the simulated time course of Shc phosphorylation to be in accordance with that observed experimentally in cells expressing normal levels of the EGFR. Similarly, k_{cat} for the EGFR-TK (k_9) must be also be maintained within a rather more narrow range than that examined in the analysis, i.e. between 6.0 and 13 min^{-1}. It is interesting to note that the fitted value of this parameter, 12 min^{-1}, is approaching the maximum of this range of appropriate values, and hence reflects an optimum balance between minimising the rate of rise in

Shc phosphorylation and maximising the extent of total phosphorylation, whilst maintaining the transient nature of the response.

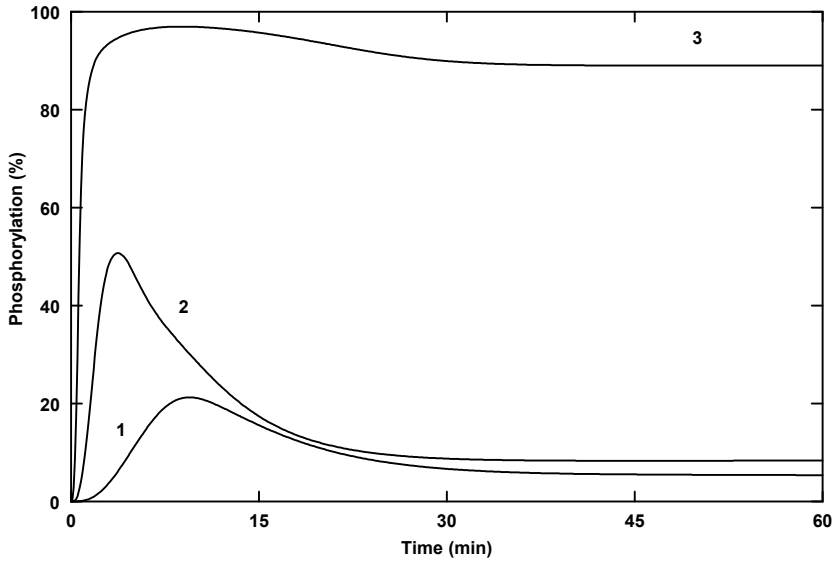

Figure 4.5 The influence of $[EGFR]_{Total}$ on the time course of EGF-induced Shc tyrosine phosphorylation

The time courses were computed over 60 minutes continuous exposure to 0.1 nM EGF, at $[EGFR]_{Total}$ = 1×10^4 molecule cell^{-1} (line 1), 1×10^5 molecule cell^{-1} (line 2) and 1×10^6 molecule cell^{-1} (line 3). Other simulation parameters are listed in Table 3.10. Phosphorylated Shc is plotted as the percentage of total Shc; the data reflect the phosphorylation status of both free and complexed Shc.

Despite having a marked effect on the time course of Shc phosphorylation, $[EGFR]_{Total}$, k_{cat} for the EGFR-TK (k_9) and [Shc] only marginally affect the timing (t_{Max}), and not the duration (p_{60}), of Ras/MAPK activation. These results particularly exemplify the stability of the Ras/MAPK cascade to quantitative changes in upstream events, which arises through the feedback regulation of cascade activation. In common with continued EGF stimulation above a given threshold, amplified or prolonged signalling by other factors upstream of the point at which the feedback mechanism operates, i.e. SOS, beyond a level that induces maximal ERK activation and SOS phosphorylation, does not affect the steady state level of cascade activation. As will be demonstrated in the following sections, it follows that the effective stability of the MAPK cascade may be forfeited through a disturbance in the feedback mechanism, which generates prolonged signalling through SOS.

Conversely, this analysis does not explain how overexpression of the EGFR generates prolonged Ras/MAPK cascade activation (278, 340, 370). One possibility is that the

inherent specificity of the receptor for SH2 domain-containing proteins (265) is compromised at high expression levels, resulting in the non-specific initiation of multiple intracellular cascades that converge upon the Ras/MAPK cascade. Likely candidates are Shc-independent routes, such as via the adaptor Crk, in conjunction with SOS (181), which may abnormally elevate Ras and ERK activation. Crk may also interact with the guanine-nucleotide exchange factor, C3G (181), which is specific for the Ras-like GTPase, Rap-1 (122), thereby activating B-Raf and the MAPK cascade in neuronal cell types (345). Whilst it has been confirmed that Crk is not normally involved in EGF-induced ERK activation (334), this protein is implicated in oncogenic signalling in fibroblasts (182). Alternatively, elevated EGFR expression may intensify signalling through parallel pathways that are normally initiated by activation of the RTK, such as via a recently discovered link between Shc/Grb2 and activation of the phosphatidylinositol 3-kinase (PI-3K)/Akt pathway (129), or through the PLCγ-PKC pathway; there is some evidence that the latter may be linked, at the level of Ras or Raf, with the MAPK cascade (33, 48, 87, 188), although this has not yet been conclusively established. These findings also seem inconsistent with the observation that Shc overexpression induces the transformation of cultured fibroblasts through enhanced Shc-Grb2 complex formation (289), and promotes neurite outgrowth in PC12 cells (285). However, these physiological responses are not necessarily associated directly with prolonged Ras or ERK activation, and may reflect augmentation of the Shc/Grb2/PI-3K/Akt pathway (129), or aberrant, non-specific interactions between Shc and other signalling molecules.

In general, it can be noted that the top-level parameters that exert the greatest influence on the time course of Shc phosphorylation and Ras activation largely correspond to concentrations of signalling molecules (EGF, EGFR and Shc), and many of the remaining parameters at this level are relatively insignificant. An increased rate of EGFR dimerization (k_4) affects the rate of EGFR activation, and thereby the initial, but not the maximal catalytic rate of the EGFR-TK; the extent of Shc phosphorylation is therefore unchanged, but the activation of Ras, and to a lesser extent, ERK, are also more rapid. However, the influence of this parameter is minimal, probably because the extent of receptor dimerization and activation are not greatly altered over the range of values examined. Furthermore, a general lack of sensitivity to parameters governing coated pit protein binding and receptor internalization (k_7 and K_{d7}; k_2, k_{-3}, k_5 and k_8) reflects the consideration that all occupied receptor dimers are catalytically active,

regardless of their location. Finally, a parallel increase in k_1 and K_{d1} for receptor-ligand binding has no discernible effect on Shc, Ras or ERK at 100 nM EGF, whilst variations in the parameters for Shc tyrosine dephosphorylation have opposing, but less pronounced effects to those associated with EGFR-TK-mediated Shc phosphorylation. Indeed, this is to be expected, since these parameters were earlier shown to have relatively little impact on the time-dependent response to EGF (sections 3.3.2.6, 3.3.2.7 and 3.3.3.8).

4.3.2.2. Intermediate module parameters

The data describing the influence of the intermediate module parameters on the time courses of Shc phosphorylation, and Ras and ERK activation, are given in Table 4.5 below. It is immediately apparent that whereas the kinetics of Ras and ERK activation are relatively insensitive to variations in the top-level module parameters, many more of the factors operating at the intermediate level of the cascade affect these variables. Evidently, there is also a reciprocal relationship between ERK p_{60} and Shc p_{60} for many of the parameters, reflecting the feedback down-regulation of Shc phosphorylation, which arises through ERK-mediated SOS phosphorylation (see section 3.3.3.6). This can be illustrated by considering a direct increase in the rate of GDP/GTP exchange on Ras (k_{13}), which enhances the extent of Ras activation, and thereby t_{Max} and p_{60} for both Ras and ERK, but adversely affects Shc phosphorylation levels. Conversely, whereas an increase in GAP and Ras-GTP association (k_{14} and K_{d14}) predictably reduces the extent of Ras and ERK activation, and delays peak activation, the level of Shc phosphorylation is elevated.

As discussed in the previous section, the extent of Shc phosphorylation is not therefore simply a function of the rate of processes that directly modulate this variable (i.e. the specific activity of the EGFR-TK and phosphatase activity), but also the ERK activation state, and reflects the changing balance between these features of the system under different conditions. Even the patterns of system sensitivity to [Grb2-SOS] and $[Ras]_{Total}$, which initially appear to contradict this view, can be accounted for in the same terms.

Table 4.5 Summary of the quantitative sensitivity analysis of the EGF signalling pathway: intermediate module parameters

The results are expressed in the form of sensitivity coefficients, S_p^{y}. All values were calculated at 100 nM

EGF.

	Shc			Ras			ERK		
Parameter	p_{Max}	t_{Max}	p_{60}	p_{Max}	t_{Max}	p_{60}	p_{Max}	t_{Max}	p_{60}
[Grb2-SOS]	0.30	-0.20	0.08	0.16	-0.20	0.12	0.02	0.10	0.21
ShcP/Grb2-SOS binding, k_{11} (K_{d11})	0.25	-0.33	0.04	0.33	-0.35	0.06	0.21	-0.23	0.11
$[Ras]_{Total}$	0.09	0.10	0.43	-0.65	0.05	-0.35	0.04	0.02	0.89
Ras-GDP/ShcP-Grb2-SOS binding, k_{12} (K_{d12})	0.04	-0.16	-0.15	0.49	-0.08	0.37	0.75	-0.13	0.69
Ras GDP/GTP exchange, k_{13}	-0.06	-0.24	-0.51	0.73	-0.20	0.15	0.56	-0.35	0.26
[GAP]	0.02	0.24	0.55	-0.65	0.21	-0.02	-0.95	0.40	-0.53
Ras-GTP/GAP binding, k_{14} (K_{d14})	0.04	0.21	0.42	-0.69	0.18	-0.24	-0.43	0.30	-0.59
GTP hydrolysis, k_{15}	0.01	0.00	0.01	-0.15	0.00	-0.13	0.00	0.09	-0.01
[Raf]	-0.05	-0.10	-0.24	0.35	-0.39	0.00	0.01	-0.41	0.62
Ras-GTP/Raf binding, k_{16} (K_{d16})	-0.01	-0.21	-0.41	0.10	-0.18	-0.36	0.42	-0.30	0.60

Increased availability of Grb2-SOS primarily enhances the overall extent of Shc phosphorylation, but also elevates the effective rate of guanine-nucleotide exchange on Ras, thus enhancing the level of Ras activation. In turn, this increases both p_{60} and t_{Max} for ERK. As illustrated by Figure 4.6A and 4.6B, an increase in p_{60} for all three signalling molecules infers a higher steady state level of system activation, in addition to prolonged phosphorylation or activation, characterized in this instance by a plateau in phosphorylation/activation status immediately following the initial response. For illustrative purposes, it can be demonstrated that this pattern is even more pronounced at levels of Grb2-SOS in excess of those considered in the sensitivity analysis, as Figure 4.6C shows. These results are consistent with experimental data indicating that the overexpression of SOS or Grb2 accelerates Ras GDP/GTP exchange and enhances ERK activation (54, 288, 311).

Since ERK activation normally initiates negative feedback regulation of the pathway through SOS phosphorylation, resulting in rapid Shc dephosphorylation and down-regulation of the Ras/MAPK cascade (Figure 4.6A), the most coherent interpretation of the data is that increased Grb2-SOS availability partly overrides this feedback mechanism (Figure 4.6B). This is achieved by limiting the impact of dissociation of the ShcP-Grb2-SOS complex, induced by SOS phosphorylation; there is still a large pool of unmodified Grb2-SOS remaining to reconstitute sufficient functionally active ShcP-Grb2-SOS complexes.

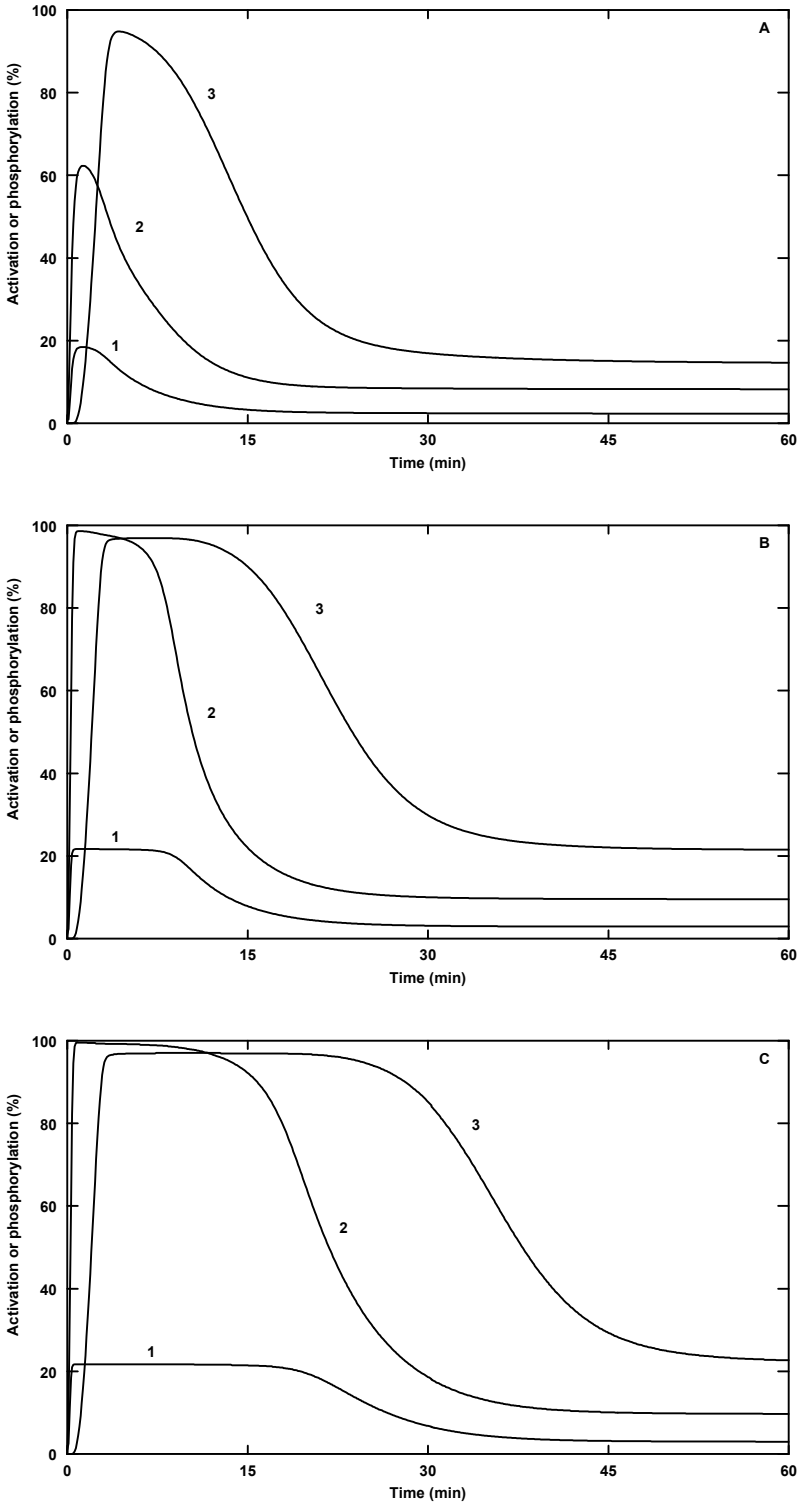

Figure 4.6 The influence of [Grb2-SOS] on the time courses of EGF-induced Shc tyrosine phosphorylation, and Ras and ERK activation

The data indicate: Ras activation (line 1), expressed as the percentage of total Ras in the GTP-bound form; Shc phosphorylation (line 2), plotted as the percentage of total Shc; and ERK activation (line 3), plotted as the percentage of total ERK in the catalytically active form. The time courses were computed over 60 minutes continuous exposure to 100 nM EGF. (**A**) [Grb2-SOS] = 2.0×10^4 molecule cell^{-1}. (**B**) [Grb2-SOS] = 2.0×10^5 molecule cell^{-1}. (**C**) [Grb2-SOS] = 5.0×10^5 molecule cell^{-1}. All other simulation parameters are listed in Table 3.3.

This has the dual effect of maintaining a higher level of signalling through SOS, thereby raising p_{60} for both Ras and ERK, and enhancing the net proportion of phosphorylated Shc that is sequestered from phosphatase activity (see section 3.3.2.6), thus increasing p_{60} for Shc; the latter is also responsible for obstructing Shc dephosphorylation at early time-points, greatly increasing p_{Max} for Shc. In contrast, a direct increase in the rate and affinity of ShcP and Grb2-SOS association (k_{11} and K_{d11}) increases p_{Max} for Shc, Ras and ERK, but has a less notable effect on p_{60} and decreases t_{Max} for all three variables, indicating that this does not result in the same degree of prolonged cascade activation. The implication is that, over the ranges of values explored, these factors do not raise the net availability of Grb2-SOS to the same degree as a direct increase in [Grb2-SOS], but are more important in determining the kinetics of pathway initialization.

The variables t_{Max} and p_{60} for Shc are also dependent on $[Ras]_{Total}$ and [GAP], as are the kinetics of Ras and ERK activation; a positive value for p_{60} again implies prolonged phosphorylation or activation, and a higher steady state level. As Figures 4.7A and 4.7B illustrate, the effect on Shc is evidently more marked than for [Grb2-SOS], as indicated by the greater magnitude of the sensitivity coefficients for $[Ras]_{Total}$ and [GAP], and the time taken to attain a steady state exceeds 60 minutes.

An increase in $[Ras]_{Total}$ was found not to produce a directly proportional increase in the actual amount of active Ras-GTP. This reflects the representation of Ras guanine-nucleotide exchange as an initial Ras-GDP/SOS binding event, with a K_d (K_{d12}; calculated from k_{12} and k_{-12}) of 6.13×10^2 molecule cell^{-1}, in comparison with a range of possible [Ras-GDP] between 1.0×10^4 and 2.0×10^5 molecule cell^{-1}, followed by an irreversible GDP/GTP exchange step. Thus, there is only a moderate increase in the actual amount of active Ras, which is paralleled by prolonged ERK activation (increased p_{60}) as apparent from Figure 4.7B, but the percentage of active Ras (p_{Max} and p_{60}) is diminished. However, increased [GAP] produces a genuine decline in the maximal level of Ras activation, which is reflected by a reduction in both p_{Max} and p_{60} for ERK, and delayed peak activation of the cascade.

Despite having opposing effects on ERK p_{60}, both Ras and GAP enhance Shc phosphorylation. In the case of GAP, this is largely correlated with a decrease in p_{60} for ERK, but the effect of Ras can be explained by considering the participation of this molecule in the protein-protein binding events that transmit the signal through the

intermediate module. An increase in $[Ras]_{Total}$ corresponds to an increase in the initial Ras-GDP level, which enhances the net extent of binding to the ShcP-Grb2-SOS complex. As SOS is assumed to be excluded from feedback phosphorylation by ERK when associated with Ras-GDP (see section 3.3.3.3), an elevated level of Ras-GDP therefore reduces net SOS phosphorylation, and consequently dissociation of the ShcP-Grb2-SOS complex leading to Shc dephosphorylation. In a manner analogous to elevated [Grb2-SOS], high $[Ras]_{Total}$ is therefore able to counteract the effects of the feedback mechanism associated with enhanced ERK activation.

The effect of increased GAP expression, or an increase in the rate and affinity of Ras-GTP/GAP binding (k_{14} and K_{d14}), can also be partly explained in these terms, since these changes both accelerate Ras-GTP hydrolysis, and thus raise the effective availability of Ras-GDP. Unlike [Grb2-SOS] therefore, neither $[Ras]_{Total}$ nor [GAP] change the maximal extent of Shc phosphorylation (p_{Max}), as they have little or no effect on the initial ShcP/Grb2-SOS binding equilibrium, but do partly determine the timing and extent of down-regulation of the initial response (t_{Max} and p_{60}), by retarding ShcP-Grb2-SOS dissociation. A general lack of sensitivity to the actual rate of Ras-GTP hydrolysis (k_{15}), except in terms of the extent of maximal and steady state Ras activation, might appear to contradict this conclusion, but the range over which this parameter was varied is considerably narrower than that represented indirectly through the variation of [GAP].

An equivalent response might also be anticipated to a direct increase in the rate and affinity of Ras-GDP/ShcP-Grb2-SOS binding (k_{12} and K_{d12}), which evidently has a positive influence on both the rate and degree of Ras and ERK activation, but results in a contrasting decline in Shc t_{Max} and p_{60}. Clearly, the explanation must be that modulation of this parameter over the range of values investigated is insufficient to overcome the feedback mechanism. This is illustrated by comparing the simulated time course at an increased rate of Ras-GDP/ShcP-Grb2-SOS association (k_{12}) shown in Figure 4.7C, with those shown for increased [Ras] or [GAP] (Figures 4.7A and 4.7B); although the steady state levels of Ras and ERK activation are clearly enhanced, the activation of ERK is not as prolonged, and neither is Shc phosphorylation.

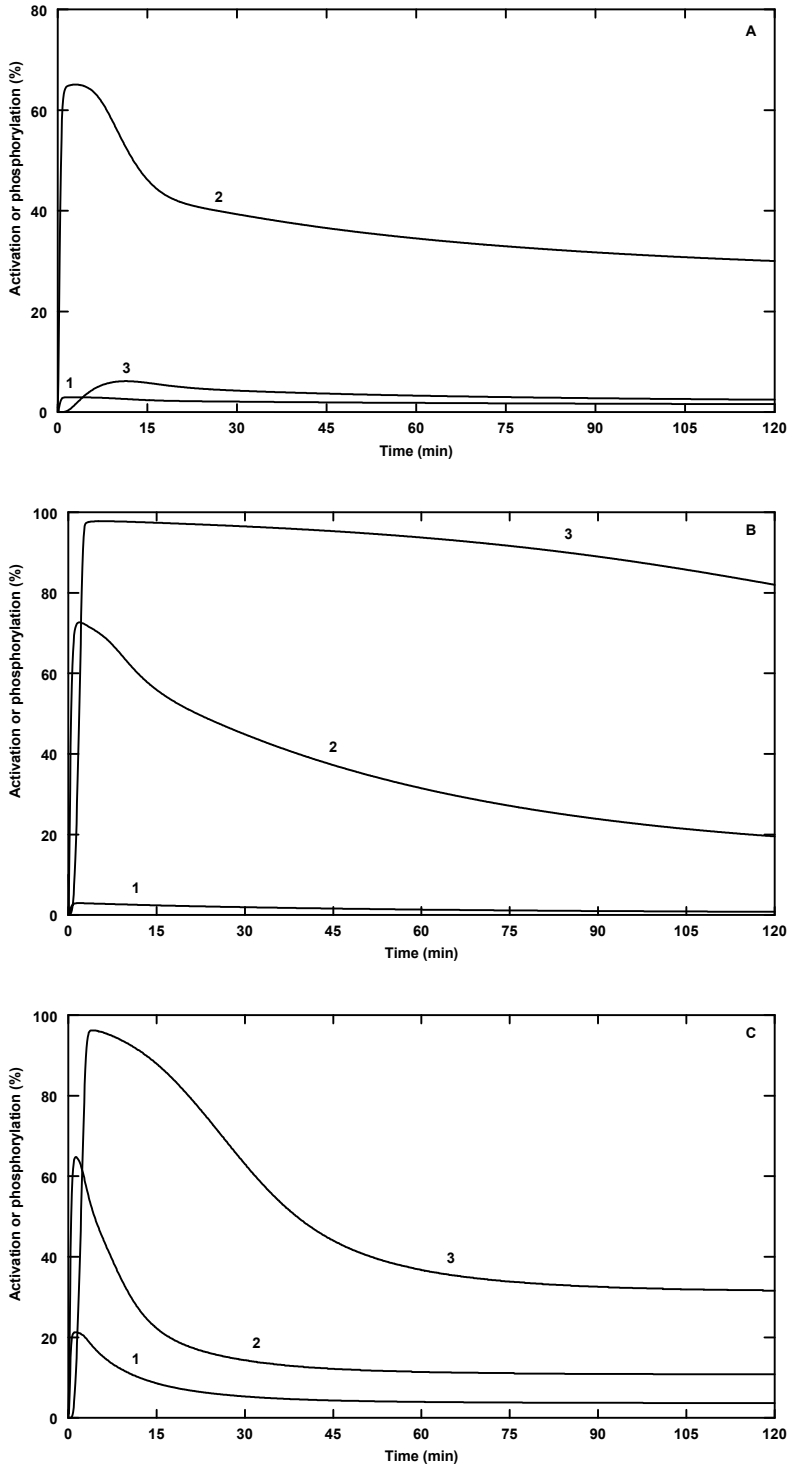

Figure 4.7 The influence of [GAP], $[Ras]_{Total}$ and the rate of Ras-GDP/ShcP-Grb2-SOS binding on the time courses of EGF-induced Shc phosphorylation, and Ras and ERK activation

The data indicate: Ras activation (line 1), expressed as the percentage of total Ras in the GTP-bound form; Shc phosphorylation (line 2), plotted as the percentage of total Shc; and ERK activation (line 3), plotted as the percentage of total ERK in the catalytically active form. The time courses were computed over 60 minutes continuous exposure to 100 nM EGF. (**A**) [GAP] = 2.0×10^5 molecule cell^{-1}. (**B**) $[Ras]_{Total} = 2.0 \times 10^5$ molecule cell^{-1}. (**C**) Ras-GDP/ShcP-Grb2-SOS binding, $k_{12} = 6 \times 10^{-2}$ molecule cell^{-1} min^{-1}. All other simulation parameters are listed in Table 3.3.

The response of the time courses of Shc, Ras and ERK to increased [Raf], shown in Figure 4.8A, provides a further perspective on the dynamics of the system. In common with increased Grb2-SOS and Ras availability, this ultimately increases the amount of catalytically active Raf and thereby enhances ERK activation, but differs by producing the expected reduction in Shc phosphorylation, through consequent activation of the feedback SOS phosphorylation loop. In addition, the effects of enhanced Raf expression on the level of Ras activation reflect the direct involvement of Raf in the binding events of the intermediate module (hence the inclusion of Raf with these parameters, although this was considered during model development to be a MAPK module component). The association of Ras-GTP with Raf or GAP are mutually exclusive events (see section 3.3.2.4), and therefore when bound to Raf, Ras-GTP is exempt from GAP-catalysed GTP hydrolysis (331). Thus, an increase in Raf availability increases the proportion of Ras-GTP bound to Raf, and thereby the total amount of activated Ras over the entire simulated time-period; p_{60} for Ras is not reduced, despite an increase in p_{60} for ERK, as the down-regulation of Ras activation is counteracted by increased [Raf].

An increase in the rate and affinity of Ras/Raf binding (k_{16} and K_{d16}) has a similarly pronounced effect on the MAPK cascade, affecting the timing of Ras/ERK activation and increasing p_{Max} and p_{60} for ERK, as illustrated by Figure 4.8B. This signifies the more rapid accumulation of the catalytically active form of Raf, which is translated through the phosphorylation cascade into a more rapid increase in the amount of activated ERK. An increased rate of Ras/Raf binding (k_{16}) also initially enhances Ras activation (p_{Max}), but is not sufficient to sustain an increased level of activation (reduced p_{60}). This pattern arises through the exclusion of a greater proportion of active Ras-GTP from GAP activity at early time-points, as in the case of an increase in Raf expression, but the accelerated conversion of Raf to the catalytically active form results in a progressive decrease in the availability of inactive Raf. This effect is less significant at very high Raf expression levels, enabling Shc phosphorylation and Ras activation to be maintained at a slightly higher level, despite inducing the same enhancement to steady state ERK activation.

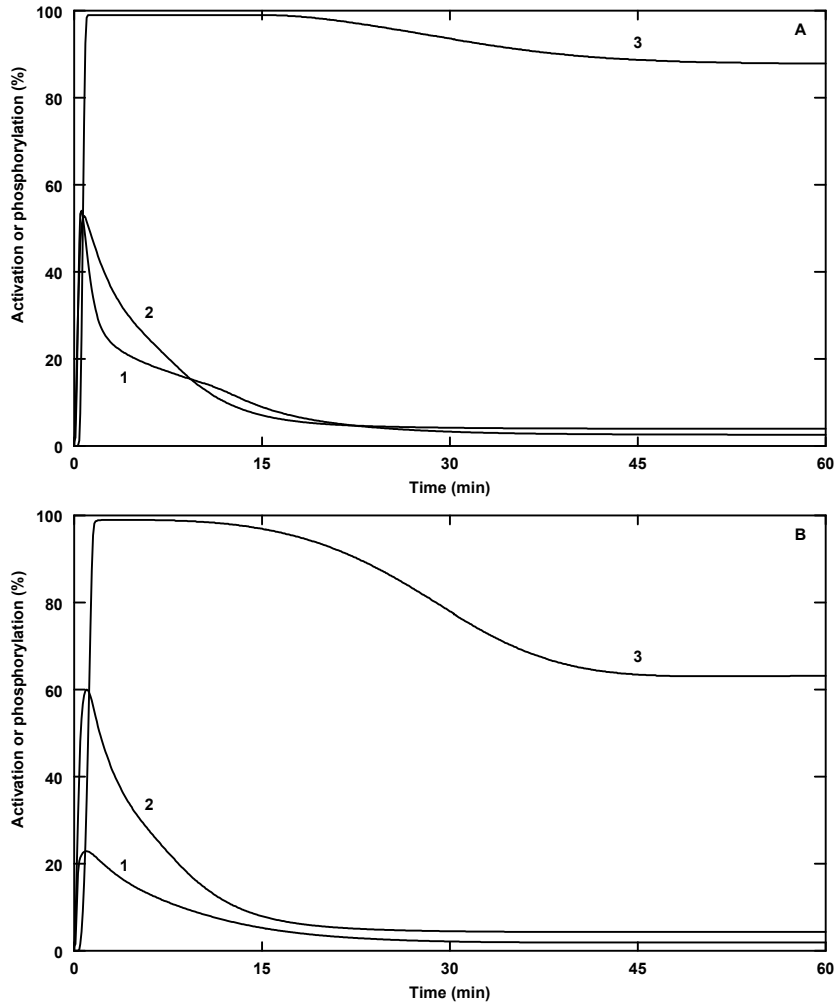

Figure 4.8 The influence of [Raf] and the rate of Ras-GTP/Raf binding on the time courses of EGF-induced Shc phosphorylation, and Ras and ERK activation

The data indicate: Ras activation (line 1), expressed as the percentage of total Ras in the GTP-bound form; Shc phosphorylation (line 2), plotted as the percentage of total Shc; and ERK activation (line 3), plotted as the percentage of total ERK in the catalytically active form. The time courses were computed over 60 minutes continuous exposure to 100 nM EGF. (**A**) [Raf] = 2.0×10^5 molecule cell^{-1}. (**B**) Ras-GTP/Raf binding, $k_{16} = 1.2 \times 10^{-2}$ molecule cell^{-1} min^{-1}.

This analysis therefore demonstrates the essentially opposing effects of Raf and GAP, and provides quantitative evidence for the importance of competition between Raf and GAP for binding to active Ras-GTP in determining the kinetics of Ras/MAPK cascade activation (see section 3.3.2.4). This is further illustrated by considering an increase in the rate and affinity of the interaction between Ras-GTP and either of these proteins (K_{d14} and k_{14}; K_{d16} and k_{16}), which have entirely contrasting, but equally profound effects on the system as a whole; these findings are therefore consistent with an earlier observation that the relative and absolute values of parameters governing the direct association of Ras with SOS, GAP and Raf are of considerable importance in

determining the rate and extent of Ras/MAPK cascade activation (section 3.3.3.7). Also notable is that the rate of Ras-GTP/GAP association (k_{14}), and the affinity of this interaction (K_{d14}), are more important in determining the initial peak level of Ras activation than the steady-state level (p_{Max} and p_{60}, respectively), confirming that the primary function of GAP-catalysed GTP hydrolysis may be in regulating maximal Ras activation (see section 3.3.3.7), with the down-regulation of this response being a subsidiary role (section 3.3.2.7).

In summary, the results presented in this section emphasise the internal stability of the MAPK cascade that arises through the cascade being embedded within a negative feedback loop, highlighted previously (section 4.3.2.1), but also demonstrate how disruption of this critical regulatory mechanism can affect the stability. An inverse relationship between ERK activation and Shc phosphorylation is also a recurrent feature, and confirms the importance of ERK-mediated SOS phosphorylation in regulating this aspect of EGF signalling (see sections 3.3.2.6 and 3.3.3.6). Thus, prolonged Shc phosphorylation, such as that generated by an increase in [GAP], is not necessarily associated with sustained Ras and ERK activation (Figure 4.7A). In contrast, an increase in [Grb2-SOS] or $[Ras]_{Total}$ (Figures 4.6B and 4.7B) prolongs activation of the entire pathway, by counteracting the effects of feedback SOS phosphorylation, i.e. the down-regulation of cascade activation.

In addition to justifying the decision to reflect the direct physical interaction of Ras with SOS, GAP and Raf separately to the catalytic processes involved in regulating Ras and Raf activation, the results therefore agree with an earlier proposal, that the availability of signalling intermediates such as Ras, SOS, GAP and Raf, could be an important regulatory feature of the EGF signalling pathway (section 3.3.2.4). Whereas modulation of the expression level of these molecules produces substantial qualitative changes in the behaviour of the system, variations in the kinetic or thermodynamic properties, over a more extensive range of experimentally determined values, do not generally result in behaviour that differs greatly from that expected, but tend to exaggerate the typical response. For example, an increase in the rate and affinity of the Ras-GDP/ShcP-Grb2-SOS interaction (k_{12} and K_{d12}) partly reinforces the feedback mechanism, by promoting Ras and ERK activation, so that any possible enhancement to Shc phosphorylation through increased Ras-GDP association is counteracted, contrasting with the effects of increased $[Ras]_{Total}$ noted above (cf. Figures 4.7B and

4.7C). It is interesting to speculate therefore, that different expression levels of signalling molecules in various cell types may be a factor in defining functional aspects of the cascade, by determining the extent or duration of Shc phosphorylation and Ras/MAPK cascade activation; this might be accomplished directly, through competition between Raf and GAP for binding to Ras-GTP, or indirectly, through modulation of the efficiency of feedback down-regulation.

4.3.2.3. The MAPK cascade module parameters

Table 4.6 encapsulates a large volume of data describing the sensitivity of the model to variations in parameters corresponding to the MAPK cascade module. Many of the results are consistent with those expected; for example, in the majority of cases, the reciprocal relationship between the extent of ERK activation and Shc phosphorylation is clear, whilst in general, the timing of peak ERK activation and Shc phosphorylation (t_{Max}) are directly correlated. Furthermore, this pattern is repeated for ERK and Ras. This can generally be linked with activation of the feedback down-regulation mechanism, comprising ERK-mediated SOS phosphorylation, and provides further quantitative evidence that the level of ERK activity is a determinant of both the Shc phosphorylation and Ras activation status (see sections 4.3.2.1 and 4.3.2.2). However, the data generated by variations in the parameters associated with the feedback loop are an exception, and will be returned to later in the discussion. In addition, none of the parameters affect the peak Shc phosphorylation level, as none are in a position to influence the ShcP-Grb2-SOS binding equilibrium, as discussed in the previous section.

Unlike any of the other parameters considered at this level, the rate of Raf activation (k_{17}) has some influence on both the steady state and initial level of Ras activation. This can again be linked with the representation of this step in the model as an initial binding equilibrium between Ras and Raf, followed by an irreversible step that releases activated Raf and Ras-GTP. An increase in the rate of the latter allows more catalytically active Raf to accumulate in a shorter time, and elevates the rate at which free Ras-GTP is made available to bind further inactive Raf. These effects synergize to enhance both the maximal extent of ERK activation (p_{Max}), by accelerating the initial rise in activated ERK (t_{Max}) and allowing this to reach a higher steady state level (p_{60}). A further consequence however, is that more free Ras-GTP is made available for binding to GAP, which combines with the feedback down-regulation mechanism to reduce the

extent of Ras activation. These results further exemplify how competition between GAP and Raf determines the pattern of responses (see section 4.3.2.2).

Table 4.6 Summary of the quantitative sensitivity analysis of the EGF signalling pathway: MAPK cascade module parameters

The results are expressed in the form of sensitivity coefficients, S_p^r; all values calculated at 100 nM EGF.

	Shc			Ras			ERK		
Parameter	p_{Max}	t_{Max}	p_{60}	p_{Max}	t_{Max}	p_{60}	p_{Max}	t_{Max}	p_{60}
Raf activation, k_{17}	0.00	-0.14	-0.24	-0.13	-0.12	-0.47	0.58	-0.22	0.32
Raf inactivation, V_{18}	0.00	0.06	0.13	0.02	0.05	0.26	-0.15	0.08	-0.25
Raf inactivation, K_{m18}	0.00	-0.03	-0.08	-0.02	-0.02	-0.26	0.00	-0.04	0.24
[MEK]	0.00	-0.22	-0.17	0.00	0.00	-0.18	0.42	-0.40	0.05
MEK phosphorylation, k_{19}, k_{21}	0.00	-0.37	-0.62	0.00	-0.08	-0.62	0.89	-0.41	0.67
MEK phosphorylation, K_{m19}, K_{m21}	0.00	0.17	0.30	0.00	0.02	0.29	-0.55	0.19	-0.29
MEK dephosphorylation, V_{20}, V_{22}	0.00	0.18	0.34	0.00	0.07	0.35	-0.78	0.07	-0.79
MEK dephosphorylation, K_{m20}, K_{m22}	0.00	-0.28	-0.56	0.00	-0.01	-0.57	0.86	-0.15	0.75
[ERK]	0.00	-0.14	-0.56	0.00	0.00	-0.54	0.00	-0.17	-0.45
ERK phosphorylation, k_{23}, k_{25}	0.00	-0.16	-0.42	0.00	0.00	-0.50	0.10	-0.21	0.53
ERK phosphorylation, K_{m21}, K_{m23}	0.00	0.22	0.25	0.00	0.03	0.26	-0.35	0.21	-0.25
ERK dephosphorylation, V_{24}, V_{26}	0.00	0.18	0.33	0.00	0.10	0.35	-0.82	0.07	-0.82
ERK dephosphorylation, K_{m24}, K_{m26}	0.00	-0.14	-0.31	0.00	0.00	-0.34	0.03	-0.06	0.44
SOS phosphorylation, k_{27}	-0.01	-0.13	-0.18	-0.01	-0.12	-0.33	-0.29	-0.15	-0.63
SOS phosphorylation, K_{m27}	0.01	0.11	0.23	0.01	0.09	0.40	0.10	0.08	0.68
SOS dephosphorylation, V_{28}	0.00	0.00	0.17	0.00	0.00	0.21	0.00	0.04	0.23
SOS dephosphorylation, K_{m28}	0.00	0.00	-0.06	0.00	0.00	-0.10	0.00	0.00	-0.18

Much of the remaining data can be considered to follow a predictable pattern. In general, an increase in the catalytic rate constants for Raf and MEK (k_{19}, k_{21}, k_{23} and k_{25}), or a reduction in the affinity of the interaction between the activated kinases and deactivating phosphatases (increased K_{m18}, K_{m20}, K_{m22}, K_{m24} and K_{m26}), is associated with an increased rate and extent of ERK activation, but reduced Shc phosphorylation and Ras activation. The effects of an increase in [MEK] also follow this pattern, since this is also an activating factor. Conversely, an increase in the rate at which the kinases are deactivated by phosphorylation (V_{18}, V_{20}, V_{22}, V_{24} and V_{26}), or a reduction in the affinity of Raf for MEK, or MEK for ERK (increased K_{m19}, K_{m21}, K_{m23} and K_{m25}), has the opposite effect. An increase in [ERK] appears to reduce the level of MAPK cascade activation, but this is again rather misleading; there is a modest increase in the actual level of activation, but activation as a percentage of total ERK is reduced.

As mentioned above, variations in the parameters associated with the feedback phosphorylation of SOS do not fit the general pattern, and necessitate further consideration. Consistent with representing a negative feedback mechanism, increasing the rate of feedback SOS phosphorylation, or the catalytic capacity of ERK (k_{27}), reduces p_{60} for Shc and Ras, but also has the almost paradoxical effect of decreasing net ERK activation. A reduction in the affinity of ERK for SOS (K_{m27}) induces an opposing response. As suggested earlier in the analysis, ERK is therefore a determinant of its own activity, through the down-regulation of Ras, in addition to the level of Shc phosphorylation (sections 4.3.2.1 and 4.3.2.2). This aptly highlights the increase in system complexity brought about by the introduction of a single feedback interaction; the activation of ERK is initially dependent upon Shc phosphorylation and Ras activity, but the latter are conversely dependent upon the variable level of ERK activity. The extent of Shc, Ras and ERK[4] phosphorylation/activation are therefore interdependent variables, so that the response of the system as a whole to modulation of one of these variables is not necessarily intuitive.

A further factor that seemingly has the potential to disrupt the interconnection between ERK activation and Shc phosphorylation is evidently the rate at which phosphorylated SOS is dephosphorylated, as indicated earlier (section 3.3.3.7), and to a lesser extent, the affinity of this interaction. As Figure 4.9 illustrates, an increase in the SOS dephosphorylation rate (V_{28}) appears to 'uncouple' Shc phosphorylation and Ras activation from ERK activation, in a manner analogous to that of increased [Grb2-SOS] or $[Ras]_{Total}$. This is achieved by increasing the net availability of Grb2-SOS for binding to phosphorylated Shc, which maintains transmission of the signal through SOS to Ras, and obstructs the dephosphorylation of phosphorylated Shc. In a sense, the interdependency of Shc, Ras and ERK is lost, with the level of ERK activity being determined by Shc and Ras, but with ERK having no complementary influence on these variables.

The data corresponding to this final level of the signalling pathway therefore further reinforce the finding that the dynamics of Ras association with SOS, GAP and Raf are of considerable importance in determining system behaviour (see section 4.3.2.2). Furthermore, the complex link between ERK and upstream components of the cascade is again highlighted, in addition to how this could be exploited within the cell

[4] In addition to Raf and MEK, but not directly considered in this analysis.

to vary the extent and duration of MAPK cascade activation. Little experimental interest has focused on feedback regulation of the cascade, other than establishing the fundamental mechanism, but it is plausible that feedback efficiency is regulated in turn by the availability of signalling molecules, either directly, by expression levels (as proposed in section 4.3.2.2), or indirectly, through modulation of the kinetics of SOS dephosphorylation. It seems reasonable that these factors could vary between particular cell types or under different conditions.

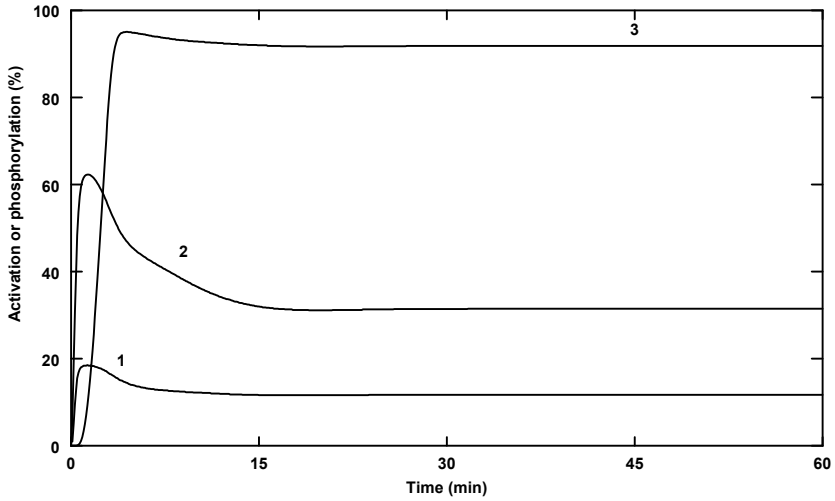

Figure 4.9 The influence of the rate of Grb2-SOS dephosphorylation on the time courses of EGF-induced Shc phosphorylation, and Ras and ERK activation
The data indicate: Ras activation (line 1), expressed as the percentage of total Ras in the GTP-bound form; Shc phosphorylation (line 2), plotted as the percentage of total Shc; and ERK activation (line 3), plotted as the percentage of total ERK in the catalytically active form. The time courses were computed over 60 minutes continuous exposure to 100 nM EGF. SOS dephosphorylation, V_{28} = 7.5 × 10^3 molecule $cell^{-1}$ min^{-1}.

4.4 Summary and Conclusions

A quantitative sensitivity analysis of the simulated EGF signalling pathway has been carried out, the results of which are presented and discussed in the sections above. The study has highlighted a number of interesting features of the model, many of which confirm earlier, unquantified observations. The concentration of EGF at which EGFR activation and down-regulation is simulated predictably has the greatest effect on the distribution of the EGFR between ligand-bound and free cell surface forms. At a saturating concentration of ligand, the effect of increased EGFR or an enhanced rate of receptor-ligand association is therefore limited, since the system is already operating

at full capacity, although these factors assume greater importance at low [EGF]. Despite the quantitative differences in receptor distribution induced by variations in the parameters for receptor-ligand binding, this aspect of system behaviour is qualitatively consistent over the range of values investigated. Nonetheless, in order to correctly reproduce the time-scale of receptor down-regulation, these parameters are clearly constrained within a fairly narrow range, as discovered when fitting parameter values for the top-level module (section 3.3.1.6). In contrast, the system is relatively unaffected by variations in the rate of receptor dimerization, as previously concluded (section 3.3.1.7). Neither is there significant response to a change in the rate of association of occupied receptors with the coated pit proteins, consistent with this representing a saturable internalization mechanism. Thus, although the concentration of EGF takes precedence in determining the influence of other parameters, the general lack of sensitivity to factors operating at this level is also likely to be a function of the limited capacity of the ligand-induced endocytic mechanism. Finally, apparent sensitivity to variations in the rate of internalization is unlikely to be physiologically relevant, since this constitutes part of a model sub-system that is an extensive simplification of real events. However, the value assigned to this parameter is necessarily invariant if the model is to reflect the time-dependent pattern of receptor down-regulation observed *in vivo*, as formerly noted (section 3.3.1.7).

The simulated EGF concentration is also of paramount importance in determining the time courses of Shc phosphorylation and Ras/MAPK cascade activation, although the response is not a simple linear increase with [EGF]. The MAPK cascade exhibits an ultrasensitive response to EGF, characterized by a steep transition from low to high peak ERK activation across a narrow range of EGF concentrations. This property is the basis of the initial response to EGF: the rapid activation of >90% of the total cellular complement of ERK. However, ERK activation is typically transient, and this maximal response is not maintained. Rather, the initial response is down-regulated through activation of a feedback loop, corresponding to ERK-mediated SOS phosphorylation. ERK activation therefore relaxes to a steady state level that is determined by the strength of the feedback signal, i.e. the extent of peak ERK activation. Above a threshold EGF concentration, at which almost maximal peak ERK activation is achieved, any further increase in [EGF] is therefore without effect on the steady state level of ERK activation, but does reduce the time taken to reach peak cascade activation.

The same feedback mechanism is responsible for generating an inverse correlation between the extent of ERK activation and the degree of Shc phosphorylation or Ras activation, but substantial variations in a number of specific parameters are capable of 'uncoupling' these interdependent variables. In each case, the effect can be associated with the disturbance of, what appears to be, a finely balanced mechanism for regulating EGF signalling to the MAPK cascade. Overexpression of the EGFR, or an increase in the catalytic activity of the EGFR-TK, results in prolonged Shc phosphorylation, since this counteracts the feedback dissociation of ShcP-Grb2-SOS, which releases phosphorylated Shc to become a target for phosphatase activity. Importantly, this is not associated with sustained Ras or ERK activation, as there is no direct effect on the phosphorylation status of the cellular pool of SOS, which thus remains effectively inactive. In general, an increase in the intensity of signalling to SOS does not affect down-regulation of the Ras/MAPK cascade; the steady-state level of Ras and ERK activation are insensitive to factors that operate above the level of feedback SOS phosphorylation, which hence confers a high degree of integral stability on the cascade/feedback system.

Conversely, the steady-state level of activation assumed by the Ras/MAPK cascade is strongly dependent upon factors that determine the relative strength or efficiency of the feedback signal. Thus, the characteristic stability is lost as a result of either direct or indirect modulation of the availability of functional SOS, such as through an increase in [Grb2-SOS] or $[Ras]_{Total}$, respectively; the latter increases the proportion of Grb2-SOS that is excluded from ERK phosphorylation through binding to Ras-GDP, and hence overall availability. As a consequence, both Shc phosphorylation and Ras/MAPK cascade activation are prolonged, as these aspects of system behaviour become effectively linked in only one direction. The steady-state level of cascade activation therefore becomes directly proportional to the intensity of the upstream stimulus. Accelerated SOS dephosphorylation produces a similar effect, by reducing the effectiveness of the feedback mechanism.

In order for the model to reproduce the experimentally derived pattern of Shc phosphorylation, the expression level of EGFR is constrained within physiological limits, and k_{cat} across an even narrower range. The analysis also suggests that EGFR overexpression is not linked with prolonged Ras or MAPK cascade activity directly via Shc, and infers that some additional mechanism may be invoked under these

conditions. Possible candidates for Shc-independent mechanisms involved in this aberrant response include Crk mediated SOS/Ras or C3G/Rap-1 activation (181), or through an interconnection with the PLCγ-PKC pathway (33, 48, 87, 188). Furthermore, Shc overexpression may effect cellular transformation through links with alternative cascades, such as the PI-3K/Akt pathway (129), rather than directly through the Ras/MAPK cascade.

Finally, it is generally apparent that the availability of signalling intermediates, such as EGFR, Grb2-SOS and Ras, but also GAP and Raf, is of considerable importance in defining the functional properties of the EGF signalling pathway represented by this particular model. As previously suggested (section 3.3.2.4), the competition between GAP and Raf for binding to active Ras-GTP is confirmed as a determining factor for the kinetics of MAPK cascade activation, as evidenced by the influence of variations in [GAP] and [Raf]. In contrast, the properties of the model appear to be less sensitive to variations in the values assumed for kinetic and thermodynamic constants. Whilst these parameters may influence quantitative aspects, such as the exact timing or extent of pathway activation, variations in these parameters across wider, experimentally determined ranges do not generally induce gross qualitative changes in the pattern of system behaviour; i.e. they do not uncouple ERK activation from Ras activation and Shc phosphorylation, and thereby significantly prolong activation of the pathway as a whole, in contrast to the typical transient response. Exceptions to this generalization are kinetic parameters that indirectly influence the availability of Grb2-SOS, such as those of the SOS dephosphorylation reaction.

This observation is significant for a number of reasons. Firstly, that the type of behaviour that the system demonstrates is robust across a range of values for kinetic parameters implies that the model is a reasonable representation of a generalized EGF signalling pathway. Furthermore, this justifies the treatment of different isoforms of signalling intermediates, which differ slightly in terms of their kinetic properties, as a single cellular pool; for example, Raf-1, A- and B-Raf, and the MEK and ERK isozymes (see sections 3.3.3.1 and 3.3.3.2). It also suggests that the functional properties of the system are resistant to moderate variations in the values of these parameters *in vivo*. Rather, it is tempting to surmise that the specific response to EGF stimulation may be modulated by variations in the actual or functional cellular complement of signalling intermediates. Detailed analysis of a representative growth factor signalling pathway has

demonstrated that the duration of pathway activation as a whole is particularly sensitive to the availability of signalling molecules. Furthermore, this aspect of growth factor signalling has been implicated in defining specific cellular responses (see section 6.1); in the PC12 cell type for example, the transient activation of Ras and the MAPK cascade, such as that induced by EGF, appears to be associated with a proliferative response, whereas the sustained activation of this system stimulated by NGF or FGF is linked with differentiation (217). An intriguing possibility is that such 'decision-making' by the cell might be regulated by the actual or effective availability of key signalling molecules; for example, SOS expression levels, or the availability of functional SOS, as determined by the efficiency of the negative feedback mechanism. This is not without precedent experimentally, as the relative expression levels of the insulin-like growth factor-1 (IGF-1) RTK substrates, IRS-1 and Shc, appear to determine whether IGF-1 receptor activation induces transformation or differentiation in 32D cells (murine haematopoietic cells) (11).

Such inferences should however, be treated with caution; whilst the model upon which this analysis is based is capable of accurately reproducing behaviour that is typical of intact cells, it may not be an entirely faithful representation of the mechanisms underlying these responses. Many of the signalling events that are represented are possibly highly simplified, and particularly the mechanism of Raf activation. Furthermore, in certain cell types there may be alternative mechanisms for activating the Ras/MAPK cascade, such as via PKC or Ca^{2+} (33, 48, 95, 188), which are not considered. Yet, that the model was able to adequately account for the experimentally observed time courses of Ras and ERK activation in the absence of alternative routes for Ras/MAPK cascade, whilst staying within quantitative limits suggested by experimental studies for activation through the SOS pathway, is consistent with the general consensus that these probably play a secondary role (85, 301); however, a more complex model would be required to test this supposition. Thus, the conclusions drawn from the analysis may only be relevant to this particular model, and the real system may be very much more stable to variations in the availability of signalling molecules. Whether such differences exist between various cell types, or under different conditions, remains to be established.

CHAPTER 5

MATHEMATICAL MODELLING APPLIED TO SIGNAL TRANSDUCTION: A CRITICAL REVIEW

5.1 INTRODUCTION

In order to examine the conclusions drawn at the close of the previous chapter within the context of prior theoretical analyses conducted by other authors, the simulation of EGF signalling in PC12 cells is compared in the current chapter with similar published mathematical models of signal transduction. The chapter begins by introducing a series of quantitative analyses of a modular component of growth factor signalling systems, phosphorylation cascades such as the MAPK cascade, and continues with a comparison of the properties predicted for these cascades in isolation, with those displayed within the context of the simulated EGF signalling pathway. In the concluding section, the structural and dynamic features of the simulation are discussed with reference to those ascribed to comparable kinetic models of EGF signalling.

5.2 THEORETICAL STUDY OF PHOSPHORYLATION CASCADES

5.2.1 BACKGROUND

Several prominent authors have previously investigated aspects of signal transduction from a theoretical perspective. The properties of interconvertible enzyme cascades, such as the MAPK cascade, which are a recurrent feature of transduction pathways and metabolism in general, have been a particular focus of attention. Pioneering work in this area was carried out by Stadtman and Chock (321), who investigated the role of covalent modification systems in metabolic regulation.

One view of the role of interconvertible enzymes is that they are modified in an 'all-or none' manner, and hence constitute 'switches' that are employed to turn metabolic pathways on and off as required. An alternative proposal is that covalent modification enables the specific activity of enzymes of regulatory importance to be varied continuously, by altering the steady state distribution of active and inactive forms; this

is regulated through interaction of the converter enzymes with allosteric effectors[5] (321). According to this view, an interconvertible enzyme only functions as a metabolic switch under extreme physiological conditions (306, 321). Using a simplified model of a covalent modification cycle, where the modifying reactions were represented using linear mass-action kinetics, Stadtman and Chock investigated the effect of variations in effector concentration on the fractional modification of the interconvertible enzyme (321). They discovered that such systems demonstrate a number of properties (306).

- Considerable capacity for amplification of the primary stimulus (corresponding to an increase in effector concentration).
- Potential for modulation of the amplitude of the maximal response (i.e. fractional modification of the target enzyme), resulting from a change in the cascade parameters, such as that caused by the action of an effector upon a converter enzyme.
- Capacity to enhance the sensitivity of the response to changes in the stimulus, i.e. to exhibit apparent cooperativity in response to increasing effector concentration, as a result of an effector acting on more than one step in the cascade; this property was later termed 'multistep ultrasensitivity' by Goldbeter and Koshland (116).
- Ability to function as biological integration systems, i.e. to generate a coherent response to numerous simultaneous stimuli, such as a coincident change in the concentration of a number of effectors.

Furthermore, it was shown that these properties were augmented in cascades consisting of more than one modification cycle, the potential for signal and sensitivity amplification increasing with each successive cycle in the cascade. Multicyclic cascades also amplify the rate at which the final target enzyme is modified, enabling them to respond rapidly to changes in effector levels (306).

Goldbeter and Koshland (116) carried out a similar quantitative analysis of covalent modification cascades however, the reactions were modelled using hyperbolic Michaelis-Menten kinetics. Hence, they were able to show that increased sensitivity to

[5] The term 'effector' has a different definition in the signal transduction field (see footnote 1, page 2), but the usage here has the meaning usually assumed in enzymology i.e. an effector is some molecule that modulates the kinetic

changes in stimulus, or apparent cooperativity, can also be obtained if one or more of the converting enzymes operates near saturation with respect to its substrate. This phenomenon was termed 'zero-order ultrasensitivity', indicating that outside the first-order domain, a relatively small change in stimulus resulted in a response that was considerably more sensitive than the Michaelis-Menten function. This was characterized by an abrupt transition from one form of the target enzyme to another, rather than a progressive increase in fractional modification. Hence, it has been suggested that zero-order ultrasensitivity may provide a mechanism for turning pathways on and off, and thereby allow phosphorylation cascades to function as metabolic switches (118). The effects of multistep and zero-order ultrasensitivity are synergistic (118), and the sensitivities at each level of a multicyclic cascade are multiplicative (180). Thus, in principle, ultrasensitivity can be significantly amplified through a multicyclic cascade, increasing the capacity for switch-like behaviour (117, 180). However, there is also the potential for any ultrasensitivity to be diminished if the parameters are not optimal, so that it is also possible for a combined subsensitive response to be obtained (118).

The conditions required in order for an interconvertible enzyme cascade to generate an ultrasensitive response were also investigated by Cárdenas and Cornish-Bowden (40). They confirmed the observation of Goldbeter and Koshland (116), that enhanced sensitivity is obtained when both converter enzymes are approaching saturation, and thus concurred that covalent modification cascades have the potential to provide a switch mechanism for turning metabolic pathways on and off (41). However, they discovered that such cascades also have the capacity to allow the fractional activity of interconvertible enzymes to vary successively, and demonstrated that the nature of the response is a function of the kinetic properties of the individual effectors and converter enzymes (41).

A more specific analysis of the properties of the MAPK cascade has been carried out by Huang and Ferrell (155). Through solving the rate equations for the cascade numerically, as well as by directly measuring ERK activation in *Xenopus* oocyte extracts, they discovered that ERK, the final enzyme in the cascade, exhibited apparent cooperative behaviour. As none of the enzymes in the cascade are known to be cooperative, they attributed this behaviour to the two-step dual phosphorylation

properties of an enzyme, whether positively or negatively.

mechanism by which both MEK and ERK are activated, as this constitutes a variation on multistep ultrasensitivity (102). Theoretical study of the cascade also indicated that some degree of ultrasensitivity would be expected even in the absence of multistep effects (102), in agreement with the proposal that ultrasensitivity may in fact be an inherent property of multicyclic cascades (26).

Ferrell and Machleder (103) have recently expanded on this work to demonstrate that, in intact *Xenopus* oocytes, a positive feedback mechanism greatly enhances the inherent ultrasensitivity of the MAPK cascade, providing an 'all-or-none' switch that apparently determines the fate of the cell. The intrinsic ultrasensitivity of the cascade supplies a stimulus threshold that must be exceeded in order for the feedback loop to be activated, but once this occurs, feedback reinforcement of the primary stimulus prevents ERK from settling at an intermediate activation state. This system therefore ensures that the cascade adopts only either a stable on or off state. Furthermore, Bhalla and Iyengar (17) have shown that positive feedback in a signal transduction network can engender system bistability, i.e. the co-existence of two possible stable steady states at the same stimulus level, separated by an unstable domain (196), as previously demonstrated for metabolic systems (141). An increase in the stimulus above the threshold for triggering the feedback mechanism will cause the system to switch to the alternative steady state, which is maintained following the decline of the stimulus to a sub-threshold level (196). Once activated, the positive feedback loop therefore ensures that the level of MAPK cascade activation is insensitive to changes in the stimulus level, and can sustain maximal ERK activation following withdrawal of the primary stimulus (17). Persistent ERK activation is associated with the transformation of certain mammalian cell types (69) and the differentiation of PC12 cells (217), but has not been experimentally linked with such a positive feedback mechanism in these cases. Finally, the effect of a negative feedback loop on the properties of the MAPK cascade, such as that provided by the ERK-dependent phosphorylation of SOS, has been investigated by Kholodenko (177). In this case, a combination of ultrasensitivity and feedback inhibition can potentially generate sustained oscillations in the level of cascade activation. This phenomenon can imitate either transient or sustained ERK activation, depending upon the period of the oscillations, and may thereby encode signals that define the cell fate, but has not yet been demonstrated experimentally (177).

Whilst an obvious role of covalent modification cascades in metabolic regulation may appear to be substantial stimulus amplification, there is no direct evidence to support this view, and the amount of amplification actually achieved, for example by the MAPK cascade, has been shown to be limited (102). Indeed, such amplification is unnecessary and may even be undesirable (189). The work discussed thus far suggests that a more probable role is sensitivity amplification, which allows a system to generate a significant response to a relatively small change in stimulus; this would enable metabolic systems to detect and respond to relatively small changes in their environment, and could be of considerable importance in metabolic regulation (116, 117). Furthermore, this property may allow an interconvertible enzyme cascade to effectively operate as a metabolic switch (41, 118, 180), allowing the system to shift between stable steady states in response to a finite change in stimulus (189). Sensitivity amplification may also be important to enable systems to distinguish between background noise and a genuine stimulus (117, 189), by reducing the sensitivity of the system at low stimulus levels (155). Hence, the capacity for the MAPK cascade to exhibit an 'all-or-none' response to a small change in stimulus may enable the system to filter out background noise, and also constitute a mechanism for effectively switching the activity of ERK on and off as required (155). This property of the cascade may be pertinent to its involvement in processes such as the initiation of mitogenesis or differentiation, which requires cells to make an abrupt shift between discrete metabolic states (155). Moreover, incorporation of the MAPK cascade within a positive or negative feedback loop, in conjunction with ultrasensitivity, further enhances the repertoire of properties that can theoretically be demonstrated (17, 103, 177), and may be important in defining the functional role of the MAPK cascade in certain cell types.

The studies described above have therefore highlighted some possible regulatory properties of modification cascades, but have been mainly concerned with whether these properties have the potential to significantly affect the activity of a single target enzyme. However, metabolic control analysis indicates that unless this enzyme exerts substantial control over metabolic flux, the overall impact of altering its activity is likely to be insignificant (101). Furthermore, specific molecular mechanisms were assumed in modelling the system. In order to analyse the effect of variations in the fractional modification of an interconvertible enzyme upon metabolic flux, as well as the likely impact of variations in effector concentration on systems containing covalent modification cascades, Small and Fell (312) have developed and utilized an extension of

metabolic control analysis. This approach does not require consideration of the molecular mechanisms involved, and is therefore likely to allow more generalized conclusions. In agreement with the work discussed above, they concluded that ultrasensitivity is likely to be generated, and thereby enhance the sensitivity of metabolic flux to an effector, only under a stringent set of conditions (312). Kholodenko and colleagues (180) have also developed an adaptation to control theory, which they have termed signal transfer analysis, to quantify the response of a covalent modification cascade to a stimulus. This is similar to modular control analysis (170, 304), but more appropriate for the study of biological information transfer (180).

In summary, several studies have suggested a number of modes of operation and functional roles for the MAPK cascade within a physiological setting, but many fail to consider how the behaviour of the MAPK cascade as an independent unit may be affected by incorporation within a more extensive signalling system, comprising several interacting modules. Thus, the cascade may have the potential to exhibit certain properties in isolation that are not displayed when embedded within a cellular signal transduction pathway, due to unforeseen constraints imposed by this environment. An exploration of this possibility, through comparison of the simulated dynamic properties of the MAPK cascade against the background of a representative signalling pathway, with the range of potential behaviours suggested by previous theoretical analyses, is conducted in the following sections.

5.2.2 INVESTIGATION OF SENSITIVITY AMPLIFICATION BY THE MAPK CASCADE

One of the most interesting results of the earlier sensitivity analysis of the simulated EGF signal transduction pathway, was that the MAPK cascade, within the confines of this system, was found to exhibit an apparently cooperative, or ultrasensitive, response to the primary stimulus, EGF (section 4.3.2.1). Thus, a threshold concentration of EGF (> 0.1 nM) initially induces a rapid and almost complete conversion of ERK between inactive and active forms, despite inducing only a 10% activation of Ras (data not shown), consistent with the reported degree of stimulus amplification demonstrated by the cascade (102). However, this peak response is not maintained, but is counteracted by feedback down-regulation, resulting in a much reduced steady state level of ERK activation. Nonetheless, the steady state response is still apparently cooperative, further implying that some aspect of the system favours ultrasensitivity.

The predicted EGF stimulus-response curves for ERK activation are reproduced in Figure 5.1 below.

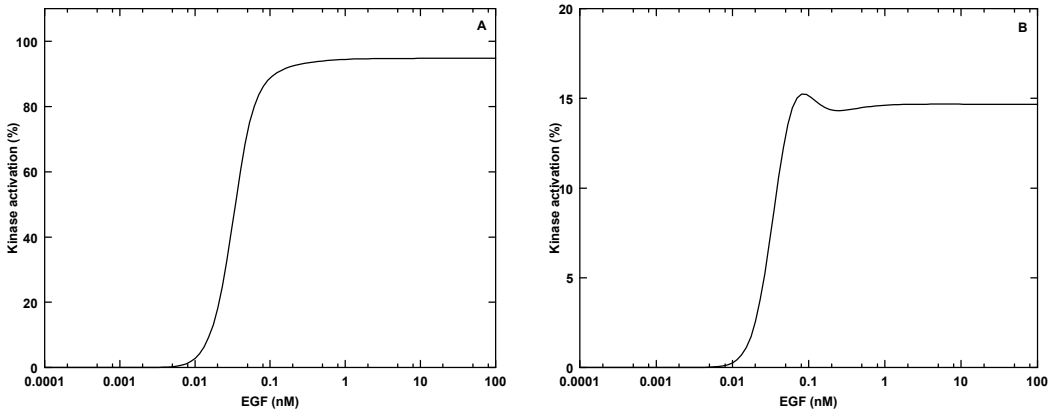

Figure 5.1 Predicted EGF stimulus-response curves for ERK activation
The curves indicate (**A**) peak activation and (**B**) steady state activation, reproduced from Figures 4.2 and 4.3. ERK activation is plotted as the percentage of total ERK in the catalytically active form. All other simulation parameters are listed in Table 3.3.

As emphasised by Huang and Ferrell (155), none of the kinases comprising the MAPK cascade are known to be cooperative, and possible sources of this type of behaviour may be the two-step dual phosphorylation mechanism by which both MEK and ERK are activated, or through partial saturation of the reactions that activate and inactive the cascade kinases. Alternatively, sensitivity amplification may simply be an inherent property of a multi-level cascade arrangement of protein kinases (26). These possibilities can be examined, firstly by comparing the kinetic properties of Raf, MEK and ERK, and the phosphatases associated with the MAPK cascade, with the cellular content of MAPK components assumed in the PC12 model. These data are summarized in Table 5.1 below.

It is apparent from the substrate concentration/K_m ratios, that although the degree of saturation of the activating reactions is greater than that of the inactivating processes, the majority are at least partially saturated. The precondition for zero-order ultrasensitivity is therefore satisfied: at least one of the reactions operates outside the first-order domain (116). It should be noted that the model was not designed with this as a prerequisite, and that these particular concentration/K_m ratios were determined through fitting of the system parameters to enable the model to reproduce

experimentally obtained time courses of Ras, MEK and ERK activation. This raises the possibility that the theoretical capacity for the MAPK cascade to exhibit ultrasensitivity is realized *in vivo*, and may be an integral feature of the EGF signalling system, not only in the PC12 cell line, but also in many others that respond in a similarly rapid, but transient manner to EGF. This property may therefore have some functional significance for growth factor signalling, a prospect that can be further explored by considering the extent to which sensitivity amplification is likely to be manifested within the cellular environment.

Table 5.1 Substrate concentrations and K_m values for the reactions of the MAPK cascade in the PC12 simulation

All values are expressed in units of molecule cell^{-1}.

Reaction	Substrate Concentration	K_m	Concentration/K_m
Raf activation	1.0×10^4	2.5×10^3 [a]	4.0
Raf inactivation	1.0×10^4	6.0×10^3	1.67
MEK activation	3.6×10^5	9.0×10^3	40
MEK inactivation	3.6×10^5	6.0×10^5	0.6
ERK activation	7.5×10^5	9.0×10^4	8.3
ERK inactivation	7.5×10^5	6.0×10^5	1.25

[a] This value corresponds to the K_d for Ras-GTP/Raf binding, which mediates the activation of Raf at the plasma membrane, through an assumed phosphorylation event.

The degree of ultrasensitivity exhibited by a cascade system of protein kinases can be quantified in terms of the steepness of the stimulus-response curve. Several slightly different approaches have previously been applied. Stadtman and Chock (321) have defined a sensitivity index, *S*, which provides an indication of the change in stimulus required to increase activation of the terminal kinase from 10% to 90%:

$$S = 8.89\ N_{0.5} / (N_{0.9} - N_{0.1}) \qquad [1]$$

where $N_{0.5}$ is the stimulus required to induce 50% of the maximal response. The constant 8.89 is a scaling factor, which relates *S* to the change in stimulus required to increase activation from 10% to 90% if the stimulus-response curve is a rectangular hyperbola, similar to the rate curve obtained for an enzyme that displays Michaelis-Menten kinetics, or a typical ligand binding curve; it can be shown that the required ligand concentration is 8.89 times the K_d for ligand binding, or that which induces 50% saturation (101). This measure of sensitivity is conceptually similar to the Hill

coefficient, used to quantify the degree of cooperativity exhibited by an allosteric protein in ligand binding. Hence, a value greater than one indicates that the system is more sensitive than the Michaelis-Menten function (ultrasensitive) and is characterized by a sigmoidal stimulus-response curve, resembling a ligand binding plot indicative of positive cooperativity. Conversely, the system is less sensitive (sub-sensitive) if the value is less than one.

Goldbeter and Koshland's (116) response coefficient is also analogous to a measure of cooperativity:

$$R_N = N_{0.9} / N_{0.1} \quad [2]$$

where N is a factor, such as ligand concentration, that determines the fractional extent of kinase activation (101). If the stimulus-response curve is a rectangular hyperbola, R_N = 81, or the ligand concentration ratio required to increase the saturation of a Michaelis-Menten enzyme from 10% to 90%. This coefficient decreases with the steepness of the curve, to a minimum of one, denoting an infinitely steep response. It is possible however, to compare R_N with a hypothetical Hill coefficient, as the two are related by the following expression:

$$R_N = (81)^{1/n_H} \quad [3]$$

where n_H = Hill coefficient[6].

It also follows from equations 2 and 3 that:

$$(81)^{1/n_H} = N_{0.9} / N_{0.1} \quad [4]$$

This equation can be rearranged to give:

$$1/n_H = \log (N_{0.9}/N_{0.1}) / \log (81) \quad [5]$$

An expression of this form was used by Huang and Ferrell (155) to quantify the steady state response of their MAPK cascade model to an upstream stimulus, in terms of the predicted Hill coefficient. In this particular study, the stimulus corresponded to the concentration of the enzyme responsible for activating the initial kinase in the cascade,

[6] Hence, where $1/n_H = 1$, as in the case of a Michaelis-Menten enzyme, $R_N = 81$.

a MAPKKK such as Raf or Mos. Over a range of assumed K_m values and concentrations for the cascade reactions and enzymes, n_H for MEK was found to vary between 1.3 and 2.4, whereas that for ERK was calculated to be between 2.4 and 9.1. However, Raf/Mos was not predicted to demonstrate an ultrasensitive response (n_H between 0.9 and 1.1), presumably since the concentration of this component was consistently assumed to be at least one order of magnitude less than the K_m for the activation reaction.

An important distinction between the MAPK cascade module of the PC12 simulation and many other mathematical models of phosphorylation cascades (116, 155, 321), lies in the regulation of cascade activation: it has generally been assumed in many analyses that the input to the cascade is an independent variable, whereas in the PC12 model, the magnitude of the input signal is dependent upon the activation state of the cascade, through feedback regulation (see section 4.3.2). In order to quantify the hypothetical response to an immediate upstream stimulus, i.e. Ras-GTP[7], and enable a direct comparison with the work of previous authors, it was necessary to disable the feedback loop that down-regulates Ras and ERK activation. Determination of Hill coefficients for the steady state response of the PC12 MAPK cascade to Ras-GTP, under these conditions, yields comparable values to those predicted by Huang and Ferrell (155): 1.2, 1.9 and 2.6, for Raf, MEK and ERK respectively. As implied by a consideration of the relative concentrations and K_m values for the components and reactions of the MAPK cascade, the system has the potential to respond with greater overall sensitivity to a small change in stimulus than predicted by the Michaelis-Menten function, in agreement with the work of many other authors (41, 116, 321). Moreover, this sensitivity is amplified at each successive level of the cascade, as shown graphically in Figure 5.2 below, corroborating previous observations made by several groups (117, 180, 306). As a consequence, although the sensitivity exhibited by ERK is actually much less than expected for a typical Michaelis-Menten enzyme at very low stimulus levels, ERK responds in an 'all-or-none' fashion once an appropriate stimulus is applied (155).

[7] Since Ras-GTP is directly responsible for activating Raf in the PC12 model, this corresponds to the immediate upstream input to the MAPK cascade represented in the model of Huang and Ferrell (155).

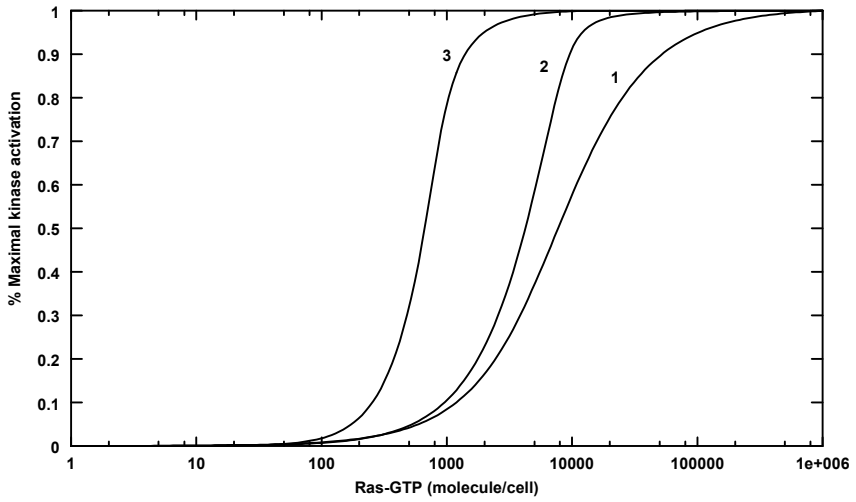

Figure 5.2 Predicted Ras-GTP stimulus-response curves for components of the PC12 cell MAPK cascade

The curves indicate the steady state response of Raf (line 1), MEK (line 2) and ERK (line 3) to Ras-GTP, predicted by the model of EGF-induced MAPK cascade activation in PC12 cells. The data are expressed as the percentage of maximal kinase activation. All other simulation parameters are listed in Table 3.3.

A high concentration of MEK, relative to the K_m values for the activating and inactivating reactions, was found by Huang and Ferrell to be the predominant factor in conferring ultrasensitivity on their model of the MAPK cascade (155). In contrast, a 10-fold reduction in either the assumed Raf, MEK or ERK concentration in the PC12 model significantly reduced, but did not eliminate the sensitivity to Ras-GTP, confirming that partial saturation of several cascade kinases and phosphatases is at least partly responsible for generating an ultrasensitive response; for example, a 10-fold decrease in Raf results in an n_H of just 1.5 for the overall response of the cascade. Any possible contribution from the two-collision mechanism of MEK and ERK dual phosphorylation can be assessed by calculating the Hill coefficients for a model in which MEK and ERK are phosphorylated at both regulatory sites through a single collision with their effectors. Although this does not affect the sensitivity of the Raf response, n_H for MEK and ERK are reduced to 1.4 and 2.0 respectively, as similarly observed by Huang and Ferrell (155), and consistent with the proposal that a two-step activation mechanism may constitute a variation on multi-step ultrasensitivity (102). Both zero-order and multi-step effects probably synergize to generate the observed ultrasensitivity of the PC12 model MAPK cascade to Ras-GTP, and hence also to EGF.

Thus, the Raf/MEK/ERK cascade of the PC12 model appears to behave in exactly the manner predicted by analyses of both generic phosphorylation cascades (116, 117, 180, 306, 321), and a representative MAPK cascade (155). Yet, the predicted degree of sensitivity amplification is actually quite modest, with the MAPK cascade responding with an overall n_H of 2.6 to Ras-GTP, in comparison with a theoretical maximum of 9.1, suggested by Huang and Ferrell (155). This is also somewhat less than the value of 4.9 determined experimentally in *Xenopus* oocyte extracts (155), although this system cannot be considered to be generally representative of mammalian cell types; the expression level of MAPKKK (Mos), MEK and ERK is typically 4 - 5 orders of magnitude greater in *Xenopus* oocytes (102), resulting in more extensive saturation of the cascade reactions. MAPK cascade ultrasensitivity may therefore be rather less significant in growth factor signalling than envisaged by many previous authors, but as an apparently inherent feature of the cascade, may still have some importance in defining the overall cellular response.

Through a propensity to amplify the sensitivity of ERK to a stimulus, and thereby facilitate an abrupt transition between stable 'off' and 'on' states of ERK activation (Figure 5.1A and 5.2), the MAPK cascade has been proposed to function as a biochemical 'switch' that instigates a shift between distinct metabolic states, such as mitogenesis and differentiation (155). This deduction was however, founded on a steady state analysis of the MAPK cascade in isolation, whereas the dynamic properties that are exhibited within the context of an extended signalling system are probably more relevant in resolving any physiological role that intrinsic ultrasensitivity may play. The consequences of regarding the MAPK cascade as an independent functional unit can be illustrated by eliminating the feedback down-regulation of cascade activation in the PC12 simulation, as in the earlier calculation of Hill coefficients for the steady state response to Ras-GTP. Figure 5.3A illustrates that this results in a high level of ERK activation being maintained indefinitely, corresponding to the stable 'on' state predicted by previous steady state analyses of the isolated cascade (102, 155).

This contrasts markedly with the pattern observed when the feedback mechanism is operational, as demonstrated by Figures 5.3B and 5.3C: in agreement with a typical experimental time course of MAPK cascade activation in the corresponding cell type (Figure 5.3C), the PC12 simulation predicts that ERK is rapidly switched 'on' [8]

[8] Corresponding to a >90% activation of ERK; see Figure 5.1A.

following an initial exposure to a stimulus of sufficient magnitude (100 nM EGF), but that ERK activation declines thereafter, reaching a level of around 15% of the peak response after 60 minutes (Figure 5.3B), which is a much less conclusive 'on' state. Whether such a low level of activation is capable of inducing a physiological effect remains to be established.

Both peak and steady state responses of ERK to EGF are estimated to have an n_H of 2.7, providing quantitative confirmation that the MAPK cascade maintains the potential to respond with enhanced sensitivity to an external stimulus when embedded in a typical signalling pathway. Nonetheless, this example of the dynamic behaviour of the MAPK cascade, within a simulated physiological setting, provides no evidence in favour of the cascade functioning as a 'metabolic switch', either in the PC12 cell line, or indeed in any cell system where the rapid down-regulation of EGF-induced Ras and ERK activation is observed (Figures 5.3B and 5.3C). Rather, the prevailing purpose of the observed sensitivity amplification may be to allow the system as a whole to detect small variations in stimulus levels (116, 117), or discriminate between background noise and a genuine signal (117, 189), by establishing a threshold that must be exceeded in order to activate the cascade (103, 155).

Not only is sensitivity predicted to be amplified at each level of a multi-level cascade, but also the rate of kinase activation (321). A further role of the cascade arrangement of Raf, MEK and ERK *in vivo* may therefore be acceleration of the rate at which ERK is activated in response to an external signal. In exceptional circumstances however, for example in the case of *Xenopus* oocytes, where positive feedback reinforces ERK activation (103), or in the absence of negative feedback (Figure 5.3A), the MAPK cascade may indeed function as a switching device; as shown repeatedly in this, and previous sections, Ras and ERK activation may be sustained by counteracting feedback down-regulation (see sections 3.3.2.6, 3.3.3.7, 4.3.2.2 and 4.3.2.3), suggesting that inactivation of this mechanism may be involved in prolonging Ras/MAPK cascade activation, and perhaps instigating PC12 differentiation, in response to NGF or FGF (see sections 4.4 and 6.1).

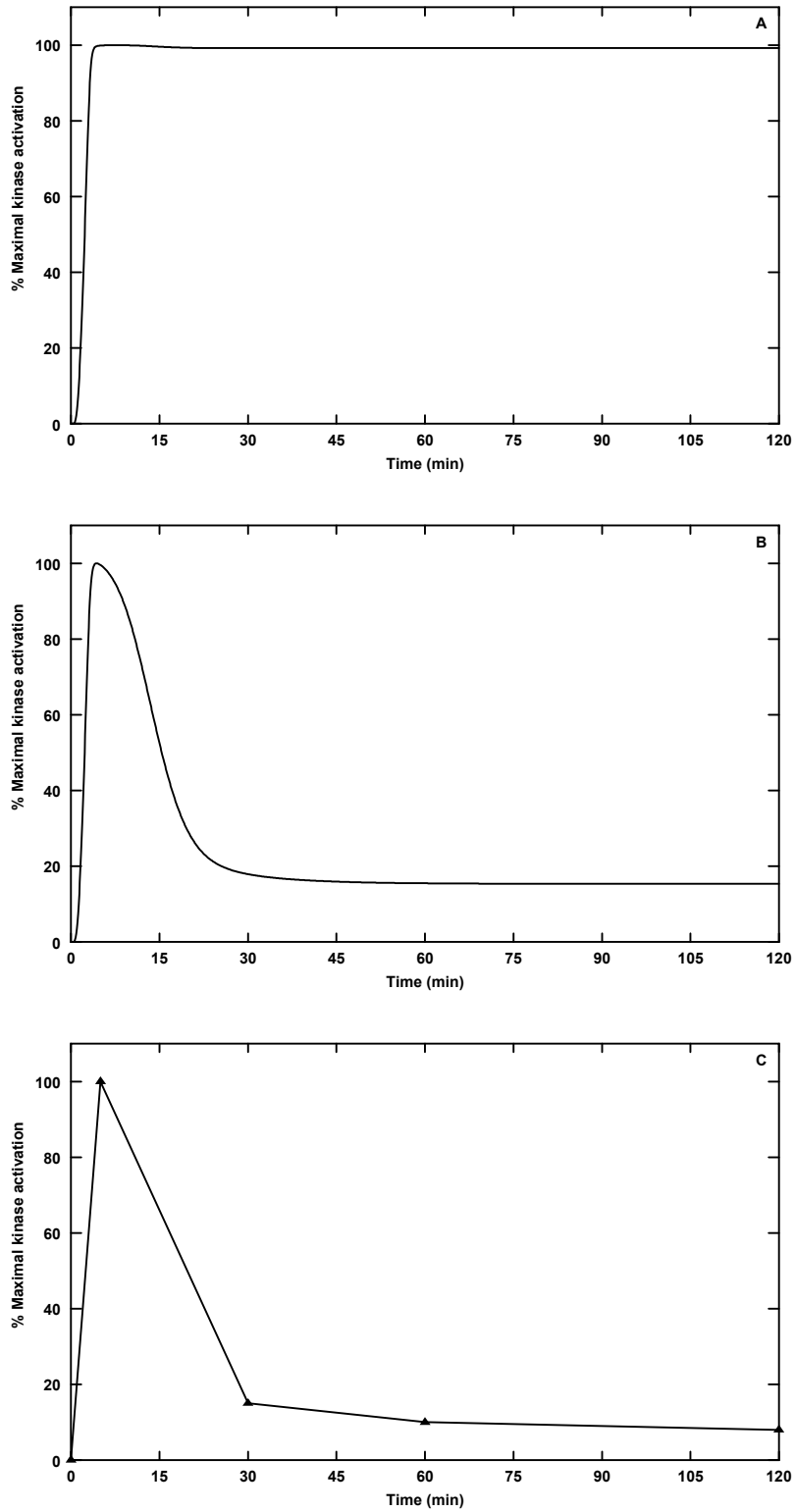

Figure 5.3 The impact of negative feedback regulation of the Ras/MAPK cascade on the time course of EGF-induced ERK activation

The curves indicate the predicted response of the PC12 cell line to 100 nM EGF, in the absence (**A**) and presence (**B**) of negative feedback regulation, and (**C**) a corresponding experimental time course, replotted from Teng *et al.* (335). The simulated time course (**B**) diverges slightly from the experimental data (**C**) after 60 minutes, as additional processes that contribute to the down-regulation of ERK activation after this time-point, such as dephosphorylation by nuclear phosphatases, have been omitted from the model (see sections 2.2.6.3 and 3.3.3.2).

A slightly different perspective on the predicted dynamic properties of the MAPK cascade has been provided by Kholodenko (177). Unlike many other theoretical analyses, this study considers the effects of negative feedback regulation in a mathematical model of the MAPK cascade, but highlights a rather extreme example of the type of behaviour that this can generate. Kholodenko has shown that, in principle, a combination of ultrasensitivity and negative feedback can give rise to sustained oscillations in ERK activation (177). In order to demonstrate this response, a reconstruction of Kholodenko's model of the MAPK cascade has been implemented in Gepasi 3.2; the predicted time course of ERK activation, induced by a threshold stimulus, is shown in Figure 5.4A below. At early time-points, the response is similar to the more typical transient pattern of EGF-induced ERK activation, shown in Figure 5.3B: there is a rapid, maximal activation of ERK, but this initial response is eventually down-regulated through the feedback inhibition of Ras activation. However, there is no attainment of a stable 'off' state, and instead a recurrent activation/inactivation cycle is initiated.

In a metabolic pathway, sustained oscillations may arise through a time delay in the cooperative feedback inhibition of an upstream enzyme, which destabilizes the system (101). The origins of this behaviour in the MAPK cascade lie in the magnitude of the feedback signal, and the degree of ultrasensitivity demonstrated by ERK to the initial stimulus, which together result in the suppression of Ras activation being disproportionately greater than the extent of ERK activation; the system effectively overcompensates. ERK activation therefore declines and approaches the basal level, but this releases the inhibition of Ras and initiates a further round of cascade activation, with the same net result.

This can be more effectively rationalized by quantifying the sensitivity of the cascade to a stimulus, and the strength of the feedback signal. For this purpose, a slightly different sensitivity index to those already introduced is more applicable:

$$R = \mathrm{d} \ln [E_n] / \mathrm{d} \ln [E_o] \qquad [6]$$

where R = overall sensitivity of the cascade, d ln $[E_n]$ = steady state fractional change in the output, i.e. ERK activation, and d ln $[E_o]$ = fractional change in the input (177), which in this case is presumed to correspond to Ras-GTP; R is therefore the slope of a tangent to a curve of ln [ERK] plotted against ln [Ras-GTP] (101).

Hence, R also corresponds to the response coefficient of metabolic control analysis, originally defined by Kacser and Burns (167), and first employed in a steady state sensitivity analysis of phosphorylation cascades by Cárdenas and Cornish-Bowden (40). Clearly, Stadtman and Chock's sensitivity index, S (321), and the Hill coefficient, n_H, used by Huang and Ferrell (155), are an approximation to R. All three measures of sensitivity are dimensionless, and as before, a value of R greater than one indicates an ultrasensitive response. However, S, n_H and furthermore, the response coefficient of Goldbeter and Koshland, R_N (116), are indicators of sensitivity over a finite range, whereas R quantifies the response of the system to a very small change in a system parameter (332).

Similarly, the feedback strength is given by:

$$f = \mathrm{d} \ln v_1 / \mathrm{d} \ln [E_n] \qquad [7]$$

where v_1 = the rate of the reaction that activates the initial kinase in the cascade (177), i.e. the rate of Raf activation, mediated by Ras-GTP. If the feedback mechanism is inhibitory, f is negative, whereas f is positive if the feedback is activating. The overall sensitivity, R, in the absence of feedback effects, is therefore modified by the factor, f, when the degree of cascade activation is regulated by a feedback loop:

$$R_f = R / (1 - f \times R) \qquad [8]$$

Negative feedback therefore decreases the overall sensitivity of the cascade to a stimulus, whilst positive feedback enhances sensitivity (177), as noted in intact *Xenopus* oocytes by Ferrell and Machleder, where feedback activation of MAPKKK increases the sensitivity, in terms of n_H, from 4.9 to 35 (103).

Although Kholodenko does not publish typical values of R and f that are likely to be associated with the distinctive behaviour illustrated in Figure 5.4A, these can be estimated from the reconstruction of this author's model, yielding values of 120 and -0.7 for R and f respectively. The value of R is therefore considerably in excess of the feasible range for n_H suggested by Huang and Ferrell (155), and arises from a high degree of saturation of the cascade reactions, with component concentrations between 10 and 20 times greater than the assumed K_m values (177). A reduction of approximately one order of magnitude in these ratios generates a stable 'on' state, much

the same as that illustrated in Figure 5.3A, rather than sustained oscillations, presumably due to the relatively weak feedback inhibition. Not surprisingly, an increase in feedback strength was found to restore the oscillating pattern of ERK activation (177).

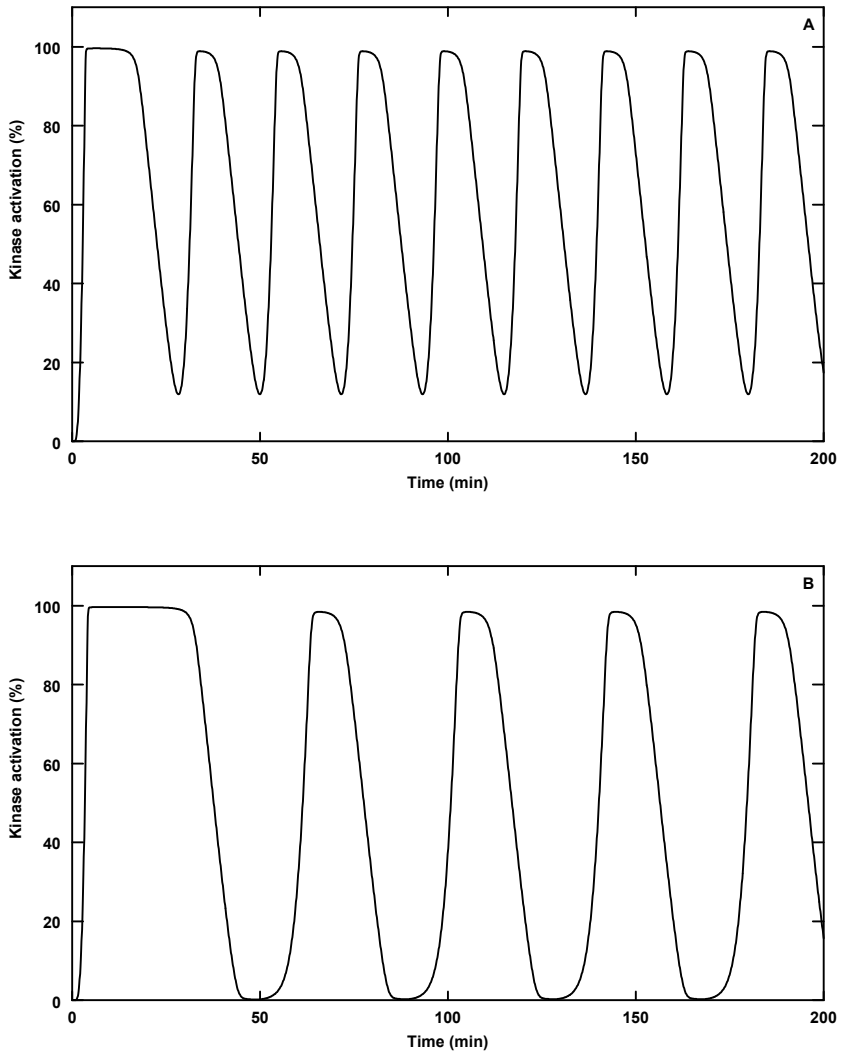

Figure 5.4 Sustained oscillations in the activation level of ERK, arising from a combination of ultrasensitivity and negative feedback regulation

The curves indicate the percentage of total ERK in the catalytically active form predicted by (**A**) a reconstruction of Kholodenko's model of the isolated MAPK cascade (177), implemented in Gepasi 3.2, and (**B**) the PC12 model of EGF-induced MAPK cascade activation. PC12 simulation parameters are listed in Table 3.3, except: $V_{18} = 9.0 \times 10^3$ molecule cell^{-1} min^{-1}; $K_{m18} = 4.8 \times 10^3$ molecule cell^{-1}; k_{19} to k_{25} (odd numbers) = 1.5 min^{-1}; V_{20}, $V_{22} = 2.7 \times 10^4$; V_{24}, $V_{26} = 1.8 \times 10^4$; K_{m19} to K_{m26}, all = 9.0×10^3 molecule cell^{-1}; $k_{27} = 0.1$ min^{-1}; $K_{m27} = 5.4 \times 10^3$ molecule cell^{-1}; $K_{m28} = 9.0 \times 10^3$ molecule cell^{-1}.

The PC12 model represents the contrasting situation, where sensitivity amplification through the cascade is comparatively low (R = 2.0)[9], but the feedback strength is more substantial (f = -1.0), resulting in a transient activation of ERK that relaxes to a stable 'off' state. By adjusting the K_m values for the MAPK cascade to those assumed by Kholodenko, and reducing the catalytic rate of activated ERK, it is possible to obtain similar oscillations in ERK activity with this more extensive model of EGF signalling, as shown in Figure 5.4B. Yet, in order to achieve this effect, it is necessary to reduce the specific activity of ERK, from the fitted value of 1.6 min^{-1} to 0.1 min^{-1}, which is well below the reported range (Table 4.1). At the lower ratios of concentration/K_m originally assumed in the PC12 model, such a reduction in the effective magnitude of the feedback signal generates a prolonged activation of Ras and ERK, as previously observed many times throughout model development and analysis (see above, and sections 3.3.2.6, 3.3.3.7 and 4.3.2), and consistent with the work of Kholodenko. However, a considerable increase in feedback strength, above that initially assumed in the PC12 model, does not cause the system to lose stability and oscillate around a steady state. Rather, lower peak and steady state activation levels are attained, although there is some indication of substantially damped oscillations, as Figure 5.5 shows.

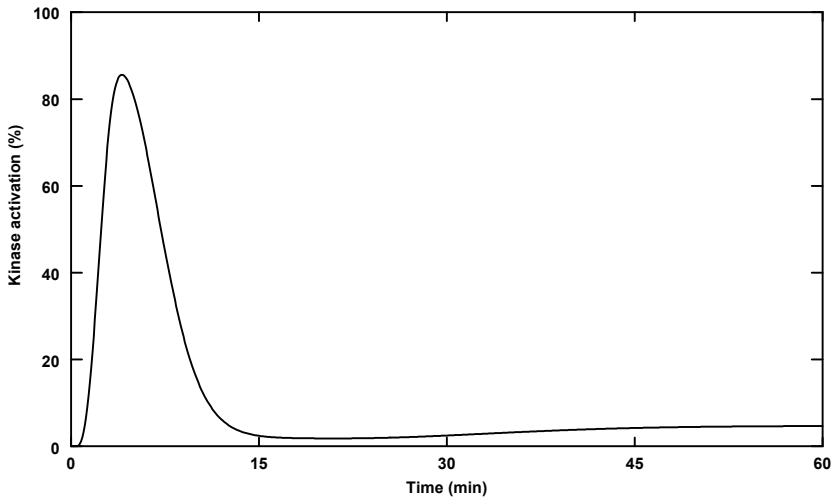

Figure 5.5 Damped oscillations in the ERK activation level arising from increased feedback strength in the PC12 model

The data are expressed as the percentage of total ERK in the catalytically active form, computed over 60 minutes continuous exposure to 100 nM EGF; k_{27} = 10 min^{-1}. All other simulation parameters are listed in Table 3.3.

[9] As noted in the text, the Hill coefficient is an approximation to the response coefficient, R, and hence the value of n_H = 2.6 for overall cascade sensitivity is slightly more than the value of R.

This disparity in the properties of the MAPK cascade predicted by the two models probably arises from differences in implementation of the feedback regulation of Ras and ERK. In a model that considers only the kinetics of MAPK cascade activation, the net effect of this regulation can be approximated by the noncompetitive or cooperative inhibition of Raf activation by ERK (177), but this is not an adequate approximation when considering the dynamic behaviour of the MAPK cascade embedded within a typical signalling pathway. Within this more realistic setting, it is not Raf activation that is directly inhibited, but Ras activation, and not through enzyme inhibition, but via the effective inactivation of SOS by covalent modification. The reversal of this inhibition therefore requires not only the cessation of the inhibitory signal, i.e. the associated decline in ERK activity, but also the reconstitution of functional SOS through dephosphorylation. Hence, in the PC12 model, feedback inhibition is not instantaneously released through the down-regulation of ERK activation, and the level of Ras activation does not immediately rebound. Rather, the inhibitory effects persist for some time after the feedback signal is withdrawn, thus ensuring that a stable 'off' state is maintained and desensitizing the system to further immediate activation, as demonstrated in several experimental studies (350, 351). It follows that a more rapid rate of SOS dephosphorylation might allow the system to oscillate, in much the same way as an increase in the ultrasensitivity of the MAPK cascade at a lower feedback strength, although Figure 5.6 shows that this does not appear to be the case. Instead, a higher steady state level of ERK activation is achieved, once again corresponding to prolonged activation of this enzyme, as observed previously (sections 3.3.3.7 and 4.3.2.3).

Thus, the set of conditions required to generate oscillations in MAPK cascade activation are quite restricted, and perhaps even rather contrived, so that this phenomenon seems unlikely to be generally evident. Nonetheless, the cycling between inactive and active enzymatic forms, coupled with the slow diffusion of phosphorylated proteins through the cytosol, is suggested to result in waves of activated kinases that travel through the cell (27), which could imitate sustained ERK activation *in vivo* (177), such as that corresponding to the 'average' response of a population of PC12 cells to NGF (217). This is an interesting possibility, but cannot be explored further without the experimental analysis of growth factor-induced MAPK cascade activation in individual cells.

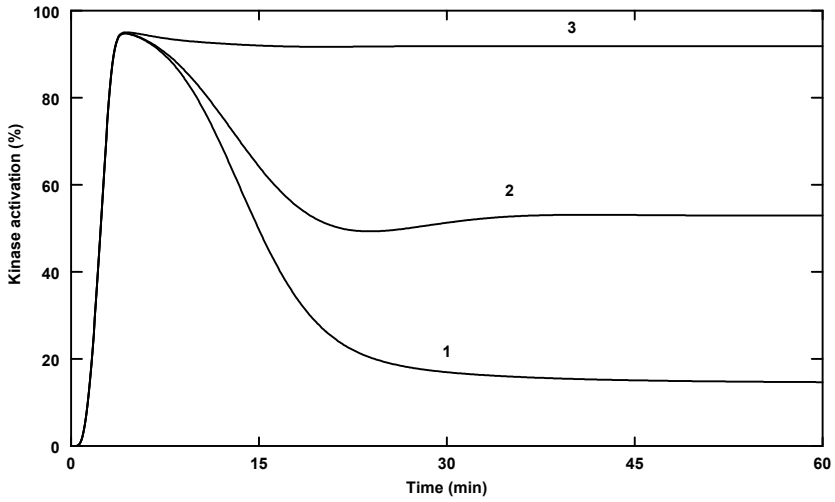

Figure 5.6 The effect of an increased rate of SOS dephosphorylation in the PC12 model

The time courses were computed over 60 minutes continuous exposure to 100 nM EGF, at V_{28} = 75 (line 1), $V_{28} = 7.5 \times 10^2$ (line 2) and $V_{28} = 7.5 \times 10^3$ (line 3). All other simulation parameters are listed in Table 3.3. The data are expressed as the percentage of total ERK in the catalytically active form.

This opening section has focused on just one possible aspect of cell signalling: sensitivity amplification by a common component of many signal transduction pathways, the MAPK cascade. By comparing the properties displayed by the cascade as an isolated functional unit and within the setting of a representative signalling system, some indication of the extent to which sensitivity amplification is exhibited within the cell, and likely physiological roles, has been provided. In order to explore further significant characteristics that the system as a whole may demonstrate, other features of the PC12 simulation are explored in more detail in the following section, with regard to similar kinetic models EGF signalling.

5.3 KINETIC MODELS OF EGF SIGNALLING

In the recent past, quantitative models of several aspects of EGF signalling have been developed, including the mathematical model of EGF-EGFR interaction at the cell surface employed as the basis for the top-level module of the simulation (112) and, as discussed above, several analyses of the MAPK cascade (155, 177). Yet, the computer simulation of EGF signal transduction developed in this project is unique as a kinetic model of growth factor signalling in a specified cell type, which integrates these, and many other, features of the pathway. However, two comparable models were published during the course of the project: that of Kholodenko and colleagues (178), representing

the early signalling events stimulated by EGF in hepatocytes; and that of Bhalla and Iyengar (17), which provides a generalized model of growth factor signalling.

5.3.1 THE MODEL OF KHOLODENKO *ET AL.*

5.3.1.1 Model description

The model developed by Kholodenko and colleagues (178) has been designed to reflect only the short term responses of isolated rat hepatocytes to EGF stimulation, and is therefore bounded by the formation of signalling complexes at the plasma membrane and the activation of PLCγ, but still represents perhaps the most comprehensive kinetic model of these events published to date.

In common with the simulation of EGF signalling in PC12 cells developed in this project (see Chapter 3), EGFR activation is mediated by the binding of EGF to the monomeric receptor, which induces EGFR dimerization, but as the time-scale is limited to within two minutes of EGF stimulation, receptor-ligand internalization is not included in the model. However, EGFR autophosphorylation, and dephosphorylation by cellular phosphotyrosine phosphatases, are explicitly represented. The hepatocyte model also considers the direct binding of Grb2 to the EGFR, and assumes that the association of the activated EGFR with either Grb2 or Shc is stable, rather than transient, and competitive. The binding of Shc to the autophosphorylated receptor results in RTK-mediated phosphorylation of Shc, enabling Grb2 to also associate with the EGFR indirectly via Shc. Hence, this particular model includes several species of signalling complex omitted from the PC12 simulation, for example, EGFR-Shc-Grb2-SOS and EGFR-Grb2-SOS complexes. Furthermore, both free and complexed Grb2-SOS may dissociate to yield independent SOS. A common assumption in both models is that only free phosphorylated Shc is a target for phosphatase activity, and that this species may also associate with Grb2 and SOS independently of the EGFR. On the whole, there are more mechanistic differences than similarities between the PC12 simulation and the hepatocyte model of Kholodenko and colleagues, yet the kinetic parameters and dynamic properties of these models are surprisingly consistent, where these features are directly comparable.

5.3.1.2 Parameter values

Table 5.2 provides a summary of the values assigned to analogous parameters of the PC12 cell simulation and the hepatocyte model of Kholodenko and colleagues; parameters for the latter have been converted to the units used in the PC12 simulation.

Table 5.2 Parameter values for the computer simulation of EGF signal transduction in PC12 cells and the model of EGF signalling in hepatocytes, developed by Kholodenko *et al.* (178)

Parameter	PC12 simulation	Hepatocyte model
Ligand binding		
[EGF], nM	1×10^2	20
$[EGFR]_{Total}$, molecule cell^{-1}	1.5×10^4	1.8×10^5
K_{d1}, M	1.9×10^{-9}	0.6×10^{-9}
k_1, M^{-1} min^{-1}	3.8×10^8	6.0×10^9
k_{-1}, min^{-1}	0.73	3.6
Dimerization		
k_4, molecule^{-1} min^{-1}	1.383×10^{-3}	1.0×10^{-3}
k_{-4}, min^{-1}	-	6.0
Shc phosphorylation		
[Shc], molecule cell^{-1}	3.0×10^4	2.7×10^5
k_9, min^{-1}	12	6.0
K_{m9}, molecule cell^{-1}	6.0×10^3	4.0×10^3
ShcP dephosphorylation		
V_{10}, molecule cell^{-1} min^{-1}	3.0×10^5	6.12×10^4
K_{m10}, molecule cell^{-1}	6.0×10^3	2.04×10^5
ShcP/Grb2-SOS binding		
[Grb2-SOS], molecule cell^{-1}	2.0×10^4	-
[Grb2], molecule cell^{-1}	-	1.53×10^5
[SOS], molecule cell^{-1}	-	6.12×10^4
K_{d11}, molecule cell^{-1}	1.9×10^3	2.86×10^3
k_{11}, molecule^{-1} minute^{-1}	2.0×10^{-3}	2.1×10^{-3}
k_{-11}, min^{-1}	3.8	6.0

In order to validate the model against a parallel experimental study of EGF signalling in isolated hepatocytes, and consider the transfer of the signal between different cellular compartments, i.e. between the extracellular and intracellular compartments, Kholodenko *et al.* rescaled the parameter values for processes occurring at the cell surface by a factor equivalent to the ratio of the average incubation medium volume and the cytoplasmic volume. To allow a direct comparison of the two models, this

rescaling was taken into account when converting the parameter values into equivalent dimensions.

A comparison of the two sets of data in Table 5.2 further highlights the differences between the models, which can generally be explained by the differing purposes for which the models were constructed, or the contrasting cellular systems they were designed to reflect. Thus, the total number of receptors assumed in the hepatocyte model is greater than that expressed by the PC12 cell line, but both are within the typical range of EGFR expression (43). Similarly, the characteristics of receptor-ligand binding are slightly different, but again the values cited for K_{d1} (43), and the forward and reverse rate constants (k_1 and k_{-1}), are consistent with the range of values measured experimentally in a variety of cell lines (112, 185, 239, 348, 360). Both studies were however, carried out at a saturating EGF concentration, and as shown previously (section 4.3.1), this negates the dependence of system behaviour on the assumed rate of ligand binding and dissociation.

Given the relative insensitivity of simulation behaviour to the actual rate of receptor-receptor association (see section 4.3.1), it is initially rather surprising that the association rate constant for the EGFR dimerization step (k_4) is almost identical in both models. However, these values were both estimated on the same premise, that the rate of receptor-receptor encounters at the cell surface represents an appropriate upper limit, and perhaps it is to be expected that similar estimates would be derived from this limiting value. More notable, is that dimerization is modelled as a reversible process in the hepatocyte model, whereas in the PC12 simulation this is effectively irreversible, since the assumed mechanism was found to be irrelevant to the behaviour of the system beyond EGFR activation (section 3.3.1.9). However, the reversibility of receptor-receptor association is likely to be a more important factor in determining the short-term responses analysed using the hepatocyte model, such as EGFR autophosphorylation, promoted by dimerization.

In the hepatocyte model, EGFR-TK-mediated Shc phosphorylation was modelled as a reversible pseudo-first-order process, whereas this was treated as an effectively irreversible, enzyme-catalysed step in the PC12 model (Figure 3.1, step 9); hence, the kinetic characterization of this key event is not directly comparable. The value of K_m cited for the hepatocyte model therefore represents an estimated K_d for EGFR-Shc

binding, but whilst this is numerically consistent with the value assigned to K_m in the PC12 simulation (K_{m9}), it is outside the range deemed appropriate in the thesis for this interaction (Table 4.1). Furthermore, the K_m for dephosphorylation of phosphorylated Shc (K_{m10}) is two orders of magnitude higher in the hepatocyte model, although the estimated maximal rates of this reaction (V_{10}) are reasonably compatible. Nonetheless, the predicted pattern of Shc phosphorylation over the initial 2 minutes following EGF stimulation is similar for both models (see section 5.3.1.3), suggesting that the incompatibilities between the mechanistic details are not significant, although any inconsistency due to the differences in the dephosphorylation kinetics would only become evident over an extended time-scale.

Finally, it is interesting that in both models, the expression level of Shc is estimated to be of the same order of magnitude as receptor expression, and that although Grb2 and SOS are represented as separate entities in the hepatocyte model, the maximum number of Grb2-SOS complexes is only three times greater than in the PC12 simulation. Moreover, in both models, the total availability of Grb2-SOS is less than that of Shc, whilst the kinetic parameters for ShcP/Grb2-SOS binding (k_{11} and k_{-11}) are remarkably similar; the forward and reverse rate constants were however, derived in the same manner, on the basis of the same reported K_d for this interaction. In general therefore, there are few gross discrepancies between the corresponding quantitative features of the models, and those that do exist do not appear to result in significant differences in model behaviour, as discussed further in the following section.

5.3.1.3 Dynamic properties

In analysing short-term EGF signalling both in isolated hepatocytes, and using the kinetic model based on this cell type, Kholodenko and colleagues were concerned with several measurable end-points: EGFR autophosphorylation; the tyrosine phosphorylation of Shc and PLCγ; and the association of Grb2, SOS and Shc with the EGFR. The PC12 simulation is moderately simplified in comparison with the hepatocyte model, and most of these aspects of system behaviour are not considered; the only directly comparable feature of both models is the predicted time course of Shc phosphorylation.

Yet, rather than highlighting a deficiency in the PC12 model, the more comprehensive approach taken by Kholodenko *et al.* to modelling the protein-protein interactions induced by EGF provides evidence that the absence of direct physical association between the activated EGFR and Grb2 or Shc is not a critical omission. Although the formation of stable complexes between the activated EGFR and Shc or Grb2-SOS is a central design feature of the hepatocyte model, these states are actually predicted to be transient when the time course is computed, i.e. sustained for less than 1 minute, despite continuous EGF stimulation (178). This observation is confirmed for Grb2 in isolated hepatocytes, the majority of which forms a complex with free phosphorylated Shc rather than the EGFR (178). Perhaps rather controversially, the transitory association of Grb2, and thereby SOS, with the activated EGFR, is proposed to underlie the transience of Ras activation in response to EGF (178). This seems unlikely, given the typical time-scale of EGF-induced Ras activation in many cell types, which peaks at around 2 minutes but declines thereafter (237, 262, 350), in comparison with the observed peak in EGFR-Grb2-SOS association 15 seconds after EGF stimulation, which rapidly diminishes to near basal levels within 1 minute (178). This hypothesis is also contradicted by evidence that EGFR-Grb2-SOS complex formation has a minor role in EGF signalling (12, 291, 292), and that Ras inactivation is correlated with feedback SOS phosphorylation (194). As the PC12 model, which does not consider these interactions, provides an accurate reflection of EGF-induced Ras activation, it seems instead that the transient nature of the association of Shc and Grb2-SOS with the EGFR has little functional significance over an extended time-scale.

A comparison of the time courses of Shc phosphorylation generated by both the hepatocyte model and the PC12 simulation, further confirms that it is not necessary to represent all possible interactions between the EGFR, Shc, Grb2 and SOS in order to provide an acceptable model of EGF-induced Grb2-SOS recruitment to the plasma membrane, even over a short time-frame. According to both models, Shc phosphorylation, and the amount of Grb2-SOS complexed with phosphorylated Shc, reach a peak within around 1 minute of EGF stimulation, which is largely maintained over the following two minutes, as shown in Figure 5.7 below. The response is slightly more rapid in the hepatocyte model, due to the greater number of receptors (178).

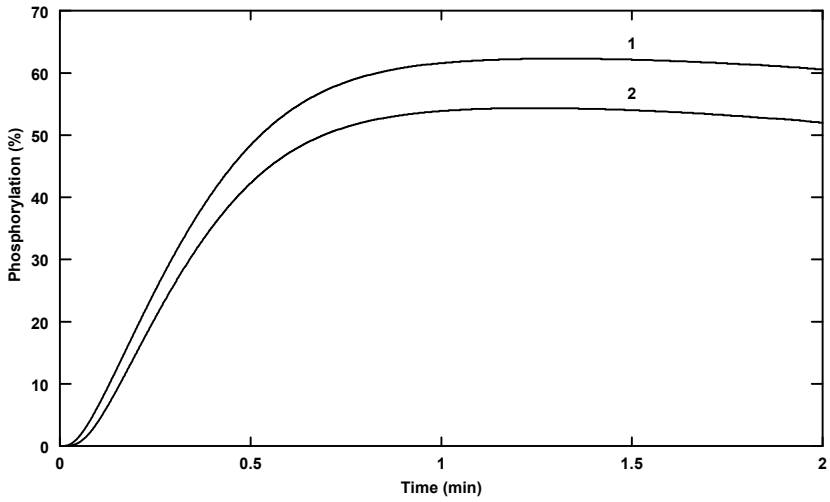

Figure 5.7 Simulated time courses of EGF-induced Shc and Shc-Grb2-SOS tyrosine phosphorylation in PC12 cells
Phosphorylated Shc is plotted as the percentage of total Shc, reflecting the phosphorylation status of both free and complexed Shc (line 1), or complexed Shc only (line 2). The time courses were computed over 2 minutes exposure to 100 nM EGF; other simulation parameters are given in Table 3.3.

A further interesting point of convergence between the two models is that the qualitative behaviour of the system appears to be largely dependent upon the relative expression levels of signalling intermediates, such as the EGFR, Shc, Grb2 or SOS, rather than the values of kinetic or thermodynamic constants (see section 4.3.2). Kholodenko *et al.* (178) suggest that the ratio of Shc:Grb2 is of particular importance in determining short-term responses, and that the cellular content of these molecules is likely to be no more than 1 or 2 orders of magnitude greater than that of the EGFR in hepatocytes. Although the criteria for assessing the relative importance of these factors differ between the two studies[10], the results of an investigation of the sensitivity of the PC12 model to variations in the availability of signalling proteins are in general agreement with these proposals: [Grb2-SOS] was found to be a significant defining factor in both the Shc phosphorylation response and Ras/MAPK cascade activation, and as the Grb2-SOS:Shc ratio approaches and exceeds unity, or the level of Grb2-SOS expression transcends that of the EGFR by more than a factor of 3, distinct qualitative changes in system behaviour are evident (see section 4.3.2.2). In addition, EGFR overexpression, represented by up to a 10-fold increase in the amount of EGFR, was found to markedly accelerate the rate of Shc phosphorylation in both models, but also prolonged phosphorylation at a peak level in the PC12 simulation (see

[10] The effect on Shc and Grb2 association with the EGFR in the case of the hepatocyte model, or on Shc phosphorylation in the PC12 model.

section 4.3.2.1). Hence, the general conclusion drawn from these analyses is also similar: that the varying expression of signalling intermediates between different cell types, or under different conditions, may also be a significant mechanism *in vivo* for modulating the dynamic response to EGF. The actual cellular content of Shc, Grb2 and SOS is however, unknown, and this supposition awaits future experimental validation.

5.3.2 THE MODEL OF BHALLA AND IYENGAR

5.3.2.1 Model description

In contrast to the model described above, which represents only selected early responses induced by the EGF stimulation of hepatocytes, Bhalla and Iyengar (17) have developed a more comprehensive kinetic model of a generic signalling network, comprising several interacting transduction pathways.

A modular approach was taken, whereby separate models of several individual signalling pathways, such as the EGF-induced activation of Ras or the MAPK cascade, were developed independently. This set of models collectively forms a library of components, which can be coupled together in various combinations to model a typical biological signalling network. The connections between pathways are formed by second messengers, or by linking an enzyme that is an integral part of one pathway with a substrate that is contained within another. One such combined model represents the EGF-induced activation of the MAPK cascade, and of PLCγ, and comprises four separate pathway modules.

The Ras activation component that forms part of this network model is very similar to the top-level module of the PC12 simulation: Ras activation is brought about via EGFR-TK-mediated phosphorylation of Shc, and the formation of a trimeric Shc-Grb2-SOS complex at the plasma membrane that is independent of the receptor. These events are stimulated by the binding of EGF to the cell surface EGFR, resulting in activation of the intrinsic RTK and subsequent internalization of the receptor; the latter is modelled as a reversible equilibrium process, and unlike the PC12 model, no measures are taken to distinguish between constitutive and ligand-induced mechanisms. Moreover, the EGFR-TK is assumed to be inactivated by internalization, even though

this process has recently been shown not to affect the capacity of the EGFR to mediate continued signalling via Ras (134), but does down-regulate PLCγ activation (136). Surprisingly, given the considerable interest that this aspect of EGF signalling has received (see Chapter 2), EGF-induced dimerization of the EGFR is also not considered. In contrast, the PC12 simulation incorporates both EGFR dimerization and the participation of internalized dimers in Ras activation.

As in the PC12 model, a direct interaction between Grb2 and the activated EGFR is not considered, but there is an important difference in the representation of the feedback mechanism that down-regulates EGF signalling: only SOS that has spontaneously dissociated from both phosphorylated Shc and Grb2 is considered to be subject to feedback phosphorylation mediated by ERK, which is seemingly without precedent in the literature (55, 61, 76, 194, 269, 286, 351). The ability of phosphorylated SOS to bind Grb2 is assumed to be unaffected, but the possibility of any interaction between Grb2-SOS(phosphorylated) and phosphorylated Shc is excluded. Both Shc and SOS dephosphorylation are also represented at this level of the model, but are treated as irreversible pseudo-first-order processes, and no particular phosphatases are specified as being associated with these events; as in both the hepatocyte and PC12 models, phosphorylated Shc is protected from phosphatase activity when associated with Grb2-SOS. However, SOS and Shc phosphorylation, and GDP/GTP exchange on Ras catalysed by the ShcP-Grb2-SOS complex, are modelled as enzyme-catalysed steps.

GAP-catalysed GTP hydrolysis on Ras is included as part of a separate module, in addition to alternative pathways for Ras activation, such as via PKC or Ca^{2+}. Also present are two other components representing PLCγ and PKC activation. The activated EGFR-TK tyrosine phosphorylates and activates PLCγ, which in turn catalyses phosphatidylinositide hydrolysis, thereby generating the second messengers, diacylglycerol (DAG) and inositol triphosphate (IP_3); the latter stimulates the release of Ca^{2+} from intracellular stores, whilst DAG activates PKC.

In general, the MAPK cascade modules of both models also share many features, but again, there are several interesting anomalies. The only Raf isoform represented in the network model is Raf-1, which is partly activated through serine phosphorylation mediated by PKC, although the role of tyrosine phosphorylation is not considered.

Once phosphorylated, Raf reversibly associates directly with Ras-GTP, in which form it is considered to be catalytically active. Thus, the Raf mechanism assumed in the network model appears to directly contradict that represented in the PC12 model, and also the general consensus apparent from the literature, i.e. that Raf activation is initiated by plasma membrane translocation, mediated by binding to Ras-GTP, where one or more phosphorylation events synergize to complete the activation process (187). Moreover, as reflected in the PC12 simulation, Raf does not need to remain associated with Ras-GTP to retain kinase activity (198), and is in fact only transiently bound to Ras-GTP (328). The reactions have presumably been modelled in this way to accommodate a direct link with the PLCγ-PKC module, which mediates a putative positive feedback mechanism in a more complex version of the model (see section 5.3.2.3).

Activated Raf is considered to catalyse the dual serine/threonine phosphorylation of MEK, but only MEK phosphorylated at both regulatory sites is presumed to be catalytically active, whereas in the PC12 model, phosphorylation at either site is sufficient to activate MEK. In turn, MEK catalyses the tyrosine and serine phosphorylation of ERK, and an assumption common to both models is that ERK is only catalytically active when phosphorylated at both sites. In addition, both models treat Raf and MEK dephosphorylation, catalysed by PP2A, as being synonymous with inactivation, but ERK is deactivated through the phosphatase activity of PP2A and an unspecified PTPase in the PC12 model, and by MKP-1 in the network model. Given that MKP-1 is a mitogen-induced nuclear enzyme, not normally expressed until at least 30 minutes after growth factor stimulation (175, 201, 337), this seems an inexplicable choice for involvement in the rapid down-regulation of ERK. Finally, an additional step, not incorporated in the PC12 simulation, is Raf deactivation mediated by ERK-dependent phosphorylation, which can be reversed by PP2A. All of these interactions, except Ras-GTP/Raf binding, are modelled as enzyme-catalysed processes.

5.3.2.2 Parameter values

The description of Bhalla and Iyengar's model given above highlights several steps that are equivalent to events modelled in the PC12 simulation, and a summary of the values assigned to the corresponding parameters is given in Table 5.3 below.

As before, where the units of the given parameters differ, these have been converted to those used in the PC12 model; although Bhalla and Iyengar expressed the rates of reactions in molecule cell^{-1}, calculated assuming a cytosolic volume of 1×10^{-12} l, concentrations and K_m values were given in Molar units (162). The authors apparently employed a conversion factor equivalent to the estimated plasma membrane protein content to determine the Molar concentrations of membrane-bound molecules.

Table 5.3 Parameter values for the computer simulation of EGF signal transduction in PC12 cells and the model of a generic EGF signalling in network, developed by Bhalla and Iyengar (17, 162)

Parameter	PC12 simulation	Network model
Ligand binding		
[EGF], nM	1×10^2	1×10^2
$[EGFR]_{Total}$, molecule cell^{-1}	1.5×10^4	1.0×10^5
K_{d1}, M	1.9×10^{-9}	5.95×10^{-8}
k_1, M^{-1} min^{-1}	3.8×10^8	2.5×10^8
k_{-1}, min^{-1}	0.73	15
Internalization/recycling of receptors		
k_{-3}, min^{-1}	0.70	0.12
k_3, min^{-1}	4.9×10^{-2}	1.98×10^{-2}
Shc phosphorylation		
[Shc], molecule cell^{-1}	3.0×10^4	3.0×10^5
k_9, min^{-1}	12	12
K_{m9}, molecule cell^{-1}	6.0×10^3	5.0×10^5
ShcP dephosphorylation		
V_{10}/K_{m10}, min^{-1}	50	0.10
ShcP/Grb2-SOS binding		
[Grb2-SOS], molecule cell^{-1}	2.0×10^4	-
[Grb2], molecule cell^{-1}	-	6.0×10^5
[SOS], molecule cell^{-1}	-	6.0×10^4
K_{d11}, molecule cell^{-1}	1.9×10^3	1.2×10^5
k_{11}, molecule^{-1} minute^{-1}	2.0×10^{-3}	5.0×10^{-5}
k_{-11}, min^{-1}	3.8	6.0

Table 5.3 Continued

Parameter	PC12 simulation	Network model
Ras-GDP/ShcP-Grb2-SOS binding		
[Ras], molecule cell^{-1}	2.0×10^4	1.2×10^5
K_{d12}, molecule cell^{-1}	6.13×10^2	3.0×10^5
Ras GDP/GTP exchange		
k_{13}, min^{-1}	15	1.2
Ras-GTP/GAP binding		
[GAP], molecule cell^{-1}	1.5×10^4	1.2×10^3
K_{d14}, molecule cell^{-1}	1.2×10^4	6.0×10^5
GTP hydrolysis		
k_{15}, min^{-1}	7.2×10^2	6.0×10^2
Ras-GTP/Raf binding		
[Raf], molecule cell^{-1}	1.0×10^4	1.2×10^5
K_{d16}, molecule cell^{-1}	2.5×10^3	1.25×10^4
k_{16}, molecule^{-1} minute^{-1}	1.2×10^{-3}	2.4×10^{-3}
k_{-16}, min^{-1}	3.0	30
Raf inactivation		
V_{18}, molecule cell^{-1} min^{-1}	9.7×10^4	4.84×10^7
K_{m18}, molecule cell^{-1}	6.0×10^3	9.39×10^6
MEK phosphorylation		
[MEK]	3.6×10^5	1.08×10^5
k_{19}, k_{21} min^{-1}	50	6.3
K_{m19}, K_{m21} molecule cell^{-1}	9.0×10^3	9.54×10^4
MEK dephosphorylation		
V_{20}, V_{22} molecule cell^{-1} min^{-1}	9.0×10^5	4.84×10^7
K_{m20}, K_{m22} molecule cell^{-1}	6.0×10^5	9.39×10^6
ERK phosphorylation		
[ERK]	7.5×10^5	2.16×10^5
k_{23}, k_{25} min^{-1}	8.3	9.0
K_{m23}, K_{m25} molecule cell^{-1}	9.0×10^4	2.57×10^4
ERK dephosphorylation		
V_{24}, molecule cell^{-1} min^{-1}	2.0×10^5	1.15×10^5
V_{26}, molecule cell^{-1} min^{-1}	4.0×10^5	1.15×10^5
K_{m24}, K_{m26} molecule cell^{-1}	6.0×10^5	4.02×10^4
SOS phosphorylation		
k_{27}, min^{-1}	1.6	6×10^2
K_{m27}, molecule cell^{-1}	6.0×10^5	1.54×10^6
SOS dephosphorylation		
V_{28}/K_{m28}, min^{-1}	3.75×10^{-3}	6.0×10^{-2}

The similarities between the two sets of data are again greater than their differences. An initial observation is that both studies were conducted at the same, saturating EGF concentration, and are therefore concerned with maximal cellular responses to EGF stimulation. Consistent with the pattern noted in the comparison of the hepatocyte and PC12 models above (section 5.3.2.1), the total number of receptors assumed in the network model is a factor of 10 greater than in the PC12 model, but is again within the typical physiological range (43). Moreover, the expression levels of the various intracellular signalling intermediates are generally regarded by all three models as being of the same order of magnitude as that of the EGFR. Hence, the concentrations of these molecules, expressed as number per cell, are consistently ten times higher in both the hepatocyte and network models than in the PC12 simulation; the only exceptions appears to be cellular concentrations of GAP, and of MEK and ERK (Table 5.3). It is also interesting to note that both Bhalla and Iyengar and Kholodenko *et al.* have presumed that the expression level of SOS is approximately 10-fold lower than that of Grb2, resulting in a total availability of Grb2-SOS complexes that is approximately equivalent to that assumed in the PC12 model. In all three models, the maximum Grb2-SOS availability is also less than the Shc expression level, and in both the network and PC12 simulations, there is twice the amount of ERK than MEK. These striking similarities between independent models of EGF signalling, developed by three different groups, further support the hypothesis that the relative numbers of signalling intermediates may have considerable importance in defining the cellular response to EGF, as proposed in sections 4.4. and 5.3.1.3.

The parameter values for ligand binding are also generally comparable, although the dissociation rate constant (k_{-1}) is 20-fold greater in the network model, resulting in a parallel discrepancy in the calculated value of K_{d1}; indeed, these values are outside the range typically specified for the EGFR in several cell types (112, 185, 239, 348, 360), and are perhaps not entirely appropriate. Other similarities may be partly coincidental, such as in the values of the parameters governing receptor internalization and recycling (k_3 and k_{-3}; source not specified), or can be ascribed to the derivation of certain values from the same sources: estimates of k_{cat} for Shc phosphorylation (k_9) and the rate constant for GTP hydrolysis (k_{15}).

Ironically, many of the remaining contrasts between the data can also be explained in these terms. In several cases, Bhalla and Iyengar have used values close to those

specified in the literature for their generic model of EGF signalling, whilst in the PC12 simulation these have been adjusted to enable the model to reproduce cell type-specific behaviour. Thus, the K_m for Shc phosphorylation catalysed by the EGFR-TK (K_{m9}) assumed in the network model is equivalent to that determined *in vitro* (257). However, during development of the PC12 model this estimate was found to be too high to account for the rapid rate of EGF-induced Shc phosphorylation typically observed *in vivo* (178, 287, 291), and was modified accordingly, within a range of acceptable values (see section 3.3.3.6). Similarly, the rate of Ras-GTP/Raf dissociation (k_{-16}) employed in the network model, and the assumed K_d for this interaction (K_{d16}), are closer to that reported for the dissociation of a Ras-GTP analogue from the RBD of Raf-1 (331). Yet, using such a high value in the PC12 model resulted in an unsatisfactory rate and extent of MEK and ERK activation, and a K_d consistent with that reported for Ras-GTP interaction with the holo-Raf molecule (229) was found to be more suitable (section 3.3.3.7). In both models, the K_d for Ras-GDP/ShcP-Grb2-SOS binding (K_{d12}) has been derived from the same reported estimate, but the network model does not consider the increase in effective affinity that arises through the localization of both Ras-GTP and ShcP-Grb2-SOS within a confined volume adjacent to the plasma membrane (see sections 3.3.2.1 and 3.3.2.5); hence, there is an apparent difference of three orders of magnitude in these values. Finally, the affinity of the Ras-GTP/GAP interaction (K_{d14}) assumed in the network model is similar to that reported in the literature (113)[11], but parameter fitting for the PC12 simulation implied that this would be significantly greater *in vivo*, possibly arising from growth-factor induced co-localization of Ras and GAP to the plasma membrane (297) (see section 3.3.3.7). However, in the network model, K_{d12} and K_{d14} are of the same order of magnitude; as shown previously in the thesis, a comparable degree of Ras-GDP/SOS and Ras-GTP/GAP binding was found to be essential in limiting the maximal level of Ras activation (section 3.3.3.7).

Other differences between the model parameters are more difficult to rationalize. Bhalla and Iyengar have assumed a 6-fold higher K_{d11} for ShcP/Grb2-SOS binding than that specified in the literature (63), whereas a 10-fold lower value was found to be more appropriate for the PC12 model, thus widening the disparity between the models. Furthermore, the rate of Ras GDP/GTP exchange (k_{13}) is at the lowest extreme of a

[11] The value cited for the network model is the K_m for GAP-catalysed GTP hydrolysis on Ras-GTP, as Ras-GTP/GAP binding was not directly represented as a physical process.

range of estimates specific for the mammalian homologue of the yeast CDC25 GEF, Ras-GRF (163, 200, 260), and is more than 10 times less than that represented in the PC12 model. The origin of the 500-fold difference in the rate of SOS phosphorylation (k_{27}) is also not apparent, but the value employed in the network model is outside the range considered to be acceptable for use in the PC12 simulation (Table 4.1), based upon experimentally determined values (281).

The kinetic characteristics of the MAPK cascade (Figure 3.1, steps 18 to 26) are generally comparable in both models; in the case of ERK phosphorylation, mediated by MEK (Figure 3.1, steps 23 and 25), both models employ almost identical parameter values. The only notable differences are between the K_m values and catalytic rates assumed for the dephosphorylation of Raf and MEK (Figure 3.1, steps 18 to 26, even numbers), and the rate constants for MEK phosphorylation, mediated by Raf (k_{19} and k_{21}). The latter is likely to be a direct reflection of the differing kinetic properties of the Raf isozymes implicit in the two models. All three Raf isozymes, Raf-1, A- and B-Raf, are involved in MEK activation in the PC12 cell line (365), but activated B-Raf has a higher catalytic activity than activated Raf-1 or A-Raf (216). The generalized model of Bhalla and Iyengar is designed to reflect the more typical response of the MAPK cascade to Raf-1 activation, observed in the majority of cell types, and therefore exhibits a slower rate of MEK, and thereby ERK activation, than the PC12 model (17). The dynamic properties exhibited by the two models are investigated in more detail in the following section.

5.3.2.3 Dynamic properties

The motivation behind the rather ambitious model of Bhalla and Iyengar was to provide a means of exploring the potential properties that a system of individual signalling pathways might display when functioning as a collective unit (17). In keeping with their objectives, this group did indeed discover that such systems can exhibit 'emergent properties', i.e. characteristic behaviour that is not evident in the isolated linear pathways, but which arises through the integration of these components into a complex signalling network (357). A simple example of this type of behaviour is provided by the negative feedback mechanism incorporated into the simulation of EGF signalling in PC12 cells, which engenders a property of the system that is not immediately intuitive, i.e. an inverse relationship between ERK and Ras activation,

which also affects the duration of Shc phosphorylation (see section 4.3.2). However, more sophisticated responses, such as the existence of multiple steady states, are demonstrated by a more elaborate version of Bhalla and Iyengar's model (17).

Due to the differing perspectives of the two models, i.e. the representation of generalized, 'high-level' properties by the network model, in contrast to the specific responses induced by EGF in a particular cell type by the PC12 model, there is little overlap in terms of directly comparable aspects of behaviour. Indeed, Bhalla and Iyengar appear not to have comprehensively validated their model against experimental observations, and have largely been concerned with the activation of only two components of the system, PLCγ and ERK. When the time course of ERK activation predicted by the network model is examined in detail, it becomes clear that this agrees in general terms with both the experimental data and the time course generated by the PC12 model, although there are some obvious quantitative differences. Bhalla and Iyengar have compared the behaviour of their model with an experimental time course of ERK activation, published by Teng *et al.* (335); this in itself is erroneous, since these data are specific for the PC12 cell system, which differs in certain, possibly significant respects from the 'average' cell type that the network model is designed to reflect (see section 3.3.3). Furthermore, whilst the data show a transient peak in EGF-induced ERK activation at around 5 minutes, which is accurately reproduced by the PC12 simulation, this is delayed by a further 5 minutes in the network model, as Figure 5.8 illustrates.

There are probably numerous reasons for this inconsistency, but as demonstrated previously, by utilizing the PC12 model in a sensitivity analysis of the EGF signalling pathway, the time-scale of MAPK cascade activation appears to depend particularly upon the values of several system parameters (see sections 4.3.2.2 and 4.3.2.3). Hence, it is likely that much of the inaccuracy shown by the network model in predicting the time-dependent pattern of ERK activation arises through the use of unfavourable parameter values for certain processes: the high K_m for Shc phosphorylation (K_{m9}); the slow rate of ShcP/Grb2-SOS association (k_{11}); a very low rate of Ras GDP/GTP exchange (k_{13}), particularly in comparison with a relatively high rate of GTP hydrolysis (k_{15}); the high rate of Ras-GTP/Raf dissociation (k_{-16}), contributing to the reduced affinity of this complex (K_{d16}); and a low rate of MEK activation (k_{19} and k_{21}). The mechanism of Raf activation assumed in the network model may also be partly

responsible for generating the lag in ERK activation: Raf is, incorrectly, considered to be catalytically active only when associated with Ras-GTP, and is liable to be modified by phosphorylation in its free state so that it is unable to bind Ras (17), both of which are likely to delay peak Raf, MEK and ERK activation.

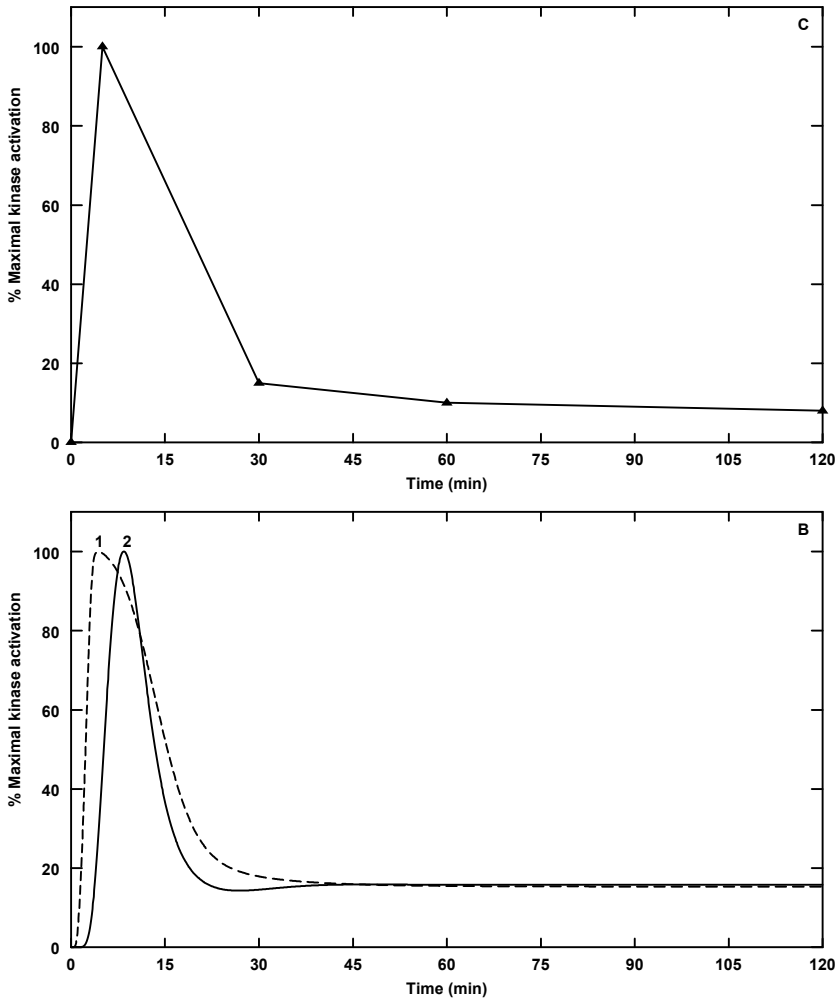

Figure 5.8 Predicted and experimental time courses of EGF-induced ERK activation

(**A**) Experimental data replotted from Teng *et al.* (335). (**B**) Response predicted by the PC12 simulation (line 1, dashed) and the network model of Bhalla and Iyengar (line 2; refs. 17 and 162). The time courses were computed over 120 minutes continuous exposure to 100 nM EGF; other simulation parameters are shown in Tables 3.3 and 5.3. The data are expressed as the percentage of maximal kinase activation.

The time courses of Shc phosphorylation and Ras activation generated by the network model have not published by Bhalla and Iyengar (17), but from a consideration of the features of the model it seems likely that these would also be erroneous; for example, Ras activation would be impeded, due mainly to the low net rate of GDP/GTP exchange (cf. k_{13} and k_{15}), and prolonged Shc phosphorylation would be expected,

partly as a result of the low catalytic efficiency of the dephosphorylation reaction (V_{10}/K_{m10}), but primarily as a consequence of the manner in which the negative feedback mechanism is implemented: SOS is assumed to be phosphorylated by ERK only when not complexed with Grb2 and Shc (17). Whilst this prevents the association of SOS with ShcP and Grb2 in a multi-protein complex, phosphorylated Shc is not released from existing complexes to become a target for PTPases; the rate of Shc dephosphorylation therefore relies upon the autonomous dissociation of the ShcP-Grb2-SOS complex. Contrary to the interdependency of these variables observed in the PC12 simulation, the steady state level of Shc phosphorylation would therefore be largely independent of ERK activity.

Reconstruction of Bhalla and Iyengar's four-module system (17, 162) in Gepasi 3.2 confirms these expectations, but also reveals that although EGF-induced Ras activation reaches an acceptable peak level (around 22%), the proportion of Ras in the GTP-bound form is subsequently maintained at more than 6 times the level observed in PC12 cells in response to continued EGF stimulation (approximately 13%), as shown in Figure 5.9 below.

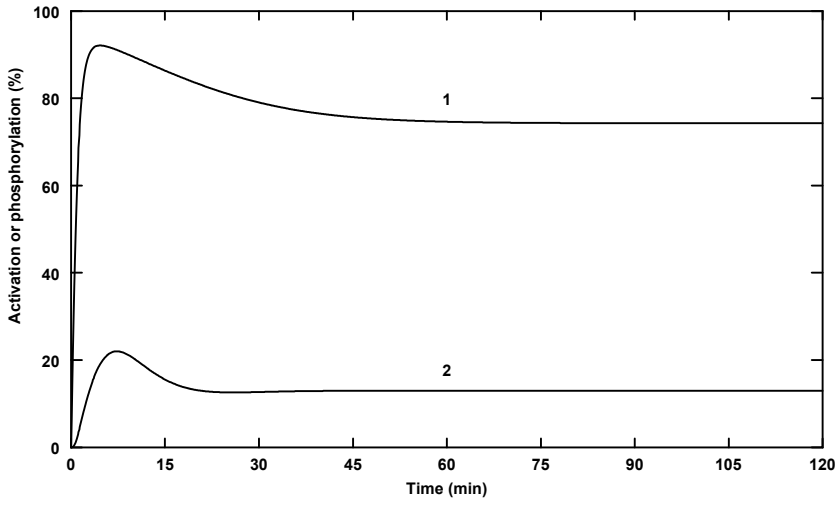

Figure 5.9 Predicted time courses of EGF-induced Shc tyrosine phosphorylation and Ras activation

The curves indicate phosphorylated Shc, plotted as the percentage of total Shc (line 1), and the percentage of total Ras in the GTP-bound form (line 2) predicted by a reconstruction of Bhalla and Iyengar's model of the EGF signalling network (17, 162), implemented in Gepasi 3.2. The simulation parameters are listed in Table 5.3.

This level of Ras activation is typically sufficient to maximally activate ERK (155), and is therefore inconsistent with the concurrent down-regulation of ERK activity

predicted by the model, shown above in Figure 5.8B. Given the fundamental importance of feedback SOS phosphorylation as a means for down-regulating Ras activity (see sections 3.3.2.6, 3.3.3.6 and 4.3.2), it is probable that this significant error also arises from the anomalous feedback mechanism implemented in the network model. Although SOS phosphorylation is presumed to hinder the formation of ShcP-Grb2-SOS complexes, in which form SOS is considered to be catalytically active, this clearly does not represent a particularly efficient mechanism for down-regulating existing complexes; these must first dissociate spontaneously, which in itself is sufficient to inactivate SOS, since this results in the diffusion of SOS away from Ras-GDP at the plasma membrane. When modelled in this way, feedback SOS phosphorylation seems almost superfluous for the rapid termination of signalling through Ras, as evidenced by Figure 5.9. This may partly account for both the relatively low rate of GDP/GTP exchange (k_{13}) employed in the network model, and the otherwise inexplicably high rate of SOS phosphorylation (k_{27}; Table 5.3). Furthermore, this could explain why the Grb2-SOS complex is assumed to dissociate at a much higher rate than that specified in the literature (1.0 min^{-1}, in comparison with 8.3×10^{-3} min^{-1}) (293), resulting in a far lower affinity than that reported ($K_d = 4.0 \times 10^5$ molecule $cell^{-1}$, compared to 9.0×10^2 molecule $cell^{-1}$) (293). These measures might reflect a largely unsuccessful attempt by the authors to minimise sustained Ras activation levels.

It is clear from the discussion above that much of the error shown by the network model in simulating the behaviour of the EGF signalling system may arise from the rather curious mechanisms assumed for both SOS inactivation and Raf activation, which are in stark contrast with those propounded in the literature and incorporated into the PC12 model. A further contributing factor, and a weakness of the model that has also been recognized by Bhalla and Iyengar, may be that the co-localization or segregation of interacting molecules is not considered (17, 162); these features of cell signalling have already been suggested to play an important regulatory role, both within this thesis (see section 3.3.3.7), and by other authors (135, 136, 179). Given the often considerable mechanistic and quantitative differences between the two models, and the failure of the network model to correctly reproduce experimentally observed time courses of EGF-induced Shc phosphorylation and Ras activation, it is notable that the pattern of MAPK cascade activation predicted by both is actually quite similar. However, this further highlights the robustness of the pathway as a mechanism for

activating the terminal kinase of the cascade, ERK, to variations in factors operating upstream, as emphasised previously (section 4.4). A further implication is that the activation state of the MAPK cascade is not a suitable end-point for appraising the behaviour of the system as a whole, and that equal consideration should also be given to the kinetics of Shc phosphorylation and Ras activation, particularly since these might also be involved in alternative pathways, such as in the activation of PI-3K (86, 129, 173).

These considerations appear to have been largely neglected by Bhalla and Iyengar, as the main purpose of their study was to explore the possibility for a signalling network to demonstrate emergent properties, such as the existence of multiple steady states at the same stimulus level, arising through the activation of a positive feedback loop (see section 5.2.1). Such a mechanism is represented in a more complex version of their model, comprising seven interacting components (17, 162), although the existence of the specified pathway *in vivo* has yet to be confirmed. The loop is proposed to connect two otherwise independent pathways that are both initiated by activation of the EGFR, the PLCγ-PKC and Ras/MAPK pathways. PKC has been reported to phosphorylate and activate Raf-1 (48, 188), whereas ERK phosphorylates and activates $cPLA_2$ (207, 240). This results in the production of arachidonic acid (AA), which acts in conjunction with DAG and Ca^{2+} generated by activated PLCγ to activate PKC (246, 310). If the external stimulus, i.e. EGF, is of sufficient amplitude and duration to induce the activation of either ERK or PLCγ above a given threshold, this will activate the positive feedback loop, resulting in an abrupt transition to a steady state characterized by maximal activation of both enzymes. Furthermore, this level of activation is sustained, even after the extracellular signal is withdrawn. However, if the initial stimulus is not of sufficient magnitude or duration, the activation levels of both enzymes revert to the basal state once the stimulus is removed (17). Such a system is therefore bistable: it can be shown to exist in one of two discontinuous steady states, at the same stimulus level, the actual state being determined by the 'history' of the system. In a sense, this type of system has a 'memory' (17); it remembers the characteristics of initial stimulus and retains a corresponding level of activation, despite a change in the stimulus, a property that is termed hysteresis (196).

This type of behaviour is illustrated in Figure 5.10, in which the response of the MAPK cascade to variations in EGF concentration over time is plotted for both a modified

version of the PC12 model, incorporating the positive feedback regulation of Raf, based on a mechanism proposed to operate in *Xenopus* oocytes by Ferrell and Machleder (103)[12], and the unmodified PC12 simulation. It is clear that reinforcement of MAPK cascade activation, through ERK-mediated Raf activation, results in a sharp transition from almost zero to maximal ERK activation, as EGF increases progressively with time, but also that this level of cascade activation is maintained, despite a reduction in the external stimulus.

The dynamic profile of the unmodified PC12 model provides a complete contrast. A stepped increase in EGF concentration with time induces a corresponding rapid, but transient rise in ERK activation, which is followed by relaxation to a lower steady state level, whilst the pattern is reversed in response to timed decrements in EGF concentration. As previously established (section 4.3.2.1), there appears to be a self-determined maximum level of steady state cascade activation, which cannot be further enhanced by increasing EGF above a certain level. Figure 5.10B also clearly demonstrates the capacity of the system to filter out background noise and remain switched 'off' at very low stimulus levels, but also to respond with a high degree of sensitivity to a change in the stimulus above an appropriate threshold; both phenomena arise from the sigmoidal, ultrasensitive response of the MAPK cascade to EGF (see section 5.2.2 above). A novel observation, which may have some physiological relevance, is that as EGF concentration is incremented with time, the amplitude of peak ERK activation is diminished and does not reach the maximal level of activation induced by acute exposure to a threshold stimulus. This is presumably because continuous exposure, to a progressively increasing stimulus, cumulatively desensitizes the system through ERK-mediated SOS phosphorylation and deactivation. As demonstrated previously, there is a delay in the reversal of SOS phosphorylation, giving rise to an extended refractory period for the reactivation of Ras, and thereby ERK (section 5.2.2).

[12] In this cell type, ERK-dependent phosphorylation promotes the stabilization and accumulation of Mos (a MAPKKK, analogous to Raf). This mechanism is not suggested to operate in the PC12 cell line, but was implemented to illustrate the typical profile of EGF-induced ERK activation observed when the MAPK cascade is embedded within a positive feedback loop. Due to the extensive modifications to the PC12 model that would have been necessary, the mechanism proposed by Bhalla and Iyengar (17) was not reproduced.

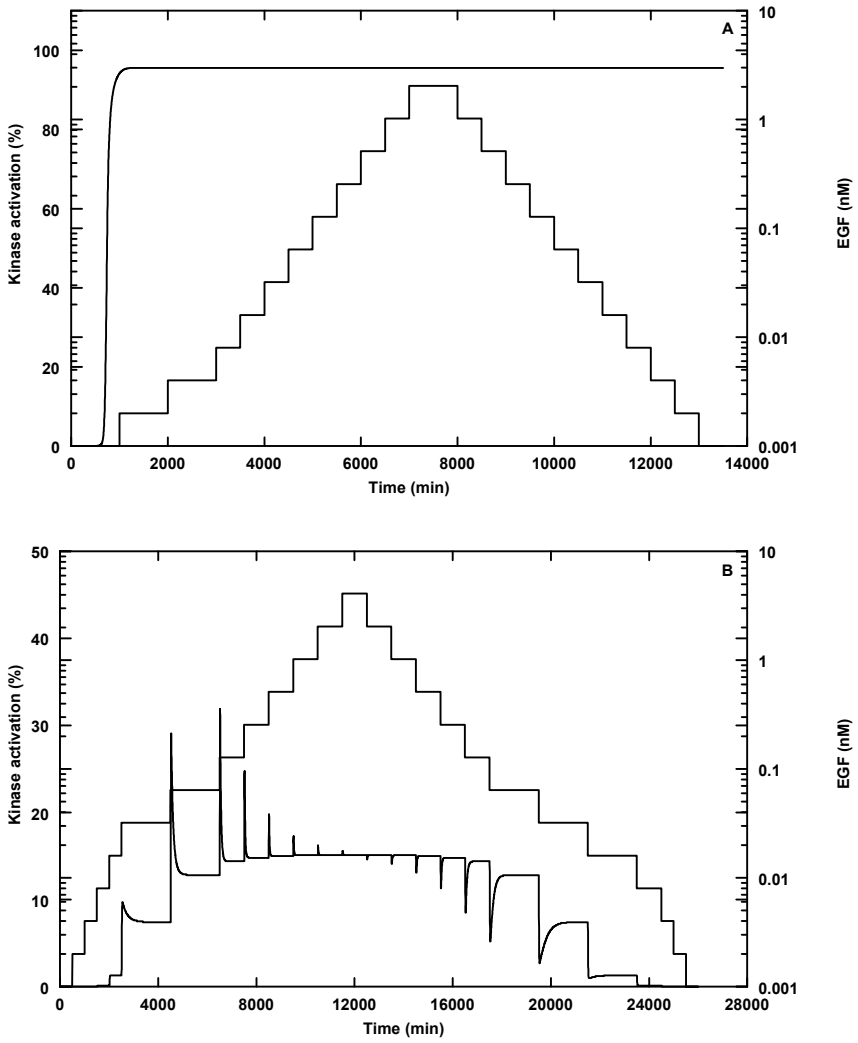

Figure 5.10 The dynamic response of ERK to a changing concentration of EGF
The curves indicate ERK activation, expressed as the percentage of total ERK in the catalytically active form (continuous line) and [EGF] (stepped line), plotted against time, in a signalling system where the MAPK cascade is regulated by (**A**) positive feedback and (**B**) negative feedback interactions. Both models were implemented in SCAMP.

The EGF signalling pathway represented by the PC12 model is clearly therefore, not bistable; indeed, it seems unlikely that the actual system would demonstrate this property, since no candidate positive feedback mechanisms been identified in this particular cell type. Thus, although PLCγ is similarly activated in PC12 cells in response to both EGF and NGF (53), which presumably results in the activation of PKC, the latter only modulates ERK activity through a Ras-dependent mechanism in this cell type (294), possibly by down-regulating GAP activity (87). There is also no evidence for the direct activation of the predominant PC12 Raf isozymes, A- or B-Raf, by PKC, and even though this enzyme can phosphorylate Raf-1 (48, 188), whether this results in increased activity towards MEK is actually questionable (212). Furthermore, neither

sustained ERK activation induced by NGF (325), nor differentiative signalling by NGF (250) or FGF (301), are dependent upon the PLCγ pathway, or PI hydrolysis, in the PC12 cell line. It therefore seems unlikely that any interaction between the PLCγ-PKC pathway and MAPK cascade mediates prolonged ERK activation in PC12 cells, but rather plays a subsidiary role in regulating the response of the Ras/MAPK cascade to growth factors (301), whilst the feedback activation of Raf through enhanced *de novo* synthesis seems, on the available evidence, to be peculiar to the *Xenopus* oocyte system (103). Such mechanisms were therefore not considered relevant to the development of a model of EGF signalling in the PC12 system.

5.4 Summary and Conclusions

The preceding sections have been concerned with further exploring the properties of the simulation of EGF signalling in PC12 cells, revealed by the comprehensive sensitivity analysis documented in Chapter 4. An integral part of this investigation has been a comparison of the features of this particular model with those of other published models of growth factor signalling systems. The account focuses initially on ultrasensitivity in the MAPK cascade. Many theoretical studies have highlighted the potential significance of this property in defining the cellular response (116, 155, 177, 321), but little attempt has been made to assess any real physiological relevance.

The MAPK cascade module of the PC12 model demonstrates an ultrasensitive response, both as an independent functional unit and within the setting of the simulated pathway, although the quantified degree of sensitivity amplification is very modest. In this case, ultrasensitivity arises from a combination of zero-order and effective multi-step effects. Yet, the analysis also indicates that the functional properties of the MAPK cascade, when embedded within a representative signalling system, depend not only upon the kinetic characteristics of the cascade reactions, but also of the other system components. Thus, although the cascade is predicted to have an inherent capacity to respond to a threshold stimulus by facilitating a rapid transition between zero and maximal ERK activation, even within a physiological setting, this is probably not generally manifested as a biochemical mechanism for switching between discrete metabolic states (155); this potential is likely to be suppressed by feedback down-regulation of the initial response. In extreme cases however, where this

mechanism is absent, perhaps in response to growth factors that stimulate prolonged ERK activation and differentiation, the MAPK cascade may indeed function as a metabolic switch. It seems more likely that sensitivity amplification, as a general property of growth factor signalling, allows the cell to respond with enhanced sensitivity to a legitimate signal, defined by a threshold level of stimulus, but to disregard background noise (103, 116, 117, 155, 189). A further function of the cascade arrangement of Raf, MEK and ERK may be to amplify the rate at which ERK is activated in response to an external signal (321).

The potential for the MAPK cascade to demonstrate sustained oscillations in the level of activation (177) was also examined, but again, rather stringent conditions were apparently necessary to generate this behaviour, corresponding to a very high degree of ultrasensitivity and relatively weak feedback inhibition. In the PC12 model, the latter equates to an assumed specific activity for activated ERK that is a factor of 10 smaller than the lowest reported value (281). Furthermore, at the more moderate degree of sensitivity amplification exhibited by the MAPK cascade of the PC12 model, this phenomenon is dependent upon certain mechanistic assumptions. If feedback inhibition is considered as essentially equivalent to noncompetitive or cooperative inhibition of Raf activation by ERK, it is possible to obtain a recurrent cycle of ERK activation/inactivation. Yet this is not directly comparable to the down-regulation of the Ras/MAPK cascade through SOS phosphorylation, the effects of which persist even after ERK has been deactivated, resulting in the attainment of a stable steady state. Hence, increased feedback strength, or accelerated SOS dephosphorylation, does not destabilize the system, but merely modifies the steady state level of cascade activation. Thus, it is concluded that sustained oscillations in ERK activity are unlikely to be observed *in vivo*, although this remains to be investigated experimentally.

The chapter continues with a systematic comparison of the simulated EGF signalling pathway in PC12 cells with two recently published models that aim to represent similar aspects of this system. The first, developed by Kholodenko and colleagues (178), provides a comprehensive model of the initial events stimulated by EGF in isolated hepatocytes. In general, this and the PC12 model are structurally similar, although the hepatocyte model considers the formation and fate of many more species of signalling complex, and also directly represents EGFR autophosphorylation and deactivation by phosphatase activity. Surprisingly, the models are also comparable in quantitative terms,

with any obvious differences originating from a consideration of different cell types. Of particular interest, is that both models assume similar ratios of EGFR to Shc, Grb2 and SOS expression levels, even though there are no primary sources that cite the cellular content of these intracellular signalling intermediates. This can perhaps be viewed as confirmation of the importance of these ratios in defining the cellular response (see section 4.3.2).

Despite the greater complexity of the hepatocyte model, in comparison with the top-level module of the PC12 simulation, the dynamic features of both are also compatible, which justifies the simplifying assumptions made in constructing the latter; clearly, any omissions in this model are not of fundamental importance in determining the short-term response of the system to EGF. In agreement with the results of a sensitivity analysis of the PC12 model (section 4.3.2), Kholodenko *et al.* also found that the qualitative behaviour of their model was significantly altered by disturbances in the ratio of signalling intermediates, but relatively unaffected by variations in kinetic or thermodynamic constants. Thus, this group have also concluded that the expression levels of signalling molecules may have a role in defining specific responses to growth factor stimulation (178).

The model of Bhalla and Iyengar (17) contrasts markedly with both Kholodenko *et al.*'s hepatocyte model and the PC12 simulation, and consists of several interconnected pathways initiated simultaneously by activation of the EGFR-TK. Again, there are many similarities in the structure of the models at the level of individual pathways, for example, the key signalling complex is trimeric ShcP-Grb2-SOS, in which form phosphorylated Shc is protected from phosphatase activity, but also some important mechanistic and quantitative differences. Thus, the EGFR is activated solely through binding EGF, and the dimerization of occupied receptors is omitted. There is also only one, non-saturable internalization mechanism, which is presumed to deactivate the RTK, whilst the interactions of Ras with SOS and GAP are modelled as enzyme-catalysed processes. Although it is admissible to view these reactions in such a way, as discussed previously, this precludes a consideration of the removal of the interacting proteins from the cellular pool, and the competition between Raf and GAP for binding Ras-GTP, which may be important regulatory features of the pathway (see sections 3.3.2.4, 4.3.2.2 and 4.3.2.3). The most remarkable anomalies are however, the mechanisms assumed for feedback down-regulation of the MAPK cascade and Raf

activation, which seemingly contradict those apparent from a review of the relevant literature.

That similar ratios of EGFR, Shc, Grb2 and SOS, in addition to Raf, MEK and ERK are assumed, further supports the hypothesis that these are generally conserved and regulate the observed response. In many other respects however, the numerical values of the model parameters differ greatly from those used in the PC12 model. These can generally be correlated with clear inconsistencies in the dynamic properties of the model, both in comparison with the PC12 simulation, and more importantly, with the available experimental data. Although the predicted time course of ERK activation is accurate in terms of the general pattern of activation, characterized by a transient peak followed by relaxation to a steady state level, the time-scale of these events is incorrect. This results from unfavourable values for a number of system parameters and the assumption that Raf is only catalytically active when associated with Ras-GTP.

The time-dependent pattern of Shc phosphorylation and Ras activation generated by the model can also be demonstrated to be in error; both variables are predicted to be maintained at high levels over the simulated time period. These discrepancies arise principally through the particular implementation of the feedback mechanism, in which SOS is only phosphorylated once dissociated from Shc and Grb2. This process does not therefore promote the release of Shc to become a target for phosphatase activity and is relatively inefficient at down-regulating Ras activity. Nonetheless, that a generally consistent pattern of ERK activation is observed, despite these clear anomalies in upstream events, further emphasises the robustness of the MAPK cascade when regulated by feedback interactions, as highlighted previously (section 4.3.2). Finally, using an extended version of their model, Bhalla and Iyengar focus on demonstrating that networks of signalling pathways demonstrate emergent properties, such as bistability arising through positive feedback interactions (17). This is not however, observed in the PC12 model. Rather, there is an increase in the response with timed increments in the level of external stimulus, until a maximum is reached, which is set by desensitization through activation of the negative feedback loop. This pattern is reversed with a subsequent decrements in the stimulus level. A reduced sensitivity of the system at very low stimulus levels, but enhanced sensitivity above a threshold stimulus is also further demonstrated in response to a progressive increase in stimulus over time.

The perspectives on EGF signalling represented by the models of Kholodenko *et al.* (178) and Bhalla and Iyengar (17) can be considered to be two extremes. The former is concerned with representing and explaining the specific responses of a particular cell type to EGF stimulation, and hence forms an *in silico* experimental system for analyzing the detailed functional and regulatory properties of a real system. In contrast, Bhalla and Iyengar are more interested in examining the potential properties that a typical growth factor signalling network might exhibit, and have therefore designed many such features 'into' the model, but have made no attempt to ascertain whether any particular behaviour is likely to be displayed within the cell. Theirs is an idealized, generic model, in which cell type specific differences in the individual pathways, or the applicability of *in vitro* data to the *in vivo* environment, are not accounted for. Hence, it does not accurately portray the majority of typical responses observed in a variety of cell types, and broadly resembles the real system in only one aspect of system behaviour: ERK activation. This suggests that it is not possible to generalize to the degree that has been attempted, whilst maintaining a coherent model. Nonetheless, this group have highlighted some interesting features of signalling networks, which may well have some physiological relevance in particular cellular systems, although this has yet to be verified.

The opposite approach has been taken in developing a simulation of EGF signalling in PC12 cells, which is therefore more comparable to the hepatocyte model of Kholodenko *et al.* Thus, a specific cell type is represented, using, where possible, appropriate data for both implementing and validating the behaviour of the model. The intention has been to accurately reproduce quantitative experimental observations, in terms of several end-points, and then through a comprehensive analysis of system properties, based on manipulation of the system parameters within appropriate limits, to explain experimental observations and examine whether or not the system is likely to display predicted behaviours. As a result, the model is in fact more detailed, although not as extensive as the network model, as it integrates many more 'low-level' processes, such as dimerization and internalization, and separates the binding of Ras with SOS, GAP and Raf from catalytic processes. It is felt that this approach provides a more realistic model that can be used as an experimental tool, and therefore has more immediate relevance to understanding growth factor signalling within the cellular environment.

CHAPTER 6

QUANTITATIVE ANALYSIS OF EGF AND NGF SIGNALLING SPECIFICITY IN PC12 CELLS

6.1 INTRODUCTION

The PC12 rat phaeochromocytoma cell line has been used extensively for studying NGF signal transduction (171), but is also responsive to other growth factors, including EGF; the latter stimulates the proliferation of PC12 cells (157), whereas NGF stimulates differentiation (126). Both EGF and NGF activate an intracellular signal transduction pathway comprising the small guanine-nucleotide binding protein, Ras, and a MAPK cascade formed by Raf, MEK and ERK protein kinases (217). In PC12 cells however, EGF induces transient activation of Ras, MEK and ERK, whilst NGF promotes sustained activation of these signalling effectors, accompanied by translocation of cytosolic ERK to the nucleus (119, 125, 139, 237, 245, 339). This observation, in conjunction with further evidence indicating that sustained activation and nuclear translocation of ERK are generally associated with PC12 differentiation (20, 69, 82, 340, 378), have been cited in support of the proposal that the duration of ERK activation may be an important factor in defining the specificity of the cellular response to growth factor stimulation (217, 245). Hence, transitory ERK activation, induced by mitogens such as EGF, may determine a proliferative response (339, 340), whereas persistent ERK activation, stimulated by NGF and other differentiation factors, may be required (20, 139), although not sufficient (343, 377, 378), for PC12 differentiation.

The basis for the quantitative differences in Ras, MEK and ERK activation induced by EGF and NGF has not been conclusively established, although differences in down-regulation of the respective cell surface RTKs have been implicated as the cause (217). This explanation assumes that growth factor signalling is attenuated by receptor internalization, but it has recently been shown that internalized EGFR is as effective as the cell surface receptor in activating Ras (134), and hence a mechanism acting downstream of the EGFR is more likely to be responsible for down-regulation of the signal generated by EGF. One possible explanation for the contrasting patterns of

Ras/MAPK cascade activation generated by EGF and NGF may therefore be that the intracellular signals induced by these growth factors are subject to differential feedback regulation, as suggested previously (section 5.2.2). Other possibilities that have been suggested include differences in binding affinities of the specific receptors for SH2 domain-containing proteins, or in RTK activities (296), or differential modulation of some factor that negatively regulates ERK, such as GAP or an ERK phosphatase (224).

The remaining sections of this chapter document an investigation of the factors influencing the kinetics of Ras/MAPK cascade activation, conducted using the computer simulation of the EGF signal transduction pathway in PC12 cells as an experimental system. The results of this analysis provide quantitative evidence that the inhibitory feedback phosphorylation of SOS is the most important factor in determining the duration of Ras/MAPK cascade activation. Hence, it is concluded that differences in feedback regulation are likely to underlie the characteristic patterns of EGF- and NGF-induced Ras, MEK and ERK activation in PC12 cells. This chapter has recently been published, in a modified form, as an independent study (25); a copy of this publication, which includes a specification of the computer simulation, is provided in Appendix II.

6.2 RATIONALE AND OBJECTIVES

The main objective of this concluding part of the project was to explain the observed quantitative differences in EGF and NGF signalling in the PC12 cell line in terms of a minimal model of Ras-mediated ERK activation, without recourse to Ras-independent mechanisms. An implicit assumption is that the pathways for EGF- and NGF-induced activation of the MAPK cascade are qualitatively identical in PC12 cells (67), and that no structural changes to the model are required in order to adequately simulate both EGF and NGF signal transduction.

In fact, many signalling events are common to these growth factors. Both EGF and NGF interact with and activate cell surface RTKs (302), and although the exact number of EGFR and NGF receptors (TrkA) varies between sub-clones of the PC12 cell line, typical expression levels of these receptors are comparable (23, 157, 244, 340). Similarly, both EGF and NGF induce an equivalent set of early responses in PC12 cells

(53), including a similar pattern of tyrosine phosphorylation of cellular proteins (213), and activate identical MEK and ERK isoforms (339).

There are however, some important distinctions between EGF and NGF signalling mechanisms; for example, Grb2 binds directly to the activated EGFR, but does not associate with the activated TrkA (133, 330). However, like EGF, NGF induces the rapid tyrosine phosphorylation of Shc, and the association of phosphorylated Shc with both the activated receptor and Grb2 (133, 253, 325). Shc has therefore been suggested to function as an adaptor between the activated TrkA and Grb2 (330), although there is no direct evidence for this proposal (12). Thus, in common with mitogenic signalling by EGF, the critical event in NGF-induced Ras activation appears to be formation of a trimeric Shc-Grb2-SOS complex (12). Since the model already reflects the predominance of this particular complex in EGF signal transduction (see section 3.3.2.2), no modifications were necessary in order to adequately portray the core sequence of signalling events initiated by NGF.

However, there have been a number of reports indicating that EGF and NGF differentially utilize additional pathways for ERK activation in PC12 cells; for example, PKA (373) and PKC (125), particularly the PKC-δ isoform (68), may contribute to ERK activation in response to NGF, but not EGF. Furthermore, NGF induces the tyrosine phosphorylation of the lipid-anchored docking protein, SNT (277) (also designated FRS2, see ref. 190), and the association of phosphorylated SNT with the activated TrkA (224). The role of this interaction is not yet certain, but SNT also binds Grb2-SOS, in addition to an alternative adaptor, Crk (224); Crk forms a complex with C3G (181), a specific GEF for the Ras-like GTPase, Rap-1 (122), which in turn is a selective activator of B-Raf (345). SNT could therefore contribute to persistent NGF-induced ERK activation (224), through a Crk/C3G/Rap-1/B-Raf pathway (377).

Nevertheless, the main focus of the investigation was to examine the potential for mechanisms associated with a linear pathway, featuring exclusively Ras-mediated ERK activation, to regulate the duration of MAPK cascade activation. Ras is apparently both an essential mediator of EGF-induced ERK activation (377), and sustained ERK activation in response to NGF, in the PC12 cell line (20). Hence, the involvement of Ras-independent pathways, which may have a subsidiary function, was not directly considered.

6.3 METHODOLOGY

An assessment of a number of factors that have been proposed to determine the kinetics of Ras/MAPK cascade activation was conducted, by employing a form of sensitivity analysis. These factors were identified with a number of system parameters: the total number of receptors; the rate of receptor internalization; the kinetic characteristics of the activated RTK; the rate of SOS phosphorylation and dephosphorylation; the catalytic activity of GAP and the rate of Raf, MEK and ERK dephosphorylation. The sensitivity of the activation state of Ras/MAPK cascade components to variations in these parameters was analysed by applying the same general approach described in sections 3.3.3.6 and 4.2; for example, to examine the effect of an increase in the affinity of the RTK for Shc, the corresponding K_m value was varied within a range bounded by the initial value and an appropriate lower limit. Parameter values were varied over a range consistent with either measured or estimated values specified in the literature (see sections 3.3.2.5 and 3.3.3.5). The data generated by this analysis were quantified and represented graphically, to enable a comparison of the relative influence of each of the parameters on the kinetics of Ras, MEK and ERK activation.

6.4 RESULTS AND DISCUSSION

It has already been demonstrated in a previous chapter (section 3.3.3.6) that the completed simulation of EGF signal transduction accurately reproduces the transient activation of Ras, MEK and ERK typically induced by continuous exposure of PC12 cells to a saturating concentration of EGF (100 nM) over a prolonged period (60 minutes). As noted above, the pattern of NGF-stimulated MAPK cascade activation in PC12 cells differs considerably from that induced by EGF; NGF has been shown to induce a rapid activation of Ras, MEK and ERK that may be largely sustained for up to several hours (5, 237, 245, 339, 340). In order to investigate the basis for this difference in EGF and NGF signalling through the MAPK kinase cascade, the simulation of EGF signal transduction has been utilized in a quantitative analysis of the factors affecting the time course of cascade activation. By individually varying the values of kinetic parameters governing a number of signalling events, the specific effect of each of these factors on the pattern of Ras, MEK and ERK activation has been determined. A summary of the results of this analysis is given in Table 6.1.

Table 6.1 The effect of variations in selected EGF signal transduction parameters on the duration MAPK cascade activation over 60 minutes simulated continuous exposure to 100 nM EGF

Parameter	Change in Value	Sustained activation		
		Ras	MEK	ERK
$[EGFR]_{total}$	↑	×	×	×
Receptor internalization, k_2, k_{-3}, k_5, k_8	↓	×	×	×
Shc phosphorylation, K_{m9}	↓	×	×	×
Shc phosphorylation, k_9	↑	×	×	×
SOS phosphorylation, k_{27}	↓	✓	✓	✓
SOS dephosphorylation, V_{28}	↑	✓	✓	✓
GAP, k_{15}	↓	✓	✓	✓
ERK PTPase, V_{24}	↓	×	×	✓
PP2A, V_{18}, V_{20}, V_{22}, V_{26}	↓	×	✓	✓

It has been proposed that the transient activation of Ras and ERK by EGF in PC12 cells may be due to attenuation of the signal at or near the level of the EGFR (339, 340). Thus, sustained Ras and ERK activation may possibly be due to prolonged activation of TrkA in comparison with the EGFR (133). Studies involving manipulation of the expression or down-regulation of growth factor receptors appear to confirm the view that the number of active cell surface receptors (278, 340, 370), and hence the strength of the signal generated (82), determine whether Ras and ERK activation are sustained. Consequently, the influence of factors affecting the number of activated cell surface receptors (these being the total number of receptors and the rate of receptor internalization) on the duration of Ras, MEK and ERK activation was investigated. Increasing the number of receptors up to 50-fold had no effect on the time course of Ras/MAPK cascade activation (Table 6.1), despite prolonging Shc phosphorylation (as demonstrated previously in section 4.3.2.1). Decreasing the rate of receptor internalization was also without effect. These results are in agreement with a recent study indicating that EGFR internalization is not likely to be the predominant mechanism for the rapid attenuation of EGF-induced Ras activation (134). Furthermore, the data suggest that EGFR overexpression is linked with sustained Ras and ERK activation through Shc-independent routes, or via parallel pathways that involve Shc (see section 4.3.2.1).

It has also been suggested that differences in the kinetics of receptor interaction with intracellular signalling intermediates might determine the duration of MAPK cascade activation (296). Thus, the influence of the affinity of the receptor for the adaptor protein, Shc, and the rate of RTK-catalysed phosphorylation of this protein were

examined, but these factors were also found to have no effect on the time course of Ras, MEK or ERK activation (Table 6.1), even though Shc phosphorylation was enhanced (as shown previously in section 4.3.2.1). Hence, these results suggest that specific differences in the number of activated receptors at the cell surface, or in the intensity of the signals generated by the receptors, do not underlie the quantitative differences in EGF and NGF signalling in PC12 cells, as manipulating the kinetic parameters of the computer simulation to increase the magnitude of ligand-induced signalling did not generate sustained Ras/MAPK cascade activation.

Since it is likely that EGF signalling is in fact down-regulated through feedback desensitization (134), mediated by MEK-dependent serine/threonine phosphorylation of SOS and resulting in dissociation of the signalling complex formed by phosphorylated Shc, Grb2 and SOS (85), the influence of factors directly affecting the persistence of the Shc-Grb2-SOS complex on the duration of Ras, MEK and ERK activation was also examined. Figure 6.1 shows that decreasing the rate of feedback SOS phosphorylation, or increasing the rate of subsequent SOS dephosphorylation, and thereby enhancing signalling via the Shc-Grb2-SOS complex, resulted in sustained activation of Ras, MEK and ERK (Table 6.1).

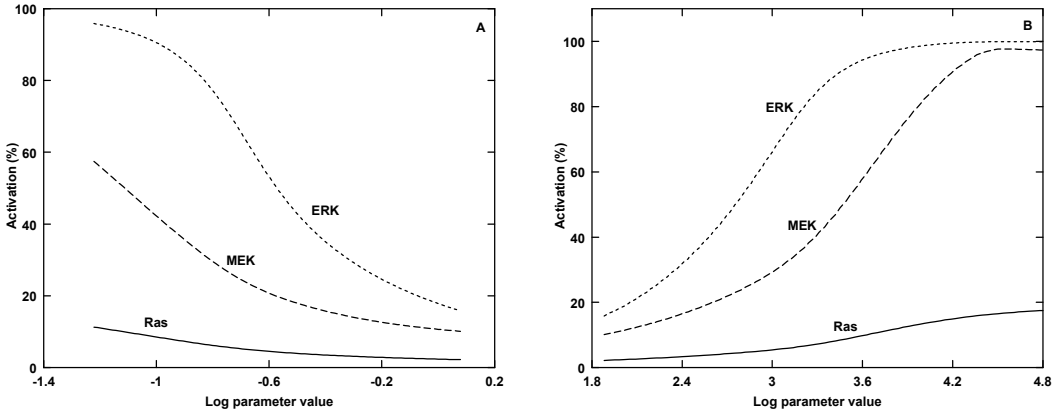

Figure 6.1 Sensitivity of the duration of Ras/MAPK cascade activation to variations in the values of kinetic parameters governing the feedback phosphorylation of SOS

The effect of (**A**) decreasing SOS phosphorylation, k_{27}, and (**B**) increasing SOS dephosphorylation, V_{28}, on the activation state of the MAPK cascade after 60 minutes simulated continuous exposure to 100 nM EGF. The curves indicate the percentage of Ras in the GTP-bound form, and the percentage of maximal MEK and ERK activation.

Furthermore, Figure 6.2 illustrates that a 40-fold increase in rate of SOS dephosphorylation generated a time course of Ras/MAPK cascade activation that is strikingly similar to that observed when PC12 cells are stimulated with NGF, rather than EGF, with the level of Ras-GTP being sustained at around 8% of total Ras (237), MEK activation maintained at around 50% of the peak value (340) and ERK activation remaining at almost the maximal level for at least 60 minutes (5, 245, 339, 340); none of the other parameters investigated had a comparable effect on the time course of Ras/MAPK cascade activation.

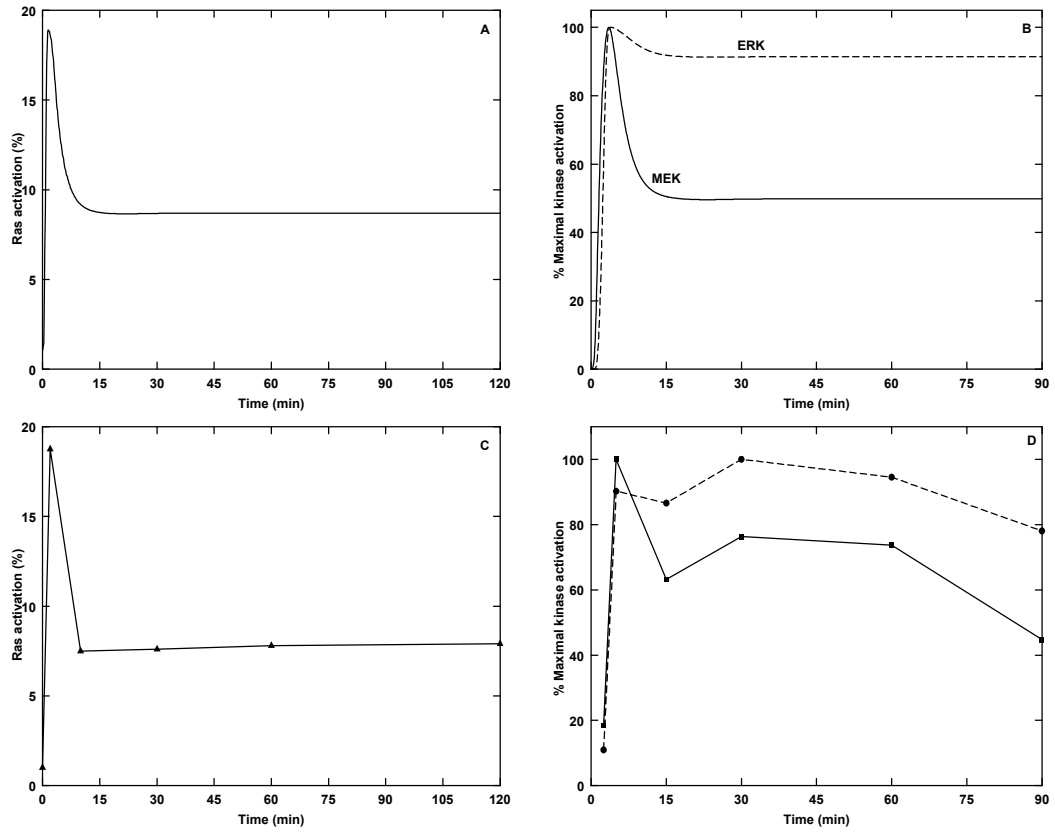

Figure 6.2 Sustained activation of the MAPK cascade resulting from a 40-fold increase in the rate of SOS dephosphorylation

Simulated time courses of (**A**) percentage of total Ras in the GTP-bound form, and (**B**) percentage of maximal MEK and ERK activation were computed over 60 minutes simulated continuous exposure to 100 nM EGF. Experimental time courses of NGF-induced (**C**) Ras activation, and (**D**) MEK (solid line) and ERK (dashed line) activation in PC12 cells, at a saturating NGF concentration, were reproduced from Muroya *et al.* (237) and Traverse *et al.* (340), respectively. SOS dephosphorylation, $V_{28} = 3 \times 10^3$ molecules cell^{-1} min^{-1}. Other simulation parameters are given in Table 3.3.

These results are consistent with earlier observations (see sections 3.3.3.7, 4.3.2.3. and 5.2.2) and experimental data showing that inhibition of the feedback phosphorylation of SOS prolongs Ras activation (194), and imply that some difference in feedback

regulation of the signals initiated by EGF and NGF could account for the quantitative differences in EGF and NGF signalling in PC12 cells. Furthermore, they support the hypothesis that NGF, but not EGF, enhances phosphatase activity towards phosphorylated SOS, resulting in sustained signalling through the Shc-Grb2-SOS complex. Although ERK is generally implicated in the feedback phosphorylation of SOS, there is evidence that additional kinases may be involved, such as the downstream target of ERK, p90 Rsk-2 (83). Moreover, the kinases responsible for catalysing SOS phosphorylation appear to vary with the cell surface receptor, with the effect on the stability of the signalling complex depending upon the site of phosphorylation (381) Hence, it is possible that EGF and NGF may induce the phosphorylation of SOS by different kinases, and thereby at distinct phosphorylation sites, resulting in differing effects on complex regulation (83); in the case of NGF, this might generate a substrate that is more readily dephosphorylated by cellular phosphatases, thus increasing the rate at which functional Shc-Grb2-SOS is reconstituted. Differential regulation of the Grb2-SOS complex by EGF and NGF in PC12 cells has in fact been observed, with EGF stimulating a small transient increase in Grb2-SOS association, and NGF inducing an initial decline in detectable Grb2-SOS complexes, followed by a phase of sustained Grb2-SOS association (154).

Another potential mechanism for regulating the duration and magnitude of MAPK cascade activation would be modulation of the activity of negative regulators of the cascade (224), but this was not supported by an analysis of the influence of the activity of GAP and protein phosphatases on the duration of cascade activation. Reducing the activity of GAP increased the duration of Ras, MEK and ERK activation (Table 6.1), although in order to sustain MEK and ERK activation at a substantial level it was necessary to virtually eliminate GAP activity, resulting in Ras activation being maintained at a level far in excess of that observed experimentally (Figure 6.3A). As no differential effect of EGF and NGF on GAP activity *in vivo* has been described, it therefore seems improbable that modulation of GAP activity represents a physiological mechanism for regulating the duration of Ras/MAPK cascade activation.

Reducing ERK PTPase activity marginally enhanced ERK activation, although this consequently amplified the feedback inhibition of Ras, and thereby diminished the activation of both Ras and MEK (Table 6.1; Figure 6.3B). Consistent with PP2A being the predominant phosphatase activity acting at all points in the MAPK cascade (228),

reducing PP2A activity had a more pronounced positive effect on the duration of both MEK and ERK activation, but again resulted in a reduction in Ras activation (Table 6.1; Figure 6.3C).

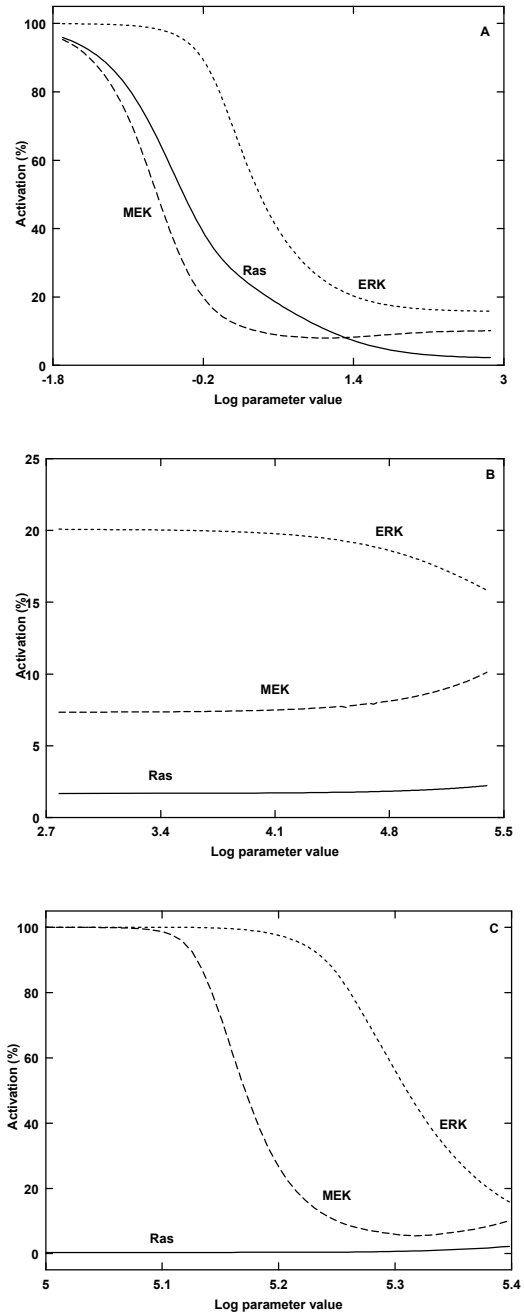

Figure 6.3 Sensitivity of the duration of MAPK cascade activation to decreasing GAP and phosphatase activity

The effect of decreasing the catalytic activity of (**A**) GAP (k_{15}), (**B**) ERK PTPase (V_{24}) and (**C**) PP2A (V_{18}, V_{20}, V_{22} and V_{26}) on the activation state of the MAPK cascade after 60 minutes simulated continuous exposure to EGF. The curves indicate the percentage of Ras in the GTP-bound form, and the percentage of maximal MEK and ERK activation.

Thus, in conjunction with experimental data showing no regulation of ERK phosphatase activity by either EGF or NGF (5), this analysis indicates that negative modulation of either ERK PTPase or PP2A activity by NGF is also unlikely to play a major role in sustaining Ras/MAPK cascade activation.

6.5 Summary and Conclusions

Through a quantitative analysis of a computer simulation of the EGF signal transduction pathway in PC12 cells, evidence has been presented that the characteristic differences in the pattern of EGF and NGF-induced Ras/MAPK cascade activation observed in PC12 cells are unlikely to be due simply to differences in the persistence or intensity of receptor signalling, or in the modulation of GAP or MAPK cascade phosphatase activity. Instead, it has been concluded that some difference in the negative feedback regulation of the cascade is predominantly responsible for determining whether activation is transient or sustained. Although other regulatory mechanisms may be involved, these are likely to play a secondary role. The results presented above clearly demonstrate that unless feedback inhibition of the signal is counteracted, intensifying the signal at the cell surface level is likely to be without effect, and enhancing ERK activation alone paradoxically reduces Ras and MEK activation, generating a pattern of activation that is incompatible with experimental observation. These findings have also been highlighted in previous sections of the thesis (3.3.3.8, 4.4 and 5.4), and hence this independent study represents a culmination of issues arising from previous work.

This analysis therefore suggests a model that accounts for the sustained activation of the Ras/MAPK cascade in PC12 cells by NGF, but not EGF. Both EGF and NGF initially activate the Ras/Raf/MEK/ERK cascade via formation of the Shc-Grb2-SOS signalling complex. In the case of the EGF, this signal is rapidly terminated through the negative feedback phosphorylation of SOS, resulting in dissociation of the Shc-Grb2-SOS complex, mediated by a kinase downstream of MEK. Similarly, in the case of NGF there is initial down-regulation of the signal through Shc-Grb2-SOS, resulting in a transient decline in the level of MEK and ERK activation by 30 minutes exposure to growth factor, which has been observed in certain studies (245, 340) and is shown in Figure 6.2D. However, the rapid reconstitution of functional Grb2-SOS, through

enhanced SOS dephosphorylation, facilitates a second sustained phase of MEK and ERK activation, which has again been observed (245, 340) and can be seen in Figure 6.2D.

Although it has been acknowledged that initial activation of the MAPK cascade is mediated by Ras and Raf-1, a parallel pathway, involving the activation of Rap-1 and B-Raf, via Crk and C3G, has been linked with the sustained phase of ERK activation (365, 377). This Ras-independent pathway may be sufficient to sustain MEK and ERK activation, but the evidence presented here implies that this mechanism alone would be associated with a decline in the Ras activation level, which is contrary to experimental observations. Hence, suppression of the feedback inhibition of Ras activation, possibly mediated through enhanced SOS dephosphorylation, is also necessary to account for all the experimentally observed effects of NGF stimulation of PC12 cells on Ras/Raf/MEK/ERK cascade activation.

Nonetheless, Crk clearly contributes to NGF signalling (377), and may function to activate Ras through SOS, in addition to mediating Rap-1 activation via C3G (181), but is apparently dispensable for EGF-induced ERK activation (334). This raises the question of why EGF does not utilize this alternative pathway for Ras activation, and the answer may once again lie in differential regulation of the status of key signalling complexes; EGF has been shown to induce the rapid dissociation of both Crk-SOS and Crk-C3G complexes (255, 256), presumably accounting for the fact that Crk is not a critical mediator of EGF signalling (334), but it seems improbable that this would occur in response to NGF, given the importance of such complexes in NGF signalling (377). The factors responsible for inducing Crk complex dissociation are not apparent, but this process is linked with the tyrosine phosphorylation status of Crk (256), which could feasibly be differentially regulated by EGF and NGF.

Although many growth factor signal transduction mechanisms have been characterized qualitatively, there is still a lack of quantitative data. Whilst these conclusions are based largely on a theoretical analysis of a current issue in growth factor signalling, this work has demonstrated that by taking a more quantitative approach to studying the regulation of cellular signalling, it is possible to gain valuable insights into areas that are still not fully understood, and determine new directions for future experimental work.

CHAPTER 7

GENERAL CONCLUSIONS

7.1 PERSPECTIVE

As stated in the initial chapter of the thesis, the draft for the project was an investigation of the properties of biological signal transduction systems, through the application of computer modelling techniques. This is obviously a rather broad directive, which was refined during the preliminary stages of the project to an analysis of the functional and regulatory features of mammalian growth factor signalling. Since the signal transducing mechanisms and pathways utilized by growth factors are central in controlling growth and differentiation in many eukaryotic cell types (298, 300), they have been a particular focus of attention for experimentalists. The signal transduction pathway of the mitogen, EGF, has perhaps been the most intensively studied, and was thus regarded as a suitable candidate for theoretical analysis.

A considerable volume of data has been generated, through reductionist approaches, describing the properties of individual components of the EGF signalling network, and likely interactions between these. Most, but debatably not all the essential elements of the system have consequently been characterized in some detail. Despite the significant advances made over the last decade, there is still great deal of uncertainty concerning how these diverse components are integrated *in vivo* to give rise to a functional signalling system, and many important questions remain unanswered. Of particular interest is how signalling specificity might be conferred when there seems to be so little scope for generating this phenomenon; many growth factors utilize similar, if not identical transduction mechanisms and systems, yet can induce very different responses, even in the same target cell type (53, 217).

Numerous descriptive models of how signals might be processed through interactions between components of the EGF signalling network have been proposed; for example, models describing EGF-induced activation of the EGFR (302), or Ras and MAPK cascade activation and down-regulation (85, 187, 221, 301). Many of these proposals are contradictory, as discussed in Chapter 2, and have not previously been verified

within an environment that can be regarded as representative of the intact cell, due to obvious technical constraints. Biological signal transmission also remains largely a qualitative field of study, with little emphasis being placed on quantitative aspects, and computer simulation has only been minimally exploited. Yet the translation of an informal description of a system into mathematical terms permits a rigorous assessment of the mechanistic assumptions and empirical evidence on which the descriptive model is founded, and can even suggest alternative interpretations of experimental observations. Hence, the development and analysis of a computational model of EGF signal transduction was anticipated to provide a novel perspective on the dynamics of cell signalling, within a simulated physiological environment, and thereby a means of furthering current understanding. The extent to which this objective was realized, and therefore the 'success' of the project, can be examined most effectively by reviewing the main points of discussion raised throughout the thesis.

7.2 ACCOMPLISHMENTS

Even during the development process, documented in Chapter 3, the model demonstrated considerable worth as a tool for evaluating proposed models of EGF signal transduction.

- An unconventional approach to modelling EGFR activation was taken, with an attempt to reconcile the many conflicting mechanistic models that have been proposed, and a number of simplifying assumptions were introduced, for example, in the presumed mechanism of Raf activation. Yet, the time-dependent behaviour of the model is consistent with experimentally observed patterns of EGF-induced EGFR down-regulation, Shc phosphorylation and Ras/MAPK cascade activation, implying that the underlying mathematical structure is compatible with events that define the real system. Furthermore, this can be viewed as validation of many of the informal models from which the mathematical formulation was derived, such as the putative mechanism of SOS-mediated Ras activation (85, 221), and also of the measures taken to integrate separate functional units into an interactive system; for example, the treatment of signalling events involving components contained within separate sub-cellular compartments.

- Although the rather controversial mechanistic details of EGFR dimerization and activation were not entirely resolved through modelling the pathway, these were not found to be of fundamental importance in defining the functional properties of the system as a whole. It was however, possible to eliminate negative cooperativity within the EGFR dimer as a source of affinity heterogeneity in ligand binding at the cell surface (366). More probable is that the association of the activated dimer with coated pit adaptor proteins gives rise to an apparent decline in ligand-binding affinity at high receptor occupancy (219). Positive cooperativity, within the solubilized EGFR dimer (199), was not excluded, although this effect would probably be obscured within the plasma membrane environment by coated pit protein binding, thus accounting for typically observed negative curvature of Scatchard plots for EGF-EGFR binding (366).

- As speculated by other authors (134-136, 179), the sub-cellular localization of signal transducing molecules was implicated in the regulation of cell signalling. Thus, the affinity of Ras for both Raf and GAP is predicted to be somewhat higher within the cell than certain *in vitro* estimates suggest (2, 113, 247, 331), perhaps indicating that the anchoring of Raf and GAP to the plasma membrane, within the vicinity of Ras, is important in regulating signal transmission through Ras. Similarly, the effective affinity of Raf for MEK, and MEK for ERK, are possibly enhanced through the association of these MAPK cascade components with scaffolding proteins, which may serve to increase signalling specificity and efficiency (110, 187). Conversely, the spatial separation of SOS from ERK and PTPase activity is possibly important in defining the kinetics of feedback SOS phosphorylation, and increasing the efficiency of this as mechanism for desensitizing the system. This mechanism was in fact, confirmed as being crucial in down-regulating not only EGF-induced Ras/MAPK cascade activation, as previously indicated by other reports (85), but also Shc phosphorylation. GAP and cellular phosphatases were demonstrated to have only secondary importance, and function to restore the basal state of system activation once signalling through Ras has been terminated by SOS deactivation. The relative affinities of SOS for Ras-GDP and GAP for Ras-GTP were however, highlighted as being involved in regulating the maximal extent of initial Ras activation.

Subsequent quantitative analysis of the model also supplied novel insights into EGF signalling, and even enabled the formulation of a new hypothesis to account for the specificity of growth factor signalling.

- A comprehensive sensitivity analysis of the simulated EGF signalling pathway, reported in Chapter 4, confirmed that the characteristics of the EGFR dimerization process have little functional significance, even at the level of cell surface events.

- The overriding importance of ERK-mediated SOS phosphorylation as a negative feedback mechanism that down-regulates and desensitizes EGF signalling through Shc and the Ras/MAPK cascade, first noted during model development, was a recurring theme throughout the analysis phase of the project. Thus, although the MAPK cascade was shown to be capable of demonstrating an ultrasensitive response to EGF, the potential for this to establish sustained maximal ERK activation is suppressed by the feedback loop. The same inhibitory mechanism is also responsible for a typically observed reciprocal relationship between the degree of ERK activation, and the extent of Shc phosphorylation or Ras activation. These variables can hence be viewed as interdependent factors, which can be 'uncoupled' by disruption of the feedback circuit.

- Above the level at which the feedback loop operates, i.e. SOS, an increase in the intensity of signalling, such as through overexpression or increased catalytic activity of the EGFR, prolongs Shc phosphorylation, but not Ras or ERK activation. Feedback down-regulation therefore endows the Ras/MAPK cascade with a high degree of stability to variations in the signal upstream of SOS, in terms of the steady state level of cascade activation; from this observation, it can be inferred that EGFR or Shc overexpression are not linked with sustained Ras and ERK activation, or cell transformation, directly through SOS, but perhaps through the aberrant activation of a parallel signalling pathway. If the magnitude or efficiency of the feedback signal is significantly altered, through gross changes in the availability of functional SOS, the stability of the cascade is lost and steady state Ras/MAPK cascade activation becomes directly proportional to the intensity of the upstream signal. Competition between GAP and Raf for binding Ras-GTP was also found to be an important determining factor for the kinetics of Ras/MAPK activation.

- Whereas changes in the availability of signalling intermediates tend to produce substantial qualitative changes in model behaviour, such as those noted above, variations in kinetic and thermodynamic constants generally influence only quantitative factors; for example, although the exact extent or timing of ERK activation may be altered, cascade activation remains characteristically transient. Notably, the only exception is the rate at which functional SOS is reconstituted. These observations not only illustrate the robustness of the model, but also suggest that this may be an inherent attribute of the real system. Thus, slight differences reported for the kinetic properties of various isoforms of signalling proteins, for example Raf (216, 264, 272, 369) and MEK (382), may be relatively insignificant in defining the cellular response. Rather, features such as the duration of ERK activation, which could be an important determinant of the cell fate (217), might be regulated by the availability of signalling intermediates. Although typical expression levels for many key signalling proteins have not been reported, it seems plausible that these would vary between cell types or under different conditions.

- Quantitative confirmation was provided in Chapter 5 that the MAPK cascade module exhibits the potential to amplify the sensitivity of the overall system response to an external stimulus, albeit to a modest degree, through partial saturation of the cascade reactions, as suggested by previous theoretical analyses of phosphorylation cascades (116, 117, 155, 180, 306, 321). Since the model as a whole is consistent with experimental data describing the time course of MAPK cascade activation, in a cell type that responds in a typical manner to EGF, ultrasensitivity could be an integral feature of the cascade *in vivo*. However, the dynamic properties of the cascade, when this is embedded within a typical signalling network, are a function of the kinetic attributes of both the cascade reactions, and other components of the system.

- It seems unlikely that the MAPK cascade constitutes a 'metabolic switch' (155), since the capacity of any inherent ultrasensitivity to enable an abrupt transition between 'off' and 'on' states of ERK activation is only transiently manifested, due to rapid feedback down-regulation of this response. An interesting corollary is that prolonged maximal ERK activation is observed when this mechanism is compromised, as noted above, and perhaps the MAPK cascade does represent a biochemical switching mechanism under such circumstances. Nonetheless, a more

general role for sensitivity amplification is likely to be in filtering out background noise (116, 117, 189), a property that is in fact demonstrated by the model, whilst the cascade arrangement of Raf, MEK and ERK may also serve to amplify the rate of ERK activation (321).

- Although a combination of ultrasensitivity and feedback inhibition can, in principle, generate sustained oscillations in ERK activation (177), this was shown to be dependent upon restrictive quantitative and mechanistic assumptions, which are incompatible with the more realistic representation of the MAPK cascade provided by the model of EGF signalling. It was therefore concluded that recurrent ERK activation/inactivation cycles are unlikely to be a general feature of growth factor signalling.

- The simulation of EGF-induced Ras/MAPK cascade activation was found to be generally in agreement with a similar, but less extensive model of EGF-induced SOS and PLC-γ activation in hepatocytes (178), despite the latter representing a more intricate array of signalling complexes. Yet, the compatibility of the two models implies that any omissions from the simulation are not critical in defining short-term responses to EGF. Furthermore, it was similarly concluded by the developers of the hepatocyte model that the relative expression levels of signalling intermediates may be an important regulatory feature of the system.

- A more complex model, which considers a network of pathways activated by the EGFR-TK (17), assumes mechanistic details that are apparently unsubstantiated by the signal transduction literature, and hence differs in several important respects from the Ras/MAPK pathway simulation. Not surprisingly, the behaviour of the two models also diverges quite considerably, and in many cases that of the network model is clearly inconsistent with typical experimental observations.

- These two published models reflect contrasting modelling approaches. Whilst the hepatocyte model aims to represent and explain specific responses to EGF in a given cell type, the network model is intended as a generic reconstruction of a typical growth factor signalling network, for investigating the potential properties such systems might exhibit. The model that forms the focus of the thesis contributes an original perspective. Whilst this is more directly comparable with the

hepatocyte model, in terms of both mathematical formulation and modelling philosophy, it greatly extends the boundaries of this model, whilst retaining a level of realism and accuracy forfeited by the more ambitious network model. This provides a more appropriate basis for employing the model as an experimental system for investigating the mechanisms of growth factor signalling.

- The final chapter documents an investigation of the possible biochemical mechanisms underlying the means by which EGF and NGF induce opposing responses in the PC12 cell line, despite activating the same signal transduction cascade. Based upon the results of a sensitivity analysis of the simulated EGF-induced activation of the Ras/MAPK cascade, a number of explanations previously offered for this phenomenon were eliminated, and a novel hypothesis was proposed. This study can in fact, be seen as the culmination of many issues raised in previous chapters. As shown repeatedly throughout the thesis, counteraction of feedback SOS phosphorylation, particularly through enhanced SOS dephosphorylation, is sufficient to sustain signalling through the Ras/MAPK cascade. Moreover, this response is consistent with that typically induced by the NGF stimulation of PC12 cells. However, an increase in signalling intensity above the level of SOS, is without effect on the duration of Ras, MEK or ERK activation, whilst directly enhancing ERK activation alone results in a reciprocal reduction in Ras activity, which is inconsistent with the experimental data. It was therefore concluded that some difference in the feedback regulation of ERK activation, possibly in the efficiency of SOS dephosphorylation, is primarily responsible for generating contrasting responses to EGF and NGF in PC12 cells, although other mechanisms may also contribute.

7.3 APPRAISAL

From the summary given in the previous section, it is clear that the primary goals of the project have been achieved: a satisfactory mathematical model of a representative signal transduction pathway has been developed and implemented as a computer simulation. Furthermore, this has been productively employed in a quantitative analysis of the system. Throughout this work, the value of a modelling approach, for tackling unresolved issues in signal transduction, has undoubtedly been demonstrated.

- It has been possible to evaluate several informal models of EGF signalling, proposed by different authors over a period of many years, and while most have been found to be consistent with experimental observations, modelling has supplied a rational basis for eliminating those that are not.

- An indication of the possible quantitative relationships within the cell has also been provided, as a counterpart to the predominantly qualitative descriptions that have previously been available.

- Computer simulation has facilitated a holistic view of biological signal transmission by a system of diverse components, uniquely illustrating the dynamics of the process.

- Equally, a far better understanding of the mechanisms that terminate the signal has been obtained.

- By providing this fresh perspective, modelling has also suggested an entirely original interpretation of an established phenomenon, for which no other satisfactory explanation has previously been supplied.

Important insights have therefore been gained into how the individual components function as part of an extended cellular network, and how their activity is regulated; these deductions are not confined to the EGF system, but can readily be extrapolated to growth factor signalling in general.

Despite the many clear benefits, there are limitations to the extent to which modelling can be applied as a technique for characterizing a system. Although it is possible to establish which of a group of competing models are credible descriptions of the real system, based on close agreement with experimental data, there can be no guarantee that any particular model is the definitive representation of actual events (141). Arguably, this can also be a failing of more traditional implementations of the 'scientific method', through which hypotheses that account for reproducible observations are proposed and tested. A general lack of numerical data, which is a particular hindrance to modelling signal transduction, also means that values for kinetic and thermodynamic constants must often be estimated from a range of feasible values, or 'fitted' to system behaviour. Even where experimentally determined values available, these are reported

for purified *in vitro* preparations, and possibly bear little resemblance to those applicable within the cell. Consequently, the values assigned to model parameters are not necessarily indicative of those *in vivo*; there may be several sets of parameter values that confer the same dynamic and steady state properties on the model, particularly when this is highly detailed (141). Finally, any new interpretation of empirical observations suggested by the model must be substantiated by further experimental work. Nevertheless, this can open a dialogue between theorists and experimentalists, which can only be desirable, and possibly even vital, in comprehending any biological system.

Modelling does not therefore stand alone and cannot be viewed as a direct alternative to more conventional methodologies. Rather, it is a complementary approach that, when applied in parallel, can afford perspectives on the behaviour of complex biochemical systems that may otherwise be unobtainable, and inspire new avenues of investigation. This has been the significant contribution made by modelling a typical growth factor signal transduction pathway, and the thesis constitutes an important step towards to resolving the cell signalling enigma. Such progress typically exposes yet more underlying questions, and this project has been no exception, but the issues that have been raised present a clear direction for future work.

7.4 Future Directions

Several issues arising from the work covered in the thesis would benefit from further investigation, and the potential for theoretical analysis to enhance understanding of growth factor signalling has been far from exhausted. Many of these advances might be achieved though improvement and extension of the current model.

Despite the success of the model in adequately representing the real system, it is greatly simplified by comparison. An obvious improvement would therefore be to eliminate many of these simplifications, where possible, with the intention of developing an even more realistic model of EGF-induced Ras/MAPK cascade activation. Some reduction in complexity is required, in order for modelling to be an aid to understanding the fundamental features of the system (141). It is therefore important to strike a balance between including processes that might add little functionality, but unnecessarily complicate the model, such as the Grb2-SOS binding equilibrium (see section 3.2.2.2), and those whose importance may have been understated. Although the measures taken

in developing a simplified representation of the system have been found to be valid when considering the specified end-points of the current model (Shc phosphorylation, and Ras/MAPK cascade activation), these might be inappropriate in an extended model of EGF signalling. Listed below are a number of possible modifications to the existing model, which allow for later model expansion.

- The inclusion of ligand-induced EGFR autophosphorylation, and subsequent dephosphorylation; although these processes are dispensable in the current implementation (see section 3.3.1.8), where the direct association of SH2 domain-containing proteins with the EGFR is not considered, they could be important when considering the stable, and possibly exclusive, binding of Shc, PLC-γ or PI-3K to the activated EGFR.

- More detailed representation of the intracellular processing of internalized receptors, and separate degradation and synthesis steps; the current representation, which introduces a time-delay and receptor recycling to approximate these events, is not entirely satisfactory and precludes an assessment of the effects of differential down-regulation of parallel signalling pathways, such as Ras and PLC-γ pathways, through EGFR internalization (134, 136).

- A refined treatment of the sub-cellular compartmentalization of signalling intermediates, for example, by specifying explicit near-membrane and cytosolic compartments, with the intention of allowing a more detailed analysis of interactions between molecules localized to the plasma membrane, and those distributed throughout the cytosol.

- A consideration of the direct association of both Grb2 and Shc with the activated EGFR, thus permitting the formation of stable EGFR-Grb2-SOS and EGFR-Shc-Grb2-SOS complexes, in addition to the independent trimeric Shc-Grb2-SOS complex.

- Modelling the direct association of GAP with the activated EGFR, and any resulting modulation of GAP catalytic activity.

- The representation of separate cellular pools of Raf-1, A-Raf and B-Raf, and the distinct activation mechanisms associated with these isoforms, enabling an

examination of the differential activation of Raf isozymes in response to different growth factors (365).

- The use of more specific estimates of kinetic and thermodynamic data, cellular concentrations of signalling intermediates, and incorporation of relevant qualitative observations (for example, concerning MAPK cascade scaffolding proteins) as these become available from published experimental studies.

These revisions would allow many of the claims made throughout the thesis to be subjected to more rigorous assessment; for example, that Shc and Grb2 only associate transiently with the activated EGFR, or that the EGFR-Grb2-SOS complex plays a minor role in activating Ras (see section 3.3.2.2). Other suppositions, such as that EGFR overexpression is linked with sustained Ras/MAPK cascade activation through Shc-independent routes, which are of lesser importance under normal circumstances (see section 4.4), could only be tested by extending the model to include interactions between parallel signalling pathways initiated by the activated EGFR. Such pathways, and the interactions between them include:

- alternative combinations of adaptors and GEFs, such as Crk/C3G, which may be responsible for activating B-Raf in neuronal cell types through Rap-1 (122, 181, 345), or Crk/SOS (181);

- the PLCγ-PKC and PI-3K pathways;

- possible interactions between PLCγ-PKC and the Ras/MAPK cascade (34, 48, 87, 188);

- a recently discovered link between the Shc/Grb2 and the PI-3K/Akt pathways (129).

Adding these features to the existing computer simulation would yield a generic model of growth factor signalling through RTKs, much the same as that attempted, albeit with only moderate success, by Bhalla and Iyengar (17), which could be readily adapted to reflect different cellular backgrounds. In principle, the development of this model would be a relatively straightforward process, using the same 'modular' approach employed previously. Extension of the current model requires only the development of

additional intermediate modules, linking 'top-level' RTK activation through Crk/SOS, Crk/C3G, PLCγ and PI-3K activation, with 'bottom-level' MAPK cascade activation, which constitutes a point of convergence for the signals initiated by these signalling effectors (233). The only limitation would be the availability of appropriate kinetic data.

This work would permit a critical re-evaluation of a number of the characteristic features of the current model, within the context of an extended system that reflects the complexity of the cell signalling network with even greater realism.

- Ultrasensitivity demonstrated by the MAPK cascade;

- Apparent integral stability of the Ras/MAPK cascade, arising from the cascade being embedded within a negative feedback loop;

- The paramount importance of this mechanism in down-regulating both Shc phosphorylation and SOS activation;

- The role that antagonism of feedback down-regulation might play in sustaining ERK activation;

- The dependence of qualitative aspects of system behaviour on the effective availability of key signalling intermediates.

Such a model would clearly also be an invaluable tool in further investigating the factors that determine the specificity of the biological response to signalling through growth factor RTKs. The current study has already revealed a clue to how such specificity might arise: the effective availability of signalling intermediates, and particularly SOS, to participate in signalling events, has the potential to regulate the kinetics of Ras/MAPK cascade activation. Since the duration of growth factor-induced ERK activation is often associated with a definitive cellular response, this could be a significant finding, which apparently the supports the proposal that distinct biological responses might be defined by quantitative, rather than qualitative factors (217).

Although this possibility has yet to be adequately investigated, there is abundant experimental evidence to support the concept of a quantitative basis for the specificity of the cellular response to the activation of particular RTKs, much of which implies

that factors operating at the level of the receptor are critical for signal definition. Thus, several studies indicate that receptor expression levels may determine the response to a particular growth factor (11, 82, 278, 340, 370), although the response is not simply dependent upon the number of receptors expressed by the cell, but rather the proportion activated by a specific ligand (51, 336). The relative affinity of the activated RTK for various SH2 domain-containing signalling effectors, such as Shc or PLCγ (251, 379), or the relative expression levels of these proteins (11), may also be defining features.

An extended model of growth factor signalling would provide an appropriate experimental system for examining the influence of these factors on the kinetic properties of key signalling events, such as the duration of ERK activation, and thereby a means of evaluating the proposed quantitative basis of signalling specificity. More specifically, this would enable a more detailed investigation of the importance of the concentrations of signalling intermediates in defining the cellular response, in comparison with the kinetic properties of these proteins. It would also provide an opportunity to explore the roles of alternative routes, such as the Crk/C3G/Rap-1/B-Raf pathway (122, 181, 345), or possible positive feedback interactions mediated by the PLCγ-PKC cascade (34, 48, 87, 188), in regulating the duration of ERK activation, and hence the biological response. This would permit the concept that differential feedback down-regulation of the Ras/MAPK cascade forms the basis of signalling specificity, at least in the PC12 cell type, to be further validated in a more representative signalling network.

7.5 Concluding Remarks

Within the pages of this thesis, many steps have been taken to furthering our understanding of a key regulatory system in cellular growth and differentiation: that of growth factor signal transduction. These advances have been made by applying an approach that is relatively new in this field, computer modelling, but through this work, the technique has proven its worth for investigating the mechanisms of cell signalling. The success of the project is only a beginning, and there are still many unresolved issues, especially pertaining to growth factor signalling networks. It is clear however,

that a modelling approach demonstrates significant potential for exploring these questions and supplying possible answers.

REFERENCES

1. Abraham, D., Podar, K., Pacher, M., Kubicek, M., Welzel, N., Hemmings, B. A., Dilworth, S. M., Mischak, H., Kölch, W. and Baccarini, M. (2000) Raf-1-associated protein phosphatase 2A as a positive regulator of kinase activation. *J Biol Chem* 275:22300-22304.
2. Ahmadian, M. R., Hoffmann, U., Goody, R. S. and Wittinghofer, A. (1997) Individual rate constants for the interaction of Ras proteins with GTPase-activating proteins determined by fluorescence spectroscopy. *Biochemistry* 36:4535-4541.
3. Albe, K. R., Butler, M. H. and Wright, B. E. (1990) Cellular concentrations of enzymes and their substrates. *J. theor. Biol.* 143:163-195.
4. Alberts, B., Bray, D., Lewis, J., Raff, M., Roberts, K. and Watson, J. D. (1994) Molecular Biology of the Cell. Garland Publishing, London.
5. Alessi, D. R., Gomez, N., Moorhead, G., Lewis, T., Keyse, S. M. and Cohen, P. (1995) Inactivation of p42 MAP kinase by protein phosphatase 2A and a protein tyrosine phosphatase, but not CL100, in various cell lines. *Curr. Biol.* 5:283-295.
6. Alessi, D. R., Saito, Y., Campbell, D. G., Cohen, P., Sithanandam, G., Rapp, U., Ashworth, A., Marshall, C. J. and Cowley, S. (1994) Identification of the sites in MAP kinase kinase-1 phosphorylated by p74^{raf-1}. *EMBO J.* 13:1610-1619.
7. Anderson, D., Koch, C. A., Grey, L., Ellis, C., Moran, M. F. and Pawson, T. (1990) Binding of SH2 domains of phospholipase Cγ1, GAP, and Src to activated growth factors. *Science* 250:979-982.
8. Anderson, N. G., Maller, J. L., Tonks, N. K. and Sturgill, T. W. (1990) Requirement for integration of signals from two distinct phosphorylation pathways for activation of MAP kinase. *Nature* 343:651-653.
9. Aronheim, A., Engelberg, D., Li, N. X., Alalawi, N., Schlessinger, J. and Karin, M. (1994) Membrane targeting of the nucleotide exchange factor Sos is sufficient for activating the Ras signaling pathway. *Cell* 78:949-961.
10. Avruch, J., Zhang, X. and Kyriakis, J. M. (1994) Raf meets Ras: completing the framework of a signal transduction pathway. *Trends Biochem. Sci.* 19:279-283.

11. Baserga, R. (1999) The IGF-I receptor in cancer research. *Exp. Cell Res.* 253:1-6.

12. Basu, T., Warne, P. H. and Downward, J. (1994) Role of Shc in the activation of Ras in response to epidermal growth factor and nerve growth factor. *Oncogene* 9:3483-3491.

13. Bellot, F., Moolenaar, W., Kris, R., Mirakhur, B., Verlaan, I., Ullrich, A., Schlessinger, J. and Felder, S. (1990) High affinity epidermal growth factor binding is specifically reduced by a monoclonal antibody, and appears necessary for early responses. *J. Cell Biol.* 110:491-502.

14. Berkers, J. A. M., van Bergen en Henegouwen, P. M. P. and Boonstra, J. (1991) Three classes of epidermal growth factor receptors on HeLa cells. *J. Biol. Chem.* 266:922-927.

15. Bertics, P. J., Chen, W. S., Hubler, L., Lazar, C. S., Rosenfeld, M. G. and Gill, G. N. (1988) Alteration of epidermal growth factor receptor activity by mutation of its primary carboxyl-terminal site of tyrosine self-phosphorylation. *J. Biol. Chem.* 263:3610-3617.

16. Bertics, P. J. and Gill, G. N. (1985) Self-phosphorylation enhances the protein-tyrosine kinase activity of the epidermal growth factor receptor. *J. Biol. Chem.* 260:14642-14647.

17. Bhalla, U. S. and Iyengar, R. (1999) Emergent properties of networks of biological signaling molecules. *Science* 283:381-387.

18. Biswas, R., Basu, M., Sen-Majumdar, A. and Das, M. (1985) Intrapeptide autophosphorylation of the epidermal growth factor receptor: regulation of kinase catalytic function by receptor dimerization. *Biochemistry* 24:3795-3802.

19. Block, C., Janknecht, R., Herrmann, C., Nassar, N. and Wittinghofer, A. (1996) Quantitative structure-activity analysis correlating Ras/Raf interaction *in vitro* to Raf activation *in vivo*. *Nature Structural Biology* 3:244-251.

20. Boglari, G., Erhardt, P., Cooper, G. M. and Szeberenyi, J. (1998) Intact Ras function is required for sustained activation and nuclear translocation of extracellular signal-regulated kinases in nerve growth factor-stimulated PC12 cells. *Eur J Cell Biol* 75:54-58.

21. Boguski, M. S. and McCormick, F. (1993) Proteins regulating Ras and its relatives. *Nature* 366:643-653.

22. Böni-Schnetzler, M. and Pilch, P. F. (1987) Mechanism of epidermal growth factor receptor autophosphorylation and high-affinity binding. *Proc. Natl. Acad. Sci. USA* 84:7832-7836.

23. Boonstra, J., Mummery, C. L., van der Saag, P. T. and de Laat, S. (1985) Two receptor classes for epidermal growth factor on pheochromocytoma cells, distinguishable by temperature, lectins, and tumor promoters. *J. Cell. Phys.* 123:347-352.

24. Borowski, P., Kornetzky, L. and Laufs, R. (1998) Properties of the proteolytically generated catalytic domain (42kDa kinase) of epidermal growth factor receptor: comparison with holoenzyme. *J. Biochem.* 123:380-385.

25. Brightman, F. A. and Fell, D. A. (2000) Differential feedback regulation of the MAPK cascade underlies the quantitative differences in EGF and NGF signalling in PC12 cells. *FEBS Lett* 482:169-174.

26. Brown, G. C., Hoek, J. B. and Kholodenko, B. N. (1997) Why do protein kinase cascades have more than one level? *Trends Biochem. Sci.* 22:288.

27. Brown, G. C. and Kholodenko, B. N. (1999) Spatial gradients of cellular phospho-proteins. *FEBS Lett.* 457:452-454.

28. Brownbridge, G. G., Lowe, P. N., Moore, K. J. M., Skinner, R. H. and Webb, M. R. (1993) Interaction of GTPase activating proteins (GAPs) with $p21^{ras}$ measured by a novel fluorescence anisotropy method: essential role of Arg-903 of GAP in activation of GTP hydrolysis on $p21^{ras}$. *J. Biol. Chem.* 268:10914-10919.

29. Brtva, T. R., Drugan, J. K., Ghosh, S., Terrell, R. S., Campbell-Burk, S., Bell, R. M. and Der, C. J. (1995) Two distinct Raf domains mediate interaction with Ras. *J Biol Chem* 270:9809-9812.

30. Buday, L. and Downward, J. (1993) Epidermal growth factor regulates $p21^{ras}$ through the formation of a complex of receptor, Grb2 adapter protein, and Sos nucleotide exchange factor. *Cell* 73:611-620.

31. Buday, L. and Downward, J. (1993) Epidermal growth factor regulates the exchange rate of guanine nucleotides on $p21^{ras}$ in fibroblasts. *Mol. Cell. Biol.* 13:1903-1910.

32. Buday, L., Warne, P. H. and Downward, J. (1995) Down-regulation of the Ras activation pathway by MAP kinase phosphorylation of SOS. *Oncogene* 11:1327-1331.

33. Burgering, B. M. T., de Vries-Smits, A. M. M., Medema, R. H., van Weeren, P. C., Tertoolen, L. G. J. and Bos, J. L. (1993) Epidermal growth factor induces phosphorylation of extracellular signal-regulated kinase 2 via multiple pathways. *Mol. Cell. Biol.* 13:7248-7256.

34. Burgering, B. M. T., Pronk, G. J., van Weeren, P. C., Chardin, P. and Bos, J. L. (1993) cAMP antagonizes p21^{ras}-directed activation of extracellular signal-regulated kinase-2 and phosphorylation of mSos nucleotide exchange factor. *EMBO J.* 12:4211-4220.

35. Burns, J. A., Cornish-Bowden, A., Groen, A. K., Heinrich, R., Porteous, J. W., Rapoport, S. M., Rapoport, T. A., Stucki, J. W., Tager, T. M., Wanders, R. J. A. and Westerhoff, H. V. (1985) Control analysis of metabolic systems. *Trends Biochem. Sci.* 10:16.

36. Cadena, D. L., Chan, C.-L. and Gill, G. N. (1994) The intracellular tyrosine kinase domain of the epidermal growth factor receptor undergoes a conformational change upon autophosphorylation. *J. Biol. Chem.* 269:260-265.

37. Cai, H., Erhardt, P., Troppmair, J., Diazmeco, M. T. and Sithanandam, G. (1993) Hydrolysis of phosphatidylcholine couples Ras to activation of Raf protein kinase during mitogenic signal transduction. *Mol. Cell. Biol.* 13:7645-7651.

38. Campbell, J. S., Seger, R., Graves, J. D., Graves, L. M., Jensen, A. M. and Krebs, E. G. (1995) The MAP kinase cascade. *Recent Progress in Hormone Research* 50:131-159.

39. Canals, F. (1992) Signal transmission by epidermal growth factor receptor: coincidence of activation and dimerization. *Biochemistry* 31:4493-4501.

40. Cárdenas, M. L. and Cornish-Bowden, A. (1989) Characteristics necessary for an interconvertible enzyme to generate a highly sensitive response to an effector. *Biochem. J.* 257:339-345.

41. Cárdenas, M. L. and Cornish-Bowden, A. (1990) Properties needed for the enzymes of an interconvertible cascade to generate a highly sensitive response. *In* Control of Metabolic Processes. A. Cornish-Bowden and M. L. Cárdenas, editors. Plenum Press, New York. 195-207.

42. Carpenter, C. D., Ingraham, H. A., Cochet, C., Walton, G. M., Lazar, C. S., Sowadski, J. M., Rosenfeld, M. G. and Gill, G. N. (1991) Structural analysis of

the transmembrane domain of the epidermal growth-factor receptor. *J. Biol. Chem.* 266:5750-5755.

43. Carpenter, G. (1987) Receptors for epidermal growth factor and other polypeptide mitogens. *Annu. Rev. Biochem.* 56:881-914.

44. Carpenter, G. and Cohen, S. (1990) Epidermal growth factor. *J. Biol. Chem.* 265:7709-7712.

45. Carraway, K. L., III and Cerione, R. A. (1991) Comparison of epidermal growth factor (EGF) receptor-receptor interactions in intact A431 cells and isolated plasma membranes. *J. Biol. Chem.* 266:8899-8906.

46. Carraway, K. L., III and Cerione, R. A. (1993) Fluorescent-labeled growth factor molecules serve as probes for receptor binding and endocytosis. *Biochemistry* 32:12039-12045.

47. Carraway, K. L., III and Cerione, R. A. (1993) Inhibition of epidermal growth-factor receptor aggregation by an antibody directed against the epidermal growth-factor receptor extracellular domain. *J. Biol. Chem.* 268:23860-23867.

48. Carroll, M. P. and May, W. S. (1994) Protein kinase-C-mediated serine phosphorylation directly activates Raf-1 in murine hematopoietic-cells. *J. Biol. Chem.* 269:1249-1256.

49. Cassel, D., Pike, L. J., Grant, G. A., Krebs, E. G. and Glaser, L. (1983) Interaction of epidermal growth factor-dependent protein kinase with endogenous membrane proteins and soluble peptide substrate. *J. Biol. Chem.* 258:2945-2950.

50. Chajry, N., Martin, P.-M., Cochet, C. and Berthois, Y. (1996) Regulation of p42 mitogen-activated-protein kinase activity by protein phosphatase 2A under conditions of growth inhibition by epidermal growth factor in A431 cells. *Eur. J. Biochem.* 235:97-102.

51. Chajry, N., Martin, P.-M., Pagès, G., Cochet, C., Afdel, K. and Berthois, Y. (1994) Relationship between MAP kinase activity and the dual effect of EGF on A431 cell proliferation. *Biochem. Biophys. Res. Comm.* 203:984-990.

52. Chang, C.-P., Lazar, C. S., Walsh, B. J., Komuro, M., Collawn, J. F., Kuhn, L. A., Tainer, J. A., Trowbridge, I. S., Farquhar, M. G., Rosenfeld, M. G., Wiley, H. S. and Gill, G. N. (1993) Ligand-induced internalization of the epidermal growth factor receptor is mediated by multiple endocytic codes analogous to

the tyrosine motif found in constitutively internalized receptors. *J. Biol. Chem.* 268:19312-19320.

53. Chao, M. V. (1992) Growth factor signaling: where is the specificity? *Cell* 68:995-997.

54. Chardin, P., Camonis, J. H., Gale, N. W., Van Aelst, L., Schlessinger, J., Wigler, M. H. and Bar-Sagi, D. (1993) Human Sos1: a guanine-nucleotide exchange factor for Ras that binds to GRB2. *Science* 260:1338-1343.

55. Chen, D., Waters, S. B., Holt, K. H. and Pessin, J. E. (1996) SOS phosphorylation and dissociation of the Grb2-SOS complex. *J. Biol. Chem.* 271:6328-6332.

56. Chen, P., Xie, H. and Wells, A. (1996) Mitogenic signaling from the EGF receptor is attenuated by a phospholipase C-γ/protein kinase C feedback mechanism. *Mol. Biol. Cell* 7:871-881.

57. Chen, R. H., Corbalan-Garcia, S. and Bar-Sagi, D. (1997) The role of the PH domain in the signal-dependent membrane targeting of Sos. *EMBO J.* 16:1351-1359.

58. Chen, R. H., Sarnecki, C. and Blenis, J. (1992) Nuclear-localization and regulation of Erk-encoded and Rsk-encoded protein-kinases. *Mol. Cell. Biol.* 12:915-927.

59. Chen, W. S., Lazar, C. S., Lund, K. A., Welsh, J. B., Chang, C.-P., Walton, G. M., Der, C. J., Wiley, H. S., Gill, G. N. and Rosenfeld, M. G. (1989) Functional independence of the epidermal growth factor receptor from a domain required for ligand-induced internalization and calcium regulation. *Cell* 59:33-43.

60. Chen, W. S., Lazar, C. S., Poenie, M., Tsien, R. Y., Gill, G. N. and Rosenfeld, M. G. (1987) Requirement for intrinsic protein tyrosine kinase in the immediate and late actions of the EGF receptor. *Nature* 328:820-823.

61. Cherniack, A. D., Klarlund, J. K., Conway, B. R. and Czech, M. P. (1995) Disassembly of Son of sevenless proteins from Grb2 during $p21^{ras}$ desensitization by insulin. *J. Biol. Chem.* 270:1485-1488.

62. Cherniack, A. D., Klarlund, J. K. and Czech, M. P. (1994) Phosphorylation of the Ras nucleotide exchange factor Son of Sevenless by mitogen-activated protein kinase. *J. Biol. Chem.* 269:4717-4720.

63. Chook, Y. M., Gish, G. D., Kay, C. M., Pai, E. F. and Pawson, T. (1996) The Grb2-mSos1 complex binds phosphopeptides with higher affinity than Grb2. *J. Biol. Chem.* 271:30472-30478.

64. Cobb, M. H. and Goldsmith, E. J. (2000) Dimerization in MAP-kinase signaling. *Trends Biochem. Sci.* 25:7-9.

65. Cochet, C., Kashles, O., Chambaz, E. M., Borrello, I., King, C. R. and Schlessinger, J. (1988) Demonstration of epidermal growth factor-induced receptor dimerization in living cells using a chemical covalent cross-linking agent. *J. Biol. Chem.* 263:3290-3295.

66. Cohen, G. B., Ren, R. and Baltimore, D. (1995) Modular binding domains in signal transduction proteins. *Cell* 80:237-248.

67. Cohen, P., Campbell, D. G., Dent, P., Gomez, N., Lavoinne, A., Nakielny, S., Stokoe, D., Sutherland, C. and Traverse, S. (1992) Dissection of the protein kinase cascades involved in insulin and nerve growth factor action. *Biochem. Soc. Trans.* 20:671-674.

68. Corbit, K. C., Foster, D. A. and Rosner, M. R. (1999) Protein kinase Cδ mediates neurogenic but not mitogenic activation of mitogen-activated protein kinase in neuronal cells. *Mol Cell Biol* 19:4209-4218.

69. Cowley, S., Paterson, H., Kemp, P. and Marshall, C. J. (1994) Activation of MAP kinase is necessary and sufficient for PC12 differentiation and for transformation of NIH 3T3 cells. *Cell* 77:841-852.

70. Cussac, D., Frech, M. and Chardin, P. (1994) Binding of the Grb2 SH2 domain to phosphotyrosine motifs does not change the affinity of its SH3 domains for Sos proline-rich motifs. *EMBO J.* 13:4011-4021.

71. Cutler, R. E., Jr., Stephens, R. M., Saracino, M. R. and Morrison, D. K. (1998) Autoregulation of the Raf-1 serine/threonine kinase. *Proc Natl Acad Sci U S A* 95:9214-9219.

72. Daum, G., Eisenmann-Tappe, I., Fries, H.-W., Troppmair, J. and Rapp, U. R. (1994) The ins and outs of Raf kinases. *Trends Biochem. Sci.* 19:474-480.

73. Davis, R. J. (1993) The mitogen-activated protein kinase signal transduction pathway. *J. Biol. Chem.* 268:14553-14556.

74. De Meyts, P., Christoffersen, C. T., Ursø, B., Wallach, B., Grønskov, K., Yakushiji, F. and Shymko, R. M. (1995) Role of the time factor in signaling

specificity: application to mitogenic and metabolic signaling by the insulin and insulin-like growth factor-I receptor tyrsoine kinases. *Metabolism* 44:1-11.

75. De Meyts, P., Ursø, B., Christoffersen, C. T. and Shymko, R. M. (1995) Mechanism of insulin and IGF-I receptor activation and signal transduction specificity. *Ann. N.Y. Acad. Sci.* 766:388-401.

76. de Vries-Smits, A. M. M., Pronk, G. J., Medema, J. P., Bugering, B. M. T. and Bos, J. L. (1995) Shc associates with an unphosphorylated form of the p21^{ras} guanine-nucleotide exchange factor, mSOS. *Oncogene* 10:919-925.

77. Dechert, U., Adam, M., Harder, K. W., Clark-Lewis, I. and Jirik, F. (1994) Characterization of protein tyrosine phosphatase SH-PTP2: study of phosphopeptide substrates and possible regulatory role of SH2 domains. *J Biol Chem* 269:5602-5611.

78. Defize, L. H. K., Boonstra, J., Meisenhelder, J., Kruijer, W., Tertoolen, L. G. J., Tilly, B. C., Hunter, T., van Bergen en Henegouwen, P. M. P., Moolenaar, W. H. and de Laat, S. W. (1989) Signal transduction by epidermal growth factor occurs through the subclass of high affinity receptors. *J. Cell Biol.* 109:2495-2507.

79. Dent, P., Chow, Y. H., Wu, J., Morrison, D. K., Jove, R. and Sturgill, T. W. (1994) Expression, purification and characterization of recombinant mitogen-activated protein-kinase kinases. *Biochem. J.* 303:105-112.

80. Dent, P., Jelinek, T., Morrison, D. K., Weber, M. J. and Sturgill, T. W. (1995) Reversal of Raf-1 activation by purified and membrane-associated protein phosphatases. *Science* 268:1902-1906.

81. Diaz, B., Barnard, D., Filson, A., MacDonald, S., King, A. and Marshall, M. (1997) Phosphorylation of Raf-1 serine 338/serine 339 is an essential regulatory event for Ras-dependent activation and biological signaling. *Mol. Cell. Biol.* 17:4509-4516.

82. Dikic, I., Schlessinger, J. and Lax, I. (1994) PC12 cells overexpressing the insulin receptor undergo insulin-dependent neuronal differentiation. *Curr. Biol.* 4:702-708.

83. Douville, E. and Downward, J. (1997) EGF induced SOS phosphorylation in PC12 cells involves p90 RSK-2. *Oncogene* 15:373-383.

84. Downward, J. (1994) The GRB2/Sem-5 adaptor protein. *FEBS Lett.* 338:113-117.

85. Downward, J. (1996) Control of Ras activation. *Cancer Surv.* 27:87-100.

86. Downward, J. (1997) Role of phosphoinositide-3-OH kinase in Ras signaling. *In* Advances in Second Messenger and Phosphoprotein Research. Vol. 31. J. Corbin and S. Francis, editors. Lippincott-Raven Publishers, Philadelphia. 1-10.

87. Downward, J., Graves, J. D., Warne, P. H., Rayter, S. and Cantrell, D. A. (1990) Stimulation of $p21^{ras}$ upon T cell activation. *Nature* 346:719-723.

88. Downward, J., Parker, P. and Waterfield, M. D. (1984) Autophosphorylation sites on the epidermal growth factor receptor. *Nature* 311:483-485.

89. Downward, J., Waterfield, M. D. and Parker, P. J. (1985) Autophosphorylation and protein kinase C phosphorylation of the epidermal growth factor receptor: effect on tyrosine kinase activity and ligand binding affinity. *J. Biol. Chem.* 260:14538-14546.

90. Egan, S. E., Giddings, B. W., Brooks, M. W., Buday, L., Sizeland, A. M. and Weinberg, R. A. (1993) Association of SOS Ras exchange protein with Grb2 is implicated in tyrosine kinase signal transduction and transformation. *Nature* 363:45-51.

91. Ehlde, M. and Zacchi, G. (1995) MIST: a user friendly metabolic simulator. *CABIOS* 11:201-207.

92. Ellis, C., Moran, M., McCormick, F. and Pawson, T. (1990) Phosphorylation of GAP and GAP-associated proteins by transforming and mitogenic tyrosine kinases. *Nature* 343:377-381.

93. Erneux, C., Cohen, S. and Garbers, D. L. (1983) The kinetics of tyrosine phosphorylation by the purified epidermal growth factor receptor kinase of A-431 cells. *J. Biol. Chem.* 258:4137-4142.

94. Fabian, J. R., Daar, I. O. and Morrison, D. K. (1993) Critical tyrosine residues regulate the enzymatic and biological activity of Raf-1 kinase. *Mol. Cell. Biol.* 13:7170-7179.

95. Farnsworth, C. L., Freshney, N. W., Rosen, L. B., Ghosh, A., Greenberg, M. E. and Feig, L. A. (1995) Calcium activation of Ras mediated by neuronal exchange factor Ras-GRF. *Nature* 376:524-527.

96. Farrar, M. A., Alberolalla, J. and Perlmutter, R. M. (1996) Activation of the Raf-1 kinase cascade by coumermycin-induced dimerization. *Nature* 383:178-181.

97. Felder, S., LaVin, J., Ullrich, A. and Schlessinger, J. (1992) Kinetics of binding, endocytosis, and recycling of EGF receptor mutants. *J. Cell Biol.* 117:203-212.

98. Felder, S., Miller, K., Moehren, G., Ullrich, A., Schlessinger, J. and Hopkins, C. R. (1990) Kinase activity controls the sorting of the epidermal growth factor receptor within the multivesicular body. *Cell* 61:623-634.

99. Felder, S., Zhou, M., Hu, P., Urena, J., Ullrich, A., Chaudhuri, M., White, M., Shoelson, S. E. and Schlessinger, J. (1993) SH2 domains exhibit high-affinity binding to tyrosine-phosphorylated peptides yet also exhibit rapid dissociation and exchange. *Mol Cell Biol* 13:1449-1455.

100. Fell, D. A. (1992) Metabolic control analysis: a survey of its theoretical and experimental development. *Biochem. J.* 286:313-330.

101. Fell, D. A. (1997) Understanding the Control of Metabolism. Portland Press, London.

102. Ferrell, J. E., Jr. (1996) Tripping the switch fantastic: how a protein kinase cascade can convert graded inputs into switch-like outputs. *Trends Biochem. Sci.* 21:460-466.

103. Ferrell, J. E., Jr. and Machleder, E. M. (1998) The biochemical basis of an all-or-none cell fate switch in *Xenopus* oocytes. *Science* 280:895-898.

104. Force, T., Bonventre, J. V., Heidecker, G., Rapp, U., Avruch, J. and Kyriakis, J. M. (1994) Enzymatic characteristics of the c-Raf-1 protein-kinase. *Proc. Natl. Acad. Sci. USA* 91:1270-1274.

105. Futter, C. E., Felder, S., Schlessinger, J., Ullrich, A. and Hopkins, C. R. (1993) Annexin-I is phosphorylated in the multivesicular body during the processing of the epidermal growth factor receptor. *J. Cell Biol.* 120:77-83.

106. Gadella, T. W. J. and Jovin, T. M. (1995) Oligomerization of epidermal growth factor receptors on A431 cells studied by time-resolved fluorescence imaging microscopy. A stereochemical model for tyrosine kinase receptor activation. *J. Cell Biol.* 129:1543-1558.

107. Gale, N. W., Kaplan, S., Lowenstein, E. J., Schlessinger, J. and Bar-Sagi, D. (1993) Grb2 mediates the EGF-dependent activation of guanine nucleotide exchange on Ras. *Nature* 363:88-92.

108. Garfinkel, D. (1981) Computer modeling of metabolic pathways. *Trends Biochem. Sci.* 6:69-71.

109. Garfinkel, D., Garfinkel, L., Pring, M., Green, S. B. and Chance, B. (1970) Computer applications to biochemical kinetics. *Annu. Rev. Biochem.* 39:473-498.

110. Garrington, T. P. and Johnson, G. L. (1999) Organization and regulation of mitogen-activated protein kinase signaling pathways. *Curr. Opin. Cell Biol.* 11:211-218.

111. Gates, R. E. and King, L. E., Jnr. (1993) Detergent solubilization is a prerequisite for aggregation-induced stimulation of epidermal growth factor (EGF) receptor kinase. *Journal of Receptor Research* 13:829-847.

112. Gex-Fabry, M. and DeLisi, C. (1984) Receptor-mediated endocytosis: a model and its implications for experimental analysis. *Am. J. Physiol.* 247:R768-779.

113. Gideon, P., John, J., Frech, M., Lautwein, A., Clark, R., Scheffler, J. E. and Wittinghofer, A. (1992) Mutational and kinetic analyses of the GTPase-activating protein (GAP)-p21 interaction: the C-terminal domain of GAP is not sufficient for full activity. *Mol. Cell. Biol.* 12:2050-2056.

114. Gill, G. N., Santon, J. B. and Bertics, P. J. (1987) Regulatory features of the epidermal growth factor receptor. *Journal of Cellular Physiology Supplement* 5:35-41.

115. Glenney, J. R., Chen, W. S., Lazar, C. S., Walton, G. M., Zokas, L. M., Rosenfeld, M. G. and Gill, G. N. (1988) Ligand-induced endocytosis of the EGF receptor is blocked by mutational inactivation and by microinjection of anti-phosphotyrosine antibodies. *Cell* 52:675-684.

116. Goldbeter, A. and Koshland Jr., D. E. (1981) An amplified sensitivity arising from covalent modification in biological systems. *Proceedings of the National Academy of Sciences, USA* 78:6840-6844.

117. Goldbeter, A. and Koshland Jr., D. E. (1982) Sensitivity amplification in biochemical systems. *In* Quarterly Review of Biophysics. Vol. 15. 555-591.

118. Goldbeter, A. and Koshland Jr., D. E. (1984) Ultrasensitivity in biochemical systems controlled by covalent modification. *J. Biol. Chem.* 259:14441-14447.

119. Gomez, N. and Cohen, P. (1991) Dissection of the protein-kinase cascade by which nerve growth factor activates MAP kinases. *Nature* 353:170-173.

120. Gorman, C., Skinner, R. H., Skelly, J. V., Neidle, S. and Lowe, P. N. (1996) Equilibrium and kinetic measurements reveal rapidly reversible binding of Ras to Raf. *J. Biol. Chem.* 271:6713-6719.

121. Gotoh, N., Tojo, A., Muroya, K., Hashimoto, Y., Hattori, S., Nakamura, S., Takenawa, T., Yazaki, Y. and Shibuya, M. (1994) Epidermal growth factor-receptor mutant lacking the autophosphorylation sites induces phosphorylation

of Shc protein and Shc-Grb2/ASH association and retains mitogenic activity. *Proc. Natl. Acad. Sci. USA* 91:167-171.

122. Gotoh, T., Hattori, S., Nakamura, S., Kitayama, H., Noda, M., Takai, Y., Kaibuchi, K., Matsui, H., Hatase, O., Takahashi, H., Kurata, T. and Matsuda, M. (1995) Identification of Rap1 as a target for the Crk SH3 domain-binding guanine nucleotide-releasing factor C3G. *Mol. Cell. Biol.* 15:6746-6753.

123. Gotoh, Y., Matsuda, S., Takenaka, K., Hattori, S., Iwamatsu, A., Ishikawa, M., Kosako, H. and Nishida, E. (1994) Characterization of recombinant *Xenopus* MAP kinase kinases mutated at potential phosphorylation sites. *Oncogene* 9:1891-1898.

124. Gotoh, Y., Nishida, E. and Sakai, H. (1990) Okadaic acid activates microtubule-associated protein kinase in quiescent fibroblastic cells. *Eur. J. Biochem.* 193:671-674.

125. Gotoh, Y., Nishida, E., Yamashita, T., Hoshi, M., Kawakami, M. and Sakai, H. (1990) Microtubule-associated-protein (MAP) kinase activated by nerve growth-factor and epidermal growth-factor in PC12 cells: identity with the mitogen-activated MAP kinase of fibroblastic cells. *Eur. J. Biochem.* 193:661-669.

126. Greene, L. A. and Tischler, A. S. (1976) Establishment of a noradrenergic clonal line of rat adrenal pheochromocytoma cells which respond to nerve growth factor. *Proc. Natl. Acad. Sci. USA* 73:2424-2428.

127. Greenfield, C., Hiles, I., Waterfield, M. D., Federwisch, M., Wollmer, A., Blundell, T. L. and McDonald, N. (1989) Epidermal growth factor binding induces a confirmational change in the external domain of its receptor. *EMBO J.* 8:4115-4123.

128. Groom, L. A., Sneddon, A. A., Alessi, D. R., Dowd, S. and Keyse, S. M. (1996) Differential regulation of the MAP, SAP and RK/p38 kinases by Pyst1, a novel cytosolic dual-specificity phosphatase. *EMBO J.* 15:3621-3632.

129. Gu, H. H., Maeda, H., Moon, J. J., Lord, J. D., Yoakim, M., Nelson, B. H. and Neel, B. G. (2000) New role for Shc in activation of the phosphatidylinositol 3-kinase/Akt pathway. *Mol. Cell. Biol.* 20:7109-7120.

130. Gullick, W. J., Downward, J. and Waterfield, M. D. (1985) Antibodies to the autophosphorylation sites of the epidermal growth factor receptor protein-tyrosine kinase as probes of structure and function. *EMBO J.* 4:2869-2877.

131. Hafner, S., Adler, H. S., Mischak, H., Janosch, P., Heidecker, G., Wolfman, A., Pippig, S., Lohse, M., Ueffing, M. and Kölch, W. (1994) Mechanism of inhibition of Raf-1 by protein kinase A. *Mol. Cell. Biol.* 14:6696-6703.

132. Haney, S. A. and Broach, J. R. (1994) Cdc25p, the guanine nucleotide exchange factor for the Ras proteins of *Saccharomyces cerevisiae*, promotes exchange by stabilizing Ras in a nucleotide-free state. *J. Biol. Chem.* 269:16541-16548.

133. Hashimoto, Y., Matuoka, K., Takenawa, T., Muroya, K., Hattori, S. and Nakamura, S. (1994) Different interactions of Grb2/Ash molecule with the NGF and EGF receptors in rat pheochromocytoma cells. *Oncogene* 9:869-875.

134. Haugh, J. M., Huang, A. C., Wiley, H. S., Wells, A. and Lauffenburger, D. A. (1999) Internalized epidermal growth factor receptors participate in the activation of $p21^{ras}$ in fibroblasts. *J. Biol. Chem.* 274:34350-34360.

135. Haugh, J. M. and Lauffenburger, D. A. (1998) Analysis of receptor internalization as a mechanism for modulating signal transduction. *J. theor. Biol.* 195:187-218.

136. Haugh, J. M., Schooler, K., Wells, A., Wiley, H. S. and Lauffenburger, D. A. (1999) Effect of epidermal growth factor receptor internalization on regulation of the phospholipase C-γ1 signaling pathway. *J. Biol. Chem.* 274:8958-8965.

137. Haystead, T. A. J., Dent, P., Wu, J., Haystead, C. M. M. and Sturgill, T. W. (1992) Ordered phosphorylation of p42 MAPK by MAP kinase kinase. *FEBS Lett.* 306:17-22.

138. Haystead, T. A. J., Weiel, J. E., Litchfield, D. W., Tsukitani, Y., Fischer, E. H. and Krebs, E. G. (1990) Okadaic acid mimics the action of insulin in stimulating protein-kinase activity in isolated adipocytes: the role of protein phosphatase-2A in attenuation of the signal. *J. Biol. Chem.* 265:16571-16580.

139. Heasley, L. E. and Johnson, G. L. (1992) The β-PDGF receptor induces neuronal differentiation of PC12 cells. *Mol. Biol. Cell* 3:545-553.

140. Heidecker, G., Kölch, W., Morrison, D. K. and Rapp, U. R. (1992) The role of Raf-1 phosphorylation in signal transduction. *Adv. Cancer Res.* 58:53-73.

141. Heinrich, R., Rapoport, S. M. and Rapoport, T. A. (1977) Metabolic regulation and mathematical models. *Prog. Biophys. Mol. Biol.* 32:1-82.

142. Heinrich, R. and Rapoport, T. A. (1974) A linear steady-state treatment of enzymatic chains: general properties, control and effector strength. *J. Biochem.* 42:89-95.

143. Hillman, G. M. and Schlessinger, J. (1982) Lateral diffusion of epidermal growth factor complexed to its surface receptors does not account for the thermal sensitivity of patch formation and endocytosis. *Biochemistry* 21:1667-1672.

144. Hofmeyr, J.-H. S. (1986) Steady-state modelling of metabolic pathways: a guide for the prospective simulator. *CABIOS* 2:5-11.

145. Holt, K. H., Kasson, B. G. and Pessin, J. E. (1996) Insulin stimulation of a MEK-dependent but ERK-independent SOS protein kinase. *Mol. Cell. Biol.* 16:577-583.

146. Holt, K. H., Waters, S. B., Okada, S., Yamauchi, K., Decker, S. J., Saltiel, A. R., Motto, D. G., Koretzky, G. A. and Pessin, J. E. (1996) Epidermal growth factor receptor targeting prevents uncoupling of the Grb2-SOS complex. *J. Biol. Chem.* 271:8300-8306.

147. Honegger, A., Dull, T. J., Szapary, D., Komoriya, A., Kris, R., Ullrich, A. and Schlessinger, J. (1988) Kinetic parameters of the protein tyrosine kinase activity of EGF-receptor mutants with individually altered autophosphorylation sites. *EMBO J.* 7:3053-3060.

148. Honegger, A. M., Dull, T. J., Felder, S., van Obberghen, E., Bellot, F., Szapary, D., Schmidt, A., Ullrich, A. and Schlessinger, J. (1987) Point mutation at the ATP binding site of EGF receptor abolishes protein-tyrosine kinase activity and alters cellular routing. *Cell* 51:199-209.

149. Honegger, A. M., Kris, R. M., Ullrich, A. and Schlessinger, J. (1989) Evidence that autophosphorylation of solubilized receptors for epidermal growth factor is mediated by intermolecular cross-phosphorylation. *Proc. Natl. Acad. Sci. USA* 86:925-929.

150. Honegger, A. M., Schmidt, A., Ullrich, A. and Schlessinger, J. (1990) Evidence for epidermal growth factor (EGF)-induced intermolecular autophosphorylation of the EGF receptor in living cells. *Mol. Cell. Biol.* 10:4035-4044.

151. Horseman, N. D., Engle, S. J. and Ralesu, A. (1997) The logic of signaling from the cell surface to the nucleus. *TEM* 8:123-129.

152. Hsu, C.-Y. J., Hurwitz, D. R., Mervic, M. and Zilberstein, A. (1991) Autophosphorylation of the intracellular domain of the epidermal growth

factor receptor results in different effects on its tyrosine kinase activity with various peptide substrates. *J. Biol. Chem.* 266:603-608.

153. Hu, C. D., Kariya, K., Tamada, M., Akasaka, K., Shirouzu, M., Yokoyama, S. and Kataoka, T. (1995) Cysteine-rich region of Raf-1 interacts with activator domain of post-translationally modified Ha-Ras. *J Biol Chem* 270:30274-30277.

154. Hu, Y. and Bowtell, D. D. L. (1996) Sos1 rapidly associates with Grb2 and is hypophosphorylated when complexed with the EGF receptor after EGF stimulation. *Oncogene* 12:1865-1872.

155. Huang, C.-Y. F. and Ferrell, J. E., Jr. (1996) Ultrasensitivity in the mitogen-activated protein kinase cascade. *Proc. Natl. Acad. Sci. USA* 93:10078-10083.

156. Hubbard, S. R., Mohammadi, M. and Schlessinger, J. (1998) Autoregulatory mechanisms in protein-tyrosine kinases. *J. Biol. Chem.* 273:11987-11990.

157. Huff, K., End, D. and Guroff, G. (1981) Nerve growth factor-induced alteration in the response of PC12 pheochromocytoma cells to epidermal growth factor. *J. Cell Biol.* 88:189-198.

158. Hunter, T. and Cooper, J. A. (1985) Protein-tyrosine kinases. *Annu. Rev. Biochem.* 54:897-930.

159. Hurwitz, D. R., Emanuel, S. L., Nathan, M. H., Sarver, N., Ullrich, A., Felder, S., Lax, I. and Schlessinger, J. (1991) EGF induces increased ligand binding affinity and dimerization of soluble epidermal growth factor (EGF) receptor extracellular domain. *J. Biol. Chem.* 266:22035-22043.

160. Inouye, K., Mizutani, S., Koide, H. and Kaziro, Y. (2000) Formation of the Ras dimer is essential for Raf-1 activation. *J Biol Chem* 275:3737-3740.

161. Iwashita, S. and Kobayashi, M. (1992) Signal transduction system for growth factor receptors associated with tyrosine kinase activity: epidermal growth factor receptor signalling and its regulation. *Cellular Signalling* 4:123-132.

162. The Iyengar laboratory Web site can be found at http://piris.pharm.mssm.edu/urilab/.

163. Jacquet, E., Baouz, S. and Parmeggiani, A. (1995) Characterization of mammalian C-CDC25^{Mm} exchange factor and kinetic propoerties of the exchange reaction intermediate p21•C-CDC25^{Mm}. *Biochemistry* 34:12347-12354.

164. Jaiswal, R. K., Moodie, S. A., Wolfman, A. and Landreth, G. E. (1994) The mitogen-activated protein kinase cascade is activated by B-Raf in response to

nerve growth factor through interaction with p21^{ras}. *Mol. Cell. Biol.* 14:6944-6953.

165. Jaiswal, R. K., Weissinger, E., Kolch, W. and Landreth, G. E. (1996) Nerve growth factor-mediated activation of the mitogen-activated protein (MAP) kinase cascade involves a signaling complex containing B-Raf and HSP90. *J. Biol. Chem.* 271:23626-23629.

166. Jelinek, T., Dent, P., Sturgill, T. W. and Weber, M. J. (1996) Ras-induced activation of Raf-1 is dependent on tyrosine phosphorylation. *Mol. Cell. Biol.* 16:1027-1034.

167. Kacser, H. and Burns, J. A. (1973) The control of flux. *Symp. Soc. Exp. Biol.* 27:65-104.

168. Kacser, H., Burns, J. A. and Fell, D. A. (1995) The control of flux. *Biochem. Soc. Trans.* 23:341-366.

169. Kacser, H. and Porteous, J. W. (1987) Control of metabolism: what do we have to measure? *Trends Biochem. Sci.* 12:5-14.

170. Kahn, D. and Westerhoff, H. V. (1991) Control theory of regulatory cascades. *J. theor. Biol.* 153:255-285.

171. Kaplan, D. R. (1998) Studying signal transduction in neuronal cells: the Trk/NGF system. *Prog. Brain Res.* 117:35-46.

172. Kaplan, D. R., Morrison, D. K., Wong, G., McCormick, F. and Williams, L. T. (1990) PDGF β-receptor stimulates tyrosine phosphorylation of GAP and association of GAP with a signaling complex. *Cell* 61:125-133.

173. Katz, M. E. and McCormick, F. (1997) Signal transduction from multiple Ras effectors. *Curr. Opin. Gen. Dev.* 7:75-79.

174. Kazlauskas, A., Ellis, C., Pawson, T. and Cooper, J. A. (1990) Binding of GAP to activated PDGF receptors. *Science* 247:1578-1581.

175. Keyse, S. M. (2000) Protein phosphatases and the regulation of mitogen-activated protein kinase signalling. *Curr. Opin. Cell Biol.* 12:186-192.

176. Khazaie, K., Dull, T. J., Graf, T., Schlessinger, J., Ullrich, A., Beug, H. and Vennstrom, B. (1988) Truncation of the human EGF receptor leads to differential transforming potentials in primary avian fibroblasts and erythroblasts. *EMBO J.* 7:3061-3071.

177. Kholodenko, B. N. (2000) Negative feedback and ultrasensitivity can bring about oscillations in the mitogen-activated protein kinase cascades. *Eur. J. Biochem.* 267:1583-1588.

178. Kholodenko, B. N., Demin, O. V., Moehren, G. and Hoek, J. B. (1999) Quantification of short term signaling by the epidermal growth factor receptor. *J. Biol. Chem.* 274:30169-30181.

179. Kholodenko, B. N., Hoek, J. B. and Westerhoff, H. V. (2000) Why signalling proteins should be recruited to cell membranes. *Cell Biology* 10:173-178.

180. Kholodenko, B. N., Hoek, J. B., Westerhoff, H. V. and Brown, G. C. (1997) Quantification of information transfer via cellular signal transduction pathways. *FEBS Lett.* 414:430-434.

181. Kiyokawa, E., Mochizuki, N., Kurata, T. and Matsuda, M. (1997) Role of Crk oncogene product in physiologic signaling. *Crit. Rev. Oncog.* 8:329-342.

182. Kizaka-Kondoh, S., Matsuda, M. and Okayama, H. (1996) CrkII signals from epidermal growth factor receptor to Ras. *Proc. Natl. Acad. Sci. U. S. A.* 93:12177-12182.

183. Klarlund, J. K., Cherniack, A. D. and Czech, M. P. (1995) Divergent mechanisms for homologous desensitization of $p21^{ras}$ by insulin and growth-factors. *J. Biol. Chem.* 270:23421-23428.

184. Klarlund, J. K., Cherniack, A. D., McMahon, M. and Czech, M. P. (1996) Role of the Raf/mitogen-activated protein kinase pathway in $p21^{ras}$ desensitization. *J. Biol. Chem.* 271:16674-16677.

185. Knauer, D. J., Wiley, H. S. and Cunningham, D. D. (1984) Relationship between epidermal growth factor receptor occupancy and mitogenic response. *J. Biol. Chem.* 259:5623-5631.

186. Koland, J. G. and Cerione, R. A. (1988) Growth factor control of epidermal growth factor receptor kinase activity via an intramolecular mechanism. *J. Biol. Chem.* 263:2230-2237.

187. Kölch, W. (2000) Meaningful relationships: the regulation of the Ras/Raf/MEK/ERK pathway by protein interactions. *Biochem. J.* 351:289-305.

188. Kölch, W., Heidecker, G., Kochs, G., Hummel, R., Vahidi, H., Mischak, H., Finkenzeller, G., Marme, D. and Rapp, U. R. (1993) Protein kinase Cα activates Raf-1 by direct phosphorylation. *Nature* 364:249-252.

189. Koshland, D. E., Jr., Goldbeter, A. and Stock, J. B. (1982) Amplification and adaptation in regulatory and sensory systems. *Science* 217:220-225.

190. Kouhara, H., Hadari, Y. R., Spivak-Kroizman, T., Schilling, J., Bar-Sagi, D., Lax, I. and Schlessinger, J. (1997) A lipid-anchored Grb2-binding protein that links FGF-receptor activation to the Ras/MAPK signaling pathway. *Cell* 89:693-702.

191. Kuroda, S., Ohtsuka, T., Yamamori, B., Fukui, K., Shimizu, K. and Takai, Y. (1996) Different effects of various phospholipids on Ki-Ras-, Ha-Ras-, and Rap1B-induced B-Raf activation. *J. Biol. Chem.* 271:14680-14683.

192. Lai, C.-C., Boguski, M., Broek, D. and Powers, S. (1993) Influence of guanine nucleotides on complex formation between Ras and CDC25 proteins. *Mol. Cell. Biol.* 13:1345-1352.

193. Lai, W. H., Cameron, P. H., Doherty II, J. J., Posner, B. I. and Bergeron, J. J. (1989) Ligand-mediated autophosphorylation activity of the epidermal growth factor receptor during internalization. *J. Cell Biol.* 109:2751-2760.

194. Langlois, W. J., Sasaoka, T., Saltiel, A. R. and Olefsky, J. M. (1995) Negative feedback regulation and desensitization of insulin- and epidermal growth factor-stimulated $p21^{ras}$ activation. *J. Biol. Chem.* 270:25320-25323.

195. Lauffenburger, D. A., Linderman, J. and Berkowitz, L. (1987) Analysis of mammalian cell growth factor receptor dynamics. *Ann. N.Y. Acad. Sci.* 506:147-162.

196. Laurent, M. and Kellershohn, N. (1999) Multistability: a major means of differentiation and evolution in biological systems. *Trends Biochem. Sci.* 24:418-422.

197. Lax, I., Mitra, A. K., Ravera, C., Hurwitz, D. R., Rubinstein, M., Ullrich, A., Stroud, R. M. and Schlessinger, J. (1991) Epidermal growth factor (EGF) induces oligomerization of soluble, extracellular, ligand-binding domain of EGFR receptor. *J. Biol. Chem.* 266:13828-13833.

198. Leevers, S. J., Paterson, H. F. and Marshall, C. J. (1994) Requirement for Ras in Raf activation is overcome by targeting Raf to the plasma membrane. *Nature* 369:411-414.

199. Lemmon, M. A., Bu, Z., Ladbury, J. E., Zhou, M., Pinchasi, D., Lax, I., Engelman, D. M. and Schlessinger, J. (1997) Two EGF molecules contribute additively to stabilization of the EGFR dimer. *EMBO J.* 16:281-294.

200. Lenzen, C., Cool, R. H., Prinz, H., Kuhlmann, J. and Wittinghofer, A. (1998) Kinetic analysis by fluorescence of the interaction between Ras and the catalytic domain of the gunanine nucleotide exchange factor $Cdc25^{Mm}$. *Biochemistry* 37:7420-7430.

201. Lewis, T. S., Shapiro, P. S. and Ahn, N. G. (1998) Signal transduction through MAP kinase cascades. *Adv. Cancer Res.* 74:49-139.

202. Li, B.-Q., Kaplan, D., Kung, H. and Kamata, T. (1992) Nerve growth factor stimulation of the Ras-guanine nucleotide exchange factor and GAP activities. *Science* 256:1456-1459.

203. Li, B.-Q., Subleski, M., Shalloway, D., Kung, H.-F. and Kamata, T. (1993) Mitogenic activation of the Ras guanine nucleotide exchange factor in NIH 3T3 cells involves protein tyrosine phosphorylation. *Proc. Natl. Acad. Sci. USA* 90:8504-8508.

204. Li, W., Batzer, A., Daly, R., Yajnik, V., Skolnik, E., Chardin, P., Bar-Sagi, D., Margolis, B. and Schlessinger, J. (1993) Guanine-nucleotide-releasing factor hSos1 binds to Grb2 and links receptor tyrosine kinases to Ras signalling. *Nature* 363:85-88.

205. Li, W., Melnick, M. and Perrimon, N. (1998) Dual function of Ras in Raf activation. *Development* 125:4999-5008.

206. Lichtner, R. B., Wiedemuth, M., Kittman, A., Ullrich, A., Schirrmacher, V. and Khazaie, K. (1992) Ligand-induced activation of epidermal growth factor receptor in intact rat mammary adenocarcinoma cells without detectable receptor phosphorylation. *J. Biol. Chem.* 267:11872-11880.

207. Lin, L. L., Wartmann, M., Lin, A. Y., Knopf, J. L., Seth, A. and Davis, R. J. (1993) $cPLA_2$ is phosphorylated and activated by map kinase. *Cell* 72:269-278.

208. Lin, M.-F. and Clinton, G. M. (1988) The epidermal growth factor receptor from prostate cells is dephosphorylated by a prostate specific phosphotyrosyl phosphatase. *Mol. Cell. Biol.* 8:5477-5485.

209. Lowenstein, E. J., Daly, R. J., Batzer, A. G., Li, W., Margolis, B., Lammers, R., Ullrich, A., Skolnik, E. Y., Bar-Sagi, D. and Schlessinger, J. (1992) The SH2 and SH3 domain containing protein Grb2 links receptor tyrosine kinases to Ras signaling. *Cell* 70:431-442.

210. Lund, K. A., Opresko, L. K., Starbuck, C., Walsh, B. J. and Wiley, H. S. (1990) Quantitative analysis of the endocytic system involved in hormone-induced receptor internalization. *J. Biol. Chem.* 265:15713-15723.

211. Luo, Z. J., Tzivion, G., Belshaw, P. J., Vavvas, D., Marshall, M. and Avruch, J. (1996) Oligomerization activates c-Raf-1 through a Ras-dependent mechanism. *Nature* 383:181-185.

212. Macdonald, S. G., Crews, C. M., Wu, L., Driller, J., Clark, R., Erikson, R. L. and McCormick, F. (1993) Reconstitution of the Raf-1-MEK-ERK signal transduction pathway *in vitro*. *Mol. Cell. Biol.* 13:6615-6620.

213. Maher, P. A. (1988) Nerve growth factor induces protein-tyrosine phosphorylation. *Proc. Natl. Acad. Sci. USA* 85:6788-6791.

214. Mansour, S. J., Candia, J. M., Matsuura, J. E., Manning, M. C. and Ahn, N. G. (1996) Interdependent domains controlling the enzymatic activity of mitogen-activated protein kinase kinase 1. *Biochemistry* 35:15529-15536.

215. Marais, R., Light, Y., Paterson, H. F. and Marshall, C. J. (1995) Ras recruits Raf-1 to the plasma membrane for activation by tyrosine phosphorylation. *EMBO J.* 14:3136-3145.

216. Marais, R., Light, Y., Paterson, H. F., Mason, C. S. and Marshall, C. J. (1997) Differential regulation of Raf-1, A-Raf, and B-Raf by oncogenic Ras and tyrosine kinases. *J. Biol. Chem.* 272:4378-4383.

217. Marshall, C. J. (1995) Specificity of receptor tyrosine kinase signaling: transient versus sustained extracellular signal-regulated kinase activation. *Cell* 80:179-185.

218. Mason, C. S., Springer, C. J., Cooper, R. G., Superti-Furga, G., Marshall, C. J. and Marais, R. (1999) Serine and tyrosine phosphorylations cooperate in Raf-1, but not B-Raf activation. *EMBO J.* 18:2137-2148.

219. Mayo, K. H., Nunez, M., Burke, C., Starbuck, C., Lauffenburger, D. and Savage, C. R., Jr. (1989) Epidermal growth factor receptor binding is not a simple one-step process. *J. Biol. Chem.* 264:17838-17844.

220. McCormick, F. (1989) Ras GTPase activating protein: signal transmitter and signal terminator. *Cell* 56:5-8.

221. McCormick, F. (1993) How receptors turn Ras on. *Nature* 363:15-16.

222. McCune, B. K. and Earp, H. S. (1989) The epidermal growth factor receptor tyrosine kinase in liver epithelial cells: the effect of ligand-dependent changes in cellular location. *J. Biol. Chem.* 264:15501-15507.

223. McLaughlin, S. and Aderem, A. (1995) The myristoyl-electrostatic switch: a modulator of reversible protein-membrane interactions. *Trends Biochem. Sci.* 20:272-276.

224. Meakin, S. O., MacDonald, J. I. S., Gryz, E. A., Kubu, C. J. and Verdi, J. M. (1999) The signaling adapter FRS-2 competes with Shc for binding to the nerve growth factor receptor TrkA: a model for discriminating proliferation and differentiation. *J. Biol. Chem.* 274:9861-9870.

225. Medema, R. H., de Vries-Smits, A. M. M., van der Zon, G. C. M., Maassen, J. A. and Bos, J. L. (1993) Ras activation by insulin and epidermal growth factor through enhanced exchange of guanine nucleotides on $p21^{ras}$. *Mol. Cell. Biol.* 13:155-162.

226. Mendes, P. (1993) GEPASI: a software package for modelling the dynamics, steady states and control of biochemical and other systems. *CABIOS* 9:563-571.

227. Mendes, P. (1997) Biochemistry by numbers: simulation of biochemical pathways with Gepasi 3. *Trends Biochem. Sci.* 22:361-363.

228. Millward, T. A., Zolnierowicz, S. and Hemmings, B. A. (1999) Regulation of protein kinase cascades by protein phosphatase 2A. *Trends Biochem. Sci.* 24:186-191.

229. Minato, T., Wang, J., Akasaka, K., Okada, T., Suzuki, N. and Kataoka, T. (1994) Quantitative analysis of mutually competitive binding of human Raf-1 and yeast adenylyl cyclase to Ras proteins. *J. Biol. Chem.* 269:20845-20851.

230. Mineo, C., Anderson, R. G. W. and White, M. A. (1997) Physical association with Ras enhances activation of membrane-bound Raf (RafCAAX). *J. Biol. Chem.* 272:10345-10348.

231. Moghal, N. and Sternberg, P. W. (1999) Multiple positive and negative regulators of signaling by the EGF-receptor. *Curr. Opin. Cell Biol.* 11:190-196.

232. Moodie, S. A., Paris, M. J., Kölch, W. and Wolfman, A. (1994) Association of MEK1 with $p21^{ras}$•GMPPNP is dependent on B-Raf. *Mol. Cell. Biol.* 14:7153-7162.

233. Mordret, G. (1993) MAP kinase kinase: a node connecting multiple pathways. *Biol. Cell* 79:193-207.

234. Morrison, D. K. and Cutler Jr., R. E. (1997) The complexity of Raf-1 regulation. *Curr. Opin. Cell Biol.* 9:174-179.

235. Mourey, R. J., Vega, Q. C., Campbell, J. S., Wenderoth, M. P., Hauschka, S. D., Krebs, E. G. and Dixon, J. E. (1996) A novel cytoplasmic dual specificity protein tyrosine phosphatase implicated in muscle and neuronal differentiation. *J. Biol. Chem.* 271:3795-3802.

236. Muda, M., Boschert, U., Dickinson, R., Martinou, J. C., Martinou, I., Camps, M., Schlegel, W. and Arkinstall, S. (1996) MKP-3, a novel cytosolic protein-tyrosine phosphatase that exemplifies a new class of mitogen-activated protein kinase phosphatase. *J. Biol. Chem.* 271:4319-4326.

237. Muroya, K., Hattori, S. and Nakamura, S. (1992) Nerve growth factor induces rapid accumlulation of the GTP-bound form of $p21^{ras}$ in rat pheochromocytoma PC12 cells. *Oncogene* 7:277-281.

238. Murthy, U., Basu, M., Sen-Majumdar, A. and Das, M. (1986) Perinuclear location and recycling of epidermal growth factor receptor kinase: immunofluorescent visualization using antibodies directed to kinase and extracellular domains. *J. Cell Biol.* 103:333-342.

239. Myers, A. C., Kovach, J. S. and Vukpavlovic, S. (1987) Binding, internalization, and intracellular processing of protein ligands: derivation of rate constants by computer modeling. *J. Biol. Chem.* 262:6494-6499.

240. Nemenoff, R. A., Winitz, S., Qian, N. X., Vanputten, V., Johnson, G. L. and Heasley, L. E. (1993) Phosphorylation and activation of a high-molecular-weight form of phospholipase-A2 by p42 microtubule-associated protein-2 kinase and protein-kinase-C. *J. Biol. Chem.* 268:1960-1964.

241. Nesterov, A., Kurten, R. C. and Gill, G. N. (1995) Association of epidermal growth factor receptors with coated pit adaptins via a tyrosine phosphorylation-regulated mechanism. *J. Biol. Chem.* 270:6320-6327.

242. Nesterov, A., Lysan, S., Vdovina, I., Nikolsky, N. and Fujita, D. J. (1994) Phosphorylation of the epidermal growth factor receptor during internalization in A-431 cells. *Arch. Biochem. Biophys.* 313:351-359.

243. Nesterov, A., Reshetnikova, G., Vinogradova, N. and Nikolsky, N. (1990) Functional state of the epidermal growth factor-receptor complexes during their internalization in A-431 cells. *Mol. Cell. Biol.* 10:5011-5014.

244. Ng, N. F. L. and Shooter, E. M. (1993) Activation of $p21^{ras}$ by nerve growth factor in embryonic sensory neurons and PC12 cells. *J. Biol. Chem.* 267:25329-25333.

245. Nguyen, T. T., Scimeca, J. C., Filloux, C., Peraldi, P., Carpentier, J.-L. and Van Obberghen, E. (1993) Co-regulation of the mitogen-activated protein kinase, extracellular signal-regulated kinase 1, and the 90-kDa ribosomal s6 kinase in PC12 cells - distinct effects of the neurotrophic factor, nerve growth factor, and the mitogenic factor, epidermal growth factor. *J. Biol. Chem.* 268:9803-9810.

246. Nishizuka, Y. (1992) Intracellular signaling by hydrolysis of phospholipids and activation of protein kinase C. *Science* 258:607-614.

247. Nixon, A. E., Brune, M., Lowe, P. N. and Webb, M. R. (1995) Kinetics of inorganic phosphate release during the interaction of p21ras with the GTPase-activating proteins, p120-GAP and neurofibromin. *Biochemistry* 34:15592-15598.

248. Northwood, I. C. and Davis, R. J. (1988) Activation of the epidermal growth factor receptor tyrosine kinase in the absence of receptor oligomerization. *J. Biol. Chem.* 263:7450-7453.

249. Northwood, I. C. and Davis, R. J. (1989) Protein kinase C inhibition of the epidermal growth factor receptor tyrosine kinase activity is independent of the oligomeric state of the receptor. *J. Biol. Chem.* 264:5746-5750.

250. Obermeier, A., Bradshaw, R. A., Seedorf, K., Choidas, A., Schlessinger, J. and Ullrich, A. (1994) Neuronal differentiation signals are controlled by nerve growth factor receptor/Trk binding sites for SHC and PLCγ. *EMBO J.* 13:1585-1590.

251. Obermeier, A., Tinhofer, I., Grunicke, H. H. and Ullrich, A. (1996) Transforming potentials of epidermal growth factor and nerve growth factor receptors inversely correlate with their phospholipase Cγ affinity and signal activation. *EMBO J.* 15:73-82.

252. Odaka, M., Kohda, D., Lax, I., Schlessinger, J. and Inagaki, F. (1997) Ligand binding enhances the affinity of dimerization of the extracellular domain of the epidermal growth factor receptor. *J. Biochem.* 122:119-121.

253. Ohmichi, M., Matuoka, K., Takenawa, T. and Saltiel, A. R. (1994) Growth factors differentially stimulate the phosphorylation of Shc proteins and their association with Grb2 in PC-12 pheochromocytoma cells. *J Biol Chem* 269:1143-1148.

254. Ohtsuka, T., Shimizu, K., Yamamori, B., Kuroda, S. and Takai, Y. (1996) Activation of brain B-Raf protein kinase by Rap1B small GTP- binding protein. *J. Biol. Chem.* 271:1258-1261.

255. Okada, S. and Pessin, J. E. (1996) Interactions between Src homology (SH) 2/SH3 adapter proteins and the guanylnucleotide exchange factor SOS are differentially regulated by insulin and epidermal growth factor. *J. Biol. Chem.* 271:25533-25538.

256. Okada, S. and Pessin, J. E. (1997) Insulin and epidermal growth factor stimulate a conformational change in Rap1 and dissociation of the CrkII-C3G complex. *J. Biol. Chem.* 272:28179-28182.

257. Okada, S., Yamauchi, K. and Pessin, J. E. (1995) Shc isoform-specific tyrosine phosphorylation by the insulin and epidermal growth factor receptors. *J. Biol. Chem.* 270:20737-20741.

258. Okada, T., Masuda, T., Shinkai, M., Kariya, K. and Kataoka, T. (1996) Post-translational modification of H-Ras is required for activation of, but not for association with, B-Raf. *J. Biol. Chem.* 271:4671-4678.

259. Opresko, L. K., Chang, C.-P., Will, B. H., Burke, P. M., Gill, G. N. and Wiley, H. S. (1995) Endocytosis and lysosomal targeting of epidermal growth factor receptors are mediated by distinct sequences independent of the tyrosine kinase domain. *J. Biol. Chem.* 270:4325-4333.

260. Orita, S., Kaibuchi, K., Kuroda, S., Shimizu, K., Nakanishi, H. and Takai, Y. (1993) Comparison of kinetic properties between 2 mammalian Ras p21 GDP-GTP exchange proteins, Ras guanine nucleotide-releasing factor and Smg GDP dissociation stimulator. *J. Biol. Chem.* 268:25542-25546.

261. Oshima, M., Sithanandam, G., Rapp, U. R. and Guroff, G. (1991) The phosphorylation and activation of B-Raf in PC12 cells stimulated by nerve growth factor. *J. Biol. Chem.* 266:23753-23760.

262. Osterop, A. P. R. M., Medema, R. H., v.d. Zon, G. C. M., Bos, J. L., Moller, W. and Maassen, J. A. (1993) Epidermal-growth-factor receptors generate Ras.GTP more efficiently than insulin receptors. *Eur. J. Biochem.* 212:477-482.

263. Panayotou, G., Gish, G., End, P., Truong, O., Gout, I., Dhand, R., Fry, M. J., Hiles, I., Pawson, T. and Waterfield, M. D. (1993) Interactions between SH2 domains and tyrosine-phosphorylated platelet-derived growth factor β-receptor sequences: analysis of kinetic parameters by a novel biosensor-based approach. *Mol Cell Biol* 13:3567-3576.

264. Papin, C., Denouel Galy, A., Laugier, D., Calothy, G. and Eychene, A. (1998) Modulation of kinase activity and oncogenic properties by alternative splicing reveals a novel regulatory mechanism for B-Raf. *J. Biol. Chem.* 273:24939-24947.

265. Pawson, T. and Gish, P. (2000) Protein-protein interactions define specificity in signal transduction. *Genes and Development* 14:1027-1047.

266. Pawson, T. and Schlessinger, J. (1993) SH2 and SH3 domains. *Curr. Biol.* 3:434-442.

267. Pearse, B. M. F. and Robinson, M. S. (1990) Clathrin, adaptors, and sorting. *Annu. Rev. Cell Biol.* 6:151-171.

268. Pelicci, G., Lanfrancone, L., Grignani, F., McGlade, J., Cavallo, F., Forni, G., Nicoletti, I., Grignani, F., Pawson, T. and Pelicci, P. G. (1992) A novel transforming protein (Shc) with an SH2 domain is implicated in mitogenic signal transduction. *Cell* 70:93-104.

269. Porfiri, E. and McCormick, F. (1996) Regulation of epidermal growth factor receptor signaling by phosphorylation of the Ras exchange factor hSOS1. *J. Biol. Chem.* 271:5871-5877.

270. Posner, I., Engel, M. and Levitzki, A. (1992) Kinetic model of the epidermal growth factor (EGF) receptor tyrosine kinase and a possible mechanism of its activation by EGF. *J. Biol. Chem.* 267:20638-20647.

271. Posner, I. and Levitzki, A. (1994) Kinetics of phosphorylation of the SH2-containing domain of phospholipase Cγ1 by the epidermal growth factor receptor. *FEBS Lett.* 353:155-161.

272. Pritchard, C. A., Samuels, M. L., Bosch, E. and McMahon, M. (1995) Conditionally oncogenic forms of the A-Raf and B-Raf protein-kinases display different biological and biochemical properties in NIH 3T3 cells. *Mol. Cell. Biol.* 15:6430-6442.

273. Pronk, G. J., de Vries-Smits, A. M. M., Buday, L., Downward, J., Maassen, J. A., Medema, R. H. and Bos, J. L. (1994) Involvement of Shc in insulin- and epidermal growth factor-induced activation of p21^{ras}. *Mol. Cell. Biol.* 14:1575-1581.

274. Prowse, C. N., Hagopian, H. C., Cobb, M. H. and Lew, J. (2000) Catalytic reaction pathway for the mitogen-activated protein kinase ERK2. *Biochemistry* 39:6258-6266.

275. Qiu, M. S. and Green, S. H. (1991) NGF and EGF rapidly activate p21^{ras} in PC12 cells by distinct, convergent pathways involving tyrosine phosphorylation. *Neuron* 7:937-946.

276. Quilliam, L. A., Huff, S. Y., Rabun, K. M., Wei, W., Park, W., Broek, D. and Der, C. J. (1994) Membrane-targeting potentiates guanine-nucleotide exchange factor Cdc25 and Sos1 activation of Ras transforming activity. *Proc. Natl. Acad. Sci. USA* 91:8512-8516.

277. Rabin, S. J., Cleghon, V. and Kaplan, D. R. (1993) SNT, a differentiation-specific target of neurotrophic factor-induced tyrosine kinase activity in neurons and PC12 cells. *Mol. Cell. Biol.* 13:2203-2213.

278. Raffioni, S. and Bradshaw, R. A. (1995) Staurosporine causes epidermal growth-factor to induce differentiation in PC12 cells via receptor up-regulation. *J. Biol. Chem.* 270:7568-7572.

279. Rensland, H., John, J., Linke, R., Simon, I., Schlichting, I., Wittinghofer, A. and Goody, R. S. (1995) Substrate and product structural requirements for binding of nucleotides to H-ras p21: the mechanism of discrimination between guanosine and adenosine nucleotides. *Biochemistry*.

280. Resing, K. A., Mansour, S. J., Hermann, A. S., Johnson, R. S., Candia, J. M., Fukasawa, K., van de Woude, G. F. and Ahn, N. G. (1995) Determination of v-Mos-catalyzed phosphorylation sites and autophosphorylation sites on MAP kinase kinase by ESI/MS. *Biochemistry* 34:2610-2620.

281. Robinson, M. J., Harkins, P. C., Zhang, J., Baer, R., Haycock, J. W., Cobb, M. H. and Goldsmith, E. J. (1996) Mutation of position 52 in ERK2 creates a nonproductive binding mode for adenosine 5'-triphosphate. *Biochemistry* 35:5641-5646.

282. Rousseau, D. L., Staros, J. V. and Beechem, J. M. (1995) The interaction of epidermal growth factor with its receptor in A431 cell membranes: a stopped-flow fluorescence anisotropy study. *Biochemistry* 34:14508-14518.

283. Roy, S., Lane, A., Yan, J., McPherson, R. and Hancock, J. F. (1997) Activity of plasma membrane-recruited Raf-1 is regulated by Ras via the Raf zinc finger. *J Biol Chem* 272:20139-20145.

284. Rozakis-Adcock, M., Fernley, R., Wade, J., Pawson, T. and Bowtell, D. (1993) The SH2 and SH3 domains of mammalian Grb2 couple the EGF receptor to the Ras activator mSos1. *Nature* 363:83-85.

285. Rozakis-Adcock, M., McGlade, J., Mbamalu, G., Pelicci, G., Daly, R., Li, W., Batzer, A., Thomas, S., Brugge, J., Pelicci, P. G., Schlessinger, J. and Pawson, T. (1992) Association of the Shc and the Grb2/Sem-5 SH2-containing proteins is implicated in activation of the Ras pathway by tyrosine kinases. *Nature* 360:689-692.

286. Rozakis-Adcock, M., Vandergeer, P., Mbamalu, G. and Pawson, T. (1995) MAP kinase phosphorylation of mSos1 promotes dissociation of mSos1-Shc and mSos1-EGF receptor complexes. *Oncogene* 11:1417-1426.

287. Ruff-Jamison, S., McGlade, J., Pawson, T., Chen, K. and Cohen, S. (1993) Epidermal growth factor stimulates the tyrosine phosphorylation of SHC in the mouse. *J. Biol. Chem.* 268:7610-7612.

288. Sakaue, M., Bowtell, D. and Kasuga, M. (1995) A dominant-negative mutant of mSos1 inhibits insulin-induced Ras activation and reveals Ras-dependent and Ras-independent insulin signaling pathways. *Mol. Cell. Biol.* 15:379-388.

289. Salcini, A. E., McGlade, J., Pelicci, G., Nicoletti, I., Pawson, T. and Pelicci, P. G. (1994) Formation of Shc-Grb2 complexes is necessary to induce neoplastic transformation by overexpression of Shc proteins. *Oncogene* 9:2827-2836.

290. Sano, M. (1992) Chromatographic resolution and characterization of a nerve growth factor-dependent kinase that phosphorylates microtubule-associated protein-1 and protein-2 in PC12 cells. *J. Neurochem.* 59:1263-1272.

291. Sasaoka, T., Langlois, W. J., Leitner, J. W., Draznin, B. and Olefsky, J. M. (1994) The signaling pathway coupling epidermal growth factor receptors to activation of p21*ras*. *J. Biol. Chem.* 269:32621-32625.

292. Sasaoka, T., Rose, D. W., Jhun, B. H., Saltiel, A. R., Draznin, B. and Olefsky, J. M. (1994) Evidence for a functional role of Shc proteins in mitogenic signaling induced by insulin, insulin-like growth factor-1, and epidermal growth factor. *J. Biol. Chem.* 269:13689-13694.

293. Sastry, L., Lin, W. H., Wong, W. T., Difiore, P. P., Scoppa, C. A. and King, C. R. (1995) Quantitative analysis of Grb2-Sos1 interaction: the N-terminal SH3 domain of Grb2 mediates affinity. *Oncogene* 11:1107-1112.

294. Satoh, T., Nakafuku, M. and Kaziro, Y. (1992) Function of Ras as a molecular switch in signal transduction. *J. Biol. Chem.* 267:24149-24152.

295. Sauro, H. (1993) SCAMP: a general purpose simulator and metabolic control analysis program. *CABIOS* 9:441-450.

296. Schamel, W. W. A. and Dick, T. P. (1996) Signal transduction: specificity of growth factors explained by parallel distributed processing. *Medical Hypotheses* 47:249-255.

297. Scheffzek, K., Ahmadian, M. R. and Wittinghofer, A. (1998) GTPase-activating proteins: helping hands to complement an active site. *Trends Biochem. Sci.* 23:257-262.

298. Schlessinger, J. (1986) Allosteric regulation of the epidermal growth factor receptor kinase. *J. Cell Biol.* 103:2067-2072.

299. Schlessinger, J. (1988) The epidermal growth factor receptor as a multifunctional allosteric protein. *Biochemistry* 27:3119-3123.

300. Schlessinger, J. (1988) Signal transduction by allosteric receptor oligomerization. *Trends Biochem. Sci.* 13:443-447.

301. Schlessinger, J. and Bar-Sagi, D. (1994) Activation of Ras and other signaling pathways by receptor tyrosine kinases. *Cold Spring Harb. Symp. on Quant. Biol.* 59:173-179.

302. Schlessinger, J. and Ullrich, A. (1992) Growth factor signaling by receptor tyrosine kinases. *Neuron* 9:383-391.

303. Schofl, C., Prank, K. and Brabant, G. (1994) Mechanisms of cellular information processing. *TEM* 5:53-59.

304. Schuster, S., Kahn, D. and Westerhoff, H. V. (1993) Modular analysis of the control of complex metabolic pathways. *Biophysical Chemistry* 48:1-17.

305. Serth, J., Weber, W., Frech, M., Wittinghofer, A. and Pingoud, A. (1992) Binding of the H-Ras p21 GTPase activating protein by the activated epidermal growth factor receptor leads to inhibition of the p21 GTPase activity *in vitro*. *Biochemistry* 31:6361-6365.

306. Shacter, E., Chock, P. B., Rhee, S. G. and Stadtman, E. R. (1986) Cyclic cascades and metabolic regulation. *The Enzymes* XVII:21-42.

307. Sherrill, J. M. (1997) Insufficiency of self-phosphorylation for the activation of epidermal growth factor receptor. *Biochemistry* 36:5677-5684.

308. Sherrill, J. M. (1997) Self-phosphorylation of epidermal growth factor receptor is an intermolecular reaction. *Biochemistry* 36:12890-12896.

309. Sherrill, J. M. and Kyte, J. (1996) Activation of epidermal growth factor receptor by epidermal growth factor. *Biochemistry* 35:5705-5718.

310. Shinomura, T., Asaoka, Y., Oka, M., Yoshida, K. and Nishizuka, Y. (1991) Synergistic action of diacylglycerol and unsaturated fatty acid for protein kinase C activation: its possible implications. *Proc. Natl. Acad. Sci. U. S. A.* 88:5149-5153.

311. Skolnik, E. Y., Batzer, A., Li, N., Lee, C. H., Lowenstein, E., Mohammadi, M., Margolis, B. and Schlessinger, J. (1993) The function of Grb2 in linking the insulin-receptor to Ras signaling pathways. *Science* 260:1953-1955.

312. Small, J. R. and Fell, D. A. (1990) Covalent modification and metabolic control analysis: modification to the theorems and their application to metabolic systems containing covalently modifiable enzymes. *Eur. J. Biochem.* 191:405-411.

313. Soler, C., Alvarez, C. V., Beguinot, L. and Carpenter, G. (1994) Potent SHC tyrosine phosphorylation by epidermal growth factor at low receptor density or in the absence of receptor autophosphorylation sites. *Oncogene* 9:2207-2215.

314. Sorkin, A. and Carpenter, G. (1991) Dimerization of internalized epidermal growth factor receptors. *J. Biol. Chem.* 266:23453-23460.

315. Sorkin, A. and Carpenter, G. (1993) Interaction of activated EGF receptors with coated pit adaptins. *Science* 261:612-615.

316. Sorkin, A., Waters, C., Overholser, K. A. and Carpenter, G. (1991) Multiple autophosphorylation site mutations of the epidermal growth factor receptor: analysis of kinase activity and endocytosis. *J. Biol. Chem.* 266:8355-8362.

317. Sorkin, A. and Waters, C. M. (1993) Endocytosis of growth factor receptors. *BioEssays* 15:375-382.

318. Sorkin, A. D., Teslenko, L. V. and Nikolsky, N. N. (1988) The endocytosis of epidermal growth factor in A431 cells: pH of microenvironment and the dynamics of receptor complex dissociation. *Exp. Cell Res.* 175:192-205.

319. Sorokin, A., Lemmon, M. A., Ullrich, A. and Schlessinger, J. (1994) Stabilization of an active dimeric form of the epidermal growth factor receptor by introduction of an inter-receptor disulfide bond. *J. Biol. Chem.* 13:9752-9759.

320. Spaargaren, M., Defize, L. H. K., Boonstra, J. and de Laat, S. (1991) Antibody-induced dimerization activates the epidermal growth factor receptor tyrosine kinase. *J. Biol. Chem.* 266:1733-1739.

321. Stadtman, E. R. and Chock, P. B. (1978) Interconvertible enzyme cascades in metabolic regulation. *Curr. Top. Cell. Reg.* 13:53-95.

322. Starbuck, C. and Lauffenburger, D. A. (1992) Mathematical model for the effects of epidermal growth factor receptor trafficking dynamics on fibroblast proliferation responses. *Biotechnology Progress* 8:132-143.

323. Staros, J. V., Cohen, S. and Russo, M. W. (1985) Receptor kinases in transmembrane signaling. *In* Molecular Mechanisms of Transmembrane Signaling. P. Cohen and M. D. Maunslay, editors. Elsevier, New York. 253-278.

324. Steck, T. L. (1974) The organisation of proteins in the human red blood cell membrane. *J. Cell Biol.* 62:1-19.

325. Stephens, R. M., Loeb, D. M., Copeland, T. D., Pawson, T., Greene, L. A. and Kaplan, D. R. (1994) Trk receptors use redundant signal transduction pathways involving SHC and PLC-γ1 to mediate NGF responses. *Neuron* 12:691-705.

326. Stephens, R. M., Sithanandam, G., Copeland, T. D., Kaplan, D. R., Rapp, U. R. and Morrison, D. K. (1992) 95-Kilodalton B-Raf serine/threonine kinase: identification of the protein and its major autophosphorylation site. *Mol. Cell. Biol.* 12:3733-3742.

327. Stevenson, L. E. and Frackelton, A. R. (1998) Constitutively tyrosine phosphorylated p52 Shc in breast cancer cells: correlation with ErbB2 and p66 Shc expression. *Breast Cancer Res. Treat.* 49:119-128.

328. Stokoe, D., Macdonald, S. G., Cadwallader, K., Symons, M. and Hancock, J. F. (1994) Activation of Raf as a result of recruitment to the plasma membrane. *Science* 264:1463-1467.

329. Stokoe, D. and McCormick, F. (1997) Activation of c-Raf-1 by Ras and Src through different mechanisms: activation *in vivo* and *in vitro*. *EMBO J.* 16:2384-2396.

330. Suen, K. L., Bustelo, X. R., Pawson, T. and Barbacid, M. (1993) Molecular cloning of the mouse *grb2* gene: differential interaction of the Grb2 adaptor protein with epidermal growth factor and nerve growth factor receptors. *Mol Cell Biol* 13:5500-5512.

331. Sydor, J. R., Engelhard, M., Wittinghofer, A., Goody, R. S. and Herrmann, C. (1998) Transient kinetic studies on the interaction of Ras and the Ras-binding domain of c-Raf-1 reveal rapid equilibration of the complex. *Biochemistry* 37:14292-14299.

332. Szedlacsek, S. E., Cardenas, M. L. and Cornish-Bowden, A. (1992) Response coefficients of interconvertible enzyme cascades towards effectors that act on one or both modifier enzymes. *Eur. J. Biochem.* 204:807-813.

333. Tamada, M., Hu, C. D., Kariya, K., Okada, T. and Kataoka, T. (1997) Membrane recruitment of Raf-1 is not the only function of Ras in Raf-1 activation. *Oncogene* 15:2959-2964.

334. Tanaka, M., Gupta, R. and Mayer, B. J. (1995) Differential inhibition of signaling pathways by dominant-negative SH2/SH3 adapter proteins. *Mol. Cell. Biol.* 15:6829-6837.

335. Teng, K. K., Lander, H., Fajardo, J. E., Hanafusa, H., Hempstead, B. L. and Birge, R. B. (1995) v-Crk modulation of growth factor-induced PC12 cell differentiation involves the Src homology-2 domain of v-Crk and sustained activation of the Ras/mitogen-activated protein kinase pathway. *J. Biol. Chem.* 270:20677-20685.

336. Thoresen, G. H., Guren, T. K., Sandnes, D., Peak, M., Agius, L. and Christoffersen, T. (1998) Response to transforming growth factor α (TGFα) and epidermal growth factor (EGF) in hepatocytes: lower EGF receptor affinity of TGFα is associated with more sustained activation of p42/p44 mitogen-activated protein kinase and greater efficacy in stimuation of DNA synthesis. *J. Cell. Phys.* 175:10-18.

337. Todd, J. L., Tanner, K. G. and Denu, J. M. (1999) Extracellular regulated kinases (ERK) 1 and ERK2 are authentic substrates for the dual-specificity protein-tyrosine phosphatase VHR. *J. Biol. Chem.* 274:13271-13280.

338. Traverse, S. and Cohen, P. (1994) Identification of a latent MAP kinase kinase kinase in PC12 cells as B-Raf. *FEBS Lett.* 350:13-18.

339. Traverse, S., Gomez, N., Paterson, H., Marshall, C. and Cohen, P. (1992) Sustained activation of the mitogen-activated protein (MAP) kinase cascade may be required for differentiation of PC12 cells: comparison of the effects of nerve growth factor and epidermal growth factor. *Biochem. J.* 288:351-355.

340. Traverse, S., Seedorf, K., Paterson, H., Marshall, C. J., Cohen, P. and Ullrich, A. (1994) EGF triggers neuronal differentiation of PC12 cells that overexpress the EGF receptor. *Curr. Biol.* 4:694-701.

341. Ullrich, A., Coussens, L., Hayflick, J. S., Dull, T. J., Gray, A., Tam, A. W., Lee, J., Yarden, Y., Libermann, T. A., Schlessinger, J., Downward, J., Mayes, E. L.

V., Whittle, N., Waterfield, M. D. and Seeburg, P. H. (1984) Human epidermal growth-factor receptor cDNA sequence and aberrant expression of the amplified gene in A431 epidermoid carcinoma cells. *Nature* 309:418-425.

342. Ullrich, A. and Schlessinger, J. (1990) Signal transduction by receptors with tyrosine kinase activity. *Cell* 61:203-212.

343. Vaillancourt, R. R., Heasley, L. E., Zamarripa, J., Storey, B., Valius, M., Kazlauskas, A. and Johnson, G. L. (1995) Mitogen-activated protein kinase activation is insufficient for growth factor receptor-mediated PC12 cell differentiation. *Mol Cell Biol* 15:3644-3653.

344. van Bergen en Henegouwen, P. M. P., Defize, L. H. K., de Kroon, J., van Damme, H., Verkleij, A. J. and Boonstra, J. (1989) Ligand-induced association of epidermal growth factor receptor to the cytoskeleton of A431 cells. *J. Cell. Biochem.* 39:455-465.

345. Vossler, M. R., Yao, H., York, R. D., Pan, M. G., Rim, C. S. and Stork, P. J. S. (1997) cAMP activates MAP kinase and Elk-1 through a B-Raf- and Rap1-dependent pathway. *Cell* 89:73-82.

346. Walker, F. and Burgess, A. W. (1991) Reconstitution of the high affinity epidermal growth factor receptor on cell-free membranes after transmodulation by platelet-derived growth factor. *J. Biol. Chem.* 266:2746-2752.

347. Walton, G. M., Chen, W. S., Rosenfeld, M. G. and Gill, G. N. (1990) Analysis of deletions of the carboxyl terminus of the epidermal growth factor receptor reveals self-phosphorylation at tyrosine 992 and enhanced *in vivo* tyrosine phosphorylation of cell substrates. *J. Biol. Chem.* 265:1750-1754.

348. Waters, C. M., Oberg, K. C., Carpenter, G. and Overholser, K. A. (1990) Rate constants for binding, dissociation, and internalization of EGF: effect of receptor occupancy and ligand concentration. *Biochemistry* 29:3563-3569.

349. Waters, C. M., Overholser, K. A., Sorkin, A. and Carpenter, G. (1992) Analysis of the influences of the E5 transforming protein on kinetic parameters of epidermal growth factor binding and metabolism. *J. Cell. Phys.* 152:253-263.

350. Waters, S. B., Chen, D., Kao, A. W., Okada, S., Holt, K. H. and Pessin, J. E. (1996) Insulin and epidermal growth factor receptors regulate distinct pools of Grb2-SOS in the control of Ras activation. *J. Biol. Chem.* 271:18224-18230.

351. Waters, S. B., Holt, K. H., Ross, S. E., Syu, L.-J., Guan, K.-L., Saltiel, A. R., Koretzky, G. A. and Pessin, J. E. (1995) Desensitization of Ras activation by a

feedback disassociation of the SOS-Grb2 complex. *J. Biol. Chem.* 270:20883-20886.

352. Weber, W., Bertics, P. J. and Gill, G. N. (1984) Immunoaffinity purification of the epidermal growth factor receptor. *J. Biol. Chem.* 259:14631-14636.

353. Wedegaertner, P. B. and Gill, G. N. (1989) Activation of the purified protein tyrosine kinase domain of the epidermal growth factor receptor. *J. Biol. Chem.* 264:11346-11353.

354. Wedegaertner, P. B. and Gill, G. N. (1992) Effect of carboxyl terminal truncation on the tyrosine kinase activity of the epidermal growth factor receptor. *Arch. Biochem. Biophys.* 292:273-280.

355. Weiss, F. U., Daub, H. and Ullrich, A. (1997) Novel mechanisms of RTK signal generation. *Curr. Opin. Gen. Dev.* 7:80-86.

356. Wells, A., Welsh, J. B., Lazar, C. S., Wiley, H. S., Gill, G. N. and Rosenfeld, M. G. (1990) Ligand-induced transformation by a non-internalizing epidermal growth factor receptor. *Science* 247:962-964.

357. Weng, G., Bhalla, U. S. and Iyengar, R. (1999) Complexity in biological signaling systems. *Science* 284:92-96.

358. Wiegant, F. A. C., Blok, F. J., Defize, L. H. K., Linnemans, W. A. M., Verkley, A. J. and Boonstra, J. (1986) Epidermal growth factor receptors associated to cytoskeletal elements of epidermoid carcinoma (A431) cells. *J. Cell Biol.* 103:87-94.

359. Wiley, H. S. (1988) Anomalous binding of epidermal growth factor to A431 cells is due to the effect of high receptor densities and a saturable endocytic system. *J. Cell Biol.* 107:801-810.

360. Wiley, H. S. and Cunningham, D. D. (1981) A steady state model for analyzing the cellular binding, internalization and degradation of polypeptide ligands. *Cell* 25:433-440.

361. Wiley, H. S. and Cunningham, D. D. (1982) The endocytic rate constant. *J. Biol. Chem.* 257:4222-4229.

362. Wiley, H. S., Herbst, J. J., Walsh, B. J., Lauffenburger, D. A., Rosenfeld, M. G. and Gill, G. N. (1991) The role of tyrosine kinase activity in endocytosis, compartmentation, and down-regulation of the epidermal growth factor receptor. *J. Biol. Chem.* 266:11083-11094.

363. Winston, J. T., Olashaw, N. E. and Pledger, W. J. (1991) Regulation of the transmodulated epidermal growth-factor receptor by cholera toxin and the protein phosphatase inhibitor okadaic acid. *J. Cell. Biochem.* 47:79-89.

364. Wittinghofer, A., Scheffzek, K. and Ahmadian, M. R. (1997) The interaction of Ras with GTPase-activating proteins. *FEBS Lett.* 410:63-67.

365. Wixler, V., Smola, U., Schuler, M. and Rapp, U. (1996) Differential regulation of Raf isozymes by growth versus differentiation inducing factors in PC12 pheochromocytoma cells. *FEBS Lett.* 385:131-137.

366. Wofsy, C., Goldstein, B., Lund, K. and Wiley, S. (1992) Implications of epidermal growth factor (EGF) induced EGF receptor aggregation. *Biophys. J.* 63:98-110.

367. Wu, J., Dent, P., Jelinek, T., Wolfman, A., Weber, M. J. and Sturgill, T. W. (1993) Inhibition of the EGF-activated MAP kinase signaling pathway by adenosine 3',5'-monophosphate. *Science* 262:1065-1069.

368. Wu, J., Lau, L. F. and Sturgill, T. W. (1994) Rapid deactivation of MAP kinase in PC12 cells occurs independently of induction of phosphatase MKP-1. *FEBS Lett.* 353:9-12.

369. Wu, X. Y., Noh, S. J., Zhou, G. C., Dixon, J. E. and Guan, K.-L. (1996) Selective activation of MEK1 but not MEK2 by A-Raf from epidermal growth factor-stimulated HeLa cells. *J. Biol. Chem.* 271:3265-3271.

370. Yamada, M., Ikeuchi, T., Aimoto, S. and Hatanaka, H. (1996) EGF-induced sustained tyrosine phosphorylation and decreased rate of down-regulation of EGF receptor in PC12h-R cells which show neuronal differentiation in response to EGF. *Neurochemical Research* 21:815-822.

371. Yan, M. H. and Templeton, D. J. (1994) Identification of 2 serine residues of MEK-1 that arre differentially phosphorylated during activation by Raf and MEK kinase. *J. Biol. Chem.* 269:19067-19073.

372. Yang, B., van Hoek, A. N. and Verkman, A. S. (1997) Very high single channel water permeability of aquaporin-4 in baculovirus-infected insect cells and liposomes reconstituted with purified aquaporin-4. *Biochemistry* 36:7625-7632.

373. Yao, H., York, R. D., Misra-Press, A., Carr, D. W. and Stork, P. J. (1998) The cyclic adenosine monophosphate-dependent protein kinase (PKA) is required for the sustained activation of mitogen-activated kinases and gene expression by nerve growth factor. *J Biol Chem* 273:8240-8247.

374. Yarden, Y. and Schlessinger, J. (1987) Epidermal growth factor induces rapid, reversible aggregation of the purified epidermal growth factor receptor. *Biochemistry* 26:1443-1451.

375. Yarden, Y. and Schlessinger, J. (1987) Self-phosphorylation of epidermal growth factor receptor: evidence for a model of intermolecular allosteric activation. *Biochemistry* 26:1434-1442.

376. Yarden, Y. and Ullrich, A. (1988) Growth factor receptor tyrosine kinases. *Annu. Rev. Biochem.* 57:443-478.

377. York, R. D., Yao, H., Dillon, T., Ellig, C. L., Eckert, S. P., McCleskey, E. W. and Stork, P. J. S. (1998) Rap1 mediates sustained MAP kinase activation induced by nerve growth factor. *Nature* 392:622-626.

378. Young, S. W., Dickens, M. and Tavare, J. M. (1994) Differentiation of PC12 cells in response to a cAMP analogue is accompanied by sustained activation of mitogen-activated protein kinase: comparison with the effects of insulin, growth factors and phorbol esters. *FEBS Lett* 338:212-216.

379. Zapf-Colby, A., Eichhorn, J., Webster, N. J. G. and Olefsky, J. M. (1999) Inhibition of PLC-γ1 activity converts nerve growth factor from an anti-mitogenic to a mitogenic signal in CHO cells. *Oncogene* 18:4908-4919.

380. Zhang, Z. Y., Walsh, A. B., Wu, L., McNamara, D. J., Dobrusin, E. M. and Miller, W. T. (1996) Determinants of substrate recognition in the protein-tyrosine phosphatase, PTP1. *J Biol Chem* 271:5386-5392.

381. Zhao, H., Li, Y. Y., Fucini, R. V., Ross, S. E., Pessin, J. E. and Koretzky, G. A. (1997) T cell receptor-induced phosphorylation of Sos requires activity of CD45, Lck, and protein kinase C, but not ERK. *J. Biol. Chem.* 272:21625-21634.

382. Zheng, C.-F. and Guan, K.-L. (1993) Properties of MEKs, the kinases that phosphorylate and activate the extracellular signal-regulated kinases. *J. Biol. Chem.* 268:23933-23939.

383. Zheng, C.-F. and Guan, K.-L. (1994) Activation of MEK family kinases requires phosphorylation of two conserved Ser/Thr residues. *EMBO J.* 13:1123-1131.

384. Zhou, M., Felder, S., Rubinstein, M., Hurwitz, D. R., Ullrich, A. and Schlessinger, J. (1993) Real-time measurements of kinetics of EGF binding to soluble EGF receptor monomers and dimers support the dimerization model for receptor activation. *Biochemistry* 32:8193-8198.

APPENDIX I

REACTION SCHEME DIAGRAM

APPENDIX II

PUBLISHED MATERIAL